THÈSE

Pour obtenir le grade de

DOCTEUR DE L'UNIVERSITÉ GRENOBLE ALPES

École doctorale : MSTII - Mathématiques, Sciences et technologies de l'information, Informatique
Spécialité : Mathématiques
Unité de recherche : Institut Fourier

Quelques problèmes géométriques autour des surfaces de translations

On some geometric problems about transation surfaces

Présentée par :

Julien BOULANGER

Direction de thèse :

Erwan LANNEAU PROFESSEUR DES UNIVERSITES, UNIVERSITE GRENOBLE ALPES	Directeur de thèse
Daniel MASSART MAITRE DE CONFERENCES HDR, UNIVERSITE DE MONTPELLIER	Co-directeur de thèse

Rapporteurs :

JAYADEV ATHREYA
FULL PROFESSOR, UNIVERSITY OF WASHINGTON
STEPHANE SABOURAU
PROFESSEUR DES UNIVERSITES, UNIVERSITE PARISEST CRETEIL

Thèse soutenue publiquement le **20 décembre 2023**, devant le jury composé de :

ERWAN LANNEAU PROFESSEUR DES UNIVERSITES, UNIVERSITE GRENOBLE ALPES	Directeur de thèse
DANIEL MASSART MAITRE DE CONFERENCES HDR, UNIVERSITE DE MONTPELLIER	Co-directeur de thèse
JAYADEV ATHREYA FULL PROFESSOR, UNIVERSITY OF WASHINGTON	Rapporteur
STEPHANE SABOURAU PROFESSEUR DES UNIVERSITES, UNIVERSITE PARISEST CRETEIL	Rapporteur
ELISE GOUJARD MAITRESSE DE CONFERENCES, UNIVERSITE DE BORDEAUX	Examinatrice
PASCAL HUBERT PROFESSEUR DES UNIVERSITES, AIX-MARSEILLE UNIVERSITE	Président
ANA RECHTMAN PROFESSEURE DES UNIVERSITES, UNIVERSITE GRENOBLE ALPES	Examinatrice
CORINNA ULCIGRAI FULL PROFESSOR, UNIVERSITÄT ZÜRICH	Examinatrice

Résumé

Cette thèse porte sur plusieurs problèmes relatifs aux surfaces de translation. Nous commençons par étudier l'intersection algébrique des courbes fermées sur ces surfaces, et plus précisément la question du nombre maximal d'intersections de deux courbes fermées en fonction de leur longueur. Pour cela, on étudie la quantité KVol définie par :

$$\mathrm{KVol}(X) = \mathrm{Vol}(X) \cdot \sup_{\alpha,\beta} \frac{\mathrm{Int}(\alpha,\beta)}{l(\alpha)l(\beta)},$$

le supremum portant sur l'ensemble des paires de courbes fermées sur X. On démontre en particulier que KVol est réalisé par deux systoles qui s'intersectent une fois sur chacune des surfaces de Bouw-Möller ayant une seule singularité. Plus généralement, on étudie cette quantité pour des surfaces construites à partir d'une collection de polygones convexes à angles obtus en recollant deux à deux leurs côtés, et on obtient une borne supérieure sur KVol qui est fonction de la longueur du plus petit côté des polygones.

On étudie ensuite le comportement de KVol lorsqu'on déforme une surface de translation en agissant par une matrice de $SL_2(\mathbb{R})$. Nous obtenons une formule close pour KVol dans chacun des disques de Teichmüller associés aux surfaces de Bouw-Möller à une seule singularité. Plus généralement, on donne un critère qui permet de savoir si KVol est borné sur le disque de Teichmüller d'une surface de Veech.

Enfin, on abordera la question du comportement de KVol non pas sur des disques de Teichmüller, mais sur toute la strate minimale de l'espace de modules des surfaces de translation, dans laquelle nous conjecturons que KVol est toujours plus grand que le genre de la surface. Dans cette direction, on exhibe une famille de surfaces dans chaque composante connexe de la strate minimale (et pour tout genre au moins deux) pour laquelle KVol est arbitrairement proche du genre de la surface.

Dans un second temps, on s'intéresse à la question de l'existence de points de connexions sur le double heptagone, et plus généralement le double n-gone pour $n \geq 7$ impair. On démontre que les centres des heptagones ne sont pas des points de connexion du double heptagone, ce qui répond à une question de P. Hubert et T. Schmidt.

Enfin, on abordera la question de la classification des surfaces de Veech dans une sous-variété de l'espace de modules des surfaces de translation en genre trois, le lieu des surfaces de translation ayant une involution prym. On démontre qu'il n'existe pas de surface de Veech géométriquement primitive dans $Prym(2,2)$. Ce résultat, dont la démonstration s'appuie en partie sur un programme utilisant le package *Flatsurf* de *Sage*, achève un travail initié par E. Lanneau et M. Möller.

Abstract

This thesis deals with several problems related to translation surfaces. We begin by studying the algebraic intersection of closed curves on these surfaces, and more precisely the question of the maximum number of intersections of two closed curves as a function of their length. In this purpose, we study the quantity KVol defined by :

$$\mathrm{KVol}(X) = \mathrm{Vol}(X) \sup_{\alpha,\beta} \frac{\mathrm{Int}(\alpha,\beta)}{l(\alpha)l(\beta)},$$

where the supremum is taken over pairs of closed curves on X. We show that KVol is realized by two systoles that intersect once on each of the Bouw-Möller surfaces having a single singularity as well as on the regular n-gon for n multiple of four. More generally, we study this quantity for surfaces built from a collection of convex polygons with obtuse angles by identifying their sides by pairs, and we obtain an upper bound on KVol which is a function of the length of the smallest side of the polygons.

We then study the behavior of KVol when we deform a translation surface by the action of a matrix of $SL_2(\mathbb{R})$. We give a closed formula for KVol in each of the Teichmüller discs associated to Bouw-Möller surfaces with a single singularity, as well as the regular n-gons for n multiple of four. More generally, we prove a criterion which ensures boundedness of KVol on the Teichmüller disk of a Veech surface.

Finally, we discuss the behavior of KVol on the minimal stratum of the moduli space of translation surfaces, in which we conjecture that KVol is always greater than the genus of the surface. In this direction, we exhibit a family of surfaces in each connected component of the minimal stratum (and for any genus at least two) for which KVol is arbitrarily close to the genus.

On a second part, we are interested in the question of the existence of connection points on the double heptagon, and more generally the double n-gon for $n \geq 7$ odd. It is shown that the centers of the heptagons are not connection points of the double heptagon, which answers a question of P. Hubert and T. Schmidt.

Finally, we will address the question of the classification of Veech surfaces in a sub-variety of the moduli space of translation surfaces in genus 3, namely the locus of translation surfaces having a prym involution. More precisely, we show that there is no geometrically primitive Veech surface in $Prym(2,2)$. This result, whose proof rely on a computer program using the *Flatsurf* package of *Sage*, completes a work initiated by E. Lanneau and M. Möller.

Remerciements

Tout d'abord, je tiens à remercier mes directeurs de thèse Erwan Lanneau et Daniel Massart, sans qui cette thèse n'aurait pu être, pour m'avoir encadré avec enthousiastme et bienveillance. Vous avoir comme directeurs de thèse a été une grande chance pour moi. Merci pour votre aide et votre disponibilité, et pour vos nombreuses explications (et ré-explications). Erwan, ta curiosité et ton enthousiasme sont inspirants et ont grandement contribué à ma motivation à travailler sur ces questions. Daniel, j'ai beaucoup progressé grâce à nos (longues) discussions et à tes relectures pointues. Merci à tous les deux pour vos conseils avisés tout au long de la thèse.

Durant ma thèse j'ai eu la chance de participer à de nombreuses conférences, de présenter mes travaux et d'échanger avec de nombreux spécialistes. J'ai été écouté avec beaucoup de bienveillance et d'enthousiasme, et je tiens à remercier les personnes qui contribuent à la diffusion de ces valeurs dans la communauté. Je remercie tout d'abord Pascal Hubert pour avoir accepté de faire partie de mon comité de suivi de thèse puis de mon jury, mais aussi pour son enthousiasme et ses questions qui m'ont permis de prendre du recul sur mon travail. Je remercie également Jayadev Athreya et Stéphane Sabourau pour avoir accepté de rapporter mon travail de thèse, et Elise Goujard, Ana Rechtman, et Corinna Ulcigrai pour avoir accepté de faire partie de mon jury de thèse.

En plus des membres du jury, je voudrais spécifiquement remercier Samuel Lelièvre, qui a entre autres installé Sage sur mon ordinateur deux ou trois fois, ainsi que Vincent Delecroix, Thierry Monteil et Julian Ruth pour leur aide précieuse pour Sage, et plus généralement Samantha Fairchild, Gabriella Schmidhusen, Selim Ghazouani, Charles Fougeron, Adrien Boulanger, Pierre Arnoux, Martin Möller, Pierre Dehornoy, Frédéric Faure et Curtis McMullen. Je suis particulièrement reconaissant à tout.e.s les doctorant.e.s (ou qui l'étaient) avec qui j'ai pu échanger et discuter de maths, notamment Pablo Montealegre, Magali Jay, Mingkun Liu et Jérome Carrand. Un grand merci à Sam Freedman pour m'avoir motivé à travailler sur les surfaces Prym et à Irene Pasquinelli pour avoir accepté avec enthousiasme de travailler ensemble sur KVol et les surfaces de Bouw-Möller.

Je voudrais également remercier l'équipe administrative et technique du laboratoire de Grenoble qui m'a permis de faire ma thèse dans de bonnes conditions. Je remercie les membres et les organisateurs des groupes de travail en géométrie auxquels j'ai participé. Surtout, je tiens à remercier les doctorant.e.s de l'institut Fourier (et Marie) pour la super ambiance, sans qui la thèse n'aurait clairement pas eu la même saveur (et je ne parle pas que des gateaux). Je remercie aussi les doctorants de l'IMAG qui m'ont toujours acceuilli à Montpellier dans la bonne humeur.

Enfin, je souhaite remercier tou.te.s mes ami.e.s qui m'acompagnent de près ou de loin, et dont la présence a participé et participe grandement à mon épanouissement. Merci à Ninon pour l'hébergement à Montpellier, entre autres.

Je termine par des remerciements à ma famille en général et plus spécifiquement à mes parents qui m'ont encouragé tout au long de ma scolarité, et qui sont la raison principale pour laquelle j'en suis là aujourd'hui.

Table des matières

Résumé **1**

Abstract **3**

Remerciements **5**

Introduction **9**

1 Présentation générale **15**
1.1 Intersection algébrique et KVol 15
1.1.1 Intersection algébrique et KVol 15
1.1.2 Motivations et historique 18
1.1.3 Quelques questions 21
1.2 Surfaces de translation 24
1.2.1 Définition et motivations 25
1.2.2 Quelques exemples 25
1.2.3 L'espace de modules des surfaces de translation 27
1.2.4 Action de $SL_2(\mathbb{R})$ et groupe de Veech 29
1.2.5 Connexions de selles et décomposition en cylindres 30
1.3 KVol sur les surfaces de translation 34
1.3.1 Introduction et motivations 34
1.3.2 Quelques idées préliminaires 36
1.3.3 Présentation des résultats 40
1.4 Points de connexion du double heptagone 56
1.5 Surfaces de Veech primitives dans $Prym(2,2)$ 58

2 KVol on double regular n-gons **60**

3 KVol on regular n-gons **91**

4 Surfaces made with convex polygons having obtuse or right angles **133**

5 The case of Bouw-Möller surfaces **176**

6 Lower bound for KVol on the minimal stratum of translation surfaces **216**

7 Connection points on the double heptagon **231**

8 There are no primitive Teichmüller curves on Prym(2,2) **246**

Introduction

Les surfaces de translation sont des exemples de surfaces plates à singularités coniques à la croisée de chemins entre géométrie différentielle, géométrie algébrique, dynamique, théorie des nombres, et théorie géométrique des groupes. La motivation originale à leur étude provient du fait qu'elles permettent d'étudier les trajectoires sur un billard polygonal dont les angles sont des multiples rationnels de π, grâce à une procédure de "dépliement" du billard décrite par A.B. Katok et A.N. Zemlyakov dans [ZK76]. Cette méthode est notamment utilisée par Kerchoff, Masur et Smillie pour démontrer que presque toute trajectoire dans un billard rationnel est uniquement ergodique, voir [GL08]. L'étude des surfaces de translation a pris de l'ampleur ces dernières années, avec notamment l'exploration des liens avec la théorie de Teichmüller ou avec des questions dynamiques autour du flot géodésique ou des échanges d'intervalles. On peut par exemple citer la démonstration du "Théorème de la baguette magique" par A. Eskin, M. Mirzakhani et A. Mohammadi [EMM15] qui classifie les adhérences d'orbites dans l'espace de modules des surfaces de translation, ou encore d'autres résultats récents [EFW18], [EMMW20] relatifs à la classification des courbes de Teichmüller.

Dans cette thèse, nous abordons plusieurs problèmes relatifs aux surfaces de translation. Le premier, de nature plutôt géométrique, concerne l'intersection algébrique des courbes fermées. Dans une deuxième partie, on s'intéresse à la notion de points de connexion sur certaines surfaces de Veech particulièrement symétriques, ce qui sera l'occasion d'explorer certains liens entre surfaces de translation, dynamique et théorie des nombres. Enfin, la dernière partie aborde la question de classification des courbes de Teichmüller, et plus spécifiquement l'étude de certaines surfaces de genre trois possédant une involution Prym.

Intersection algébrique et KVol. Dans une première partie, on étudie l'intersection algébrique de courbes fermées sur une surface de translation. Plus précisément, on s'intéresse à la question suivante :

Combien de fois deux courbes fermées de longueur donnée peuvent-elles s'intersecter ?

Cette question, qui fait sens pour n'importe quelle surface orientable X sur laquelle on peut mesurer les longueurs des courbes fermées (on supposera ici que la surface est munie d'une métrique riemannienne à singularités coniques), peut être quantifiée en définissant :

$$\mathrm{KVol}(X) := \mathrm{Vol}(X) \cdot \sup_{\alpha,\beta} \frac{\mathrm{Int}(\alpha,\beta)}{l(\alpha)l(\beta)}$$

le supremum portant sur l'ensemble des paires de courbes fermées sur X. La normalisation par le volume permet de rendre la quantité invariante par dilatation de la surface. Dans ce

texte, nous étudions le cas de l'intersection *algébrique*, définie en assignant un signe à chaque point d'intersection. L'étude de KVol remonte aux travaux de D. Massart dans [Mas97], où cette quantité apparaît (indirectement) comme constante de comparaison entre la norme stable et la norme de Hodge. L'étude de KVol a depuis été approfondie par D. Massart et B. Muetzel [MM14], mais de nombreuses questions restent en suspens, à commencer par la question du calcul explicite de KVol sur des exemples simples de surfaces. Dans ce contexte, S. Cheboui, A. Kessi et D. Massart ont initié l'étude de KVol sur des surfaces de translation en calculant précisément KVol sur le disque de Teichmüller de certaines surfaces à petits carreaux, voir [CKM21a].

Dans cette thèse, nous continuons dans cette direction en exposant une méthode qui permet de calculer précisément KVol sur une famille de surfaces de translation comprenant les surfaces de Bouw-Möller à une singularité. Cette méthode permet également d'obtenir une borne supérieure sur KVol pour des surfaces construites à partir de polygones convexes à angles obtus tels que les côtés d'un même polygone ne sont pas recollés entre eux. Plus précisément, on a :

Théorème A. *Soit X une surface construite à partir d'une collection de polygones $(P_i)_{i\in I}$ dont on a recollé les côtés deux à deux. On suppose :*

(H1) Les polygones sont convexes à angles obtus.
(H2) Les côtés d'un même polygone ne sont pas recollés entre eux.

Alors, pour toute paire de courbes fermées (α, β) sur la surface X, on a :

$$\frac{Int(\alpha,\beta)}{l(\alpha)l(\beta)} \leq \frac{1}{l_0^2}$$

où l_0 désigne la longueur du plus petit des côtés des polygones P_i.

Ce résultat donne une borne supérieure sur KVol (lorsque l'aire de la surface est finie). On démontre que cette borne est atteinte pour les surfaces de Bouw-Möller à une seule singularité.

Théorème B. *Soit $m, n \geq 2$ avec $mn \geq 6$. Étant données deux courbes fermées α et β sur la surface de Bouw-Möller $S_{m,n}$, on a :*

$$\frac{Int(\alpha,\beta)}{l(\alpha)l(\beta)} \leq \frac{1}{\sin(\frac{\pi}{m})^2}.$$

De plus, l'égalité est réalisée si et seulement si m et n sont premiers entre eux, et si α et β sont deux systoles qui s'intersectent, ou bien lorsque $n = 4$ et $m \equiv 3 \mod 4$ et α et β sont les deux diagonales du carré $P(0)$ (resp. $P(m-1)$).

Un résultat similaire est également valable pour les surfaces de translation construites à partir d'un seul polygone régulier ayant un nombre pair de côtés (voir Théorèmes 1.3.3 et 1.3.4).

Une fois KVol calculé sur des exemples de surfaces, on peut se demander comment cette quantité varie lorsqu'on déforme légèrement la surface. Dans le cas des surfaces de translation, on peut par exemple étudier les variations de KVol sous l'action de $SL_2(\mathbb{R})$. Formulée autrement, la question est de savoir si l'on peut donner une formule explicite pour KVol sur le disque de Teichmüller d'une surface de translation donnée. Cette question a notamment été étudiée dans [CKM21a] pour certaines surfaces à petits carreaux. Ici, on s'intéressera spécifiquement aux surfaces de Veech, et nous présenterons une méthode qui permet notamment d'étendre le calcul de KVol de certaines surfaces ayant une unique singularité à tout leur disque de Teichmüller (voir Théorème 1.3.10). Nous illustrons cette méthode dans le cas des surfaces de Bouw-Möller ayant une unique singularité en démontrant :

Théorème C. *Soient $m, n \geq 2$ premiers entre eux. Étant donnés $d, d' \in \mathbb{R} \cup \{\infty\} \simeq \partial\mathbb{H}^2$, notons $\gamma_{d,d'}$ la géodésique du demi-plan hyperbolique $\mathbb{H}^2$ dont les extrémités sont en d et d'. Soit $X = M \cdot S_{m,n}$ une surface du disque de Teichmüller de la surface de Bouw-Möller $S_{m,n}$, obtenue à partir de $S_{m,n}$ en agissant par une matrice $M = \begin{pmatrix} a & b \\ c & d \end{pmatrix} \in SL_2(\mathbb{R})$. Alors, on a :*

$$KVol(X) = K_0 \cdot \frac{1}{\cosh(\mathrm{dist}_{\mathbb{H}^2}(\frac{di+b}{ci+a}, \Gamma_{m,n} \cdot \gamma_{\infty, \pm \cot \frac{\pi}{n}}))}$$

où $K_0 > 0$ est une constante explicite qui dépend seulement de m et n, $\Gamma_{m,n}$ désigne le groupe de Veech de $S_{m,n}$ et $\mathrm{dist}_{\mathbb{H}^2}$ désigne la distance hyperbolique.

Nous calculons également KVol sur le disque de Teichmüller du n-gone régulier pour $n \equiv 0 \mod 4$, voir Théorème 1.3.9. À la différence des surfaces de Bouw-Möller, le maximum de KVol sur le disque de Teichmüller du n-gone régulier correspond (à l'action du groupe de Veech près) à une infinité de géodésiques.

Pour les surfaces de Veech ayant plusieurs singularités, la méthode d'extension au disque de Teichmüller n'est plus valable. Toutefois, nous donnons un critère qui permet de savoir si KVol est borné ou non sur un disque de Teichmüller d'une surface de Veech.

Théorème D. *KVol est borné sur le disque de Teichmüller d'une surface de Veech si et seulement si pour toute direction périodique, deux géodésiques fermées construites à partir de connexions de selles dans cette direction ne s'intersectent jamais. C'est le cas si et seulement si le diagramme des séparatrices associé à la direction périodique est planaire (en tant que graphe enrubanné).*

Ce critère permet d'obtenir le résultat suivant :

Théorème E. *Pour tous $m, n \geq 2$ avec $mn \geq 6$, KVol est borné sur le disque de Teichmüller de $S_{m,n}$.*

Un résultat similaire est valable pour le n-gone régulier (n pair), voir Théorème 1.3.11. Le Théorème 5 est à mettre en perspective avec les résultats de [CKM21a], où il est démontré que KVol n'est pas borné sur le disque de Teichmüller des surfaces à petits carreaux considérés.

Enfin, plutôt que de se restreindre à l'étude de KVol sur un disque de Teichmüller donné, on peut également chercher à étudier KVol sur chacune des strates de l'espace de modules des surfaces de translation. En genre un, cette question est relativement élémentaire et KVol est constant égal à un. En genre supérieur ou égal à deux, KVol n'est plus constant et il est facile de faire tendre KVol vers l'infini en pinçant une courbe non-séparante (mais en gardant le diamètre de la surface borné). Les surfaces intéressantes sont alors les surfaces pour lesquelles KVol est "petit". Dans ce cadre, nous étudions le cas spécifique de la strate minimale $\mathcal{H}(2g-2)$ et généralisons une construction de Cheboui, Kessi et Massart [CKM21b], ce qui nous permet d'obtenir une famille de surfaces de translation à une seule singularité dans chaque composante connexe de la strate minimale de l'espace de modules des surfaces de translation dont KVol est arbitrairement proche du genre de la surface.

Théorème F. *Soit $g \geq 2$. Pour chaque composante connexe $\mathcal{C}$ de $\mathcal{H}(2g-2)$, on a :*

$$\inf_{X \in \mathcal{C}} KVol(X) \leq g.$$

On conjecture que cette inégalité est optimale (et que, de plus, l'infimum n'est jamais atteint).

Points de connexion du double n-gone régulier. Dans une deuxième partie, on s'intéresse à la notion de point de connexion d'une surface de translation, introduite par P. Hubert et T.A. Schmidt [HS04], et qui permet notamment de construire des surfaces de translation dont le groupe de Veech est infiniment engendré. Dans [Bou], publié au *Bulletin de la SMF* et qui correspond au Chapitre 7, on s'intéresse spécifiquement au double heptagone, construit à partir de deux copies d'un heptagone régulier à recollé les côtés deux à deux, et plus généralement au double n-gone pour $n \geq 7$ impair. Ces surfaces sont, avec les n-gones réguliers pour n pair, les surfaces originales étudiées par Veech dans son article fondateur [Vee89]. Elles jouissent de propriétés dynamiques et géométriques particulières. Cependant, on ne connaît aucun point de connexion non-périodique sur ces surfaces (et plus généralement sur toute surface de translation dont le degré sur $\mathbb{Q}$ corps de trace est 3 ou plus). Les centres des n-gones, qui ne sont pas des points périodiques, sont des candidats naturels pour être des points de connexion. Pour $n = 7$ et $n = 9$, nous démontrons qu'en fait, ce n'est pas le cas :

Théorème G. *Les points centraux du double heptagone et du double nonagone ne sont pas des points de connexion.*

Nous conjecturons que ce résultat s'étend à chacun des double n-gones pour $n \geq 7$ impair.

Pour démontrer le Théorème 7, nous utilisons la notion de fraction continue de Hecke, introduite par D. Rosen dans [Ros54]. Il découle d'un résultat de T. Schmidt et M. Sheingorn [SS95] (ainsi que de la dichotomie de Veech [Vee89]) que ces fractions continues permettent de caractériser les directions périodiques sur le double n-gone : une direction sur le double n-gone est périodique si et seulement si le développement en fraction continue de Hecke de sa pente (obtenu à partir de l'algorithme de fraction continue "à l'entier supérieur ou égal") est fini.

Surfaces de Veech ayant une involution Prym. Dans la dernière partie, on s'intéresse à la question de la classification des surfaces de Veech *géométriquement primitives*. Malgré plusieurs avancées majeures récentes [EFW18] et [EMMW20], cette question semble loin d'être résolue. En genre deux, les surfaces de Veech primitives ont été classifiées dans une série d'articles de C. McMullen [McM05b], [McM05a] et [McM06a]. En genre trois, la classification n'est pas complète mais C. McMullen [McM06b] a exhibé une famille infinie de surfaces de Veech primitives. Les travaux de plusieurs personnes ont depuis montré que, en dehors de cette famille, il n'y a qu'un nombre fini de surfaces de Veech primitives (à l'action de $GL_2^+(\mathbb{R})$ près), voir [McM21, Theorem 5.5]. Cette famille infinie est constituée de surfaces munies d'une *involution Prym* et ayant une seule singularité. Une surface de translation munie d'une involution Prym peut être construite comme revêtement double d'une surface de *demi-translation* (ramifié en les singularités), voir [McM06b] ou [LN13]. Pour rechercher d'autres surfaces de Veech primitives, une idée naturelle est de s'intéresser aux surfaces de translation munies d'une involution Prym, mais ayant plusieurs singularités. Dans ce contexte, E. Lanneau et M. Möller [LM19] ont cherché les surfaces de Veech primitives dans les lieux $\mathrm{Prym}(2,1,1)$ et $\mathrm{Prym}(2,2)$. Ils démontrent qu'il n'existe pas de surface de Veech primitive dans $\mathrm{Prym}(2,1,1)$ et identifient 92 candidats dans $\mathrm{Prym}(2,2)$. Dans un travail en commun avec Sam Freedman présenté au Chapitre 8, et accepté pour publication aux *Comptes rendus de l'académie des sciences*, on s'intéresse spécifiquement à ces 92 candidats et nous démontrons qu'aucun d'entre eux n'est une surface de Veech. Autrement dit :

Théorème H. *Il n'y a pas de surfaces de Veech géométriquement primitives dans la sous-variété* $\mathrm{Prym}(2,2)$.

La démonstration s'appuie notamment sur un programme informatique qui utilise le package *Flatsurf* de *Sage*.

Publications et pré-publications de l'auteur

Les travaux présentés dans cette thèse sont en partie issus des travaux suivants, publiés ou soumis pour publication :

[1] Boulanger, J. "The central points of the double heptagon are not connection points." *Bulletin de la SMF* 150, 2 :459-472, (2023).

[2] Boulanger, J. and Freedman, S. "There are no primitive Teichmüller curves in Prym$(2, 2)$." accepted for publication at the *Comptes rendus de l'académie des sciences* (2022).

[3] Boulanger, J., Lanneau, E. and Massart, D. "Algebraic intersection in regular polygons." *arXiv 2110.14235* (2022).

[4] Boulanger, J. "Algebraic intersection, lengths and Veech surfaces." *arXiv :2309.17165* (2023).

[5] Boulanger, J. "Lower bound for KVol on the minimal stratum of translation surfaces." *arXiv :2310.00130* (2023).

De plus, un article est en préparation en collaboration avec I. Pasquinelli concernant le travail présenté aux Chapitres 4 et 5.

Chapitre 1

Présentation générale

Ce premier chapitre, en français, est voulu comme un survol informel de la thèse dans lequel nous présentons les motivations, les résultats ainsi que quelques idées clés. On commence par une introduction générale sur la quantité KVol qui sera au coeur des Chapitres 2 à 6. Dans un second temps, on introduit les surfaces de translation et présentons quelques propriétés qui nous seront utiles dans tous les chapitres suivants, et qui ne seront pas forcément rappelées. La troisième partie est consacrée à l'étude de KVol spécifiquement sur les surfaces de translation, et, après avoir donné quelques motivations et expliqué quelques idées préliminaires, nous présentons spécifiquement les résultats obtenus et développés dans les Chapitres 2 à 6, en insistant sur certaines idées qui nous ont paru importantes. Dans la quatrième partie de cette introduction, nous définissons la notion de points de connexion et abordons la question de leur caractérisation, qui est étudiée dans le Chapitre 7. Nous terminons ce chapitre en discutant la question de la classification des surfaces de Veech géométriquement primitives ayant une involution prym en genre trois, qui sera abordée dans le Chapitre 8.

1.1 Intersection algébrique et KVol

L'une des questions principales abordées dans ce texte concerne l'intersection algébrique des courbes fermées sur des surfaces. Plus spécifiquement, si la surface est munie d'une métrique qui permet de mesurer la longueur des courbes, on peut se poser la question suivante :

Combien de fois deux courbes fermées de longueur donnée peuvent-elles s'intersecter ?

Dans cette section, nous formulons la question de manière plus précise en commençant par définir l'intersection algébrique de deux courbes sur une surface ainsi que la quantité KVol au coeur de cette thèse qui décrit l'intersection maximale de deux courbes d'une longueur donnée. Nous présenterons ensuite les motivations et les questions principales reliées à KVol.

1.1.1 Intersection algébrique et KVol

Étant donné deux courbes fermées (et lisses) α et β sur une surface orientable X, on peut se demander comment compter le nombre de fois que les deux courbes s'intersectent.

On pourrait faire un décompte naïf en comptant un par un les points d'intersection, mais il pourrait y avoir un nombre infini de points d'intersection si les courbes ne sont pas en position transverse, comme sur la partie gauche de la Figure 1.1. Dans ce cas, une idée pourrait être de déformer légèrement l'une des deux courbes pour rendre l'intersection transverse comme sur la partie droite de la Figure 1.1, et ainsi obtenir un nombre fini de points d'intersection. On arrive alors à la conclusion qu'une bonne notion d'intersection doit être préservée par petite déformation des courbes en question.

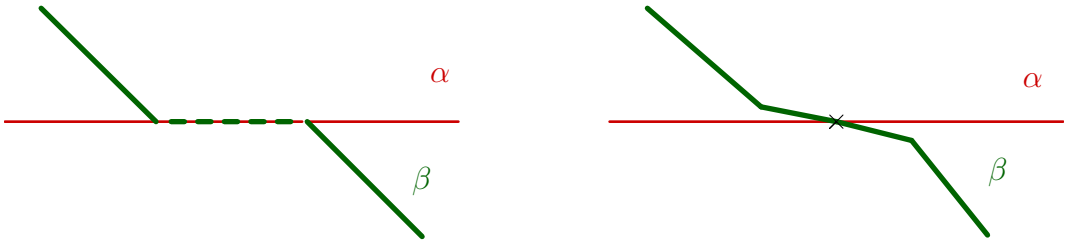

FIGURE 1.1 – Lorsque l'intersection n'est pas transverse, on peut déformer légèrement les courbes pour la rendre transverse.

Dès lors, on peut définir deux notions distinctes d'intersection :

— L'intersection *géométrique* est définie comme le nombre minimal de points d'intersection sur tous les représentants de la classe d'homotopie libre de α et β en position transverse.

— L'intersection *algébrique* est définie pour deux courbes α et β en position transverse en orientant chacune des courbes et en comptant chaque intersection avec un signe $+1$ ou -1 comme sur la Figure 1.2. On définit ensuite :

$$\mathrm{Int}(\alpha, \beta) = \sum_P \mathrm{Int}_P(\alpha, \beta).$$

De cette manière, on évite de compter l'intersection lorsque deux courbes "zigzaguent" entre elles. En fait, l'intersection algébrique de deux courbes est invariante par déformation continue des courbes. Mieux, l'intersection algébrique de deux courbes est invariante si l'on remplace les courbes par des courbes dans la même classe d'homologie. Ainsi, l'intersection algébrique définit une forme bilinéaire symplectique (i.e. antisymétrique et non-dégénérée) sur le groupe d'homologie $H_1(X, \mathbb{Z})$, que l'on peut alors étendre directement à $H_1(X, \mathbb{R})$. En particulier, on a toujours $\mathrm{Int}(\alpha, \alpha) = 0$. Ce n'est pas le cas pour l'intersection géométrique : la courbe α de la Figure 1.3 s'auto-intersecte une fois.

Dans toute la suite, on s'intéressera à l'intersection algébrique, et on utilisera la notation $\mathrm{Int}(\alpha, \beta)$ pour désigner l'intersection algébrique de deux courbes α et β. Une définition plus rigoureuse de l'intersection algébrique consiste à associer à chaque courbe fermée α une 1-forme différentielle ω_α par dualité de Poincaré. L'intersection algébrique de α et β se définit alors comme $\mathrm{Int}(\alpha, \beta) = \int_X \omega_\alpha \wedge \omega_\beta$. Formulé autrement, l'intersection algébrique en homologie est Poincaré duale au produit extérieur en cohomologie. Cette définition s'étend aux

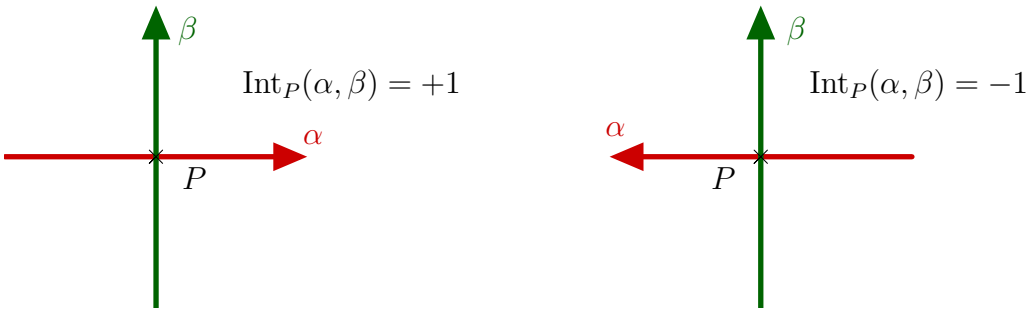

FIGURE 1.2 – Signe en un point d'intersection.

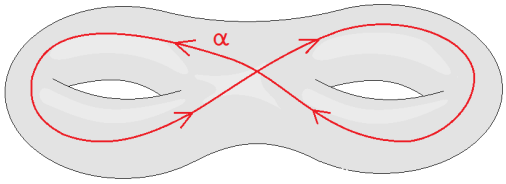

FIGURE 1.3 – Dans cet exemple $\mathrm{Int}_{geom}(\alpha, \alpha) = 1$.

variétés de dimension paire pour obtenir une forme d'intersection sur le groupe d'homologie d'ordre la moitié de la dimension. Toutefois, nous nous intéresserons dans ce texte seulement au cas des surfaces, et la définition de l'intersection algébrique pour des courbes en position transverse en comptant chaque point d'intersection avec un signe nous suffira.

Avec une telle définition, on peut se demander s'il est possible pour deux courbes de longueur donnée d'avoir une intersection arbitrairement grande. Cela nécessite bien sûr d'avoir défini un moyen de mesurer la longueur de courbes. On suppose donc ici qu'on a une métrique (ici, riemannienne avec éventuellement des singularités coniques isolées) qui nous le permette.

Prenons par exemple le cas où la surface X est un tore avec la métrique induite sur la surface par restriction de la métrique euclidienne de $\mathbb{R}^3$, et considérons la courbe fermée α comme sur la Figure 1.4. Pour qu'une courbe fermée intersecte non-trivialement la courbe α, elle doit alors faire tout le tour de l'anse, dans le sens transverse. Plus généralement, chaque intersection d'une courbe fermée β avec α nécessite de faire un tour de l'anse, à moins de revenir en arrière, ce qui reviendrait à compter une intersection négative ! Ainsi, on a besoin d'une certaine longueur pour intersecter un certain nombre de fois la courbe α. Par contraposée, une courbe β d'une longueur donnée ne peut intersecter α qu'un nombre de fois proportionnel à sa longueur.

Plus généralement, si X est une surface compacte, un argument de compacité de la boule unité de l'espace projectif sur $H^1(X, \mathbb{R})$ (qui est alors un espace vectoriel de dimension finie) montre que deux courbes de longueur donnée ne peuvent pas s'intersecter plus d'un certain nombre de fois. Une manière de quantifier ce phénomène est alors de définir la quantité suivante :

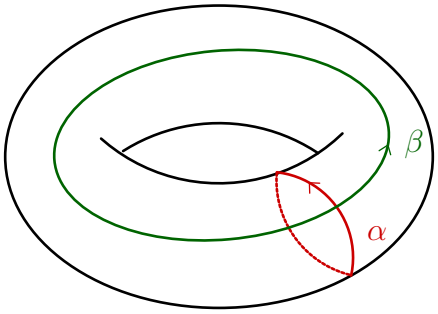

FIGURE 1.4 – Exemple d'un tore. Chaque intersection positive avec α nécéssite de faire tout le tour du tore dans le sens transverse.

$$\mathrm{K}(X) = \sup_{\alpha,\beta} \frac{\mathrm{Int}(\alpha,\beta)}{l(\alpha)l(\beta)}$$

où le supremum est pris sur l'ensemble des courbes fermées sur X, et $l(\alpha)$ (resp. $l(\beta)$) désigne la longueur de α (resp. β) pour la métrique considérée. En pratique, puisqu'on veut maximiser l'intersection par unité de longueur, on peut se restreindre au cas où α et β sont des géodésiques fermées, et même des géodésiques fermées simples par un argument de "convexité", voir [MM14, Lemme 3.1].

Il est à noter qu'une telle quantité a également été récemment étudiée dans le cas de l'intersection géométrique, voir [Tor23]. On verra dans le paragraphe suivant quelques motivations qui nous font considérer cette quantité plutôt qu'une autre, notamment le lien avec la *norme stable*, mais on peut d'ores et déjà noter un rapport de proportionnalité entre l'intersection avec α et la longueur de β (pour α fixé), comme illustré dans l'exemple du tore.

En pratique, pour comparer la valeur de K pour deux surfaces différentes, il est utile de normaliser cette quantité en multipliant par le volume de la surface, lorsque ce dernier est bien défini et fini. On définit alors :

$$\mathrm{KVol}(X) = \mathrm{Vol}(X) \cdot \sup_{\alpha,\beta} \frac{\mathrm{Int}(\alpha,\beta)}{l(\alpha)l(\beta)}$$

de sorte que KVol soit invariant par dilatation de la surface.

1.1.2 Motivations et historique

Comparaison de normes en homologie

La première occurrence connue de l'auteur de K ou de KVol remonte à l'étude de la norme stable d'une surface fermée munie d'une métrique Riemanienne par D. Massart dans sa thèse [Mas97]. K apparaît alors comme constante de comparaison entre la norme stable $\|\cdot\|_s$ et la norme L^2 $\|\cdot\|_2$, deux normes définies sur $H^1(X,\mathbb{R})$. Puisque $H^1(X,\mathbb{R})$ est un $\mathbb{R}$-espace vectoriel de dimension finie, les deux normes sont équivalentes. La relation entre les deux normes s'énonce alors comme suit :

Théorème 1.1.1 ([Mas97] et [MM14]). *On suppose que X est une surface fermée munie d'une métrique Riemanienne. Alors pour tout $h \in H_1(X, \mathbb{R})$, on a*

$$\|h\|_s \leq \sqrt{Vol(X)}\|h\|_2 \leq KVol(X)\|h\|_s$$

De plus, ces bornes sont optimales.

Avant de donner une interprétation géométrique de ce résultat, commençons par donner une définition informelle des deux normes en question.

La norme stable. La norme stable peut se définir de plusieurs manières. Dans le cas d'une surface compacte orientable sans bord de genre $g \geq 1$ muni d'une métrique riemannienne, on peut utiliser la définition suivante, voir [Mas97] :

Définition 1.1.2 (Norme stable sur $H_1(X, \mathbb{Z})$). Étant donnée une courbe fermée γ, on définit $\|\gamma\|$ comme la plus petite longueur des représentants de la classe γ. En particulier, pour une surface à courbure négative ou nulle, la norme stable d'une classe d'homologie entière est juste la longueur d'un représentant géodésique.
Pour une classe d'homologie entière $\gamma = \sum r_i[\gamma_i]$ (les coefficients r_i étant des entiers relatifs et les γ_i des courbes fermées), on définit $\|\gamma\|_s := \sum r_i\|\gamma_i\|_s$.

On étend alors cette définition à $H_1(X, \mathbb{R})$ par densité des classes d'homologie rationnelles.

La norme L^2. De son côté, la norme L^2 est plus naturelle à définir en utilisant les classes de cohomologie. Étant donné une 1-forme différentielle ω, on définit :

$$\|\omega\|_2 = \int_X \|\omega_x\|^2 \mathrm{dVol}(x)$$

On étend alors cette définition aux classes de cohomologie en posant, pour $c \in H^1(X, \mathbb{R})$, $\|c\|_2 := \inf_{[\omega]=c} \|\omega\|_2$. Cette norme est aussi appelée norme de Hodge, car l'infimum dans la définition est en fait un minimum, et il est réalisé par l'unique 1-forme harmonique de la classe de cohomologie [GH94]. La norme L^2 en cohomologie induit une norme en homologie par dualité de Poincaré (également appelée norme L^2).

Pour interpréter KVol en tant que constante de comparaison des normes stables et L^2, on peut s'intéresser à la boule unité de chacune de ces normes. La norme L^2 étant euclidienne, la boule unité est strictement convexe. À l'inverse, la boule unité de la norme stable est généralement bien plus sauvage, voir [Mas97]. Notons que la forme de la boule unité de la norme stable de tores plats fendus a récemment été étudiée par P. Montealegre.

L'exemple du tore plat

Lorsque la surface est un tore plat, on peut facilement calculer KVol : un tel tore peut être représenté comme un cylindre dans $\mathbb{R}^3$ dont on identifie les deux extrémités (éventuellement avec une rotation, on parle alors de *"twist"*). En prenant α comme l'un des cercles transverses

au cylindre et β une courbe traversant une fois le cylindre (dans le cas où il n'y a pas de twist, une telle courbe est fermée), on a exactement une intersection et $l(\alpha)l(\beta)$ est exactement l'aire du tore, de sorte que, si X désigne notre tore plat, on a

$$\frac{\mathrm{Int}(\alpha,\beta)}{l(\alpha)l(\beta)} = \frac{1}{\mathrm{Aire}(X)}$$

En fait, ceci est aussi vrai lorsque le tore possède un twist non nul : si le twist est rationnel, on peut continuer à traverser le cylindre jusqu'à ce que la courbe se referme ; et si le twist est irrationnel, on peut continuer à faire des traversées du cylindre jusqu'à ce que la courbe devienne très proche de se refermer (de sorte qu'on peut la refermer avec une toute petite longueur). On obtient alors une suite β_n de courbes fermées (en refermant la courbe après n tours) telle que :

$$\frac{\mathrm{Int}(\alpha,\beta_n)}{l(\alpha)l(\beta_n)} \xrightarrow[n\to\infty]{} \frac{1}{\mathrm{Aire}(tore)}.$$

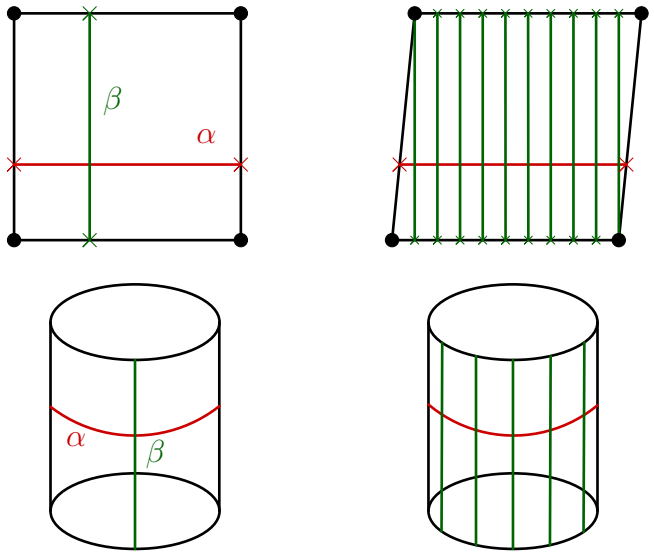

FIGURE 1.5 – Exemples de paires de courbes maximisant le rapport d'intersection divisé par le produit des longueurs dans le cas d'un tore carré (à gauche) et d'un tore avec twist rationnel (à droite).

Pour ce choix de α, il est clair qu'on ne peut pas obtenir de plus grands rapports. En fait, on peut montrer que c'est le meilleur rapport que l'on puisse obtenir, quelles que soient les courbes α et β choisies. Une personne familière avec la géométrie des tores plats pourrait remarquer qu'il suffit, étant donné une géodésique α, de découper le tore le long de α pour obtenir un cylindre plat, ce qui nous permet d'appliquer le même argument. Ceci nous permet de conclure que

$$\mathrm{KVol}(X) = 1.$$

Ce résultat n'a rien d'anodin, car dans le cas des tores plats la norme stable coïncide avec la norme L^2 (à normalisation près). En fait, c'est le seul cas où cela arrive :

Théorème 1.1.3 ([MM14]). *Soit X une surface compacte, orientable, sans bord de genre $g \geq 1$ et muni d'une métrique riemannienne. Alors*

$$KVol(X) \geq 1$$

avec égalité si et seulement si X est un tore et la métrique est plate.

On peut remarquer que l'inégalité sur KVol découle directement du Théorème 1.1.1. L'apport du Théorème 1.1.3 est de dire que la norme stable et la norme L^2 coïncident si et seulement si la surface est un tore plat. Ce résultat découle du fait que les formes harmoniques sont de norme constante uniquement dans le cas d'un tore plat, voir [BK04].

1.1.3 Quelques questions

Les paragraphes précédents, et notamment l'exemple du tore plat, suscitent un certain nombre de questions. En particulier, on peut se demander :

Question 1.1.4. Peut-on calculer explicitement KVol pour d'autres familles de surfaces ?

En général, le supremum dans la définition de KVol rend le calcul explicite difficile, car on pourrait imaginer que le supremum n'est pas un maximum, c'est-à-dire que les paires de courbes qui permettent de s'approcher de KVol sont des courbes de plus en plus longues mais qui s'intersectent beaucoup.

En fait, l'argument esquissé dans l'exemple du tore plat permet de calculer KVol sur certaines surfaces, à savoir des surfaces de translation ayant un modèle en escalier particulièrement symétrique. Les surfaces de translation sont des surfaces plates à singularités coniques, elles seront définies à la section suivante. Nous verrons que la géométrie des surfaces de translation ressemble à celle des tores plats avec notamment une notion de *décomposition en cylindres*. C'est cette question du calcul explicite de KVol qui a orienté les travaux de S. Cheboui, A. Kessi et D. Massart dans [CKM21a] et [CKM21b], ainsi que le travail de cette thèse dans les Chapitres 2, 3, 4 et 5. En particulier, nous présentons une méthode qui permet de calculer KVol sur une famille de surfaces de translation construite à partir de polygones semi-réguliers, les *surfaces de Bouw-Möller* (à une singularité). On verra également comment étendre le calcul de KVol à des déformations des surfaces de Bouw-Möller en utilisant leurs symétries.

Une autre question intéressante est la suivante :

Question 1.1.5. À quelle(s) condition(s) le supremum dans la définition de KVol est-il un maximum ?

En d'autres termes, on peut se demander quels sont les cas où KVol est plutôt réalisé par des paires de courbes relativement courtes s'intersectant peu ou bien par des paires de courbes avec l'une au moins dont la longueur tend vers l'infini mais qui s'intersectent beaucoup de fois. Dans le cas d'un tore plat, on a vu que KVol est réalisé par une paire de courbes explicite lorsque le twist est rationnel, alors que le supremum n'est pas un maximum lorsque le twist est irrationnel. Dans le cas d'une surface de plus grand genre, on s'attend à ce que ce phénomène ne se produise plus, car une géodésique longue traversant un cylindre aura tendance à sortir du cylindre et à aller se promener dans d'autres parties de la surface, perdant

beaucoup de longueur sans gagner d'intersection. C'est notamment le cas pour les surfaces dites *de Veech*, pour lesquelles un feuilletage dans une direction non-périodique est toujours uniquement ergodique. En particulier, KVol est toujours un maximum pour une surface de Veech de genre au moins deux. On verra par exemple que pour les surfaces de Bouw-Möller à une singularité, KVol est toujours réalisé par une paire de systoles qui s'intersectent une fois.

De manière générale, on peut chercher à comparer KVol et le *volume systolique* défini par :

$$\mathrm{Volsys}(X) = \mathrm{Vol}(X) \cdot \sup_{\alpha} \frac{1}{l(\alpha)^2}$$

le supremum portant sur toutes les courbes fermées et homologiquement non-triviales. Une courbe α maximisant le supremum est appelée une systole (homologique) et on note $\mathrm{sys}(X)$ la longueur d'une telle systole. Un premier élément de réponse à cette question est donné par D. Massart et B. Muetzel, qui démontrent dans [MM14] le résultat suivant :

Théorème 1.1.6. *Étant donné une surface fermée de genre $g \geq 1$ munie d'une métrique riemannienne, on a*

$$\frac{Vol(X)}{2\mathrm{sys}(X)\mathrm{diam}(X)} \leq KVol(X) \leq 9 \cdot \mathrm{Volsys}(X). \tag{1.1}$$

où $\mathrm{diam}(X)$ *désigne le diamètre de* X*.*

Ce résultat, très général et dont la démonstration est élémentaire, n'a pas de raison d'être optimal. Cependant, c'est un résultat intéressant car le volume systolique a été largement étudié (voir, entre autres, [Gro83], [Kap00], [Sch93], [BS94], [BPS12], [Bal]) Par exemple, deux systoles sur une surface hyperbolique fermée ne s'intersectent qu'une seule fois (voir [FP15]). Le résultat est le même sur une surface de translation à une singularité, en utilisant les propriétés de la décomposition Delaunay (voir [BG21]).

Dans le cas des surfaces hyperboliques (à courbure constante -1), Massart et Muetzel démontrent :

Théorème 1.1.7 ([MM14])**.** *Il existe des constantes $A(g), B(g) > 0$ dépendant uniquement du genre g de la surface X, et telle que, dès que* $\mathrm{sys}(X)$ *est suffisamment petit, on a :*

$$\frac{A(g) \cdot Vol(X)}{\mathrm{sys}(X)|\log(\mathrm{sys}(X))|} \leq KVol(X) \leq \frac{B(g) \cdot Vol(X)}{\mathrm{sys}(X)|\log(\mathrm{sys}(X))|}$$

Ce résultat peut être vu comme un résultat "asymptotique" pour KVol lorsque la surface X s'approche du bord de l'espace de modules des surfaces hyperboliques. Il est à noter qu'un résultat similaire a été récemment obtenu dans le cas de l'intersection géométrique, voir [Tor23]. Par ailleurs, même si plusieurs problèmes faisant intervenir l'intersection (notamment géométrique) ont été étudiés dans le cas des surfaces hyperboliques (avec par exemple [Mir08], [Lal14] et [Cha21] autour de questions de comptage de géodésiques sous contrainte d'auto-intersection – géométrique donc –), on ne sait pas grand chose de plus pour KVol sur les surfaces hyperboliques. Il est notamment difficile de calculer précisément KVol sur une

surface hyperbolique donnée.

Dans la suite, nous nous intéresserons plutôt au cas des surfaces de translation. On peut alors se demander s'il est possible d'améliorer la constante dans la borne supérieure de l'équation 1.1 pour les surfaces de translation. Nous verrons notamment comment obtenir un résultat de comparaison dans le cas de surfaces construites à partir de polygones convexes à angles obtus.

Pour terminer, remarquons qu'il est facile de faire tendre KVol vers l'infini en pinçant une courbe non-séparante mais en gardant le diamètre et le volume borné (voir Équation 1.1), mais que, comme indiqué dans l'énoncé du Théorème 1.1.3, KVol ne peut pas être arbitrairement petit. En particulier, le Théorème 1.1.3 donne une borne générale sur KVol atteinte uniquement en genre un, et il est naturel de se demander si l'on peut améliorer cette borne si l'on se restreint aux surfaces de genre $g \geq 2$. Plus précisément :

Question 1.1.8.

$$\text{Que vaut } \mathcal{K}(g) := \inf_{X \text{ de genre } g} \mathrm{KVol}(X) \,?$$

L'infimum est-il réalisé ? Si oui, quelles sont les propriétés des surfaces qui réalisent l'égalité ?

Autrement dit, existe-t-il une obstruction topologique qui empêche KVol de se rapprocher de 1 pour des surfaces de genre plus grand ? Pour cette question, nous supposerons que la métrique est riemannienne avec éventuellement des singularités isolées. Une intuition naïve est que pour une surface de genre g, la meilleur rapport *Intersection/produit des longueurs* est atteint lorsque l'une des courbes tourne autour de la plus petite anse, et l'autre tourne autour de cette anse une fois dans le sens transverse par le plus court chemin. Pour diminuer KVol il faudrait alors avoir une surface particulièrement symétrique et on aurait $\mathrm{KVol}(X) \geq g$ pour n'importe quelle surface de genre g. Toutefois, cette idée n'est pas suffisamment précise, car, d'une part les cylindres ne sont pas toujours plats en général et donc le rapport *Intersection/produit des longueurs* n'est pas forcément égal à l'aire du cylindre pour une configuration comme dans le cas du tore, et d'autre part la présence de singularités modifie la géométrie de la surface. Par exemple, P. Buser et P. Sarnak dans [BS94] ont exhibé une famille de surfaces hyperboliques $(X_g)_{g\in\mathbb{N}^*}$ (une surface pour chaque genre g) telle qu'il existe $C > 0$ avec :

$$\mathrm{VolSys}(X_g) \leq C \cdot \frac{g}{\log(g)^2}.$$

En particulier, le Théorème 1.1.6 implique que :

$$\mathrm{KVol}(X_g) \leq C' \cdot \frac{g}{\log(g)^2}$$

et en particulier :

$$\mathcal{K}(g) \leq C' \cdot \frac{g}{\log(g)^2}.$$

Concernant la borne inférieure, le Théorème 3.12 de [BKP18] permet de démontrer que :

Théorème 1.1.9. *Il existe une constante $c > 0$ telle que pour tout $g \geq 2$ et toute surface hyperbolique X de genre g, on a :*

$$KVol(X) \geq c\frac{g}{\log(g)^2}$$

Notons qu'un résultat similaire est valable pour l'intersection géométrique (voir [Tor23]), et on peut obtenir la borne inférieure en démontrant que sur une surface hyperbolique on peut toujours trouver une courbe α en forme de huit de longueur au plus $c' \log(g)$. Il serait intéressant de savoir si cette croissance en $\frac{g}{(\log(g)^2}$ est toujours valable pour les surfaces à courbure négative (ou nulle) variable.

Une autre direction pour aborder cette question est de s'intéresser aux surfaces plates. En effet, on s'attend à ce que l'infimum de KVol sur l'ensemble des surfaces ayant une métrique Riemanienne à courbure négative ou nulle et avec (éventuellemnt) des singularités coniques soit réalisé en particulier pour des surfaces plates par morceaux à singularités coniques, car on peut concentrer la courbure en des singularités coniques tout en faisant diminuer KVol, voir [KS21, Proposition 3.1] dans le cas où l'on considère la systole plutôt que KVol. Notons toutefois que le procédé de concentration de la courbure en des singularités de [KS21, Proposition 3.1] fait apparaître *beaucoup* de singularités, et il y a très peu de chances d'obtenir des surfaces de translation, qui ont peu de singularités coniques et dont les angles sont des multiples de 2π.

En particulier, il est possible que l'asymptotique en $\frac{g}{\log(g)^2}$ ne soit pas atteinte pour des surfaces de translation, notamment celles ayant peu de singularités en comparaison du genre. Dans [Bou23b] (Chapitre 6), nous étudions le cas spécifique des surfaces de translation à une seule singularité, en donnant des exemples de familles de surfaces dont l'asymptotique de KVol est en g. La méthode de construction de ces surfaces généralise une construction de Cheboui, Kessi et Massart faite en genre deux, voir [CKM21b]. De plus, nous conjecturons que cette asymptotique en g est en fait optimale, et plus précisément :

Conjecture 1.1.10. *Pour toute surface de translation X de genre g à une seule singularité, on a :*

$$KVol(X) > g.$$

1.2 Surfaces de translation

Avant de poursuivre, nous définissons les surfaces de translation et en donnons quelques propriétés. Cela nous permettra d'énoncer précisément les résultats obtenus au cours de la thèse dans la section suivante. Cette section constitue un survol informel autour de la notion de surface de translation : nous nous contentons de donner les définitions qui nous seront utiles ainsi que quelques idées géométriques. Pour plus de détails, il existe de nombreux survols, notamment [Mas00], [HS06], [Mas22], [Wri16] ou encore [Zor06].

1.2.1 Définition et motivations

Une surface de translation est une surface topologique X de genre g muni d'un atlas de cartes défini en dehors d'un ensemble fini de singularités Σ, et telle que les applications de changement de cartes sont des translations du plan. On munit également la surface d'une direction privilégiée, bien définie grâce à la structure de translation. Une telle structure est assez spécifique car, puisque les translations préservent la métrique euclidienne de $\mathbb{R}^2$, la surface hérite automatiquement de la métrique euclidienne de $\mathbb{R}^2$. En particulier, on peut mesurer la longueur des courbes et définir des géodésiques, qui sont alors des lignes droites par morceaux, changeant éventuellement de direction en passant par une singularité. De plus, les singularités (éléments de Σ) sont des singularités coniques d'angle multiple de 2π.

Une autre manière d'appréhender ces surfaces est de les voir comme les surfaces obtenues à partir d'un ensemble de polygones tel que chaque côté est apparié avec un autre côté, parallèle et de même longueur. Par exemple, le tore obtenu à partir d'un carré adont on a recollé les côtés opposés est une surface de translation, et n'a pas de singularités. Nous présentons d'autres exemples classiques de surfaces de translation dans le prochain paragraphe. Il est à noter que les singularités sont forcément des sommets des polygones car on peut définir une carte locale autour de chaque point à l'intérieur d'un polygone ou à l'intérieur d'une arête (le voisinage étant dans ce dernier cas obtenu comme le recollement de deux demi-disques). Comme c'est le cas pour le tore, les sommets ne sont pas forcément tous des singularités sur la surface de translation induite par recollement des arêtes.

Une troisième possibilité équivalente consiste à définir une surface de translation comme une surface de Riemann munie d'une 1-forme holomorphe ω. On dit que ω est alors une différentielle abélienne et ses zéros correspondent aux singularités de la surface de translation. De plus, les cartes locales au voisinage de points réguliers peuvent être obtenues en intégrant ω.

Les surfaces de translation interviennent notamment dans le contexte de l'étude des trajectoires sur une table de billard polygonale [1] en utilisant la construction de Katok-Zemlyakov [ZK76] qui consiste à "déplier" le billard pour ramener l'étude des trajectoires à l'étude du flot directionnel sur une surface de translation, et sont étroitement liées à la dynamique des échanges d'intervalles, qui généralisent les rotations sur le cercle. Les surfaces de translation sont à la croisée des chemins entre dynamique, géométrie et théorie des nombres et sont encore largement étudiées aujourd'hui, avec par exemple de récents résultats importants comme [EMM15], [EFW18] or [EMMW20].

1.2.2 Quelques exemples

Commençons par l'exemple d'un polygone en forme de L dont on a identifié les côtés parallèles et de même longueur comme sur la Figure 1.6. Comme on peut le voir, la surface correspondante est de genre deux. De plus, tous les sommets du polygone sont identifiés en un seul point sur la surface correspondante, et on peut voir que tourner autour de la singularité nécessite de parcourir un angle 6π. Notons également que replier la surface permet de

1. avec des angles multiples rationnels de π

calculer l'intersection des courbes A, B, C et D en la singularité.

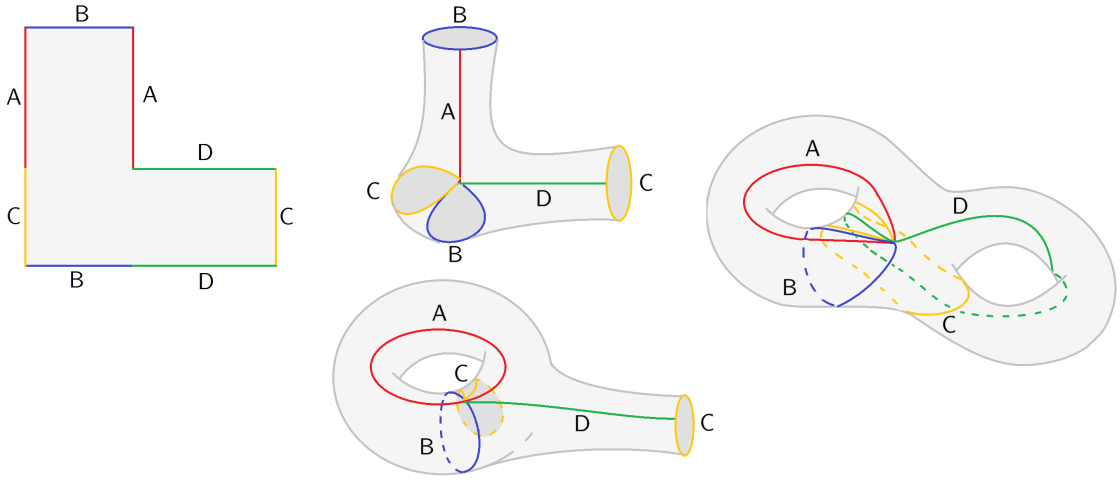

FIGURE 1.6 – Une surface de translation en forme de L de genre deux.

Le n-gone régulier. Un autre exemple de surface de translation est donné par les polygones réguliers ayant un nombre pair de côtés. On recolle alors deux à deux les côtés parallèles. Pour l'octogone, la surface obtenue est de genre deux et n'a qu'une seule singularité d'angle 6π tandis que pour le décagone la surface possède deux singularités distinctes, chacune d'angle 4π (la surface est encore de genre deux). Plus généralement :

— Si $n = 4m$, la surface de translation obtenue à partir d'un n-gone régulier est de genre m avec une seule singularité d'angle $(4m-2)\pi$.

— Si $n = 4m+2$ la surface obtenue est aussi de genre m mais possède deux singularités, chacune d'angle $2m\pi$.

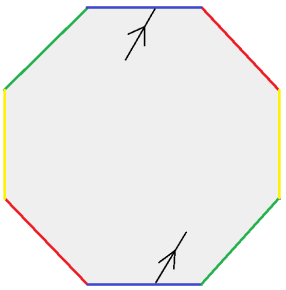

FIGURE 1.7 – L'octogone dont on a identifié les côtés parallèles est une surface de translation de genre 2 avec une singularité d'angle 6π.

De manière générale, on peut appliquer la formule de Riemann-Roch pour obtenir une relation entre le genre et la somme des ordres des singularités : pour une surface de translation

de genre g ayant N singularités coniques d'angles respectifs $2(k_i+1)\pi$, $1 \leq i \leq N$, on a :

$$\sum_i k_i = 2g-2.$$

L'entier k_i est appelé *l'ordre de la singularité* i. Notons qu'il est parfois utile de rajouter des singularités factices dans l'ensemble Σ, on parle alors de singularité d'ordre zéro. C'est typiquement le cas pour les tores plats où l'on peut rajouter une singularité factice qui fait office de "point de référence" pour construire des courbes fermées.

Le double n-gone. Lorsqu'on part d'un polygone régulier ayant un nombre impair de côtés, une manière de construire une surface de translation est d'utiliser deux copies du polygone dont l'une est une copie miroir de l'autre. On recolle ensuite les côtés parallèles deux à deux, comme sur la Figure 1.8. On obtient alors une surface appelée *double n-gone* (régulier), de genre $m := \frac{n-1}{2}$ et avec une seule singularité conique d'angle $(2n-4)\pi = (4m-2)\pi$. Cette famille de surfaces, construite par Veech [Vee89], constitue avec les n-gones réguliers (n pair) les premiers exemples de ce qui s'appelle maintenant les surfaces de Veech et qui possèdent notamment des propriétés dynamiques intéressantes.

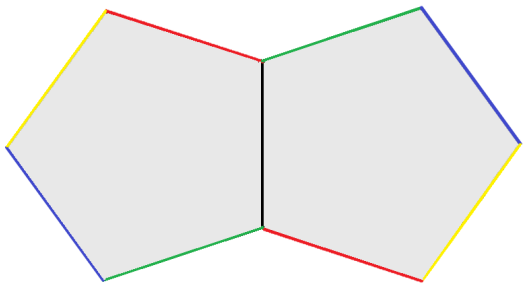

FIGURE 1.8 – Le double pentagone.

Surfaces de Bouw-Möller. La famille des doubles n-gones réguliers ($n \geq 3$ impair) fait partie d'une famille de surfaces plus générale, les *surfaces de Bouw-Möller* [BM10], [Hoo12], [DPU19]. Étant donné deux entiers $m, n \geq 2$ avec $mn \geq 6$, on associe une surface de Bouw-Möller $S_{m,n}$ construite à partir de m polygones semi-réguliers ayant n ou $2n$ côtés [Hoo12], et ayant $pgcd(m,n)$ singularités. Le double n-gone (n impair) correspond à la surface $S_{2,n}$ et les surfaces $S_{3,4}$ et $S_{4,3}$ sont représentées Figure 1.9. Ces surfaces ont la particularité d'avoir un grand groupe de symétrie : comme on va le voir, les surfaces de Bouw-Möller sont exactement les surfaces de translation dont le groupe de Veech est un groupe triangulaire [BM10].

1.2.3 L'espace de modules des surfaces de translation

L'ensemble de toutes les surfaces de translation peut être muni d'une structure géométrique. Pour cela, commençons par dire que deux surfaces de translation obtenues à partir de polygones sont équivalentes si l'une peut être obtenue à partir de l'autre en découpant les

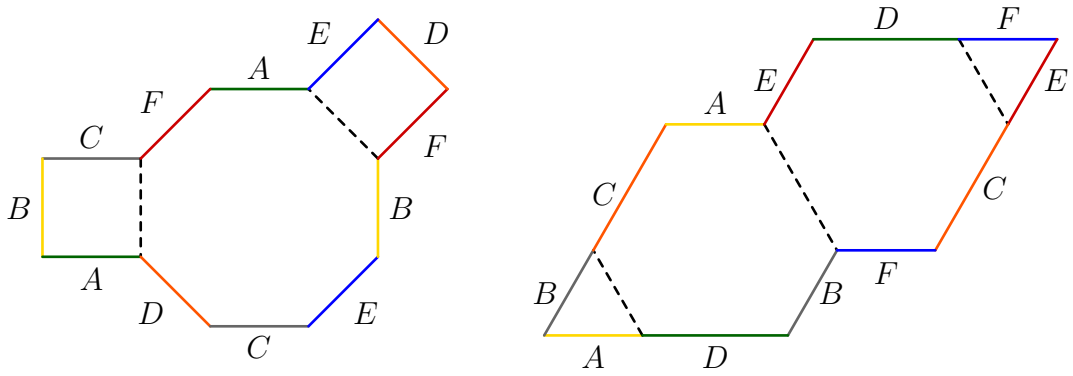

FIGURE 1.9 – Les surfaces de Bouw-Möller $S_{3,4}$ et $S_{4,3}$.

polygones qui la composent et en recollant certaines arêtes pour obtenir une nouvelle famille de polygones. On définit alors l'espace de modules des surfaces de genre g comme :

$$\mathcal{H}_g = \{\text{Surface de translation de genre } g\}/ \text{ découpage-collage}$$

Ce dernier espace est une variété différentielle : on peut déformer une surface de translation définie à partir de polygones en modifiant légèrement les polygones qui la définissent, tout en gardant la contrainte de parallélisme et la contrainte sur les longueurs. Un choix de vecteurs paramétrant les polygones fournit des coordonnées locales sur $\mathcal{H}_g$, on parle de *coordonnées des périodes*, voir par exemple [Wri16]. De la sorte, le genre reste fixe mais aussi le nombre de singularités et l'espace des surfaces de translation est naturellement stratifié : étant donnés des entiers strictement positifs g et $k_1, \dots, k_N$ vérifiant

$$\sum_i k_i = 2g - 2$$

on définit l'espace de modules $\mathcal{H}(k_1, \dots, k_N)$ des surfaces de translation ayant N singularités d'ordres respectifs $k_1, \dots, k_N$, et on a

$$\mathcal{H}_g = \sqcup \mathcal{H}(k_1, \dots, k_N).$$

Cette définition informelle ne doit rien au hasard et provient de la définition de l'espace de modules des surfaces de Riemann $\mathcal{M}_g$, défini pour $g \geq 1$ comme l'ensemble des surfaces de Riemann à biholomorphisme près. En voyant une surface de translation comme une surface de Riemann munie d'une 1-forme holomorphe, deux surfaces de translation (X_1, ω_1) et (X_2, ω_2) sont équivalentes si et seulement si il existe un biholomorphisme f de $X_1 \backslash \{\text{singularités de } X_1\}$ vers $X_2 \backslash \{\text{singularités de } X_2\}$ et telle que $f^*\omega_2 = \omega_1$. L'espace de modules des surfaces de translation $\mathcal{H}_g$ est donc un fibré au-dessus de $\mathcal{M}_g$. De plus, les coordonnées locales sont données en intégrant la 1-forme sur une base de l'homologie (relative aux singularités).

M. Kontsevich et A. Zorich [KZ03] ont classifié les composantes connexes de chaque strate $\mathcal{H}(k_1, \cdots, k_n)$. Un cas qui nous intéressera tout particulièrement est le cas de $\mathcal{H}(2g-2)$ qui possède trois composantes connexes lorsque $g \geq 4$: une composante *hyperelliptique* et deux

autres composantes distinguées par *l'invariant de Arf* qui correspond aussi à la parité de la structure spin associée à la surface de translation. Notons enfin que $\mathcal{H}(2)$ est connexe (toutes les surfaces de translation de $\mathcal{H}(2)$ sont hyperelliptiques) et $\mathcal{H}(4)$ possède deux composantes connexes, l'une hyperelliptique et l'autre composée des surfaces de translation ayant une structure spin impaire.

1.2.4 Action de $SL_2(\mathbb{R})$ et groupe de Veech

L'interprétation d'une surface de translation comme ensemble de polygones ayant des côtés parallèles identifiés permet de voir que l'espace des surfaces de translation est muni d'une action de $GL_2^+(\mathbb{R})$, provenant de l'action linéaire de $GL_2^+(\mathbb{R})$ sur $\mathbb{R}^2$. Étant donné un ensemble de polygones du plan euclidien ayant des côtés parallèles et de même longueur identifiés deux à deux, l'action de $GL_2^+(\mathbb{R})$ préserve l'égalité des longueurs et le parallélisme mais aussi l'orientation. Ainsi, l'action d'une matrice produit une nouvelle surface de translation. Sur l'atlas de cartes, cela correspond à post-composer chaque carte par l'action induite sur $\mathbb{R}^2$ par la matrice $A \in GL_2(\mathbb{R})$. Deux surfaces de translation sont dites *affinement équivalentes* si elles sont dans la même orbite.

Dans la suite, on considérera également l'action restreinte à $SL_2(\mathbb{R})$, car elle a l'avantage de préserver l'aire de la surface. Enfin, deux sous-groupes à un paramètre méritent d'être distingués : le sous-groupe $\{g_t = \begin{pmatrix} e^t & 0 \\ 0 & e^{-t} \end{pmatrix}, t \in \mathbb{R}\}$ induit le *flot géodésique de Teichmüller*, et $\{h_s = \begin{pmatrix} 1 & s \\ 0 & 1 \end{pmatrix}, s \in \mathbb{R}\}$ induit le *flot horocyclique de Teichmüller*.

Groupe de Veech. Comme on l'a vu dans le paragraphe précédent, une surface de translation dans l'espace de modules peut avoir plusieurs représentations sous forme d'une collection de polygones dont les côtés sont identifiés, de sorte que le stabilisateur (sous l'action de $SL_2(\mathbb{R})$) d'une surface de translation X donnée est parfois non trivial. Le stabilisateur de la surface X sous l'action de $SL_2(\mathbb{R})$ est appelé le *groupe de Veech* de X, et sera noté $SL(X)$. Par exemple :

- La matrice $\begin{pmatrix} 1 & 1 \\ 0 & 1 \end{pmatrix}$ appartient au groupe de Veech du tore carré, voir Figure 1.10.
- La matrice $\begin{pmatrix} \cos(\frac{2\pi}{5}) & \sin(\frac{2\pi}{5}) \\ \sin(\frac{2\pi}{5}) & \cos(\frac{2\pi}{5}) \end{pmatrix}$, correspondant à la rotation d'angle $\frac{2\pi}{5}$, appartient au groupe de Veech du double pentagone.

Il est à noter que l'action d'un élément du groupe de Veech induit un *difféomorphisme affine* de la surface [2], c'est-à-dire un difféomorphisme qui s'exprime de manière affine dans les cartes (la partie linéaire correspondant à la matrice du groupe de Veech en question).

Une matrice stabilisant une surface de translation devant préserver l'aire, on a $SL(X) \subset SL_2(\mathbb{R})$. En fait, Veech a montré que le groupe de Veech $SL(X)$ d'une surface de translation X est un sous-groupe discret de $SL_2(\mathbb{R})$, autrement dit un groupe Fuchsien, voir

2. et parfois plusieurs lorsqu'il y a plusieurs moyens de découper et recoller la surface pour revenir à la surface initiale.

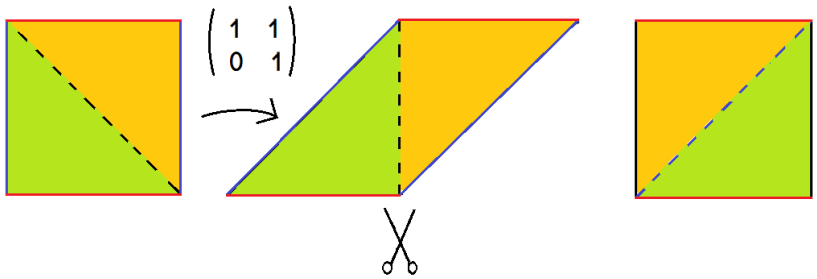

FIGURE 1.10 – L'action de la matrice $\begin{pmatrix} 1 & 1 \\ 0 & 1 \end{pmatrix}$ sur le tore carré induit un difféomorphisme affine du tore.

[Vee89]. Par exemple, le groupe de Veech du tore carré est $SL_2(\mathbb{Z})$ et le groupe de Veech du double n-gone est conjugué au groupe de Hecke d'ordre n défini pour $n \geq 3$ par $H_n := < \begin{pmatrix} 1 & \Phi_n \\ 0 & 1 \end{pmatrix}, \begin{pmatrix} 0 & 1 \\ -1 & 0 \end{pmatrix} >$, avec $\Phi_n = 2\cos(\frac{\pi}{n})$, voir [Vee89], [Mon05]. Remarquons que $H_3 = SL_2(\mathbb{Z})$ est le groupe de Veech d'un tore (construit à partir de deux triangles).

Disque de Teichmüller. Avec cette définition du groupe de Veech, l'orbite d'une surface de translation sous l'action de $SL_2(\mathbb{R})$ s'identifie à $SL(X)\backslash SL_2(\mathbb{R})$. En quotientant à droite par l'action de $SO(2)$, c'est-à-dire en oubliant la direction privilégiée, on obtient le *disque de Teichmüller* de la surface X, identifié à $SL(X)\backslash\mathbb{H}^2$ et qui est alors une surface hyperbolique (avec de possibles points coniques). Une classe particulièrement intéressante de surfaces de translation est celle des surfaces dont le groupe de Veech est un réseau dans $SL_2(\mathbb{R})$, c'est-à-dire que le disque de Teichmüller correspondant est de volume fini. Le disque de Teichmüller se projette alors en une courbe complexe fermée dans $\mathcal{M}_g$. De telles surfaces sont appelées des *surfaces de Veech* et, comme on va le voir, ont des propriétés dynamiques intéressantes. Par exemple, le double n-gone est une surface de Veech et son disque de Teichmüller s'identifie au quotient de $\mathbb{H}^2$ par le groupe de Hecke H_n, voir Figure 1.11. Plus généralement, le disque de Teichmüller de la surface de Bouw-Möller $S_{m,n}$ s'identifie au quotient de $\mathbb{H}^2$ par un groupe triangulaire $\Delta(m, n, \infty)$ et on peut représenter un domaine fondamental de $S_{m,n}$ comme sur la Figure 1.12. On peut remarquer que $S_{m,n}$ et $S_{n,m}$ sont dans le même disque de Teichmüller (à normalisation près), voir [Hoo12]. Enfin, lorsque n est pair le n-gone régulier est également une surface de Veech, dont nous avons représenté un domaine fondamental en Figure 1.13. Notons que ces familles de surfaces sont les seules familles connues de surfaces de Veech *primitives* en grand genre. Nous reviendrons plus en détail sur la question de la classification des surfaces de Veech primitives en 1.5.

1.2.5 Connexions de selles et décomposition en cylindres

On a vu qu'une surface de translation est munie d'une métrique plate, héritée de la structure euclidienne de $\mathbb{R}^2$, et que, en particulier, les géodésiques sont des lignes droites (par morceaux). Le seul moyen pour une géodésique de changer de direction est de passer par une singularité. On définit alors une *séparatrice* comme un segment géodésique qui part

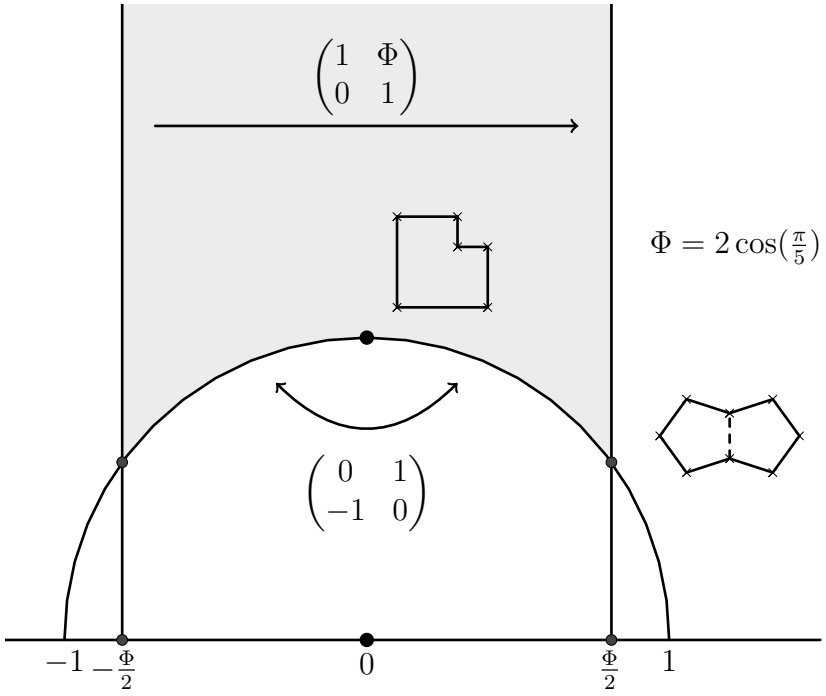

FIGURE 1.11 – Un domaine fondamental pour le disque de Teichmüller du double pentagone. Le double pentagone correspond aux deux coins identifiés tandis que le point d'affixe i correspond à une surface en L appelée le L d'or.

d'une singularité, et une *connexion de selles* comme un segment géodésique qui va d'une singularité à une autre (et donc *connecte* les singularités). Concrètement, sur une surface donnée par un ensemble de polygones, une connexion de selles est une trajectoire géodésique entre deux sommets qui représentent une singularité. La trajectoire géodésique est constituée de segments dans la même direction, identifiés entre eux via les recollements des côtés des polygones. En mettant bout à bout ces segments on obtient un vecteur de $\mathbb{R}^2$ appelé *vecteur d'holonomie* associé à la connexion de selles.

Une spécificité des surfaces de translation est que toute géodésique fermée est homologue à une union de connexions de selles[3]. Plus précisément, au voisinage de chaque géodésique fermée qui n'est pas une union de connexion de selles, on a un *cylindre* de géodésiques fermées dans la même direction, comme sur la Figure 1.14. On peut alors étendre le cylindre en un cylindre maximal qui est bordé de connexions de selles, de sorte que la géodésique fermée initiale est homologue à l'union des connexions de selles bordant le cylindre.

Un cas qui nous intéresse particulièrement est celui où toutes les géodésiques dans une direction sont des géodésiques fermées. La surface est alors *décomposable en cylindres* dans la direction correspondante, comme sur la Figure 1.15. D'après un résultat de Veech, c'est notamment le cas pour une surface de Veech dans n'importe quelle direction qui possède une géodésique périodique. Plus précisément, on a le résultat suivant, connu sous le nom

3. Mis à part le cas du genre un où il n'y a pas de singularités, donc pas de connexions de selles, auquel cas on peut *marquer un point* en le considérant comme une singularité factice, d'ordre zéro.

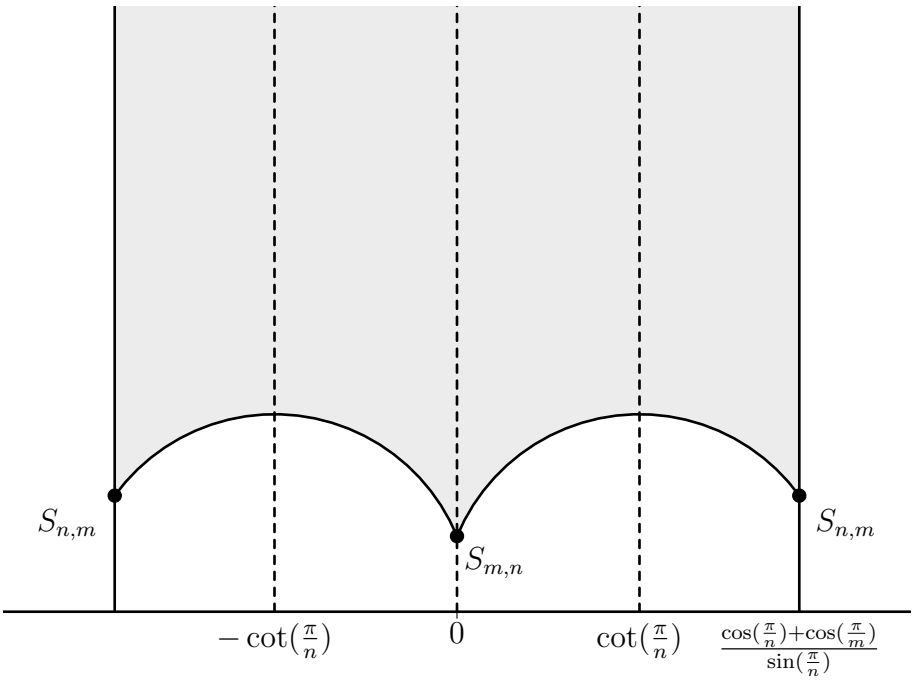

FIGURE 1.12 – Un domaine fondamental du disque de Teichmüller de $S_{m,n}$.

d'alternative de Veech :

Théorème 1.2.1 ([Vee89]). *Soit X une surface de Veech. Pour toute direction $\theta \in \mathbb{S}^1$ le flot dans la direction θ sur la surface X est ou bien périodique ou bien uniquement ergodique. De plus, dans le premier cas, la surface est décomposable en cylindres et les modules*[4] *des cylindres sont commensurables.*

En particulier, les surfaces de Veech sont particulièrement adaptées pour le calcul de KVol, car on peut espérer adapter l'argument utilisé pour calculer KVol sur le tore.

Une autre propriété qui mérite d'être mentionnée est le fait que les directions périodiques d'une surface de Veech sont encodées dans le groupe de Veech. Plus précisément, on a :

Théorème 1.2.2 ([Vee89], voir aussi [HS06]). *Les directions périodiques sont exactement les directions propres des matrices paraboliques du groupe de Veech.*

En particulier, les classes de conjugaison d'éléments paraboliques du groupe de Veech correspondent exactement aux combinatoires possibles des décompositions en cylindres. Cela permet de déduire qu'une surface de Veech possède un nombre fini de décompositions en cylindres à l'action du groupe de Veech près. Plus précisément, les classes d'équivalences de décomposition en cylindres sont en bijection avec les cusps du disque de Teichmüller associé à la surface de Veech.

4. Le module d'un cylindre est le rapport *hauteur/longueur*.

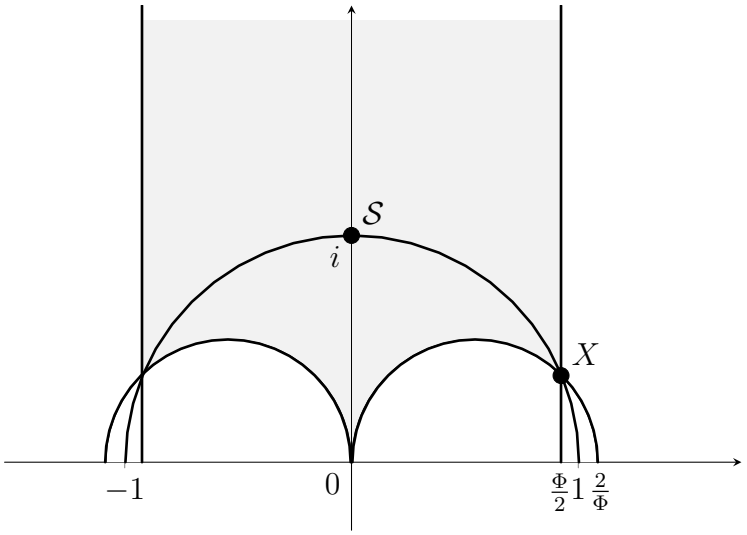

FIGURE 1.13 – Un domaine fondamental pour le disque de Teichmüller du n-gone régulier, n pair.

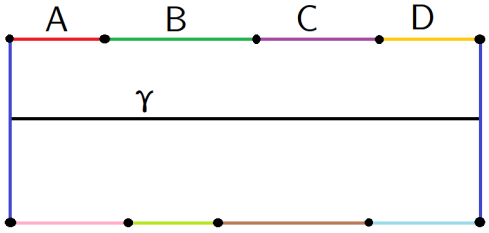

FIGURE 1.14 – Un cylindre maximal autour de la géodésique fermée γ. La géodésique γ est homologue à l'union des connexions de selles $A \cup B \cup C \cup D$.

Une question intéressante est celle de caractériser algébriquement les directions périodiques. Kenyon et Smillie [KS00] ont démontré que pour une surface de Veech convenablement normalisée, les pentes des directions périodiques appartiennent à une extension algébrique de $\mathbb{Q}$, le *corps de trace*. Le corps de trace est le corps engendré par les traces des éléments du groupe de Veech (de la surface normalisée). Il coïncide avec le *corps d'holonomie* engendré par coordonnées des vecteurs holonomie des connexions de selles de la surface normalisée, et est une extension algébrique sur $\mathbb{Q}$ de degré au plus le genre de la surface.

Lorsque le corps de trace est $\mathbb{Q}$ ou une extension quadratique de $\mathbb{Q}$, les directions périodiques sont exactement celles dont les pentes appartiennent au corps de trace (voir [McM05b] ou [Bos88]), mais l'inclusion peut être stricte lorsque le corps de trace est de degré au moins 3 sur $\mathbb{Q}$, voir [AS09]. En particulier, dans le cas spécifique du double n-gone la question de caractériser algébriquement les directions périodiques est toujours ouverte à partir de $n = 7$. Nous reviendrons sur cette question en 1.4.

Un exemple de décomposition en cylindres : le modèle en escalier du double n-gone. Lorsque n est impair, le double n-gone régulier, grâce à ses propriétés de symé-

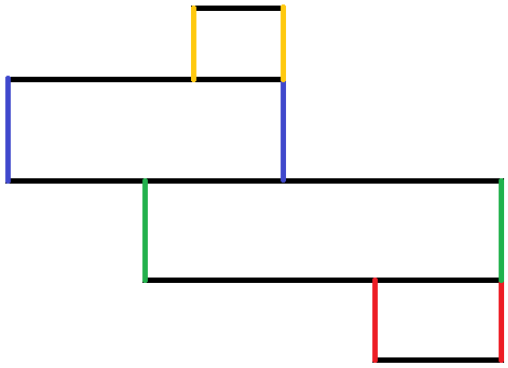

FIGURE 1.15 – Exemple de surface décomposée en cylindres horizontaux.

trie, est affinement équivalent à une surface de translation en escalier comme sur la Figure 1.16. Ce modèle, décrit dans [Vee89] (voir aussi [Mon05] et [Bou]), possède $\frac{n-1}{2}$ cylindres horizontaux et $\frac{n-1}{2}$ cylindres verticaux, qui ont tous le même module égal à $\frac{1}{\Phi_n}$. En fait, à l'action de $SL_2(\mathbb{R})$ près, la décomposition en cylindres dans n'importe quelle direction est exactement celle du modèle en escalier. Notons que pour $n = 5$, le modèle en escalier correspondant au double pentagone est un L dont les proportions sont données par le nombre d'or $\Phi_5 = 2\cos(\pi/5)$: cette surface est parfois appelée le "L d'or".

De manière similaire, lorsque n est pair le n-gone régulier possède un modèle en escalier, mais cette fois les directions horizontales et verticales ne sont pas équivalentes : tous les cylindres horizontaux et verticaux ont le même module égal à $\frac{1}{\Phi_n}$ sauf un cylindre (horizontal ou vertical selon que n est congru à 0 ou 2 modulo 4) qui a un module de $\frac{2}{\Phi_n}$. On peut montrer que, à l'action de $SL_2(\mathbb{R})$ près, toutes les décompositions en cylindres du n-gone régulier sont équivalentes ou bien à la direction horizontale ou bien la verticale (en remarquant par exemple que le disque de Teichmüller du n-gone régulier possède exactement deux cusps).

1.3 KVol sur les surfaces de translation

Dans cette section, nous présentons les résultats de cette thèse ainsi que leur organisation. On commencera par voir plus en détail quelques motivations spécifiques pour l'étude de KVol sur les surfaces de translation ainsi que quelques idées clés déjà présentes dans les travaux de S. Cheboui, A. Kessi et D. Massart, [CKM21a] et [CKM21b].

1.3.1 Introduction et motivations

Comme nous l'avons vu en 1.1.2, bien que la question à l'origine de KVol s'énonce simplement, il est difficile d'y apporter une réponse quantitative précise. La première motivation pour regarder KVol sur les surfaces de translation est alors de trouver des exemples de surfaces sur lesquelles on peut calculer précisément KVol. Le premier avantage est qu'on peut espérer pouvoir s'inspirer de la méthode de calcul de KVol sur le tore plat. Un deuxième avantage est que les géodésiques des surfaces de translation sont des morceaux de lignes

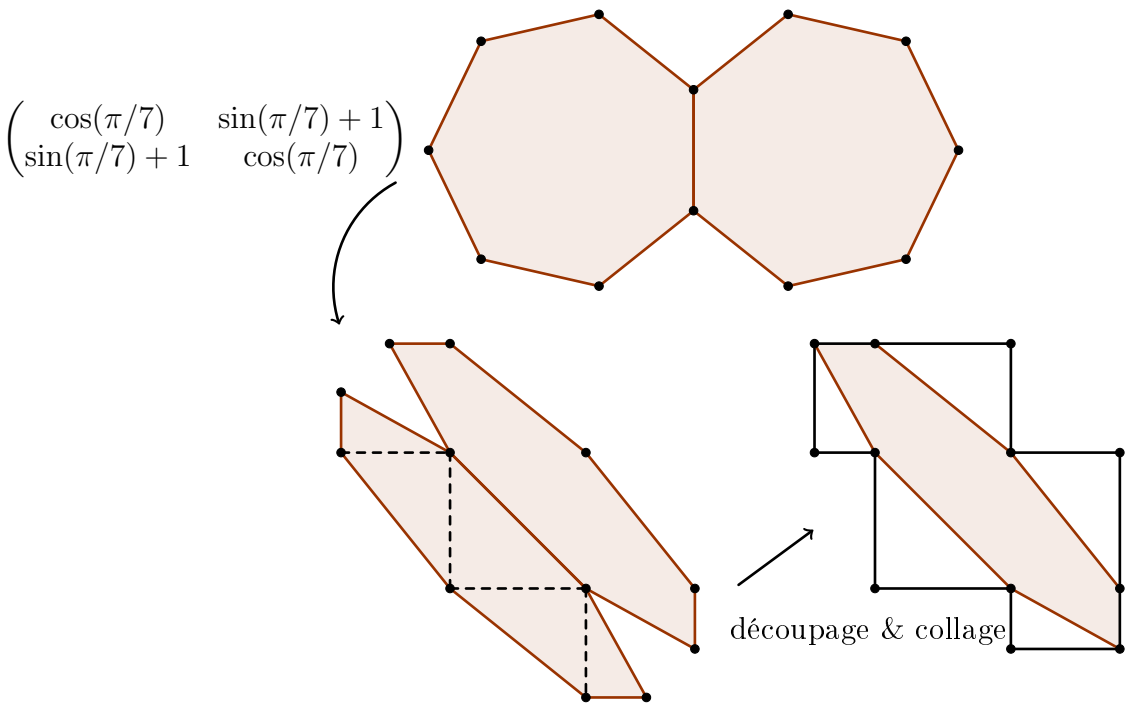

FIGURE 1.16 – Passage du double heptagone à son modèle en escalier.

droites, dont la longueur est facilement calculable. Cela permet par exemple d'obtenir des résultats précis concernant la systole, notamment lorsqu'il n'y a qu'une seule singularité, voir [BG21], [JP19] ou [CHMWS22].

Comme on l'a vu dans la section précédente, toute géodésique fermée sur une surface de translation est homologue à une union de connexions de selles. On peut alors remplacer le supremum dans la définition de KVol par un supremum sur toutes les paires de courbes fermées (α, β) qui s'écrivent comme union de connexions de selles.

Un cas particulièrement adapté est lorsque la surface de translation considérée n'a qu'une seule singularité, de sorte que toutes les connexions de selles sont automatiquement des courbes fermées. On peut alors écrire :

$$\mathrm{KVol}(X) = \mathrm{Vol}(X) \cdot \sup_{\alpha,\beta} \frac{\mathrm{Int}(\alpha,\beta)}{l(\alpha)l(\beta)},$$

le supremum étant cette fois pris uniquement sur les paires de connexions de selles. En particulier, les connexions de selles étant des lignes droites, toutes les intersections ont le même signe hormis une possible intersection en la singularité (que l'on peut calculer en regardant l'ordre cyclique des courbes autour de la singularité, comme nous le verrons au paragraphe suivant).

En fait, tous les exemples connus de calculs explicites de KVol sont des surfaces de translation à une seule singularité. Dès qu'il y a plusieurs singularités, certaines géodésiques fermées

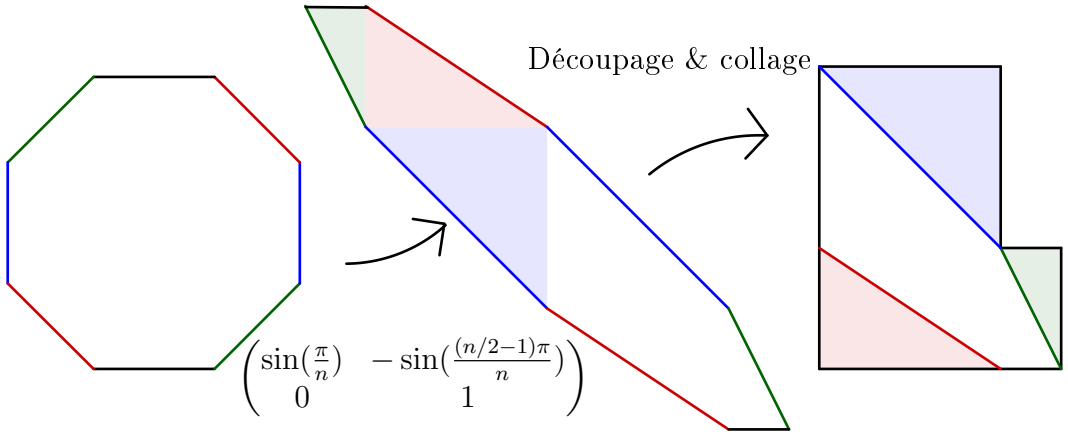

FIGURE 1.17 – Passage de l'octogone régulier à son modèle en escalier.

simples peuvent être des unions de connexions de selles dans des directions différentes, et cela suffit à rendre le calcul bien plus difficile.

L'étude de KVol sur les surfaces de translation a été initiée par S. Cheboui, A. Kessi et D. Massart [CKM21a] et [CKM21b]. Pour étendre la méthode de calcul de KVol sur le tore, il faut non pas chercher à calculer KVol sur une surface particulière, mais plutôt sur tout un disque de Teichmüller d'une surface de Veech en utilisant le fait qu'une surface de Veech est décomposable en cylindres dans n'importe quelle direction périodique. Dans la section suivante, nous présentons brièvement les idées qui ont permis à S.Cheboui, A.Kessi et D.Massart de calculer KVol sur le disque de Teichmüller de certaines surfaces à petits carreaux. Une question naturelle est alors de se demander si l'on peut étendre la méthode pour le calcul de KVol sur d'autres surfaces.

Dans les Chapitres 2, 3 et 5, nous explorons le cas de surfaces construites à partir de polygones (semi-)réguliers, et on développe deux idées dont la première permet d'estimer KVol sur une large classe de surfaces de translation (indépendamment du disque de Teichmüller), et la seconde permet d'étendre la méthode de calcul de KVol sur les disques de Teichmüller introduite dans [CKM21a]. Par ailleurs, on démontre un critère pour que KVol soit borné dans le disque de Teichmüller d'une surface de Veech, et ce indépendamment du nombre de singularités. Enfin, nous étudions au Chapitre 6 le comportement de KVol sur les surfaces de translation à une singularité lorsque le genre grandit.

1.3.2 Quelques idées préliminaires

Calculs d'intersections singulières. Comme on l'a vu, hormis dans le cas des tores, les surfaces de translation présentent des singularités coniques. De plus, bien que toutes les intersections non-singulières entre deux connexions de selles aient le même signe, ce n'est pas forcément le cas des intersections en une singularité. Une manière de calculer l'intersection de deux courbes en une singularité est de dessiner la figure locale obtenue en tournant autour de la singularité, comme sur la Figure 1.18. De la sorte, on peut par exemple montrer que

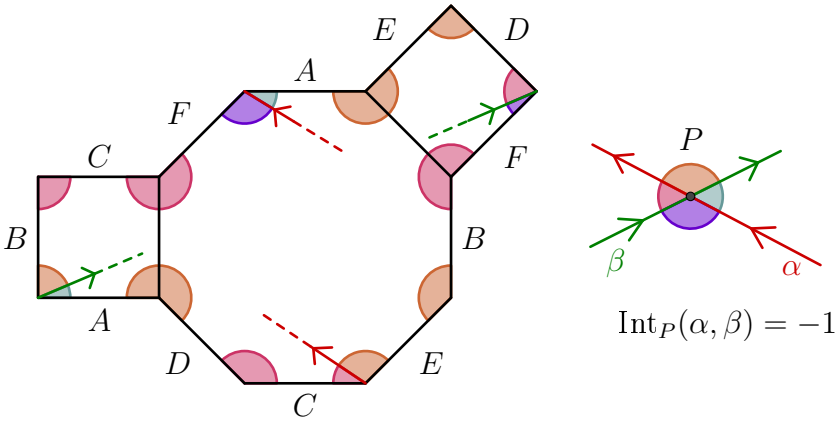

FIGURE 1.18 – Dans cet exemple, les courbes α et β s'intersectent en la singularité, le signe est donné par $\mathrm{Int}_P(\alpha,\beta) = -1$.

deux côtés du double n-gone s'intersectent toujours, ou qu'il existe au moins deux systoles de $S_{m,n}$ qui s'intersectent lorsque m et n sont premiers entre eux, voir Chapitre 5.

Décomposition en cylindres dans une direction périodique. Pour calculer KVol sur une surface de translation, une première idée développée dans [CKM21a] peut être de s'inspirer de la méthode de calcul de KVol sur le tore, en utilisant la décomposition d'une surface (de Veech) en cylindres dans une direction périodique. Plus précisément, étant donné une courbe α sur une surface de Veech X, on peut décomposer la surface en cylindres dans la direction de α. Un exemple est donné à la Figure 1.19 dans le cas d'une surface de genre deux décomposée en deux cylindres. Sur cet exemple, la surface est déjà décomposée en cylindres dans la direction de la courbe α dessinée, et on voit facilement que chaque intersection (non-singulière) avec α requiert une longueur au moins $h(C_2)$, la hauteur du cylindre du bas. Cela permet de dire que pour toute connexion de selles β, on a :

$$\frac{\mathrm{Int}(\alpha,\beta)}{l(\alpha)l(\beta)} \leq \frac{1}{l(\alpha)h(C_2)}.$$

En fait, en raison d'une possible intersection singulière, cette conclusion ne tient que lorsque la courbe β intersecte α non-singulièrement au moins une fois, ou lorsque $h(C_2) \leq h(C_1)$. D'autre part, il pourrait arriver que deux courbes fermées dans la même direction s'intersectent en la singularité (on verra que c'est le cas par exemple pour la surface à trois carreaux de la Figure 1.30). Cependant, mis à part ces quelques restrictions, cela permet d'obtenir une borne qui dépend uniquement de la géométrie de la décomposition en cylindres. Notons enfin que la quantité $h(C_2)l(\alpha)$ correspond à l'aire d'un rectangle et est donc invariante par l'action du groupe de Veech. La borne obtenue dépend donc uniquement de la décomposition en cylindres *à l'action de* $SL_2(\mathbb{R})$ *près*.

Plus généralement, pour n'importe quelle décomposition en cylindres obtenue en découpant dans la direction de la courbe α sur une surface de Veech X, on peut trouver $C_0 > 0$

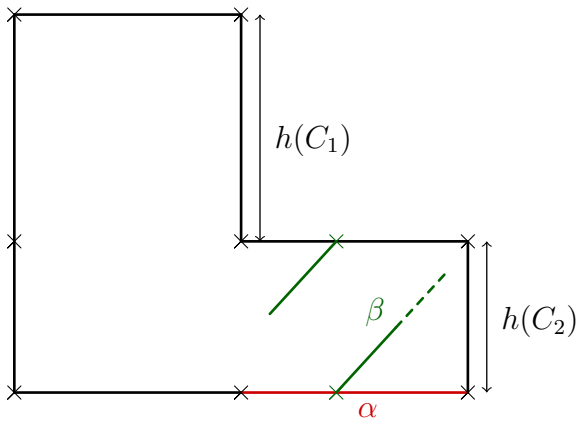

FIGURE 1.19 – Dans cet exemple, chaque intersection non-singulière d'une courbe β avec α nécessite d'avoir traversé verticalement le cylindre avant l'intersection et de traverser verticalement le cylindre après l'intersection.

qui dépend de la décomposition en cylindres et tel que pour tout β qui n'est pas dans la direction de α, on a

$$\frac{\mathrm{Int}(\alpha,\beta)}{l(\alpha)l(\beta)} \leq C_0.$$

Étant donné qu'il n'y a qu'un nombre fini de décompositions en cylindres possibles dans le disque de Teichmüller d'une surface de Veech (à action de $SL_2(\mathbb{R})$ près), cette première idée permet déjà de donner une borne supérieure pour KVol dans tout le disque de Teichmüller d'une surface de Veech à une singularité dont les connexions de selles parallèles ne s'intersectent pas. On verra que l'on peut étendre cet argument dans le cas où il y a plusieurs singularités.

Et lorsqu'il y a du twist ? L'argument précédent permet d'obtenir une majoration du rapport $\frac{\mathrm{Int}(\alpha,\beta)}{l(\alpha)l(\beta)}$ pour n'importe quel choix de β. Cependant, cette majoration n'est optimale que lorsque la décomposition en cylindres obtenue ne possède pas de twist. En effet, à la différence du tore pour lequel il suffisait de prendre une géodésique verticale sans ce soucier du fait qu'elle soit fermée ou minimale, une courbe verticale sur une surface de translation de genre supérieur avec un twist non nul aura tendance à sortir du cylindre dont fait partie la courbe α. Or, si elle sort du cylindre, on perd de la longueur sans gagner d'intersection, et le rapport *Intersection/produit des longueurs* aura tendance à diminuer fortement. En fait, on conjecture :

Conjecture 1.3.1. *Si X est une surface de Veech de genre au moins deux, alors le supremum dans la définition de KVol est en fait un maximum.*

Dès lors, plutôt que de chercher à maximiser KVol en utilisant des courbes verticales, une idée est plutôt de suivre les courbes qui réalisent le maximum de KVol sur la surface sans twist et d'espérer qu'après un petit twist ce sera toujours la même paire de courbes qui réalise

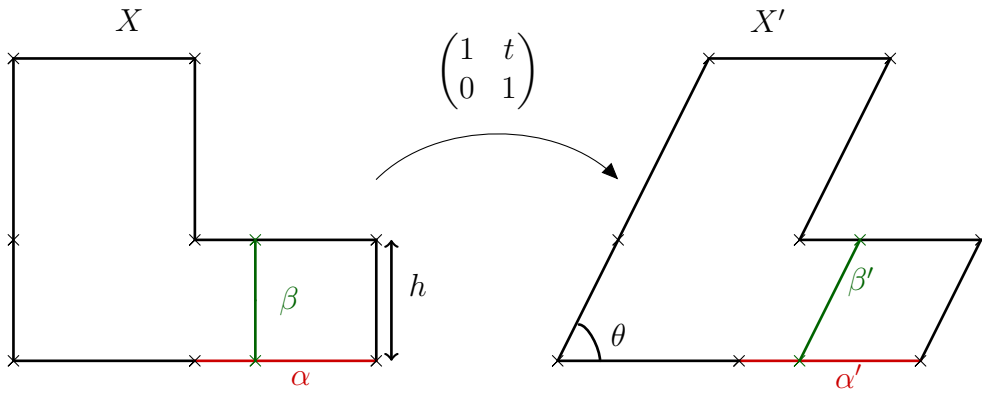

FIGURE 1.20 – Après un twist horizontal, la longueur de β a été multipliée par $\sqrt{1+t^2} = \frac{1}{\sin\theta}$.

le maximum de KVol. On peut quantifier la variation du rapport *Intersection/produit des longueurs* à la suite d'un twist : étant donnée une surface X à angles droits comme sur la Figure 1.20, nous pouvons appliquer un twist horizontal représenté par l'action d'une matrice de la forme $\begin{pmatrix} 1 & t \\ 0 & 1 \end{pmatrix}$ pour obtenir une nouvelle surface X'. Considérons deux connexions de selles α et β sur X, α étant horizontale, et notons α' et β' les images respectives de α et β par l'action du twist, comme sur la Figure 1.20. La longueur de α' est la même que celle de α, tandis que la longueur de β' est $l(\beta') = h\sqrt{1+t^2} = \frac{h}{\sin\theta}$. Puisque l'action affine préserve la forme symplectique d'intersection, celle-ci est inchangée et on a :

$$\frac{\mathrm{Int}(\alpha', \beta')}{l(\alpha')l(\beta')} = \frac{1}{hl(\alpha)} \sin\theta.$$

En particulier, si le maximum dans la définition de $\mathrm{KVol}(X)$ est réalisé uniquement par la paire de courbes (α, β), alors par continuité de KVol après un twist suffisamment petit ce sera la paire de courbes (α', β') image de (α, β) qui réalisera le maximum pour $\mathrm{KVol}(X')$, et on aura $\mathrm{KVol}(X') = \mathrm{KVol}(X)\sin\theta$. L'idée fondamentale à retenir est que, pour calculer KVol dans le disque de Teichmüller d'une surface de Veech, il faut considérer les courbes α et β non pas sur une surface en particulier, mais s'intéresser également à leurs images dans chacune des surfaces du disque de Teichmüller.

Une manière de rendre cette approche explicite est d'écrire, pour deux connexions de selles α et β non-parallèles :

$$\frac{\mathrm{Int}(\alpha, \beta)}{l(\alpha)l(\beta)} = \frac{\mathrm{Int}(\alpha, \beta)}{\alpha \wedge \beta} \cdot \sin\theta(X, \alpha, \beta) \tag{1.2}$$

où $\theta(X, \alpha, \beta)$ est l'angle que forment les directions des connexions de selles α et β sur la surface X, et $\alpha \wedge \beta$ est le produit vectoriel des vecteurs d'holonomie, qui vaut également $l(\alpha)l(\beta)\sin\theta(X, \alpha, \beta)$. L'intérêt est que le rapport $\frac{\mathrm{Int}(\alpha,\beta)}{\alpha\wedge\beta}$ est invariant par l'action de $SL_2(\mathbb{R})$. Tout le travail est alors d'une part d'estimer cette quantité pour α et β données, et d'autre part d'obtenir l'expression de $\sin\theta(X, \alpha, \beta)$ lorsque la surface X (et les courbes α et β) varient sous l'action de $SL_2(\mathbb{R})$. Tandis que la première partie est spécifique à chaque

disque de Teichmüller considéré, nous verrons que $\sin\theta(X,\alpha,\beta)$ s'exprime de manière élégante, voir également [CKM21a, Lemme 2.5]. Remarquons que l'expression ci-dessus n'est évidemment pas valable lorsque α et β sont parallèles et s'intersectent : ce cas problématique doit être traité à part en regardant chaque décomposition en cylindres qui induit des connexions de selles parallèles qui s'intersectent. Nous reviendrons plus en détail sur cette idée et sur le calcul de KVol sur certains disques de Teichmüller spécifiques.

Ces deux idées préliminaires ont permis à S. Cheboui, A. Kessi et D. Massart [CKM21a] de calculer KVol dans le disque de Teichmüller des surfaces à petits carreaux hyperelliptiques en forme d'escalier. Nous reprenons ces idées pour calculer KVol sur d'autres exemples de surfaces de translation.

1.3.3 Présentation des résultats

Dans cette section nous présentons les résultats de la thèse relatifs à KVol, qui peuvent se grouper en trois parties :

1. Premièrement, nous calculons KVol sur des surfaces spécifiques (indépendamment du disque de Teichmüller) en découpant les connexions de selles de sorte à pouvoir estimer simultanément intersection et longueurs. Cette méthode de découpage permet d'obtenir une borne supérieure pour KVol pour une large classe de surfaces de translation, et l'égalité plus spécifiquement dans le cas des surfaces de Bouw-Möller à une singularité. On verra que la technique s'étend également au $2m$-gone régulier, $m \geq 4$.
2. Nous calculons ensuite précisément KVol sur certains disques de Teichmüller. Dans cette partie, l'idée principale est d'utiliser à la fois les idées préliminaires et les résultats sur certaines surfaces spécifiques pour pouvoir calculer KVol sur tout le disque de Teichmüller en démontrant un résultat de "comparaison des sinus". Nous traitons le cas du double $(2m+1)$-gone dans un premier temps, puis plus généralement des surfaces de Bouw-Möller ainsi que du $2m$-gone régulier. Bien que le calcul explicite de KVol ne soit possible avec cette méthode que dans le cas de surfaces à une seule singularité, nous donnons un critère pour que KVol soit borné dans le disque de Teichmüller d'une surface à plusieurs singularités.
3. Enfin, nous aborderons la question de la borne inférieure de KVol sur l'ensemble de toutes les surfaces de translation de $\mathcal{H}(2g-2)$. Plus précisément, on décrit plusieurs familles de surfaces pour chaque genre $g \geq 3$ et dont KVol est arbitrairement proche de g, l'infimum conjectural de KVol sur $\mathcal{H}(2g-2)$. Cela généralise une construction de S. Cheboui, A. Kessi et D. Massart [CKM21b].

Calcul de KVol sur certaines surfaces particulières

Une des premières motivations de ce travail de thèse a été de trouver des exemples de surfaces sur lesquelles on pouvait calculer KVol explicitement. Nous nous sommes intéressés spécifiquement aux surfaces originales de Veech, le double n-gone régulier pour n impair et le n-gone régulier pour n pair, pour lesquelles nous calculons KVol dans [BLM22] pour le double n-gone régulier, puis dans [Bou23a] pour le n-gone régulier (dans le cas à deux singularités

nous ne donnons qu'une borne supérieure pour KVol, non-optimale). Enfin, nous étendons les méthodes utilisées pour le calcul de KVol dans un cadre plus général qui comprend le cas des surfaces de Bouw-Möller, voir Chapitres 4 et 5. Plus précisément, en notant X_n le double n-gone régulier lorsque $n \geq 5$ impair et le n-gone régulier lorsque $n \geq 8$ est pair, on a les résultats suivants :

Théorème 1.3.2 (Cas du double n-gone)**.** *Lorsque $n \geq 5$ est impair, le double n-gone régulier X_n vérifie :*

$$KVol(X_n) = \frac{n}{2} \cot \frac{\pi}{n}$$

De plus, KVol est réalisé uniquement par les paires de côtés des n-gones, qui s'intersectent deux à deux en la singularité.

Théorème 1.3.3 (Cas du n-gone régulier, n multiple de 4)**.** *Lorsque $n = 4m \geq 8$ est un multiple de 4, le n-gone régulier vérifie :*

$$KVol(X_n) = \frac{n}{4} \cot \frac{\pi}{n}$$

De plus, KVol est réalisé uniquement par les paires de côtés du $4m$-gone, qui s'intersectent deux à deux en la singularité.

Théorème 1.3.4 (Cas du n-gone régulier, n non-multiple de 4)**.** *Lorsque $n = 4m + 2$ est pair mais n'est pas un multiple de 4, on a :*

$$KVol(X_n) < \frac{n}{4} \cot \frac{\pi}{n}.$$

Remarquons que dans ce dernier cas, la surface possède deux singularités distinctes, et la borne que nous obtenons ne correspond pas à une paire de géodésiques fermées sur la surface, c'est pourquoi on obtient une inégalité stricte. Pour obtenir ces résultats, l'idée principale est de découper les connexions de selles en plus petits morceaux (non fermés) dont on peut estimer à la fois les longueurs et les intersections, ce qui permet de majorer KVol. Dans les deux premiers cas, on montre ensuite que les majorations obtenues sont optimales en étudiant spécifiquement l'intersection des systoles. Cette méthode se généralise au cas de surfaces de translation construites à partir de polygones convexes, sous certaines hypothèses :

Théorème A. *Soit X une surface de translation construite à partir d'une collection de polygones P_i. On suppose que :*

(H1) Chaque polygone est convexe à angles obtus ou droits,
(H2) Les côtés d'un même polygone ne sont pas recollés ensemble.

Alors

$$KVol(X) \leq \frac{Vol(X)}{l_0^2},$$

où l_0 désigne la longueur du plus petit côté des polygones.

En fait, ce résultat ne se restreint pas uniquement au cadre des surfaces de translation, mais est en fait vrai pour n'importe quelle surface plate vérifiant les hypothèses (H1) et (H2), avec seulement quelques modifications dans la partie technique de la démonstration. De plus, l'inégalité est optimale dans le cas des surfaces de Bouw-Möller à une seule singularité :

Théorème B. *Soit $m, n \geq 2$ avec $mn \geq 6$. On a :*

$$KVol(S_{m,n}) \leq \frac{Vol(S_{m,n})}{\sin(\pi/m)^2}$$

De plus, l'égalité est réalisée si et seulement si $pgcd(m, n) = 1$ (c'est-à-dire que $S_{m,n}$ possède une seule singularité). Dans ce cas, KVol est alors atteint uniquement par les paires de systoles qui s'intersectent une fois.

Rappelons que lorsque n est impair, $X_n = S_{2,n}$ de sorte que le Théorème 1.3.2 est une conséquence directe du Théorème B. Toutefois, nous avons énoncé ce résultat séparément car la démonstration est plus simple dans ce cas particulier. Notons par ailleurs que le n-gone régulier (pour n pair) ne vérifie pas les hypothèses du Théorème A, et de fait l'hypothèse qu'il n'y a pas d'identifications entre les arêtes d'un même polygone est nécessaire à la preuve que nous donnons. Nous discuterons des hypothèses du Théorème A dans un prochain paragraphe.

L'idée du découpage. Étant donnée une surface décrite à l'aide d'une collection de polygones avec des identifications et deux géodésiques fermées α et β sur cette surface (qui sont alors des lignes droites par morceaux, passant possiblement par une ou plusieurs singularités), on peut décider de décomposer chacune des deux géodésiques en segments plus courts (non fermés) en découpant à chaque fois que la géodésique traverse une arête d'un polygone. Cela donne une subdivision $\alpha = \alpha_1 \cup \cdots \cup \alpha_k$ (resp. $\beta = \beta_1 \cup \cdots \cup \beta_l$), que l'on peut appeler la *subdivision polygonale*.

Ce découpage naïf permet d'avoir un contrôle sur l'intersection entre α et β car alors deux segments ne peuvent s'intersecter qu'une fois au plus, et cela uniquement s'ils sont dans le même polygone. Concernant les longueurs, cela dépend très fortement de la forme du polygone, mais dans l'exemple d'un polygone convexe à angles obtus (ou droits), on peut obtenir une bonne estimation des longueurs. Pour cela, on distingue deux types de segments :

— Les segments *non-adjacents* qui vont d'un côté du polygone à un côté non-adjacent du polygone.

— Les segment *adjacents* qui vont d'un côté du polygone à un côté adjacent du polygone.

Lorsque l'une des extrémités du segment est une singularité, on comptera le segment comme un segment non-adjacent. Par exemple, sur la Figure 1.21 les segments α_2 et α_4 sont des segments adjacents tandis que α_1, α_3 et α_5 sont non-adjacents.

On peut se convaincre que les segments non-adjacents ont une longueur supérieure à la longueur du plus petit côté du polygone (convexe à angles obtus). Concernant les segments adjacents, l'idée est de les grouper par deux : comme on peut le voir grâce à la Figure 1.22, la

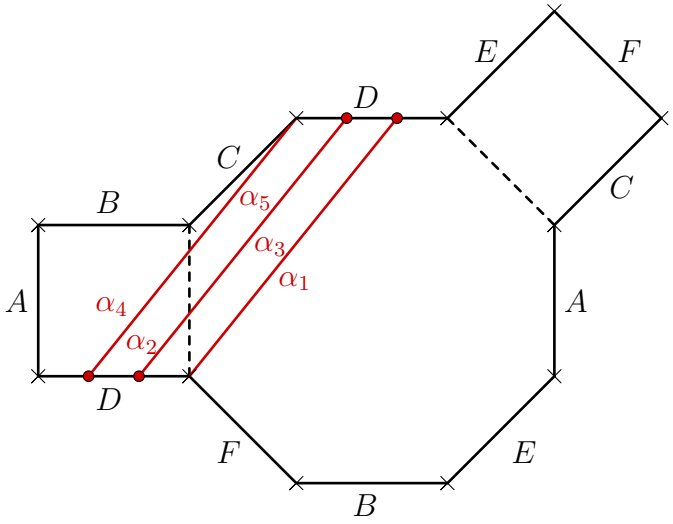

FIGURE 1.21 – Exemple d'une connexion de selle α décomposée en 5 segments $\alpha_1, \alpha_2, \alpha_3, \alpha_4$ et α_5. Les segments α_2 et α_4 sont des segments adjacents tandis que α_1, α_3 et α_5 sont non-adjacents.

longueur totale de deux segments adjacents *consécutifs* est au moins égale à la longueur du côté des polygones qu'ils partagent (grâce à l'hypothèse sur les angles). Bien que les segments adjacents ne viennent pas toujours par paire, on verra que c'est le cas pour le double n-gone et le n-gone régulier, ce qui nous permet de faire des calculs explicites.

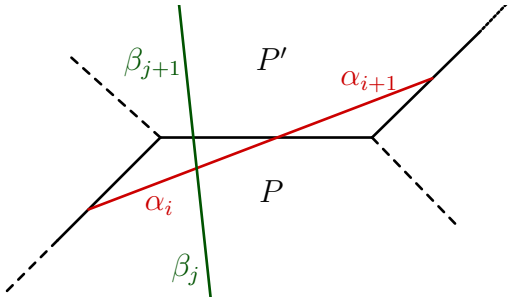

FIGURE 1.22 – La longueur de deux segments adjacents consécutifs est au moins égale à la longueur du côté qu'ils traversent. De plus l'intersection entre α_i et β_j permet de déduire qu'il n'y a pas d'intersection entre α_{i+1} et β_{j+1}, qui sont pourtant dans le même polygone.

Revenons maintenant aux intersections. On a vu que deux segments quelconques ne peuvent s'intersecter qu'une fois, et ce à la condition supplémentaire d'être dans le même polygone (nous supposons ici qu'il n'y a pas d'intersections sur les arêtes des polygones, ce que l'on peut supposer quitte à déformer légèrement α ou β à condition que ni α ni β ne soit une arête d'un polygone, ce dernier cas pouvant être traité à part). On peut aller plus loin en remarquant que si un segment *adjacent* α_i intersecte un segment β_j, il existe une arête du polygone contenant une extrémité de α_i et une extrémité de β_j, et alors on

se rend compte que les segments $\alpha_{i'}$ et $\beta_{j'}$ consécutifs le long de cette arête ne peuvent pas s'intersecter alors même qu'ils sont dans le même polygone. Par exemple, sur la Figure 1.22, α_i et β_j s'intersectent et partagent une arête extrémale, de sorte que α_{i+1} et β_{j+1} ne peuvent pas s'intersecter alors qu'ils sont tous deux contenus dans le même polygone P'. Remarquons cependant que cet argument n'est pas valable lorsque le segment β_j est un segment dont l'une des extrémités est un sommet d'un polygone, mais malgré ce cas particulier, la philosophie générale est qu'*une intersection avec un segment adjacent retire une intersection potentielle* et permet de compenser la petite longueur des segments adjacents en retirant des intersections.

Plus précisément, lorsque les côtés d'un même polygone ne sont pas recollés pour construire la surface de translation, on peut démontrer :

Proposition 1.3.5. *Notons*

- *p_α (resp. p_β) le nombre de segments non-adjacents de α (resp. β),*
- *q_α (resp. q_β) le nombre maximal de paires de segments adjacents consécutifs dans la décomposition polygonale de α (resp. β).*

Alors le nombre d'intersections non-singulières $|\alpha \cap \beta|$ des géodésiques fermées α et β vérifie :

$$|\alpha \cap \beta| \leq (p_\alpha + q_\alpha)(p_\beta + q_\beta)$$

Cette proposition, combinée à une bonne estimation des longueurs, permet essentiellement de démontrer le Théorème A.

Comparaison entre KVol et le volume systolique. Dans le cas où X est une surface qui vérifie les hypothèses du Théorème A, et si l'on suppose de plus que tous les sommets des polygones sont identifiés en une seule singularité, le plus petit côté des polygones est alors une courbe fermée simple, qui est de plus une systole, et on a

$$\mathrm{KVol}(X) \leq \mathrm{Volsys}(X).$$

Ce résultat est à comparer avec le résultat du Théorème 1.1.6, qui donnait l'estimée $\mathrm{KVol}(X) \leq 9\mathrm{Volsys}(X)$. On peut alors se poser la question de la meilleure constante possible dans cette inégalité dans le cas spécifique des surfaces de translation. Une première chose à remarquer est que la constante 1 valable dans le cas des polygones convexes à angles obtus sans identifications des arêtes d'un même polygone n'est pas valable en général : la surface en L construite à partir de 6 triangles équilatéraux (voir Figure 1.23) fournit un exemple de surface de translation X à une singularité telle que :

$$\mathrm{KVol}(X) = 3 = \frac{2}{\sqrt{3}}\mathrm{Volsys}(X).$$

Nous conjecturons que la surface en L équilatéral réalise la borne supérieure de la comparaison entre KVol et le volume systolique, plus précisément :

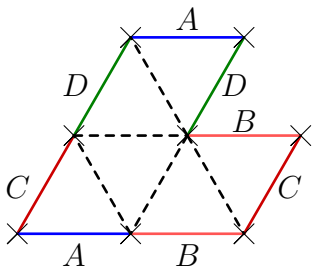

FIGURE 1.23 – Le L équilatéral.

Conjecture 1.3.6. *Pour toute surface de translation X à une singularité, on a*

$$KVol(X) \leq \frac{2}{\sqrt{3}}\text{Volsys}(X).$$

De plus, l'inégalité est optimale pour tout genre g, et le cas d'égalité comprend les surfaces équilatérales $St(2g-1)$.

Une idée pour démontrer ce résultat pourrait être d'adapter la méthode de découpage dans les cas où les hypothèses du Théorème A ne sont pas vérifiées. Toutefois, la méthode de découpage seule ne semble pas suffisante pour démontrer la Conjecture 1.3.6, pour plusieurs raisons :

- D'une part, il faut pouvoir traiter le cas de surfaces construites à partir de polygones convexes dont les angles ne sont pas obtus. Mais si les angles ne sont pas supposés obtus ou droits, la longueur d'une paire de segments adjacents consécutifs peut être arbitrairement petite, comme sur l'exemple de la Figure 1.24. En particulier, notre méthode n'a aucune chance de s'adapter à moins de supposer :

  (H1') La somme de deux angles consécutifs autour d'un sommet donné est toujours supérieure ou égale à π.

  En supposant (H1'), le fait d'avoir des angles obtus n'intervient que dans l'étude des longueurs et l'estimation des intersections reste inchangée. Ainsi, il suffit d'adapter la partie sur l'estimation des longueurs dans la démonstration du Théorème A pour obtenir un résultat similaire. Plus précisément, on a :

  Théorème 1.3.7. *Soit X une surface de translation construite à partir d'une collection de polygones $(P_i)_{i\in I}$ vérifiant (H1') et (H2). Notons θ_0 l'angle minimal entre les côtés des polygones P_i, et l_0 la longueur du plus petit côté des polygones. On suppose $\theta_0 \geq \frac{1}{2}\arccos\frac{8}{9}$. Alors*

  $$KVol(X) \leq \frac{Vol(X)}{\sin(\theta_0)^2 l_0^2}$$

  Bien qu'énoncé sous la contrainte $\theta_0 \geq \frac{1}{2}\arccos\frac{8}{9} \simeq 0.076\pi$, nous pensons que ce résultat est vrai pour tout $\theta_0 > 0$.

  Enfin, remarquons que le Théorème 1.3.7 n'est pas suffisant pour résoudre la Conjecture 1.3.6, car, en laissant de côté l'hypothèse sur les identifications d'arêtes, on obtient $\text{KVol}(X) \leq \frac{4}{3}\text{Volsys}(X)$ dans le cas du L équilatéral.

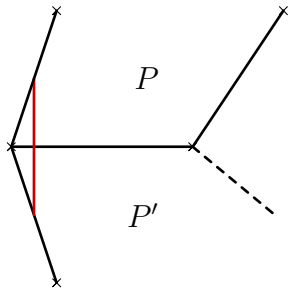

FIGURE 1.24 – Si on ne suppose pas que les angles des polygones sont obtus ou droits, la longueur totale de deux segments adjacents consécutifs peut être arbitrairement petite.

- Concernant les identifications d'arêtes d'un même polygone, nous avons vu dans le cas du n-gone régulier pour n pair (Théorèmes 1.3.3 et 1.3.4) que la conclusion des Théorèmes A et 1.3.7 peut rester valable. En fait, nous conjecturons que ces deux théorèmes restent valables sans l'hypothèse sur les identifications des arêtes. Toutefois, une preuve utilisant la méthode de découpage telle quelle nécessiterait une estimation bien plus fine des longueurs et une étude spécifique de certaines configurations problématiques. Remarquons toutefois que l'argument de découpage permet facilement de démontrer que pour une surface X construite à partir d'une collection de polygones (P_i) vérifiant (H1) mais pas (H2), on a :
$$\mathrm{KVol}(X) \leq 4\frac{\mathrm{Vol}(X)}{l_0^2},$$
où l_0 désigne la longueur du plus petit côté des polygones.
- Enfin, dans le cas où les sommets ne sont pas tous identifiés au même point sur la surface, il pourrait ne pas y avoir de courbe fermée de longueur l_0. Cette dernière hypothèse semble difficile à prendre en compte en utilisant l'argument de découpage. Une conjecture optimiste serait que le Théorème A reste vrai en remplaçant la longueur du plus petit côté des polygones par la systole, indépendamment du nombre de singularités.

Et si la surface n'est pas plate ? Remarquons pour terminer que cette méthode est essentiellement combinatoire et n'a pas de raison d'être spécifique aux surfaces plates. On pourrait par exemple imaginer estimer KVol sur certaines surfaces hyperboliques (ayant potentiellement des singularités coniques) en utilisant ces résultats. Toutefois, la condition d'avoir tous les angles obtus ou droits est généralement difficile à obtenir pour une surface hyperbolique n'ayant pas de singularités (les angles ayant plutôt tendance à être petits).

L'extension au disque de Teichmüller

Une fois KVol calculé sur une surface particulière du disque de Teichmüller, on peut utiliser la continuité de KVol pour estimer KVol pour des surfaces proches, mais sans aucun contrôle sur la taille du voisinage. Dans cette section, nous expliquons comment utiliser

l'estimation de KVol sur une surface particulière (qui dans nos exemples correspond exactement à un coin du domaine fondamental) avec la méthode de calcul de KVol sur le disque de Teichmüller vue en §1.3.2, pour calculer précisément KVol sur les disques de Teichmüller des surfaces de Bouw-Möller d'une part, et du n-gone régulier pour $n = 4m$ d'autre part. Pour formaliser les résultats, on utilise la paramétrisation du disque de Teichmüller de ces surfaces obtenues en §1.2.4. Ces résultats peuvent se résumer à l'aide des Figures 1.25, 1.26 et 1.27. Essentiellement, on démontre que KVol peut se calculer sur le disque de Teichmüller de chacune de ces surfaces simplement en regardant la distance de la surface considérée par rapport à une famille de géodésiques du disque de Teichmüller.

Théorème 1.3.8 (Cas du double n-gone)**.** *Soit $n \geq 5$ impair. Pour toute surface X dans le disque de Teichmüller du double n-gone régulier, représentée par un point dans le domaine fondamental de la Figure 1.25, on a*

$$KVol(X) = K_0 \cdot \frac{1}{\cosh(d_{\mathbb{H}^2}(X, \gamma_{0,\infty}))}$$

où $K_0 > 0$ est une constante explicite qui dépend de n, $\gamma_{0,\infty}$ désigne la géodésique d'extrémités 0 et ∞ et $d_{\mathbb{H}^2}$ désigne la distance hyperbolique.
Cette quantité s'exprime aussi sous la forme

$$KVol(X) = K_0 \sin\theta(X, 0, \infty),$$

où $\theta(X, 0, \infty)$ est l'angle qui définit le voisinage banane *de la géodésique $\gamma_{0,\infty}$ qui passe par X, comme sur la Figure 1.25. (Étant donnés $d, d' \in \mathbb{R} \cup \{\infty\}$ distincts, le voisinage banane de la géodésique $\gamma_{d,d'}$ qui passe par X est l'ensemble $\{z \in \mathbb{H}^2, d(z, \gamma_{d,d'}) = d(X, \gamma_{d,d'})\}$.)*

Avant de poursuivre, remarquons que l'égalité $\sin\theta(X, 0, \infty) = \dfrac{1}{\cosh(d_{\mathbb{H}^2}(X, \gamma_{0,\infty}))}$ est vraie en toute généralité et se démontre par un simple calcul de géométrie hyperbolique. Plus généralement, étant donné deux directions $d, d' \in \mathbb{R} \cup \{\infty\} \simeq \partial\mathbb{H}^2$ distinctes, on a $\sin\theta(X, d, d') = \dfrac{1}{\cosh(d_{\mathbb{H}^2}(X, \gamma_{d,d'}))}$ où $\gamma_{d,d'}$ désigne la géodésique hyperbolique d'extrémités d et d' et $\sin\theta(X, d, d')$ désigne l'angle défini par le voisinage banane de $\gamma_{d,d'}$ passant par X, comme sur la Figure 1.28.

Théorème 1.3.9 (Cas du n-gone régulier à une singularité)**.** *Soit $n = 4m \geq 8$. Pour toute surface X dans le disque de Teichmüller du n-gone régulier, représentée par un point dans le domaine fondamental de la Figure 1.26, on a*

$$KVol(X) = K_0 \cdot \frac{1}{\cosh(d_{\mathbb{H}^2}(X, \mathcal{G}))}$$

où K_0 est une constante explicite qui dépend de n et

$$\mathcal{G} = \bigcup_{k \in \mathbb{N}^* \cup \{\infty\}} \Gamma \cdot \gamma_{\infty, 1/k\Phi}$$

Ici, Γ désigne le groupe de Veech du modèle en escalier associé au n-gone régulier, et $\Phi = \Phi_n := 2\cos(\pi/n)$.

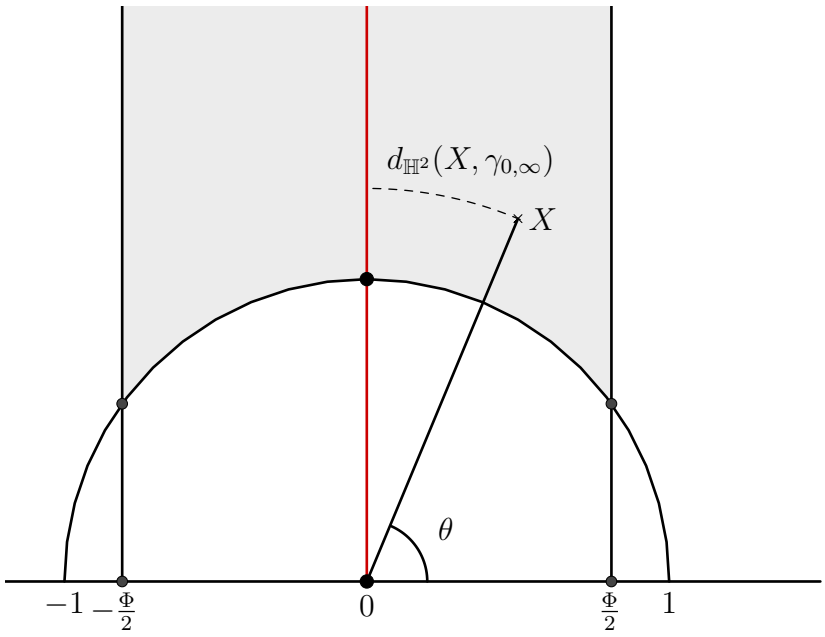

FIGURE 1.25 – Dans le domaine fondamental du le disque de Teichmüller du double pentagone, on a $\mathrm{KVol}(X) = K_0 \sin\theta = K_0 \frac{1}{\cosh(d_{\mathbb{H}^2}(X,\gamma_{0,\infty}))}$.

Théorème C (Cas des surfaces de Bouw-Möller)**.** *Pour tous $m, n \geq 3$ avec $m \wedge n = 1$ et toute surface X dans le disque de Teichmüller de la surface de Bouw-Möller $S_{m,n}$, représentée par un point dans le domaine fondamental de la Figure 1.27, on a*

$$KVol(X) = K_0 \cdot \frac{1}{\cosh(d_{\mathbb{H}^2}(X, \gamma_{\cot(\pi/n),\infty} \cup \gamma_{-\cot(\pi/n),\infty}))}$$

où $K_0 > 0$ est une constante explicite qui dépend de m et n.

Remarquons que le cas des surfaces à plusieurs singularités ne peut être traité ici, tant à cause du fait que nous n'avons pas de calcul précis pour KVol sur les surfaces spécifiques (uniquement une borne inférieure) que parce que la méthode d'extension au disque de Teichmüller n'est valable que pour des surfaces avec une seule singularité.

Une question d'interpolation. Les démonstrations des Théorèmes 1.3.8, 1.3.9 et C suivent la même logique : prenons l'exemple du double pentagone pour en expliquer l'idée. Comme on l'a vu en §1.2.4, un domaine fondamental pour le disque de Teichmüller du double pentagone peut être représenté par un triangle hyperbolique avec un cusp dont les deux angles non nuls sont $\frac{\pi}{5}$. Le double pentagone est représenté par le coin du domaine fondamental (les deux coins étant identifiés). Au vu des résultats précédents, nous disposons des informations suivantes :

— Le calcul de KVol sur le double pentagone (Théorème 1.3.2), en plus de nous donner l'expression exacte de KVol, nous donne précisément les courbes qui réalisent le maximum (ce sont les paires de côtés des pentagones).

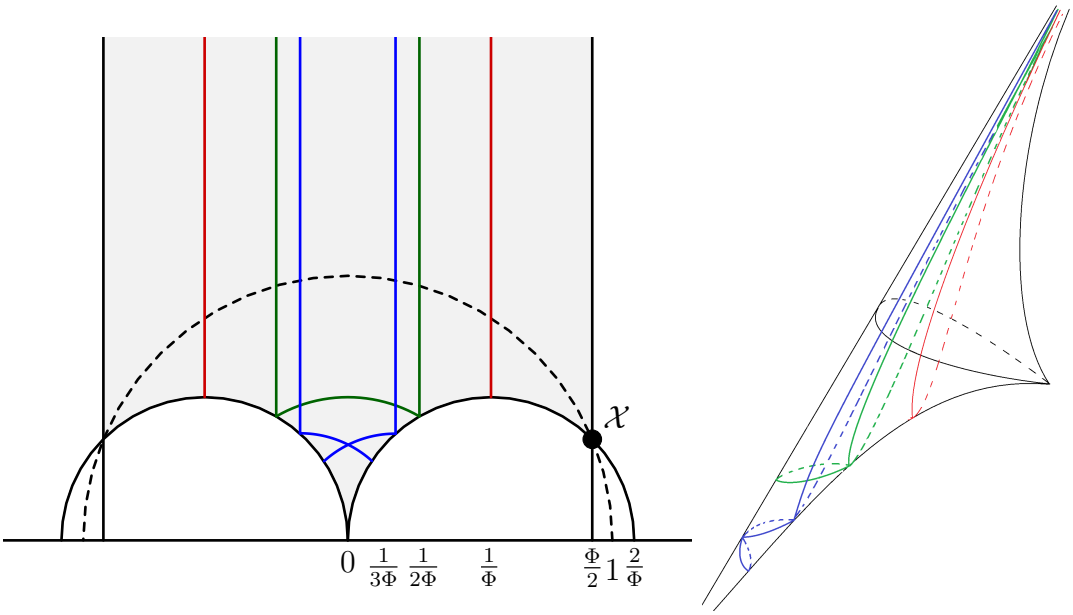

FIGURE 1.26 – Les géodésiques $\gamma_{\infty,\frac{1}{k\Phi}}$ pour $k = 1, 2, 3$ et leurs images par le groupe de Veech qui intersectent le domaine fondamental. A droite, les mêmes géodésiques sur la surface quotient $\mathbb{H}^2/\Gamma$.

— De plus, en utilisant le fait que dans n'importe quelle direction périodique, la décomposition en cylindres est celle du L d'or à action du groupe de Veech près, on peut montrer que $\mathrm{KVol}(X) \leq \frac{2\Phi-1}{(\Phi-1)^2}$ sur tout le disque de Teichmüller. L'égalité est évidemment réalisée dans le cas du L d'or (placée au point i dans le domaine fondamental), mais aussi pour les images du L d'or par le flot géodésique vertical (placées en ai pour $a \geq 1$). De plus, pour toutes ces surfaces, KVol est réalisé par l'image des courbes α et β de la Figure 1.29.

En particulier, ce sont les mêmes courbes qui réalisent le maximum dans la définition KVol dans le double pentagone et dans les surfaces en L situées sur la géodésique $\gamma_{0,\infty}$. L'idée fondatrice est alors de démontrer que c'est le cas sur tout le domaine fondamental en interpolant sur tout le reste du disque de Teichmüller.

Pour cela, on commence par choisir une surface de base S_0 du disque de Teichmüller (par exemple, dans le cas des doubles n-gones on choisit le modèle en escalier associé) puis on définit, étant donné deux directions périodiques distinctes d et d' sur S_0, la quantité :

$$K(d, d') = \max_{\alpha,\beta} \frac{\mathrm{Int}(\alpha, \beta)}{\alpha \wedge \beta}$$

le maximum portant sur l'ensemble (fini) des connexions de selles sur S_0 de directions respectives d et d'. Ensuite, on démontre que pour une surface de translation dont les géodésiques parallèles ne s'intersectent pas, on a :

$$\mathrm{KVol}(X) = \sup_{d,d' \in \mathcal{P}, d \neq d'} K(d, d') \cdot \sin\theta(X, d, d').$$

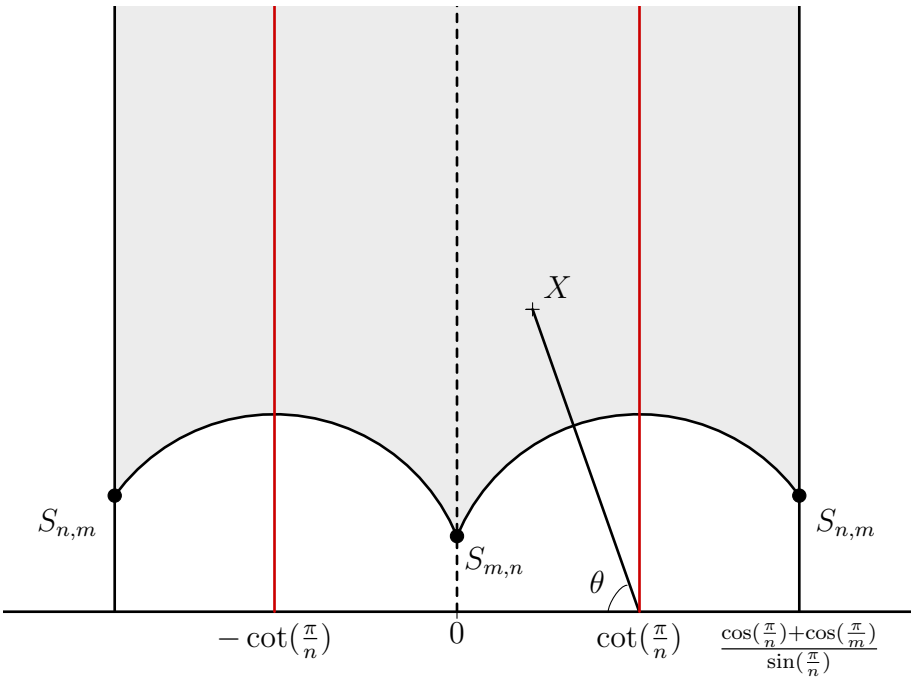

FIGURE 1.27 – Le domaine fondamental pour le disque de Teichmüller $S_{m,n}$ et les géodésiques $\gamma_{\infty,\pm\cot(\pi/n)}$. L'angle θ mesure la distance entre X et la géodésique $\gamma_{\infty,\cot(\pi/n)}$

où $\theta(X,d,d')$ est l'angle défini par le voisinage banane de la géodésique hyperbolique $\gamma_{d,d'}$ passant par X comme sur la Figure 1.28, et $\mathcal{P}$ est l'ensemble des directions périodiques sur la surface S_0. Enfin, nous démontrons un résultat de "comparaison des sinus" en géométrie hyperbolique, qui peut s'énoncer comme suit :

Théorème 1.3.10. *Soient $a,b,c \in \mathbb{R}$ avec $|b| \leq |c|$. Notons $\mathcal{D}$ le polygone hyperbolique défini par les géodésiques $\gamma_{a,\infty}$, $\gamma_{a+b,\infty}$ and $\gamma_{a-c,a+c}$, et X_0 le point d'intersection de $\gamma_{a+b,\infty}$ et $\gamma_{a-c,a+c}$ (qui existe grâce à l'hypothèse $|b| \leq |c|$). Supposons de plus que l'angle entre les géodésiques $\gamma_{a+b,\infty}$ et $\gamma_{a+c,a-c}$ est de la forme $\frac{\pi}{n}$ pour $n \geq 2$, de sorte que le groupe G engendré par les réflexions par rapport aux géodésiques $\gamma_{a+b,\infty}$ et $\gamma_{a-c,a+c}$ est un groupe dihédral. Soit $\mathcal{P}$ un sous-ensemble de $\partial\mathbb{H}^2$ stable par l'action de G et contenant au moins ∞, a et $a+2b$. Soit $K(\cdot,\cdot) : \mathcal{P} \times \mathcal{P}\backslash\Delta \to \mathbb{R}$ une fonction symétrique en ses deux coordonnées (Δ est la diagonale $\{(x,x), x \in \mathcal{P}\}$) et invariante sous l'action diagonale de G.*

Supposons de plus que :

(H1) Pour tous $d,d' \in \mathcal{P}$ distincts,

$$K(d,d')\sin(X_0,d,d') \leq K(\infty,a)\sin\theta(X_0,\infty,a)$$

(H2) Pour tous $d,d' \in \mathcal{P}$ distincts,

$$K(d,d') \leq K(\infty,a)$$

(H3) Pour tous $d,d' \in \mathcal{P}$ distincts tels que $\gamma_{d,d'}$ intersecte $\mathcal{D}$ et $(d,d') \neq (\infty,a)$,

$$K(d,d') \leq \sin(\frac{\pi}{4})K(\infty,a)$$

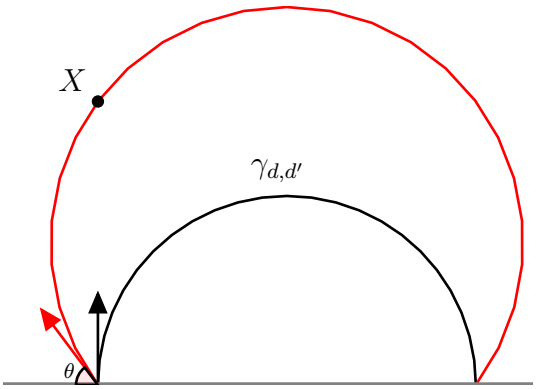

FIGURE 1.28 – Définition de l'angle $\theta(X, d, d')$.

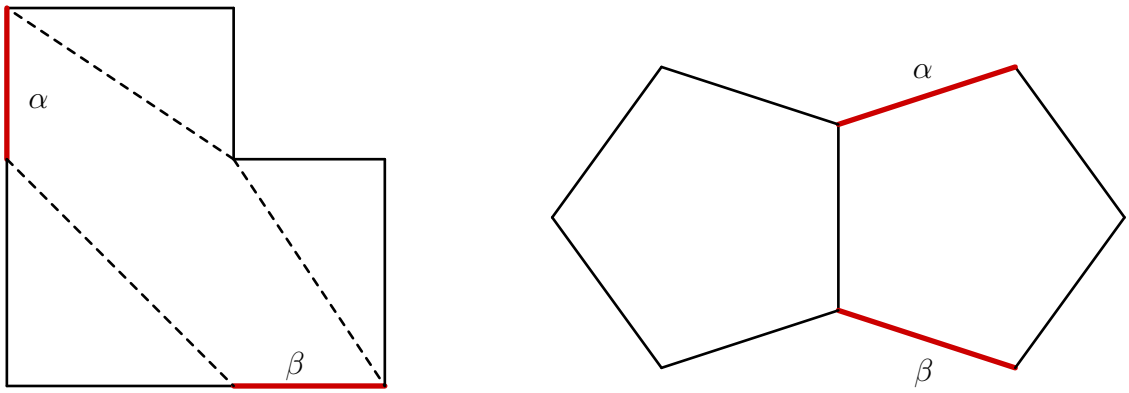

FIGURE 1.29 – Ce sont les mêmes courbes qui réalisent KVol sur le double pentagone et sur son modèle en escalier.

(H4) Pour tous $d, d' \in \mathcal{P}$ distincts tels que $\gamma_{d,d'}$ intersecte $\mathcal{D}$ et $(d, d') \neq (\infty, a)$,

$$K(d, d') \leq \frac{\sin\theta(X_0, \infty, a)}{\sin\theta(X_0, a, a + 2b)} K(\infty, a)$$

Alors, pour tout $X \in \mathcal{D}$ et tous $d, d' \in \mathcal{P}$ distincts :

$$K(d, d') \sin(X, d, d') \leq K(\infty, a) \sin\theta(X, \infty, a).$$

Dans notre cadre, $\mathcal{P}$ sera l'ensemble des directions périodiques de la surface S_0. L'objectif est alors d'étudier $K(\cdot, \cdot)$ pour montrer que les hypothèses du Théorème 1.3.10 sont vérifiées pour les paramètres a, b et c correspondant au domaine fondamental du disque de Teichmüller considéré, la surface S_0 étant placée en i.

Le cas des surfaces à plusieurs singularités. Dans le cas des surfaces de translation à plusieurs singularités, les géodésiques fermées simples n'ont pas toujours de direction bien

définie car elles pourraient être union de connexions de selles (non fermées) dans des directions différentes, et la méthode d'extension au disque de Teichmüller ne fonctionne plus. Toutefois, on peut quand même utiliser les décompositions en cylindres pour donner un critère pour que KVol reste borné sur le disque de Teichmüller d'une surface de Veech. Plus précisément :

Théorème D ([Bou23a])**.** *KVol est borné sur le disque de Teichmüller d'une surface de Veech X si et seulement si deux courbes fermées qui s'expriment comme union de connexion de selles parallèles ne s'intersectent jamais.*

Il est à noter que la preuve de ce résultat permet de donner une borne explicite (mais non optimale) en fonction du disque de Teichmüller considéré (à condition d'avoir une description explicite des décompositions en cylindres). Notamment, nous donnons une borne explicite pour KVol sur le disque de Teichmüller du n-gone régulier avec deux singularités ($n \equiv 2 \mod 4$) dans [Bou23a].

Théorème 1.3.11. *Soit $n \equiv 2 \mod 4$, $n \geq 10$. Pour toute surface X dans le disque de Teichmüller du n-gone régulier, on a :*

$$KVol(X) \leq \frac{n}{4} \cot(\frac{\pi}{n}).$$

Théorème E. *Pour tous $m, n \geq 2$ avec $mn \geq 6$, KVol est borné sur le disque de Teichmüller de $S_{m,n}$.*

Bien que le critère du Théorème D soit assez facile à vérifier dans le cas du n-gone régulier, le cas des surfaces de Bouw-Möller requiert un peu plus d'attention. Pour étudier les intersections des courbes parallèles (et donc pouvoir appliquer le critère ci-dessus), une méthode est d'utiliser les *diagrammes de séparatrices* introduits par M. Kontsevich et A. Zorich [KZ03], qui sont des graphes munis d'un ordre cyclique à chaque arête (aussi appelés *graphes enrubannés*, voir [EMM13]) qui encodent justement l'ordre cyclique des connexions de selles horizontales en les singularités. Par exemple, le diagramme associé à la décomposition en cylindres horizontale de la surface à trois carreaux est représenté en Figure 1.30. On peut déduire d'un tel graphe les intersections entre connexions de selles, ou entre courbes fermées qui sont des union de plusieurs connexions de selles (dans le cas où il y a plusieurs singularités). Plus précisément, on a :

Théorème 1.3.12. *Les courbes fermées parallèles ne s'intersectent pas si et seulement si le diagramme de séparatrices associé à chacune des décompositions en cylindres est planaire.*

Nous utilisons ce résultat dans le cas des surfaces de Bouw-Möller pour démontrer le Théorème E. (Pour être tout à fait exact, nous utilisons en fait la version duale du diagramme de séparatrices, qui est planaire si et seulement si le diagramme de séparatrices l'est, et qui a l'avantage de se déduire plus directement de la décomposition en cylindres.) Un corollaire combinatoire du Théorème 1.3.12 est qu'il existe toujours des courbes fermées parallèles qui s'intersectent si une surface de genre g possède une décomposition en $g-1$ cylindres ou moins. De plus, la réciproque est vraie s'il n'y a qu'une seule singularité. Par exemple, dans $\mathcal{H}(2)$, la classification des surfaces de Veech donnée par McMullen [McM05a] implique que :

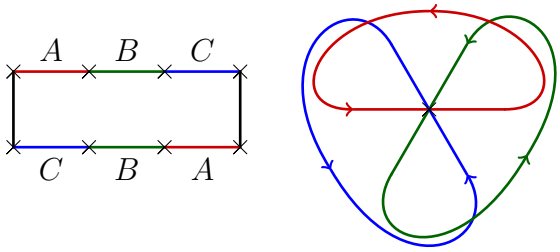

FIGURE 1.30 – La surface à trois carreaux et son diagramme de séparatrices horizontales.

Théorème 1.3.13. *Dans $\mathcal{H}(2)$, KVol est borné sur le disque de Teichmüller d'une surface de Veech X si et seulement si X est non arithmétique.*

Plus généralement, ce critère permet de démontrer que KVol est borné sur le disque de Teichmüller de n'importe quelle surface de Veech *algébriquement primitive* ayant une seule singularité, car alors toutes les décompositions en cylindres ont exactement g cylindres. Notons par ailleurs que, dès qu'il y a plusieurs singularités, on peut construire des surfaces arithmétiques ayant un disque de Teichmüller sur lequel KVol est borné : la surface présentée en Figure 1.31 possède, à l'action de $SL_2(\mathbb{R})$ près, deux décompositions en cylindres, et les diagrammes de séparatrices associés sont planaires. On peut trouver des exemples similaires en genre trois et quatre, mais ces exemples sont toujours dans la strate principale. Ainsi, on peut se poser la question suivante :

Question 1.3.14. Est ce que toute surface de Veech arithmétique de $\mathcal{H}(2g-2)$ possède au moins une direction ayant $g-1$ cylindres ou moins ? Réciproquement, est-ce qu'il existe des surfaces de Veech non-arithmétiques de $\mathcal{H}(2g-2)$ avec une direction ayant $g-1$ cylindres ou moins ?

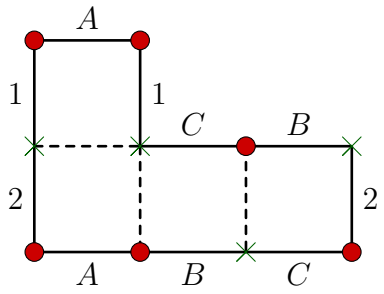

FIGURE 1.31 – Un exemple de surface à petit carreaux ayant un disque de Teichmüller sur lequel KVol est borné.

Une borne inférieure pour KVol en genre g ?

Dans cette partie, on s'intéresse à l'infimum de KVol sur les surfaces de translation de genre g. Comme on l'a vu dans la section introductive, l'asymptotique de l'infimum de KVol

sur toutes les surfaces riemanniennes de courbure négative ou nulle de genre g est de l'ordre de $\frac{g}{\log(g)^2}$. Toutefois, dans le cas spécifique des surfaces de translation à une seule singularité, on conjecture que

$$\inf_{X\in\mathcal{H}(2g-2)} \mathrm{KVol}(X) = g.$$

Dans cette direction, nous construisons des familles $(L_{g,n})$ de surfaces de $\mathcal{H}(2g-2)$ pour chaque genre $g \geq 3$ dont $\mathrm{KVol}(L_{g,n})$ tend vers g lorsque n tend vers l'infini, pour g fixé. Cette construction généralise un résultat de [CKM21b] obtenu en genre deux. Nous adaptons également la construction pour chacune des composantes connexes de $\mathcal{H}(2g-2)$. En particulier, on démontre :

Théorème F ([Bou23b]). *Pour chaque composante connexe $\mathcal{C}$ de $\mathcal{H}(2g-2)$, on a :*

$$\inf_{X\in\mathcal{C}} KVol(X) \leq g.$$

Les surfaces $L_{g,n}$ sont des surfaces à petits carreaux dont le nombre de carreaux tend vers l'infini avec n et g. Un modèle de $L_{3,4}$ et $L_{4,3}$ est donné à la Figure 1.32.

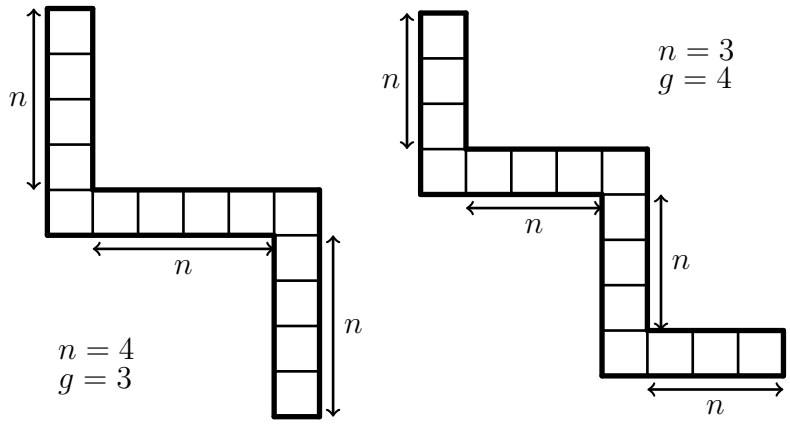

FIGURE 1.32 – La surface $L_{3,4}$ à gauche, et $L_{4,3}$ à droite. Les identifications sont telles que la surface est décomposée en cylindres dans les directions horizontale et verticale.

Questions et Perspectives

Pour terminer cette section, nous mentionnons quelques questions qui nous paraissent intéressantes et qui n'ont pas forcément été abordées dans les parties précédentes.

KVol sur $\mathcal{H}(2)$. Dans le paragraphe précédent, nous avons exhibé des familles de surfaces de $\mathcal{H}(2g-2)$ (pour chaque $g \geq 2$ et chaque composante connexe de $\mathcal{H}(2g-2)$) ayant un KVol arbitrairement proche de g, et conjecturons que cette borne est optimale. Cependant, démontrer que cette borne est optimale est difficile, et ce même en genre deux. Une idée parmi d'autres pourrait être d'utiliser la classification des surfaces de Veech en genre deux et les méthodes d'extension au disque de Teichmüller pour montrer que KVol est supérieur à 2 sur n'importe quelle surface de Veech et conclure par densité. Une autre idée pourrait être

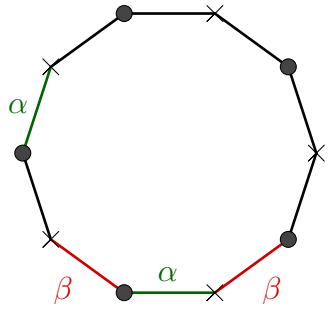

FIGURE 1.33 – Dans cet exemple, les courbes α and β (orientées de sorte à ce que les courbes aient une orientation bien définie) s'intersectent deux fois.

par exemple d'estimer KVol sur des modèles en L de plus en plus généraux. Par exemple, il est facile de démontrer que KVol est strictement plus grand que deux pour une surface en L à base carrée.

KVol pour le décagone. Dans les paragraphes précédents, nous avons vu qu'il était difficile de calculer KVol pour des surfaces de translation à plusieurs singularités. Plus précisément, il n'existe aucun exemple de surface de translation ayant au moins deux singularités dont on sait calculer précisément KVol. Un premier candidat pourrait être le décagone, qui possède deux singularités et pour lequel une méthode de découpage plus sophistiquée pourrait permettre de calculer KVol. Plus précisément, nous conjecturons que KVol pour le décagone est réalisé par deux paires de côtés du décagone qui forment deux courbes fermées, comme sur la Figure 1.33. Remarquons toutefois que la méthode de découpage telle quelle n'est pas suffisante, et il faudrait raffiner à la fois le décompte des intersections et des longueurs. Une idée serait d'utiliser les diagrammes de transition et d'aller une étape plus loin dans la concaténation : au lieu de seulement regrouper les segments adjacents par deux, on pourrait regrouper les segments en plus grands nombres et dans chacun des (très nombreux) cas obtenir une estimation plus précise des longueurs et des intersections. Plus généralement, on peut imaginer déduire d'une suite de côtés intersectés une estimation précise sur la longueur.

Étude de KVol sur le feuilletage du noyau. Comme nous avons étudié KVol sur les disques de Teichmüller de surfaces de Veech, on pourrait se demander ce qu'il se passe lorsqu'on se restreint à un autre sous espace de l'espace des modules : le feuilletage du noyau. Par exemple, étant donné une surface de $\mathcal{H}(1,1)$ représentée par deux tores fendus recollés le long d'une fente : on peut se demander comment varie KVol en fonction des variations de la taille de la fente.

La distribution des rapports. En nous intéressant à KVol, on cherche à maximiser le rapport *Intersection/produit des longueurs*. Une question alternative pourrait être de se demander quelle est la distribution du rapport *Intersection/produit des longueurs* choisi sur toutes les paires de géodésiques fermées.

Analyse asymptotique. En continuant dans cette direction, on peut se demander le rapport *Intersection/produit des longueurs* obtenu en choisissant deux géodésiques "au hasard" sur la surface. On pourrait par exemple espérer obtenir un résultat asymptotique sur le rapport *Intersection / produit des longueurs* lorsque la longueur des courbes augmente, dans l'esprit de [Lal14] pour les auto-intersections sur les surfaces hyperboliques.

1.4 Points de connexion du double heptagone

Nous terminons cette introduction en présentant deux travaux autour des surfaces de translation qui ne font pas intervenir KVol. Dans le premier, [Bou], issu de l'article *Central points of the double heptagon are not connection points* publié au *Bulletin de la SMF*, on s'intéresse aux directions des connexions de selles dans le double n-gone pour n impair et à la question reliée des points de connexions.

Étant donné une surface de translation, on a déjà vu qu'une séparatrice est un segment géodésique qui part d'une singularité et qu'une connexion de selles est un segment géodésique qui va d'une singularité à une autre. Un *point de connexion* est un point (non-singulier) de la surface de translation telle que toute séparatrice passant par ce point s'étend en une connexion de selles. Par exemple, les points ayant une orbite finie sous l'action du groupe affine (appelés *points périodiques*) sont des points de connexion, dits *triviaux*. Une motivation pour l'étude des points de connexions (non-périodiques) est qu'ils permettent de construire des surfaces de translation dont le groupe de Veech est infiniment engendré, voir [HS04].

Les points de connexions d'une surface à petits carreaux (obtenue à partir d'un revêtement ramifié en un point du tore carré) sont exactement les points à coordonnées rationnelles (et coïncident donc avec les points périodiques). Pour une surface de translation dont le corps de trace est de degré 2 sur $\mathbb{Q}$, il n'y a qu'un nombre fini de points périodiques et les points de connexion ne sont plus nécessairement périodiques. Plus précisément, l'étude des directions périodiques des surfaces de Veech ayant un corps de trace quadratique implique que les points de connexion sont exactement les points à coordonnées dans le corps de trace sur la surface normalisée. Cependant, dès que le corps de trace est de dégré 3 ou plus sur $\mathbb{Q}$, ce résultat ne tient plus (voir [AS09]) et on ne connaît aucun exemple de point de connexion non-périodique. Dans [Bou], nous nous intéressons au cas du point central du double heptagone, et nous démontrons :

Théorème G. *Dans le double heptagone, les centres des heptagones ne sont pas des points de connexion.*

Ce résultat est surprenant car le double heptagone est l'exemple le plus naturel de surface de Veech dont le corps de trace est cubique et les centres des heptagones sont des points non-périodiques et pourtant géométriquement particuliers : ce sont donc de bons candidats à être des points de connexion non-périodiques (en particulier, on pouvait espérer arriver à démontrer géométriquement que c'étaient des points de connexion). Cela répond (par la négative) à une question de P. Hubert et T. Schmidt.

Pour démontrer le Théorème G, il suffit d'exhiber une séparatrice qui passe par l'un des points centraux et qui ne s'étend pas en une connexion de selles. Au vu du Théorème 1.2.2, une manière de garantir qu'une séparatrice ne s'étend pas en une connexion de selles consiste à montrer que la direction de cette séparatrice ne correspond pas à une direction d'un point fixe parabolique d'un élément du groupe de Veech. Ici, nous exhibons une séparatrice dont la direction est une direction propre d'un élément hyperbolique du groupe de Veech. Les directions propres hyperboliques et paraboliques d'un groupe Fuchsien étant distinctes, cela démontre le résultat.

Pour ce faire, on traduit la notion de direction propre hyperbolique et parabolique à l'aide du développement en fractions continues de Hecke. Les fractions continues de Hecke ont été introduites dans les années cinquante par Rosen [Ros54].

On a vu que le groupe de Veech du double heptagone est conjugué au groupe de Hecke d'ordre 7, engendré par les matrices $T = \begin{pmatrix} 1 & \Phi_7 \\ 0 & 1 \end{pmatrix}$ et $S = \begin{pmatrix} 0 & -1 \\ 1 & 0 \end{pmatrix}$. De plus, tout nombre réel peut s'écrire sous la forme d'une fraction continue (négative) de Hecke :

$$x = a_0\Phi_7 - \cfrac{1}{a_1\Phi_7 - \cfrac{1}{a_2\Phi_7 - \cdots}}$$

Un nombre réel peut avoir plusieurs développements en fraction continue sous cette forme mais nous choisirons ici le développement obtenu à partir de l'algorithme de fraction continue au multiple de Φ_7 supérieur, décrit dans [SS95]. On a alors :

Théorème 1.4.1 ([SS95]). — *Les directions paraboliques sont exactement les directions dont la pente d s'écrit sous la forme d'une fraction continue de Hecke finie.*

— *Les directions hyperboliques sont exactement les directions dont la pente d s'écrit sous la forme d'une fraction continue de Hecke infinie périodique à partir d'un certain rang.*

La partie de l'énoncé correspondant aux éléments paraboliques s'obtient en remarquant que :

$$a_0\Phi_7 - \cfrac{1}{a_1\Phi_7 - \cfrac{1}{\cdots - \cfrac{1}{a_n\Phi_7}}} = T^{a_0}ST^{a_1}S\cdots ST^{a_N}S(\infty),$$

de sorte qu'une fraction continue finie correspond exactement à l'image de ∞ par un élément du groupe de Veech, et donc à une direction parabolique. Réciproquement, puisque le domaine fondamental associé au groupe de Hecke d'ordre n ne possède qu'un seul cusp, toutes les directions paraboliques sont images de ∞ par un élément de H_n et donc s'écrit sous la forme d'une fraction continue finie. Dans [Bou], nous utilisons en fait une version accélérée de l'algorithme de fractions continues décrite dans [DL18].

Questions et perspectives. Une première question serait de savoir si les points centraux du double n-gone régulier sont des points de connexion pour $n \geq 11$ impair. Nous conjecturons que, comme pour le double heptagone et le double nonagone, ce ne sont pas des points de connexion.

Par ailleurs, le problème de trouver des points de connexion sur le double heptagone (et plus généralement sur le double n-gone pour $n \geq 7$ impair) est étroitement relié à la

question de la caractérisation des directions périodiques. Plus précisément, on aimerait avoir une description algébrique de ces directions. Cette question a été étudiée dès les années 1970 [Leu67], [Bor73] et [BR73] puis plus récemment [HMTY08], [AS09], [CS12], [CS13]. On a par exemple le résultat suivant :

Théorème 1.4.2 ([AS09]). *Tous les éléments de $\mathbb{Q}[\Phi_n]$ ont un développement en fractions continues de Hecke fini si et seulement si $n \in \{3, 4, 5, 6, 8, 10, 12\}$.*

Dans les autres cas, on ne sait pas caractériser algébriquement les directions paraboliques.

1.5 Surfaces de Veech primitives dans $Prym(2, 2)$

Pour terminer cette introduction, nous présentons un travail écrit en collaboration avec Sam Freedman et accepté pour publication dans les *Comptes rendus de l'Académie des sciences*. voir [BF22]. On s'intéresse au problème de classification des surfaces de Veech primitives. Plus précisément, nous utilisons le package Flatsurf développé sur Sage pour démontrer qu'il n'y a pas de surfaces de Veech primitives dans le lieu $Prym(2, 2)$ de $\mathcal{H}(2, 2)$ des surfaces de translation ayant une involution Prym, ce qui achève un travail initié par E. Lanneau et M. Möller [LM19].

Introduction et motivations. Comme nous l'avons vu dans la Section 1.2, parmi toutes les surfaces de translation certaines jouissent de propriétés dynamiques et géométriques particulières : les surfaces de Veech. La question de classifier ces surfaces de Veech est centrale en dynamique de Teichmüller. Une méthode pour classifier les surfaces de Veech peut-être de commencer par chercher celles qui sont *géométriquement primitives*, c'est-à-dire qui ne proviennent pas d'un revêtement d'une autre surface de Veech.

En fait, on connaît assez peu de telles surfaces : on a déjà rencontré les surfaces de Bouw-Möller et le n-gone régulier, mais ce sont les seules familles infinies que l'on connaît en dehors de familles spécifiques en genre 2, 3 ou 4. Pour une présentation des surfaces de Veech connues, on pourra consulter le survol récent [McM21] (voir aussi [Möl18] et [LM19]).

Les surfaces de Veech primitives en genre 2 ont été classifiées dans une série d'articles de C. McMullen [McM05b], [McM05a] et [McM06a]. En genre 3, à part un nombre fini de disques de Teichmüller, toutes les surfaces de Veech géométriquement primitives sont contenues dans un sous-ensemble de l'espace de modules, voir [McM21, Theorem 5.5]. Ce sous-ensemble est constitué des surfaces de translation qui possèdent une involution Prym et qui n'ont qu'une seule singularité. En considérant la surface de translation comme une surface de Riemann X de genre g munie d'une 1-forme holomorphe ω, une involution Prym est une involution $\rho \in \mathrm{Aut}(X)$ telle que $\rho^*(\omega) = -\omega$ (on dit que ω est anti-invariante par ρ) et telle que le quotient X/ρ est de genre $g-2$. Ces surfaces peuvent également s'obtenir à partir de *surfaces de demi-translation* en prenant un revêtement double ramifié en les singularités.

Surfaces de Veech ayant une involution prym. Parmi les surfaces munies d'une involution Prym, on sait ([McM06b, Theorem 3.1]) que celles qui sont des surfaces de Veech sont parmi les surfaces munies d'une *multiplication réelle* par $\mathcal{O}_D := \mathbb{Z}[\sqrt{D}]$, avec $D \in \mathbb{N}$.

Plus précisément, il existe un endomorphisme de la variété jacobienne T, auto-adjoint (pour la forme d'intersection sur la jacobienne) et $\mathbb{C}$-linéaire. Notons qu'un endomorphisme de la jacobienne est automatiquement $\mathbb{R}$-linéaire, mais être $\mathbb{C}$-linéaire impose une vraie restriction. Dans le cas des surfaces Prym, on demande également que T préserve les formes holomorphes anti-invariantes par l'involution Prym ρ. Le polynôme minimal de T est alors de degré deux et son discriminant D est appelé le discriminant associé à la surface (X, ω). Une famille infinie de surfaces de Veech a été ainsi identifiée dans la strate minimale $\mathcal{H}(4)$, qui généralise la construction de McMullen en genre deux, voir [McM06b]. De plus, en genre trois, on sait qu'il n'existe qu'un nombre fini de surfaces de Veech (à l'action de $GL_2^+(\mathbb{R})$ près) en dehors de cette famille, voir [McM21, Théorème 5.5].

Dans l'espoir de trouver d'autres surfaces de Veech, on peut commencer par en chercher parmi les surfaces ayant une involution Prym et une multiplication réelle, mais avec plusieurs singularités. Dans ce contexte, E. Lanneau et M. Möller [LM19] se sont attelés à la recherche des courbes de Teichmüller contenues dans $\mathrm{Prym}(2,1,1)$ et $\mathrm{Prym}(2,2)$. En distinguant selon le discrimant et en utilisant une *condition de torsion* démontrée par M. Möller [Möl04], ils démontrent qu'il n'y a pas de surfaces de Veech primitives dans $\mathrm{Prym}(2,1,1)$ et identifient 92 candidats dans $\mathrm{Prym}(2,2)$. En collaboration avec Sam Freedman, nous avons implémenté ces 92 surfaces et utilisé le package Flatsurf développé dans sage (voir [DRW21, Annexe B]) pour démontrer :

Théorème H. *Il n'y a pas de surfaces de Veech géométriquement primitives dans* $\mathrm{Prym}(2,2)$.

En particulier, le seul cas qui n'a pas encore été regardé est le cas de $\mathrm{Prym}(1,1,1,1)$, qui semble plus technique. Par ailleurs, il est à noter que, en dehors du lieu Prym, K. Winsor [Win22] à démontré récemment que le 14-gone régulier engendre le seul disque de Teichmüller algébriquement primitif dans la composante hyperelliptique de $\mathcal{H}(2,2)$.

Chapitre 2

KVol on double regular n-gons

Résumé en français. Ce chapitre correspond à l'article [BLM22], écrit en collaboration avec E. Lanneau et D. Massart et soumis pour publication, dans lequel nous calculons KVol pour les doubles n-gones ($n \geq 5$ impair). Nous développons ensuite la méthode d'extension au disque de Teichmüller qui permet de calculer KVol sur tout le disque de Teichmüller du double n-gone pour $n \geq 5$ impair. C'est cette méthode que l'on généralisera au Chapitre 5.

Les deux premières sections constituent respectivement une introduction à KVol et aux surfaces de translation (avec un point spécifique sur le double n-gone). Dans la section 3, on présente un premier critère pour borner KVol sur un disque de Teichmüller d'une surface de translation à une seule singularité, ce qui constitue une première étape pour la démonstration du Théorème D, qui sera démontré dans le chapitre suivant. Dans la Section 4, on démontre le Théorème 1.3.2. Dans les Sections 5 et 6, on introduit le matériel nécessaire à l'étude de KVol sur les disques de Teichmüller, qui sera réutilisé aux chapitres suivants dans des contextes légèrement différents. La Section 6 est également dédiée au calcul d'estimées qui permettront de démontrer le Théorème 1.3.8. Enfin, nous démontrons dans la Section 7 une version faible du Théorème 1.3.10 spécifique au double n-gone. Les arguments de la Section 7 seront réutilisés au Chapitre 5 pour démontrer le Théorème 1.3.10 en toute généralité.

ALGEBRAIC INTERSECTION FOR A FAMILY OF VEECH SURFACES

JULIEN BOULANGER, ERWAN LANNEAU, AND DANIEL MASSART

1. Introduction

Our objects of study are translation surfaces and their geodesics. These structures arise in the study of rational polygonal billiards and more generally in Teichmüller dynamics. This paper focuses on computing relations between lengths of geodesics and their intersections on those surfaces.

1.1. **Motivation and results.** For any closed (meaning compact, connected, without boundary) oriented surface X, the algebraic intersection endows the first homology group $H_1(X,\mathbb{R})$ with a symplectic bilinear form denoted $\mathrm{Int}(\cdot,\cdot)$. When X is endowed with a Riemannian metric g (possibly with singularities), one can ask the following question: how much can two curves of a given length intersect? Namely, what is

$$\mathrm{KVol}(X) := \mathrm{Vol}(X,g)\cdot \sup_{\alpha,\beta} \frac{\mathrm{Int}(\alpha,\beta)}{l_g(\alpha) l_g(\beta)}, \tag{1}$$

where the supremum ranges over all piecewise smooth closed curves α and β in X, and $l_g(\cdot)$ denotes the length with respect to the Riemannian metric. It is readily seen that multiplying by the volume $\mathrm{Vol}(X,g)$ makes the quantity invariant by rescaling the metric g. This function is well defined, finite (see [MM14]) and continuous in the metric.

Recent work [CKM21a, CKM21b] provides new estimates of KVol on the Teichmüller curve of some arithmetic translation surfaces (X,ω). In this paper we study the most natural family of non-arithmetic Teichmüller curves $(\mathcal{T}_n)_{n\geq 5}$, generated for $n\geq 5$ by the original Veech surface described in [Vee89], namely the surface arising from the unfolding of a right-angled triangle with angles $(\pi/2, \pi/n, (n-2)\cdot\pi/2n)$. For odd n, $\mathcal{T}_n$ is canonically identified with $\mathbb{H}^2/\Gamma_n$ where Γ_n is the Hecke triangle group of signature $(2,n,\infty)$ (see §2.1 and §4). In this context, we establish the first known explicit formula for KVol (beyond the case of the moduli space of flat tori, see [MM14]):

Theorem 1.1. *For odd integer $n\geq 5$, and any $(X,\omega)\in\mathcal{T}_n$, we have*

$$KVol(X,\omega) = \frac{\frac{n}{2}\cot\frac{\pi}{n}\cdot\frac{1}{\sin\frac{\pi}{n}}}{\cosh d_{\mathrm{hyp}}(X,\gamma_{0,\infty})},$$

where $\gamma_{0,\infty}$ is the hyperbolic geodesic in $\mathbb{H}^2$ with endpoints 0 and ∞.

2020 *Mathematics Subject Classification.* Primary: 37E05. Secondary: 37D40.
Key words and phrases. Lyapunov exponents.

In particular KVol is real analytic on $\mathcal{T}_n$ except along the geodesic with endpoints $\cos\frac{\pi}{n}$ and ∞.

1.2. **Context and history.** While KVol is a close cousin of the systolic ratio $\sup_\alpha \frac{\mathrm{Vol}(X,g)}{l_g(\alpha)^2}$, very little is known on the function KVol. For any Riemannian surface (X,g), we have $\mathrm{KVol}(X,g)\geq 1$, and equality holds if and only if (X,g) is a flat torus [MM14]. Almost all of the obvious questions about KVol on hyperbolic surfaces are currently open. In this paper we propose to continue the study of KVol as a function on the moduli space of translation surfaces, originally initiated by the third named author in [CKM21a, CKM21b]. The surface X is called a translation surface if it is equipped with a translation structure, that is, an atlas of charts such that all transition functions are translations in $\mathbb{R}^2$. We assume that the chart domains cover all the surface X except for finitely many points called singularities. The translation structure induces the structure of a smooth manifold and a flat Riemannian metric on X punctured at the singular points. We require that the metric have a cone type singularity at each singular point. Although geodesics on X are piecewise straight lines, they can be quite complicated: they may be unions of saddle connections with different directions.

More specifically, in [CKM21a], KVol is studied for ramified covers of the torus (or arithmetic Teichmüller curves). It is proved in [CKM21a] that KVol, defined on the Teichmüller disc of the surface tiled with three squares, is unbounded, but it does have a minimum, achieved at a surface, unique modulo symmetries, and otherwise fairly undistinguished. The interesting surfaces, i.e. the three square surfaces, and the surface tiled with six equilateral triangles, are local maxima, with $\mathrm{KVol}=3$, where 3 should be thought of as the ratio of the total area of the surface, to the area of the smallest cylinder of closed geodesics. The local maxima are not locally unique, they come in hyperbolic geodesics, in the Teichmüller curve viewed as a quotient of the hyperbolic plane by a Fuchsian group.

In the current paper, we extend the study to non arithmetic Teichmüller curves.

1.3. **KVol on non arithmetic Teichmüller curves.** Teichmüller curves are isometrically immersed algebraic curves in the moduli space of Riemann surfaces. These arise as $\mathrm{SL}(2,\mathbb{R})$-orbit (or Teichmüller disc) of special flat surfaces that are called Veech surfaces. For $n=2m+1\geq 5$ we will denote by X_0 the original Veech surface [Vee89] arising from the unfolding a right-angled triangle with angles $(\pi/2,\pi/n,(n-2)\cdot\pi/2n)$, also referred to as the *double regular $n-$gon*. The surface X_0 lies in the stratum $\mathcal{H}(n-3)$ and its genus is $\mathrm{genus}(X_0)=(n-1)/2$. From Theorem 1.1, we deduce the

Corollary 1.2. *For any $X\in\mathcal{T}_n$ the following holds*

$$\frac{n}{2}\cot\frac{\pi}{n}\leq \mathit{KVol}(X)\leq \frac{n}{2}\cot\frac{\pi}{n}\cdot\frac{1}{\sin\frac{\pi}{n}}.$$

Moreover the bounds are sharp and:

(1) The maximum of the function KVol on $\mathcal{T}_n$ is achieved, precisely, along $\gamma_{0,\infty}$, that is, by images of the right-angled staircases under the Teichmüller geodesic flow (see Figure 1).
(2) The minimum of the function KVol on $\mathcal{T}_n$ is achieved, uniquely, at X_0.

Finally, in the definition of KVol, the supremum is achieved by pairs of curves that are (images of) pairs of sides of the double regular $n-$gon.

Remark 1.3. The case of the regular $4m$-gon is dealt with in a forthcoming paper of the first author. When $n \equiv 2 \mod 4$, the surface X_n belongs to a stratum with two conical points. This case is combinatorially a bit more complicated and we set it aside for future work.

Unlike the three-square surface case [CKM21a], KVol is bounded on the Teichmüller discs of the double regular $n-$gon. More generally we show

Theorem 1.4. *The function KVol is bounded on the Teichmüller disc of $X \in \mathcal{H}(2)$ if and only if X is a primitive Veech surface i.e. X is not arithmetic.*

The same discussion applies to the Teichmüller disc of surfaces in the Prym eigenform loci in $\mathcal{H}(4)$ and $\mathcal{H}(6)$ (see [LN14]) by looking at possible cylinder diagrams. We suspect that KVol is never bounded from above on the Teichmüller disc of arithmetic Veech surfaces. The first author recently obtained an example of a non arithmetic Teichmüller disc where KVol is *unbounded*.

Remark 1.5. Another difference with [CKM21a] is that the minimum of KVol on $\mathcal{T}_n$ is achieved, uniquely, by the most interesting surface in the disc, namely the double $n-$gon. On the other hand, similarly to the three-square case, the local maxima, which are also global maxima are achieved along hyperbolic geodesics in the Teichmüller disc, which correspond to surfaces with a right-angled template, see Figure 1.

1.4. **Comparison of norms.** The quantity KVol appears naturally in the comparisons between the stable norm $||\cdot||_s$ and the Hodge norm. More precisely (see [Mas97, MM14]):

$$||\cdot||_s \leq \sqrt{\mathrm{Vol(M,g)}}||\cdot||_{\mathrm{Hodge}} \leq \mathrm{KVol}(M,g)||\cdot||_s$$

The upper bound is sharp. More recently, in the context of quadratic differentials, a new comparison between Hodge and Teichmüller norms has been established in [KW22]. The latter is useful for the proof of effective versions of results on dynamics of mapping class groups (see the work [AH22]). It would be interesting to establish an analogue of Theorem 1.1 for the Hodge and Teichmüller norms and see wether it gives better effective results on mapping class groups.

1.5. **Organization of the paper.** In §2.1 we recall prerequisites on translation surfaces, Veech groups, Veech surfaces, and we describe the right-angled staircase models for our surfaces. In §3 we explain why KVol is bounded on some Teichmüller curves. In §4 and §5 we explain how to interpret KVol geometrically, in terms of hyperbolic distance on the Teichmüller curve (identified with a quotient of $\mathbb{H}^2$ by a Fuchsian group), and we give an upper bound for

KVol on the Teichmüller curve. In particular this proves that the maximum is achieved by the staircase surfaces.

In §6 we perform the first main step of the proof: we compute KVol for the double n-gon, by a geometric method, carefully looking at how saddle connections intersect depending on their directions.

In §7 we perform the second main step of the proof: we interpolate, by analytical methods, between the double n-gon and the staircase surfaces, thus proving that the minimum is achieved, uniquely, by the former.

Acknowledgments. This work has been partially supported by the LabEx PERSYVAL-Lab (ANR-11-LABX-0025-01) funded by the French program Investissement d'avenir.

2. Background

2.1. **Preliminaries.** We review useful results concerning flat surfaces, Veech groups and Teichmüller curves. For a general introduction to translation surfaces and their moduli spaces, we refer the reader to the surveys [Zor06, Wri16, Mas22] and the references therein. Throughout this paper, $\mathcal{H}(k_1, \dots, k_r)$ will denote the stratum of moduli space of Abelian differentials ω on Riemann surfaces X of genus $g \geq 1$, having r zeros, of orders k_i for $i = 1, \dots, r$, or equivalently of angles $2\pi(k_i + 1)$. For simplicity we will simply denote X for the pair (X, ω) if the context is clear.

As previously mentioned, geodesics on translation surfaces can be complicated. However for X in the minimal stratum $\mathcal{H}(2g-2)$, any geodesic is homologous to a union of *closed* saddle connections. Hence the supremum in Equation (1) can be taken over all saddle connections of the surface.

We denote the holonomy vector of a saddle connection α by $\overrightarrow{\alpha} = \int_\alpha \omega \in \mathbb{R}^2$. By abuse of notation we will often confuse $\overrightarrow{\alpha}$ with α. We have $l(\alpha) = ||\overrightarrow{\alpha}||$.

A Teichmüller curve is an isometrically immersed complex curve in the moduli space of Riemann surfaces. The projection of a closed $\mathrm{GL}_2(\mathbb{R})$-orbit to the moduli space of Riemann surfaces is a Teichmüller curve, so as is common we will also refer to closed $\mathrm{GL}_2(\mathbb{R})$-orbits as Teichmüller curves in $\mathcal{H}(k_1, \dots, k_r)$. A point on a closed $\mathrm{GL}_2(\mathbb{R})$-orbit is called a Veech surface. Equivalently a translation surface is a Veech surface if and only if its Veech group is a lattice in $\mathrm{SL}_2(\mathbb{R})$. The easiest examples of Teichmüller curves are orbits of arithmetic surfaces (namely ramified covers of the two-torus). Veech [Vee89] discovered a family of non arithmetic surfaces arising from a right-angled triangle with angles $(\pi/2, \pi/n, (n-2)\cdot\pi/2n)$ by the unfolding construction described in [ZK76]. We give a description of these surfaces in the next section.

2.2. **The staircase model for the double $n-$gon.** For $n \geq 3$, the surface X_0 (arising from the unfolding of a right triangle with angles $(\pi/2, \pi/n, (n-2)\pi/2n)$) can be described as follows (see [ZK76, Vee89])

- If $n \geq 8$ is even then X_0 is the quotient of the regular $n-$gon (with radius 1) by gluing opposite sides by translation. Moreover, if $n = 4m$ for $m \geq 2$ the surface belongs to the stratum $\mathcal{H}(2m-2)$, while if $n = 4m+2$ it belongs to the stratum $\mathcal{H}(m-1, m-1)$.

- If $n \geq 5$ is odd, then X_0 is the quotient of the double of the regular $n-$gon (with radius 1) by gluing opposite sides by translation. It belongs to the stratum $\mathcal{H}(n-3)$.

As mentioned in the introduction we will focus on the latter case and in the sequel we will assume $n = 2m+1$ is an odd integer.

The double n-gon X_0 has a staircase model S_0 in its $\mathrm{GL}_2(\mathbb{R})$-orbit, drawn in Figure 1 and described in [Mon05], which we shall use with a few modifications (see also [Vee89, §5]). In order to exhibit the Veech group and a fundamental

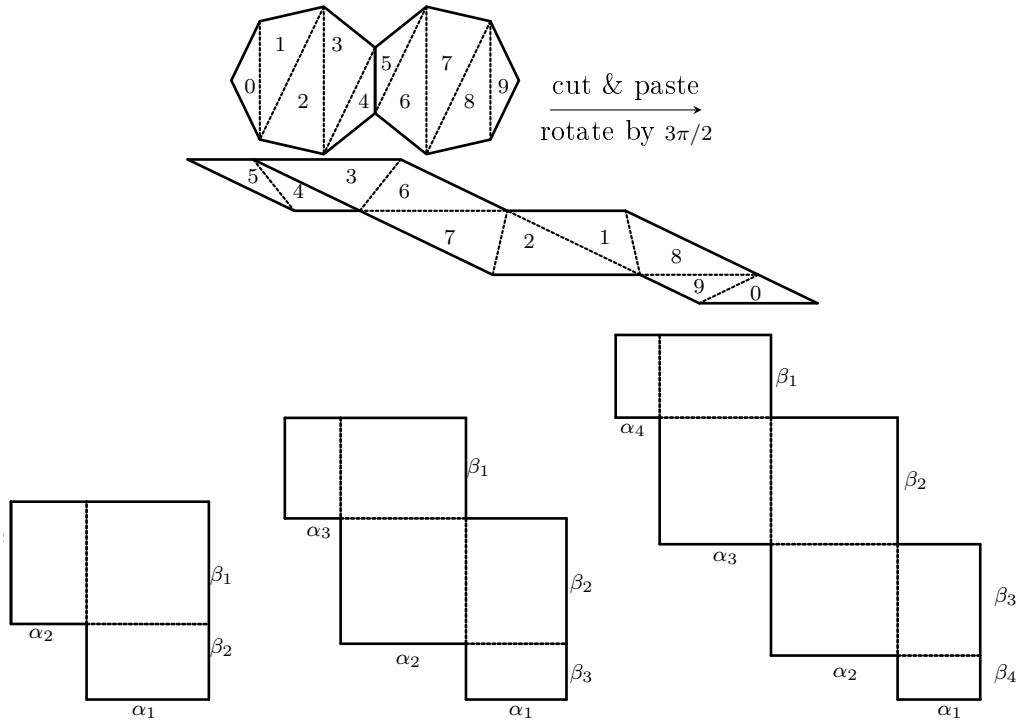

FIGURE 1. Above, the double $(2m+1)-$gon X_0 is cut into $2(2m-1)$ triangles, which are re-arranged into a slanted stair-shape, whose slanted sides are then rotated and sheared to create the right-angled stair-shape S_0. Below, a staircase model S_0 for X_0 ($n = 2m+1$), for $m = 2, 3, 4$, with parameters $(\alpha_i, \beta_i)_{i=1,\dots,m}$. The surface S_0 for $m = 2$ is usually shown rotated by 180 degrees, as the golden L (see [DFT11], [DL19]).

domain, one needs to compute the dimensions of the m horizontal cylinders of S_0. This immediately follows from [Vee89, §5]: for $k = 1, \dots, m$, the core curve of the kth cylinder of S_0 is given by $\alpha_{k-1} + \alpha_k$ (with the dummy condition

$\alpha_0 := 0$), and its height is β_{m-k+1}. From [Vee89, §5] we draw:

$$(2)\quad l(\alpha_k) = l(\beta_k) = \sin\frac{2k\pi}{n},\ \text{for any } k = 1, \dots, m,\ \text{and } \mathrm{Vol}(S_0) = \frac{n}{2}\cos\frac{\pi}{n}.$$

In particular all moduli are the same and equal to

$$\frac{height}{width} = \frac{\sin\frac{2(m-k+1)\pi}{n}}{\sin\frac{2(k-1)\pi}{n} + \sin\frac{2k\pi}{n}} = \frac{\sin\frac{(2k-1)\pi}{n}}{2\sin\frac{2(k-1+k)\pi}{2n}\cos\frac{2(k-1-k)\pi}{2n}} = \frac{1}{2\cos\pi/n}.$$

From this knowledge, it is easy to construct affine homeomorphisms of S_0 whose derivative maps (outside the singularity) are parabolic elements. We describe the Veech group of S_0 in the next section.

2.3. **Veech group and fundamental domain.** For $n \geq 3$, we denote by Γ_n the Hecke triangle group of level n (or signature $(2, n, \infty)$) generated by

$$T = \begin{pmatrix} 1 & \Phi_n \\ 0 & 1 \end{pmatrix} \text{ and } R = \begin{pmatrix} 0 & -1 \\ 1 & 0 \end{pmatrix},\ \text{setting } \Phi_n = 2\cos\frac{\pi}{n}.$$

In the following we will simply use the notation Φ for Φ_n. The group Γ_n, acting on the hyperbolic plane $\mathbb{H}^2$, has a fundamental domain $\mathcal{D}$ depicted in Figure 2. It is comprised between the vertical geodesics with abscissae $-\Phi/2$ and $\Phi/2$, and the geodesic with endpoints ± 1. The Veech group of S_0 coincides with Γ_n. In the fundamental domain the staircase model S_0 is represented by the point i, while X_0 corresponds to the lower corners of $\mathcal{D}$ (the intersection between a vertical boundary and the circular boundary).

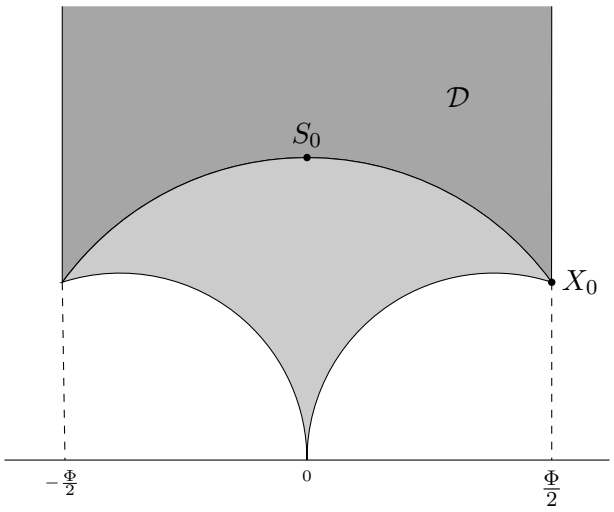

FIGURE 2. A fundamental domain $\mathcal{D}$ of the Veech group of the staircase model of the double regular $(2m+1)$-gon, along with its reflection in the geodesic $(-1, 1)$.

3. Boundedness of KVol on Teichmüller discs

Before studying the maximum of KVol on Teichmüller discs, we give a criterion to ensure that it is indeed a bounded function. We conclude this section with a proof of Theorem 1.4.

We can first notice that if there are two parallel saddle connections α, β on $X \in \mathcal{H}(n-3) = \mathcal{H}(2m-2)$ having non trivial intersection then applying the Teichmüller geodesic flow in the orthogonal direction of α, β, we get for all $t > 0$

$$\mathrm{KVol}(g_t X) \geq \frac{1}{e^{-2t}|\alpha||\beta|}.$$

Thus KVol is not bounded on the Teichmüller disc of X. Actually, this remark applies to a large class of translation surfaces (of genus at least two): those decomposed into a single metric cylinder, as we will see below.

Before proving Lemma 3.1 we recall the notion of the angle of a horizontal saddle connection on a surface whose horizontal foliation has only closed leaves. The union of all (horizontal) saddle connections and the singularity defines a finite oriented graph Γ. Orientation on the edges comes from the canonical orientation of the horizontal foliation. At the singularity p the direction of saddle connections attached to p alternates (between directions toward p and from p) as we follow the clockwise order. For a saddle connection γ one can count the number of different sectors between the two directions it determines. This gives an angle $(2k+1)\pi$ well defined modulo $2(2m-1)\pi$. Observe that if γ has angle π then it is the boundary of a metric cylinder embedded into the surface.

Lemma 3.1. *If X has a cylinder decomposition all of whose boundary saddle connections have trivial intersection pairwise, then there is a saddle connection with angle π. In particular if X has a one cylinder decomposition and* $\mathrm{genus}(X) > 1$ *then there are two parallel saddle connections intersecting non trivially.*

Proof. We consider the saddle connection γ having the smallest angle $(2k+1)\pi$ at p (see Figure 3). Assume $k > 0$. Then γ determines $2k+1$ sectors and so $2k$ saddle connections $\beta_1, \ldots, \beta_{2k}$. Since the angle of γ is minimal, no β_i can begin and end inside the sector of angle $(2k+1)\pi$ cut by γ. Therefore the intersection of β_i with γ is non trivial for every $i = 1, \ldots, k$. □

From this observation and the fact that one-cylinder surfaces are dense, we immediately deduce that KVol is not bounded on any connected component of $\mathcal{H}(2m-2)$ for $m \geq 2$. Similarly, since KVol is a continuous function, it is not bounded on the Teichmüller disc of a generic (with respect to the Masur–Veech measure) surface X. Veech surfaces are exceptionally symmetric translation surfaces and are not generic if $m \geq 2$. For those surfaces one has the following converse.

Proposition 3.2. *KVol is bounded on the Teichmüller disc of a Veech surface in $\mathcal{H}(2m-2)$ if there are no parallel saddle connections intersecting non trivially.*

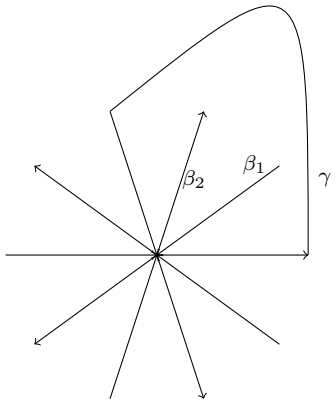

FIGURE 3. A separatrix diagram in $\mathcal{H}(6)$. The singularity p has conical angle 10π and α has angle 3π (or 7π modulo 10π)

Proof of Proposition 3.2. Let us consider only surfaces which have total area 1. Let X be a Veech surface. Let θ be the angle associated to two periodic directions (d, d') having saddle connections α, β with nontrivial intersections. The hypothesis ensures that $d \neq d'$, so that up to swapping d and d' we may assume $\theta \in]0, \pi[$. Then, any intersection between a saddle connection α with direction d, and a saddle connection β with direction d', if it occurs outside the singularity, is positive. Therefore, given two saddle connections α and β, with respective directions d and d', either $\mathrm{Int}(\alpha, \beta) = -1$, in which case α and β intersect only once, at the singularity, or $\mathrm{Int}(\alpha, \beta) \geq 0$.

By Veech dichotomy, X is decomposed into cylinders $C_1, \ldots, C_r$ (of heights $h_1(d), \ldots, h_r(d)$) with direction d and saddle connections α_i. Observe that in the minimal stratum $\mathcal{H}(2m-2)$ the number of cylinders r is bounded by the genus m of the surface. We can subdivide β by looking at the intersections $\mathrm{Int}(\alpha_k, \beta)$. This gives:

$$l(\beta) \cdot \sin\theta = \sum_{k=1}^{r} h_k(d)\mathrm{Int}(\alpha_k, \beta) = \sum_{k=1}^{r} c_k(d)\frac{\mathrm{Int}(\alpha_k, \beta)}{l(\alpha_k)}, \tag{3}$$

where $c_k(d) = h_k(d) \cdot l(\alpha_k)$ represents the area of an embedded parallelogram supported on α_k. We write $l(\alpha_k)l(\beta) = \alpha_k \wedge \beta / \sin\theta$, so

$$1 = \sum_{k=1}^{r} c_k(d)\frac{\mathrm{Int}(\alpha_k, \beta)}{\alpha_k \wedge \beta}.$$

Writing in a slightly different way:

$$1 = \sum_{\mathrm{Int}>0} c_k(d)\frac{\mathrm{Int}(\alpha_k, \beta)}{\alpha_k \wedge \beta} - \sum_{\mathrm{Int}=-1} \frac{c_k(d)}{\alpha_k \wedge \beta}.$$

By [Vor96], there are no small triangles in X *i.e.* there exists $M > 0$, depending only on X, such that $|\alpha_k \wedge \beta| > M$ (this is actually the easy part of the characterization of Veech surfaces in [SW10]). In particular since $c_k(d) \leq \text{Area(X)} = 1$, we have

$$\sum_{\text{Int}=-1} \frac{c_k(d)}{\alpha_k \wedge \beta} < r \cdot \frac{1}{M} < C$$

for some uniform constant $C = C(X)$ (recalling $r \leq m$). Thus

$$\frac{\text{Int}(\alpha_k, \beta)}{\alpha_k \wedge \beta} < \frac{1+C}{c_k(d)} < \frac{1+C}{M}.$$

Hence $\dfrac{\text{Int}(\alpha_k, \beta)}{l(\alpha_k) l(\beta)}$ is uniformly bounded on the Teichmüller disc of X. Since $\text{Area}(X) = 1$, KVol is uniformly bounded as well. □

In $\mathcal{H}(2)$ we have a more precise description.

Proof of Theorem 1.4. By [McM07] Teichmüller discs are either dense or closed. So if X is not a Veech surface, KVol is not bounded from above on its Teichmüller disc. For Veech surfaces, a quick inspection of possible cylinder diagrams leads to the following observation: for two-cylinder decompositions, there are no parallel saddle connections with non trivial intersections. Now a Veech surface in genus two is either primitive or square-tiled. By [McM05, Corollary A.2], square-tiled surfaces all admit one-cylinder decompositions. Since primitive Veech surfaces in $\mathcal{H}(2)$ do not have one-cylinder decompositions, we get the desired result. □

4. $\text{SL}_2(\mathbb{R})$−action and directions in the Teichmüller disc

The action of $\text{SL}_2(\mathbb{R})$ on moduli spaces provides a powerful tool to study the dynamics of the translation flow on X. This group is also acting affinely on surfaces, preserving the intersection form. Saddle connections are mapped to saddle connections, but lengths are not preserved in general. The right quantity to consider is not the length of α or β but rather the quantity $\overrightarrow{\alpha} \wedge \overrightarrow{\beta} = l(\alpha) l(\beta) \sin\theta$, where θ is the angle between the holonomy vectors $\overrightarrow{\alpha}, \overrightarrow{\beta}$ associated to α, β. The wedge product is invariant under $\text{SL}_2(\mathbb{R})$ and is twice the area of a (virtual) triangle delimited by α and β.

This observation motivates the following definition.

Definition 4.1. For $d \in \mathbb{R}P^1$, we say that a saddle connection in S_0 has direction d if it has direction d in the plane template of Figure 1. For $M \in \text{GL}_2^+(\mathbb{R})$ we say that a saddle connection α in $M \cdot S_0$ has direction d if $M^{-1} \cdot \alpha$ has direction d in S_0.

This is a bit counter-intuitive because α may not have direction d in a plane template for $M \cdot S_0$, but it makes sense with the following

Proposition 4.2. *Using the identifications* [1]

$$\Psi : d = [x : y] \in \mathbb{R}P^1 \mapsto -\frac{x}{y} \in \mathbb{R} \cup \{\infty\} \equiv \partial\mathbb{H}^2$$

and, for $M = \begin{pmatrix} a & b \\ c & d \end{pmatrix} \in SO_2(\mathbb{R})\backslash GL_2^+(\mathbb{R})$,

$$\chi : M \cdot S_0 \in \mathcal{T}_n \mapsto \frac{di+b}{ci+a} \in \mathbb{H}^2,$$

the locus of surfaces in $\mathcal{T}_n$ *where the directions* d *and* d' *make an (unoriented) angle* $\theta \in]0, \frac{\pi}{2}]$ *is the banana neighbourhood*

$$\gamma_{d,d',r} = \{z \in \mathbb{H}^2 : d_{\mathrm{hyp}}(z, \gamma_{d,d'}) = r\}$$

where $\cosh r = \dfrac{1}{\sin\theta}$, $\gamma_{d,d'}$ *denotes the hyperbolic geodesic with endpoints* $\Psi(d)$ *and* $\Psi(d')$, *and* d_{hyp} *is the hyperbolic distance.*

In particular, the locus of surfaces in $\mathcal{T}_n$ *where the directions* d *and* d' *are orthogonal is the hyperbolic geodesic with endpoints* $\Psi(d)$ *and* $\Psi(d')$.

Notation 4.3. In the rest of the paper, we denote by $\theta(X, d, d')$ the angle between the directions d and d' in the surface $X = M \cdot S_0$. Notice that Proposition 4.2 gives

$$\cosh d_{hyp}(X, \gamma_{d,d'}) = \frac{1}{\sin\theta(X, d, d')}.$$

Proof of Proposition 4.2. For $\theta \in]0, \frac{\pi}{2}]$ and $u, v \in \mathbb{R}^2$ with equivalence classes $d \neq d'$ we define

$$\mathcal{M}(d, d', \theta) = \{M \in GL_2^+(\mathbb{R}) : \min(\mathrm{angle}(\pm Mu, \pm Mv), \mathrm{angle}(\pm Mv, \pm Mu)) = \theta\}.$$

Observe that $\mathcal{M}(d, d', \theta)$ is well defined (it only depends on the equivalence classes d, d' because the angles are taken modulo π) and equivariant by right multiplication: if $G \in GL_2^+(\mathbb{R})$ then

$$\mathcal{M}(d, d', \theta).G = \mathcal{M}(G^{-1}d, G^{-1}d', \theta). \tag{4}$$

Denote $\bar{\mathcal{M}}(d, d', \theta)$ the projection of $\mathcal{M}(d, d', \theta)$ to $\mathbb{H}^2$. Observe that $\mathcal{M}(d, d', \theta)$ is invariant by left multiplication by $SO_2(\mathbb{R})$, so any matrix in $GL_2^+(\mathbb{R})$ that projects to an element of $\bar{\mathcal{M}}(d, d', \theta)$, is actually in $\mathcal{M}(d, d', \theta)$.

Let us look at the case $d = (\bar{1}_0) = \infty$ and $d' = (\bar{0}_1) = 0$. Observe that in that case $\bar{\mathcal{M}}(d, d', \theta)$ is invariant by $z \mapsto \lambda z$, for any $\lambda > 0$. Indeed, take $\lambda > 0$ and $z \in \bar{\mathcal{M}}(d, d', \theta)$, and let

$$M = \begin{pmatrix} a & b \\ c & d \end{pmatrix}$$

[1] Note that χ defines a right action of $GL_2^+(\mathbb{R})$. See [Mas22, Section 6.1], as to why we should quotient by $SO_2(\mathbb{R})$ on the left, and act by $GL_2^+(\mathbb{R})$ on the right.

be an element of $\mathcal{M}(d,d',\theta) \subset GL_2^+(\mathbb{R})$ which projects to z. Then the matrix

$$M' = \begin{pmatrix} a & b \\ c & d \end{pmatrix} \begin{pmatrix} 1 & 0 \\ 0 & \lambda \end{pmatrix} \in GL_2^+(\mathbb{R})$$

projects to λz. But the equivalence class, in $\mathbb{R}P^1$, of $\left(\begin{smallmatrix} 1 & 0 \\ 0 & \lambda \end{smallmatrix}\right)\left(\begin{smallmatrix} 1 \\ 0 \end{smallmatrix}\right)$ (resp. $\left(\begin{smallmatrix} 1 & 0 \\ 0 & \lambda \end{smallmatrix}\right)\left(\begin{smallmatrix} 0 \\ 1 \end{smallmatrix}\right)$), is d (resp. d'), and we have seen that $\mathcal{M}(d,d',\theta)$ only depends on the equivalence classes d, d', so $M \in \mathcal{M}(d,d',\theta)$ entails $M' \in \mathcal{M}(d,d',\theta)$. Therefore $\lambda z \in \bar{\mathcal{M}}(d,d',\theta)$.

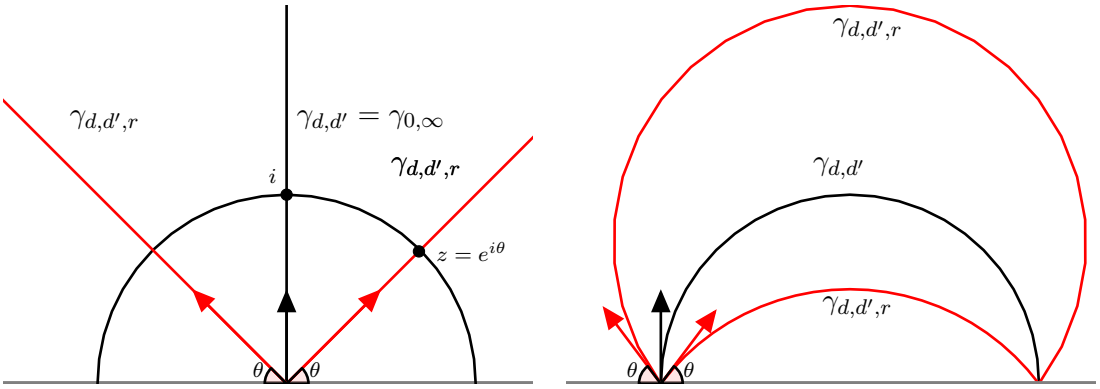

FIGURE 4. The set $\gamma_{d,d',r}$ for $\cosh r = \frac{1}{\sin\theta}$.

Thus, to determine $\bar{\mathcal{M}}(d,d',\theta)$, it suffices to determine its intersection with the horizontal straight line $\{y = 1\}$, which we parametrize as

$$\left\{ i + \cot\alpha : \alpha \in]0,\pi[\right\}$$

A corresponding set of matrices in $GL_2^+(\mathbb{R})$ is given by

$$\left\{ \begin{pmatrix} 1 & \cot\alpha \\ 0 & 1 \end{pmatrix} : \alpha \in]0,\pi[\right\}$$

which sends $\left(\begin{smallmatrix} 1 \\ 0 \end{smallmatrix}\right)$ and $\left(\begin{smallmatrix} 0 \\ 1 \end{smallmatrix}\right)$ to, respectively, $\left(\begin{smallmatrix} 1 \\ 0 \end{smallmatrix}\right)$ and $\left(\begin{smallmatrix} \cot\alpha \\ 1 \end{smallmatrix}\right)$. The angle of the latter vectors is α, so $\bar{\mathcal{M}}(d,d',\theta) \cap \{y = 1\} = \{\left(\begin{smallmatrix} \cot\theta \\ 1 \end{smallmatrix}\right)\}$. Therefore, $\bar{\mathcal{M}}(d,d',\theta)$ is the half-line which starts at the origin, with co-slope $\cot\theta$. This is precisely $\gamma_{d,d',r}$ with $\cosh r = \frac{1}{\sin\theta}$, since the hyperbolic distance from $z = e^{i\theta}$ to the geodesic $\gamma_{0,\infty}$ is realized by the geodesic η parameterized by $\eta(t) = e^{it}$ for $t \in [\theta, \pi/2]$, so that by definition

$$r = \mathrm{d}_{hyp}(z, \gamma_{d,d'}) = l_{\mathrm{hyp}}(\eta) = \int_\theta^{\pi/2} \frac{dt}{\sin t} = \frac{1}{2}\log\frac{1+\cos\theta}{1-\cos\theta},$$

thus $\cos\theta = \frac{e^{2r}-1}{e^{2r}+1}$, and

$$\sin\theta = \sqrt{1-\cos^2\theta} = \sqrt{1-\left(\frac{e^{2r}-1}{e^{2r}+1}\right)^2} = \frac{2e^r}{e^{2r}+1} = \frac{1}{\cosh r}.$$

Now let us consider the general case. Pick $G \in GL_2^+(\mathbb{R})$ taking directions d, d' to $\left(\begin{smallmatrix} 1 \\ 0 \end{smallmatrix}\right) = \infty$ and $\left(\begin{smallmatrix} 0 \\ 1 \end{smallmatrix}\right) = 0$ respectively. Then, by Equation 4,

$\mathcal{M}(\infty,0,\theta).G = \mathcal{M}(d,d',\theta)$, so $\bar{\mathcal{M}}(d,d',\theta)$ is the image of $\bar{\mathcal{M}}(\infty,0,\theta)$ by the orientation-preserving isometry of $\mathbb{H}^2$ corresponding to the action of G. One verifies that this isometry sends ∞ and 0 to the images of the directions d and d' by the identification $\mathbb{R}P^1 \simeq \partial\mathbb{H}^2$ via the opposite of the co-slope, respectively. This finishes the proof. □

5. Another look at KVol

Recall that the function KVol can be expressed as a supremum over saddle connections α, β in (1). We will use the invariance of $\mathrm{Int}(\cdot,\cdot)$ for the affine action of $\mathrm{SL}_2(\mathbb{R})$ on translation surfaces and the invariance of $\wedge$ for the linear action of $\mathrm{SL}_2(\mathbb{R})$ on $\mathbb{R}^2$ in order to have a more suitable formula to work with. In the sequel we will use the notation $K(X)$:

$$\mathrm{KVol}(X) = \mathrm{Vol}(X) \cdot K(X).$$

Proposition 5.1. *Let $\mathcal{P}$ be the set of periodic directions in $X = M \cdot S_0$ for some $M \in \mathrm{SL}_2(\mathbb{R})$. Then*

$$K(X) = \sup_{\substack{d,d' \in \mathcal{P} \\ d \neq d'}} K(d,d') \cdot \sin\theta(X,d,d'),$$

where $K(d,d') = \sup_{\substack{\alpha \subset S_0 \text{ in direction } d \\ \beta \subset S_0 \text{ in direction } d'}} \frac{\mathrm{Int}(\alpha,\beta)}{\alpha\wedge\beta}$ and $\theta(X,d,d')$ is the angle given in Notation 4.3.

Observe that the quantity $K(d,d')$ is invariant under the diagonal action of the Veech group Γ. Moreover $\sin\theta(X,d,d') = 1/\cosh r$, where r is the hyperbolic distance between X and the geodesic $\gamma_{d,d'}$, by Proposition 4.2.

Proof of Proposition 5.1. Given two saddle connections $\alpha, \beta \subset X$ having directions d, d' (in X) and making an angle θ, one has $\alpha \wedge \beta = l(\alpha)l(\beta)\sin\theta$. Notice that parallel saddle connections do not intersect in X, so we will assume $d \neq d'$. By definition these saddle connections are the images by M of saddle connections $\alpha', \beta' \subset S_0$ having directions d, d' (in S_0), and thus $M \in \mathcal{M}(d,d',\theta)$. In particular the projection of M to $\mathbb{H}^2$, that is $X \in \bar{\mathcal{M}}(d,d',\theta)$, gives $\theta = \theta(X,d,d')$.

Now, by definition (see (1)),

$$\sup_{\alpha,\beta}\frac{\mathrm{Int}(\alpha,\beta)}{l(\alpha)l(\beta)} = \sup_{\substack{d,d'\in\mathcal{P}\\ d\neq d'}}\ \sup_{\substack{\alpha\subset X \text{ in direction } d\\ \beta\subset X \text{ in direction } d'}}\frac{\mathrm{Int}(\alpha,\beta)}{l(\alpha)l(\beta)}$$

$$= \sup_{\substack{d,d'\in\mathcal{P}\\ d\neq d'}}\ \sup_{\substack{\alpha\subset X \text{ in direction } d\\ \beta\subset X \text{ in direction } d'}}\frac{\mathrm{Int}(\alpha,\beta)}{\alpha\wedge\beta}\cdot\sin\mathrm{angle}(\alpha,\beta)$$

$$= \sup_{\substack{d,d'\in\mathcal{P}\\ d\neq d'}}\ \sup_{\substack{M^{-1}\alpha\subset S_0 \text{ in direction } d\\ M^{-1}\beta\subset S_0 \text{ in direction } d'}}\frac{\mathrm{Int}(M^{-1}\alpha,M^{-1}\beta)}{M^{-1}\alpha\wedge M^{-1}\beta}\cdot\sin\theta(X,d,d')$$

$$= \sup_{\substack{d,d'\in\mathcal{P}\\ d\neq d'}} K(d,d')\cdot\sin\theta(X,d,d')$$

as desired. □

We end this section with the following computation of $K(0,\infty)$ and $K(0,\Phi)$, for later use.

Proposition 5.2. *The following hold:*

(i) $K(0,\infty)=\frac{1}{l(\alpha_m)^2}$ *and* $K(0,\Phi)=\frac{1}{\Phi}\cdot K(0,\infty)$.

(ii) $\forall (d,d')\notin\Gamma_n\cdot(0,\infty)$, $K(d,d')\leq K(0,\Phi)$.

Proof of Proposition 5.2. (i) We use the notations of Figure 1. The directions $d=0$ and $d'=\infty$ correspond to the vertical and the horizontal, respectively. By definition

$$K(0,\infty)=\sup_{\substack{\alpha\subset S_0 \text{ horizontal}\\ \beta\subset S_0 \text{ vertical}}}\frac{\mathrm{Int}(\alpha,\beta)}{l(\alpha)l(\beta)}=\sup_{i,j=1,\dots,m}\frac{\mathrm{Int}(\alpha_i,\beta_j)}{l(\alpha_i)l(\beta_j)}$$

A quick look at the intersections shows that $\mathrm{Int}(\alpha_i,\beta_j)\in\{0,\pm1\}$. Moreover, $l(\alpha_k)=l(\beta_k)=\sin 2k\pi/(2m+1)\geq\sin\pi/(2m+1)$ and equality is realized for $k=m$. Since $\mathrm{Int}(\alpha_m,\beta_m)\neq 0$, we draw $K(0,\infty)=\dfrac{1}{l(\alpha_m)l(\beta_m)}=\dfrac{1}{l(\alpha_m)^2}$.

The discussion for the directions $d=0$ and $d'=\Phi$ is similar. They correspond to the vertical and the direction of the diagonal of horizontal cylinders. It is clear that

$$K(0,\Phi)=\sup_{\substack{\alpha\subset S_0 \text{ vertical}\\ \beta\subset S_0 \text{ diagonal of a horizontal cylinder}}}\frac{\mathrm{Int}(\alpha,\beta)}{l(\alpha)l(\beta)}$$

is maximal for $\alpha=\beta_m$ and $\beta=\alpha_1+\beta_m$. And we have $K(0,\Phi)=\frac{\mathrm{Int}(\alpha,\beta)}{\alpha\wedge\beta}=\frac{1}{l(\alpha_1)l(\beta_m)}=\frac{1}{\Phi}K(0,\infty)$.

(ii) Let $(d,d')\notin\Gamma\cdot(0,\infty)$. Since $K(d,d')$ is invariant under the diagonal action of the Veech group and d is a periodic direction, we can assume $d=\infty$,

and, up to a horizontal shear, $d' \in]0, \Phi[$. Notice that given a geodesic β in direction d', every intersection with any of the α_i requires a vertical length $l(\alpha_1)$ (this is where we use the fact that d' is not vertical), that is

$$\forall i \in \{1, \cdots, m\},\ l(\beta) \sin\theta(S_0, d, d') \geq l(\alpha_1) \mathrm{Int}(\alpha_i, \beta).$$

Hence

$$\forall i \in \{1, \cdots, m\},\ \frac{\mathrm{Int}(\alpha_i, \beta)}{l(\alpha_i) l(\beta) \sin\theta(S_0, d, d')} \leq \frac{1}{l(\alpha_1) l(\alpha_i)}$$

But $l(\alpha_i) l(\beta) \sin\theta(S_0, d, d') = \alpha_i \wedge \beta$, and $l(\alpha_i) \geq l(\alpha_m)$, so that the last equation reduces to

$$\forall i \in \{1, \cdots, m\},\ \frac{\mathrm{Int}(\alpha_i, \beta)}{\alpha_i \wedge \beta} \leq \frac{1}{l(\alpha_1) l(\alpha_m)} = \frac{1}{\Phi} K(0, \infty),$$

where the last equality follows from (i). This concludes the proof of Proposition 5.2. □

6. Computation of KVol for the double $(2m+1)$-gon

In this section we show that $\mathrm{KVol}(X_0)$ is realised by pairs of sides of the double $(2m+1)$-gon:

Proposition 6.1. *For every pair of saddle connections α and β on X_0, we have:*

$$\frac{Int(\alpha, \beta)}{l(\alpha) l(\beta)} \leq \frac{1}{l_0^2}$$

where l_0 is the length of the side of the $(2m+1)$-gon.
Moreover, equality is achieved if and only if α and β are two distinct sides of the regular $(2m+1)$-gon.

In particular, since the directions $d = 0$ and $d' = \infty$ represent sides of the double $(2m+1)$-gon, we deduce the following:

Corollary 6.2. *For $X = X_0$ the double $(2m+1)$-gon, we have:*

$$K(X_0) = K(0, \infty) \cdot \sin\theta(X_0, 0, \infty)$$

The main idea of the proof of Proposition 6.1 is to subdivide both saddle connections α and β into segments of length at least l_0 such that each segment of α intersect each segment of β at most once. While, strictly speaking, we do not achieve that, we still get estimates good enough for our purpose, see Lemma 6.7.

6.1. Sectors and transition diagrams.

Let α and β be two saddle connections on the double $(2m+1)$-gon. We partition the set of possible directions into $2m+1$ sectors of angle $\frac{\pi}{2m+1}$, as in Figure 5 for the double heptagon.

To each sector Σ_i there is associated a *transition diagram* which encodes the admissible sequences of intersections with the sides of the double $(2m+1)$-gon, as in [DL19, §3]. Such a diagram looks like:

$$e_{\sigma_i(1)} \leftrightharpoons e_{\sigma_i(2)} \leftrightharpoons \cdots \leftrightharpoons e_{\sigma_i(2n)} \leftrightharpoons e_{\sigma_i(2m+1)}$$

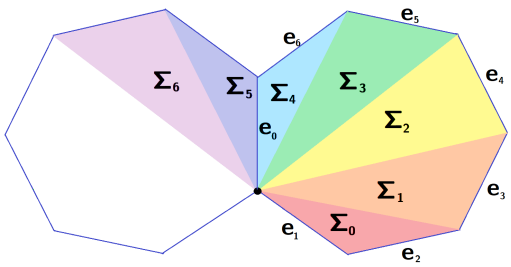

FIGURE 5. The seven sectors for the double heptagon.

with $\sigma_i \in \mathfrak{S}_{2m+1}$, and it means that for any curve α in sector Σ_i, each intersection of α with $e_{\sigma_i(j)}$ is preceded and followed by an intersection with either $e_{\sigma_i(j-1)}$ or $e_{\sigma_i(j+1)}$ [2]. In particular, each intersection with $e_{\sigma_i(1)}$ (resp. $e_{\sigma_i(2m+1)}$) is preceded (and followed) by an intersection with $e_{\sigma_i(2)}$ (resp. $e_{\sigma_i(2m)}$). We say that the side $e_{\sigma_i(1)}$ (resp. $e_{\sigma_i(2m+1)}$) is *sandwiched* by $e_{\sigma_i(2)}$ (resp. $e_{\sigma_i(2m)}$) in the sector Σ_i.

For the sake of completeness, we provide the seven possible transition diagrams for the double heptagon.

$$
\begin{aligned}
&\Sigma_0 : e_1 \leftrightharpoons e_2 \leftrightharpoons e_0 \leftrightharpoons e_3 \leftrightharpoons e_6 \leftrightharpoons e_4 \leftrightharpoons e_5\\
&\Sigma_1 : e_5 \leftrightharpoons e_6 \leftrightharpoons e_4 \leftrightharpoons e_0 \leftrightharpoons e_3 \leftrightharpoons e_1 \leftrightharpoons e_2\\
&\Sigma_2 : e_2 \leftrightharpoons e_3 \leftrightharpoons e_1 \leftrightharpoons e_4 \leftrightharpoons e_0 \leftrightharpoons e_5 \leftrightharpoons e_6\\
&\Sigma_3 : e_6 \leftrightharpoons e_0 \leftrightharpoons e_5 \leftrightharpoons e_1 \leftrightharpoons e_4 \leftrightharpoons e_2 \leftrightharpoons e_3\\
&\Sigma_4 : e_3 \leftrightharpoons e_4 \leftrightharpoons e_2 \leftrightharpoons e_5 \leftrightharpoons e_1 \leftrightharpoons e_6 \leftrightharpoons e_0\\
&\Sigma_5 : e_0 \leftrightharpoons e_1 \leftrightharpoons e_6 \leftrightharpoons e_2 \leftrightharpoons e_5 \leftrightharpoons e_3 \leftrightharpoons e_4\\
&\Sigma_6 : e_4 \leftrightharpoons e_5 \leftrightharpoons e_3 \leftrightharpoons e_6 \leftrightharpoons e_2 \leftrightharpoons e_0 \leftrightharpoons e_1
\end{aligned}
\tag{5}
$$

6.2. **Construction of the subdivision.** Let us denote by Σ_α (resp. Σ_β) the sector of α (resp. β), and σ_α (resp. σ_β) the corresponding permutation. Now, we cut α (resp. β) at each intersection with a non-sandwiched side in the sector Σ_α (resp. Σ_β). We get a decomposition $\alpha = \alpha_1 \cup \cdots \cup \alpha_k$ and $\beta = \beta_1 \cup \cdots \cup \beta_l$ with $k, l \geq 1$ and each segment is either (see Figure 6):

- A non-sandwiched segment which goes from one side to another non-adjacent side of one of the $(2m+1)$-gons.
- A sandwiched segment which intersects a sandwiched side in its interior. Such segments go through both $(2m+1)$-gons (see Figure 7).
- an initial or final segment α_1, α_k, β_1, β_l. We also call such segments non-sandwiched.

Notation 6.3. When a segment α_i (or β_j) intersects the side e which is sandwiched by e' in the corresponding sector, we say that α_i is of type $e' \to e \to e'$.

Remark 6.4. For a sandwiched segment α_i of type $e' \to e \to e'$, there is a parallelogram $P(e', e) \subset X_0$ with the following property: one of its sides is e' and one of its diagonals is e. The segment α_i goes from one e'-side to the opposite side. The closure of $P(e', e)$ is a cylinder.

[2] Unless it reaches a singularity.

Notice that for each sector Σ_i, the sides of the $(2m+1)$-gon which are sandwiched in Σ_i are those having direction in the boundary of Σ_i. For instance, the sides of the double heptagon which are sandwiched in the sector Σ_0 are e_1 and e_5 (see Figure 5).

Moreover, the side of the $(2m+1)$-gon with direction in $\Sigma_i \cap \Sigma_{i-1}$ is sandwiched in both sectors Σ_i and Σ_{i-1}, but in Σ_i it is sandwiched by its successor in the cyclic order (modulo $2m+1$), while in Σ_{i-1} it is sandwiched by its predecessor. For instance, e_1 is sandwiched by e_2 in Σ_0, while it is sandwiched by e_0 in Σ_{2m} (Σ_6 for the double heptagon).

Since no two sectors have the same pair (sandwiched side, sandwiching side), prescribing the type of α_i automatically tells which sector the direction of α belongs to.

Remark 6.5. If α is a diagonal of the double $(2m+1)$-gon, the sector is not uniquely defined. However, in such cases α is not divided into pieces and $k = 1$.

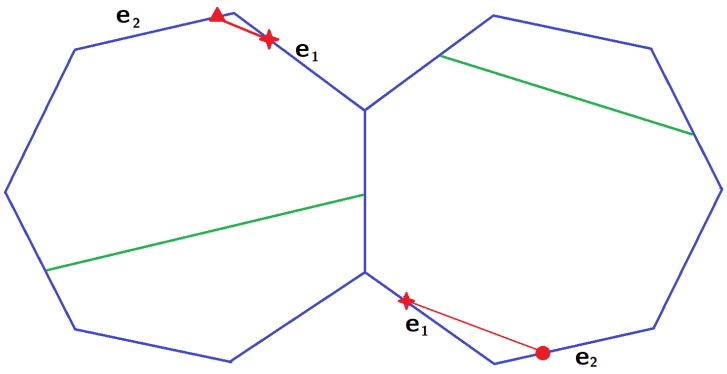

FIGURE 6. Examples of non-sandwiched segments in green and a sandwiched segment in red. The sandwiched segment is of type $e_2 \to e_1 \to e_2$. Remark that the points ◯ and △ on the side e_2 are not the same.

The next two lemmas are the reason for this peculiar way of subdivising saddle connections.

Lemma 6.6. *Every segment of α (resp. β) has length at least l_0, with equality if and only if α (resp. β) is a side of the double $(2m+1)$-gon.*

Proof. A non-sandwiched segment goes from one side (or vertex) of a $(2m+1)$-gon to a *non-adjacent* side in the same $(2m+1)$-gon. So its length is a least l_0.

Now take a sandwiched segment α_i which intersects a sandwiched side e in its interior. If the type of α_i is $e' \to e \to e'$, then by Remark 6.4, α_i goes from the side e' of $P(e', e)$ to the opposite side of $P(e', e)$. In particular the length of α_i is no less than that of e' which is l_0. □

6.3. **Study of the intersections.** In this section, we investigate the possible intersections between the segments of α and β. First observe that α_i and β_j can have nontrivial intersections on the interior of the sides of a sector Σ_α. However if this happen, we can slightly deform α as follows. We change the slope of α_i and α_{i+1} so that the new segment α_i' intersects β_j in the interior of Σ_α the same number of times α_i intersects β_j. We choose the deformation small enough so that we do not create new intersections with the others segments. The new path $\alpha' = \alpha_1 \cup \cdots \cup \alpha_i' \cup \alpha_{i+1}' \cup \cdots \cup \alpha_k$ is homologous to α by construction. In the sequel we will simply use α instead of α'.

Now, since β is made of segments of straight lines in the same direction, and α is made of segments whose directions are close to a given direction, all non-singular intersections have the same sign. In particular, adding the possible singular intersection, it gives:

$$Int(\alpha, \beta) \leq \sum_{i,j} |Int(\alpha_i, \beta_j)| + 1 \tag{6}$$

where $|Int(\alpha_i, \beta_j)|$ is the geometric intersection between α_i and β_j.

Lemma 6.7. *If α and β are not both diagonals, then $Int(\alpha, \beta) \leq kl$.*

Proof of Lemma 6.7. We will show that $\sum_{i,j} |Int(\alpha_i, \beta_j)| \leq kl-1$. Let us fix i, j. We first observe that if either α_i or β_j is a non-sandwiched segment, then α_i and β_j intersect at most once (possibly on a side). Indeed a non-sandwiched segment goes from one side to another non-adjacent side of one of the $(2m+1)$-gons. In particular it is a segment that is contained entirely in one of the $(2m+1)$-gons. A sandwiched segment consists of two straight lines, not contained in the same $(2m+1)$-gon. Hence in total they intersect at most once.

Thus it remains to consider the case where α_i and β_j are sandwiched segments. Up to a rotation and a symmetry, we can assume α_i is of type $e_2 \to e_1 \to e_2$ (see Figure 5). The sector determined by α is necessarily Σ_0.

Now if β_j is sandwiched but neither e_1 nor e_2 appear in the type of β_j, then α_j is contained in the parallelogram $P(e_k, e_l)$ (defined in Remark 6.4) for some $e_k, e_l \notin \{e_1, e_2\}$. In particular α_i does not intersect this parallelogram, and so not β_j either.

Eventually it remains to treat the following cases where β_j is of type:

(1)	$e_0 \to e_1 \to e_0$	(2)	$e_1 \to e_0 \to e_1$
(3)	$e_1 \to e_2 \to e_1$	(4)	$e_2 \to e_1 \to e_2$
(5)	$e_2 \to e_3 \to e_2$	(6)	$e_3 \to e_2 \to e_3$

In all situations but (3), we can show that α_i and β_j intersects at most once. We proceed case by case.

Case (1): Recall that α_i is contained in the parallelogram $P(e_2, e_1)$ and goes from one e_2-side to the opposite side. Let us denote by e, e' the two other sides of $P(e_2, e_1)$. Similarly β_j is contained in another parallelogram $P(e_0, e_1)$ sharing the same diagonal, and β_j goes from one side e_0 to the opposite side. We can see that the intersection of $P(e_2, e_1)$ with $P(e_0, e_1)$ is connected: it is a

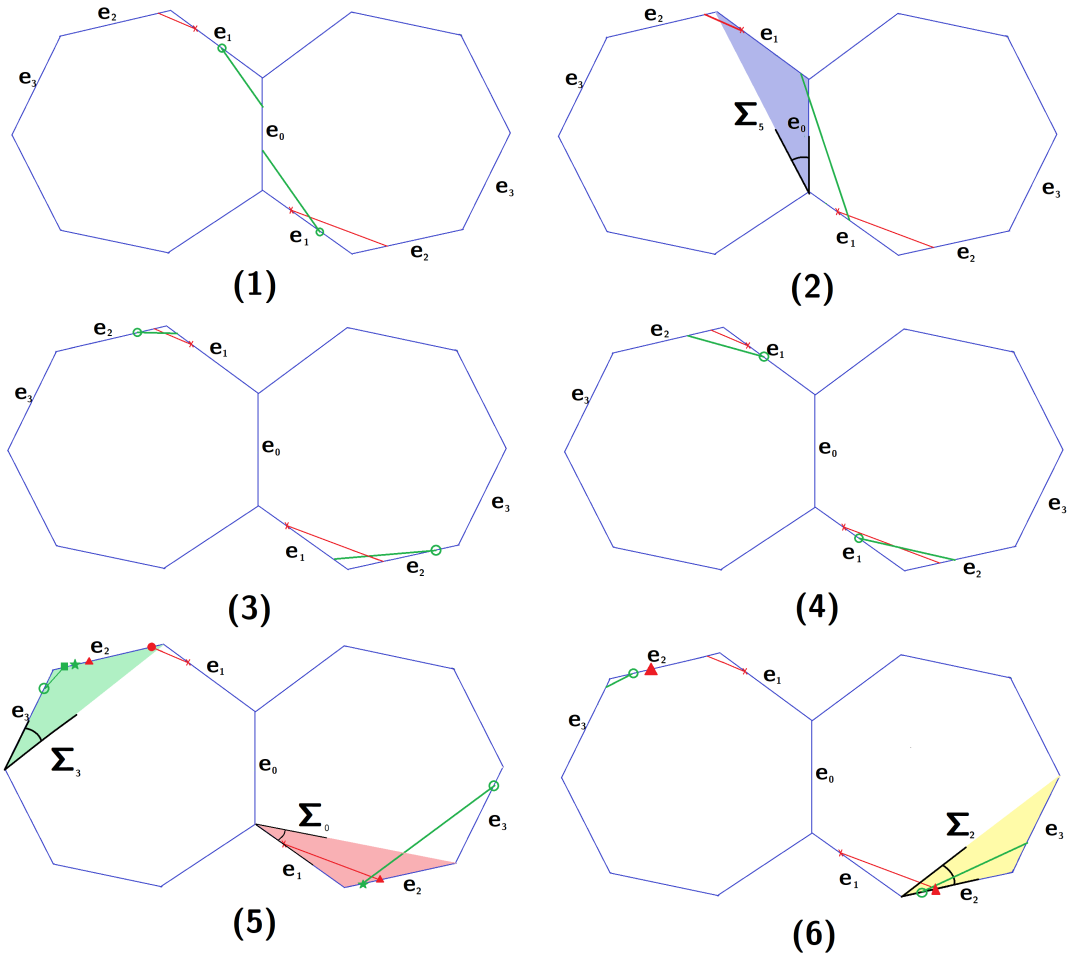

FIGURE 7. The six different cases where α_i (in red) and β_j (in green) are sandwiched and intersect.

parallelogram. In particular the intersection of β_j with $P(e_2, e_1)$ goes from the side e to the side e' and thus intersects α_i exactly once (see Figure 8).

Case (4): By Remark 6.4 α_i and β_j are contained in the *same* $P(e_2, e_1)$. They both go from one side e_2 to the opposite. In particular they intersect at most once.

Case (2): By (5), since e_0 is sandwiched by e_1, the direction of β lies in the sector Σ_5. Moreover β_j lies in the parallelogram $P(e_1, e_0)$ and goes from the side e_1 to the opposite (see Figure 9). The segments α_i and β_j intersect each other at most twice. Assume by contradiction $\alpha_i \cap \beta_j = \{p, q\}$ with $p \neq q \in X_0$. Since p and q belong to different parts of the segment α_i, they belong to different copies of the $(2m+1)$-gon. The slope s of the holonomy vector defined by pq coincide with the slope of β and thus belongs to the sector Σ_5 *i.e.* $\text{slope}(e_4) \leq s \leq 0$

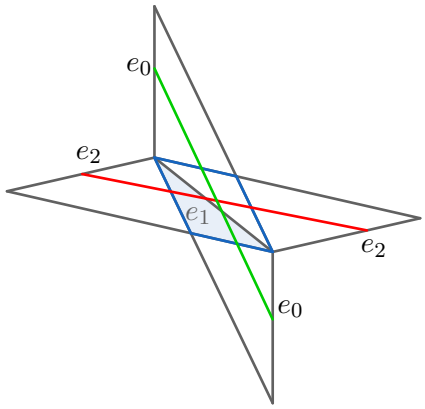

FIGURE 8. Case 1 re-drawn

(with equality iff β is a diagonal). On the other hand, the intersection of α_i with the two sides e_1 on the plane template of Figure 9 determines two points c and d.

By construction the slope s satisfies $s \leq \text{slope}(cd)$. Since $\text{slope}(cd) = \text{slope}(e_4)$ we get that β is a diagonal. We run into a contradiction because $\beta_j = \beta$ is not sandwiched (see beginning of Section 6.2), and therefore $\text{Int}(\alpha_i, \beta_j) \leq 1$.

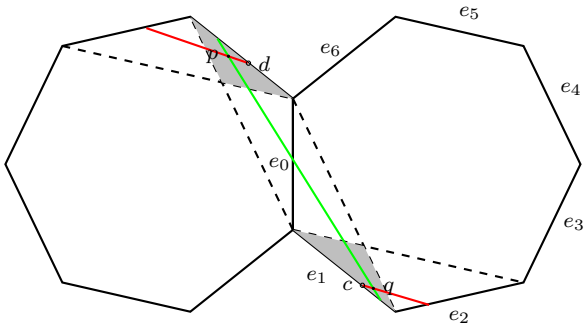

FIGURE 9. The parallelogram $P(e_1, e_0)$ and two intersections in Case (2): $\beta \notin \Sigma_5$

Case (6): This case is the same as Case (2) rotating by an angle $\frac{2\pi}{2m+1}$ and swapping α_i and β_j.

Case (5): By (5), since e_3 is sandwiched by e_2, the direction of β lies in the sector Σ_3 and β is contained in the parallelogram $P(e_2, e_3)$. In particular its slope verifies $s \geq \text{slope}(e_6)$. The segment α_i intersects $P(e_2, e_3)$ with two connected components. One such component intersects one side e_2 at a point a while the other component intersects the other side e_2 at a point b (which project in the double $(2m+1)$-gon to the red bullet and the red triangle in Figure 7 Case

(5)). As in Case (2) the segments α_i and β_j intersect each other at most twice. Assume by contradiction $\alpha_i \cap \beta_j = \{p, q\}$ with $p \neq q \in P(e_2, e_3)$. Necessarily $\text{slope}(ab) \geq \text{slope}(pq) = s$. Since $\alpha \in \Sigma_0$ we can check that $\text{slope}(ab) \leq \text{slope}(e_6)$ (recall that the slope of α_i' is very close to the slope of α_i).

Thus $s = \text{slope}(e_6)$ and β is a diagonal: we again run into a contradiction because $\beta_j = \beta$ is not sandwiched. Therefore $\text{Int}(\alpha_i, \beta_j) \leq 1$ as desired.

Conclusion: Setting aside case (3) which will be considered below, we have for every i, j, $|Int(\alpha_i, \beta_j)| \leq 1$. In particular $\sum_{i,j} |Int(\alpha_i, \beta_j)| \leq kl$. Recall that we want the left quantity to be less than $kl - 1$ instead of kl; the desired bound comes from the following observation: up to permuting α and β, we may assume α is not a diagonal. Then α_1 is non-sandwiched and lies in one of the $(2m+1)$-gons while the second non-sandwiched α_i lies in the other $(2m+1)$-gon[3]. In particular, since β_1 is non sandwiched, it lies in one of the two $(2m+1)$-gons and it cannot intersect both α_1 and the next non-sandwiched α_i.

In particular, $\sum_{i,j} |Int(\alpha_i, \beta_j)| \leq kl - 1$. Hence, by Formula 6, we get that $Int(\alpha, \beta) \leq kl$.

Treating case (3). In this paragraph we assume there are indices i, j such that α_i is sandwiched of type $e_2 \to e_1 \to e_2$ and β_j is sandwiched of type $e_1 \to e_2 \to e_1$. In this case, α_i and β_j could intersect twice, but we will show that if this happens then there is an index j' such that α_i and $\beta_{j'}$ don't intersect. Hence the conclusion $\sum_{i,j} |Int(\alpha_i, \beta_j)| \leq kl$ will still hold (and in fact the inequality will be strict, as we require).

To do that let us assume $\alpha_{i_0}, \ldots, \alpha_{i_0+p}$ (resp. $\beta_{j_0}, \ldots, \beta_{j_0+q}$) are consecutively sandwiched of type $e_2 \to e_1 \to e_2$ (resp. $e_1 \to e_2 \to e_1$), this sequence being maximal (i.e α_{i_0-1} and α_{i_0+p+1} – resp. β_{j_0-1} and β_{j_0+q+1} – are not sandwiched). An example of such a configuration is depicted in Figure 11 for $p = q = 0$ and in Figure 12 for $p = q = 3$. We claim that there are at most $(p+3)(q+2)$ intersections between $\alpha_{i_0-1} \cup \alpha_{i_0} \cup \cdots \cup \alpha_{i_0+p} \cup \alpha_{i_0+p+1}$ and $\beta_{j_0-1} \cup \beta_{j_0} \cup \cdots \cup \beta_{j_0+q} \cup \beta_{j_0+q+1}$, while there are $(p+3)(q+3)$ pairs of segments.

Indeed, in this configuration $\alpha_{i_0-1} \cup \alpha_{i_0} \cup \cdots \cup \alpha_{i_0+p} \cup \alpha_{i_0+p+1}$ and $\beta_{j_0-1} \cup \beta_{j_0} \cup \cdots \cup \beta_{j_0+q} \cup \beta_{j_0+q+1}$ go through the cylinder $P(e_2, e_1)$ defined by e_1 and e_2, as in Figure 11. Now, instead of cutting β each time it crosses e_1 we can cut β each time it crosses e_2. Notice that β crosses e_1 once more than it crosses e_2, so it gives a decomposition $\beta_{j_0-1} \cup \cdots \cup \beta_{j_0+q} \cup \beta_{j_0+q+1} = \tilde{\beta}_{j_0} \cup \cdots \cup \tilde{\beta}_{j_0+q} \cup \tilde{\beta}_{j_0+q+1}$ with only $q+2$ segments while each $\tilde{\beta}_j$ for $j \in [\![j_0, j_0+q+1]\!]$ can intersect each of the α_i for $i \in [\![i_0 - 1, i_0 + p + 1]\!]$ at most once, which leaves at most $(p+3)(q+2)$ intersections.

[3]Notice that the last non-sandwiched segment before a sequence of sandwiched segments and the next non-sandwiched segment after such a sequence lie in different $(2m+1)$-gons, as in Figures 11 and 12.

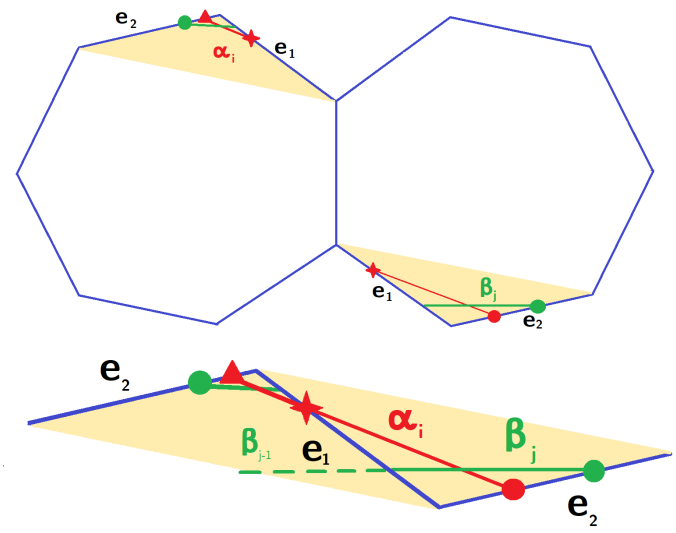

FIGURE 10. α_i and β_j could intersect twice in the configuration of case 3. Below, a closer look at the cylinder $P(e_2, e_1)$. In the example of this picture, α_i does not intersect β_{j-1}.

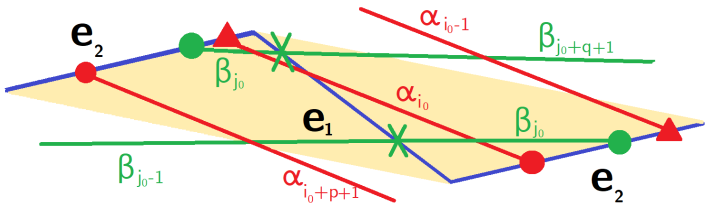

FIGURE 11. $\alpha_{i_0-1} \cup \alpha_{i_0} \cup \cdots \cup \alpha_{i_0+p} \cup \alpha_{i_0+p+1}$ and $\beta_{j_0-1} \cup \beta_{j_0-1} \cup \cdots \cup \beta_{j_0+q} \cup \beta_{j_0+q+1}$ for $p = q = 0$. There are only six intersections but nine pairs of segments.

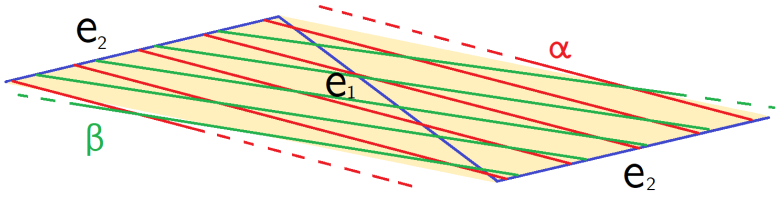

FIGURE 12. $\alpha_{i_0-1} \cup \alpha_{i_0} \cup \cdots \cup \alpha_{i_0+p} \cup \alpha_{i_0+p+1}$ and $\beta_{j_0-1} \cup \beta_{j_0-1} \cup \cdots \cup \beta_{j_0+q} \cup \beta_{j_0+q+1}$ for $p = q = 3$. There are only ten intersections but thirty-six pairs of segments.

In conclusion, summing with all other segments yields $\sum_{i,j} |Int(\alpha_i, \beta_j)| < kl$. Adding the possible singular intersection, we get the desired result. This concludes the proof of Lemma 6.7 □

6.4. **Conclusion.** We are now able to prove the main proposition of this section.

Proof of Proposition 6.1. If either α or β is not a diagonal, then:

- $l(\alpha)l(\beta) > kl \cdot l_0^2$ by Lemma 6.6,
- $Int(\alpha,\beta) \leq kl$ by Lemma 6.7,

In particular, we have:

$$\frac{Int(\alpha,\beta)}{l(\alpha)l(\beta)} < \frac{1}{l_0^2}$$

as desired.

Otherwise, both α and β are diagonals. Then:

(1) either none of them is a side of a $(2m+1)$-gon and then:
   (a) $l(\alpha)l(\beta) \geq 4\cos^2(\frac{\pi}{2m+1})l_0^2 > 2l_0^2$ because the shortest diagonals of the $(2m+1)$-gon which are not sides have length $2\cos(\frac{\pi}{2m+1})l_0$.
   (b) $Int(\alpha,\beta) \leq 2$ because there is at most one non-singular intersection and one singular intersection.

   In particular, $\frac{Int(\alpha,\beta)}{l(\alpha)l(\beta)} < \frac{1}{l_0^2}$.

(2) or α (up to a change in names) is a side, and then:
   (a) $Int(\alpha,\beta) \leq 1$ as there is no non-singular intersection,
   (b) $l(\alpha)l(\beta) \geq l_0^2$ with equality if and only if both α and β are sides of a $(2m+1)$-gon.

   In particular, we have $\frac{Int(\alpha,\beta)}{l(\alpha)l(\beta)} \leq \frac{1}{l_0^2}$ with equality if and only if both α and β are sides of a $(2m+1)$-gon.

This concludes the proof of Proposition 6.1. □

7. Extension to the Teichmüller disc

In this section, we finally show our main result:

Theorem 7.1. *For any surface X in the Teichmüller disc of the double $(2m+1)$-gon, we have:*

$$K(X) = K(0,\infty)\sin\theta(X,0,\infty). \tag{7}$$

Theorem 1.1 follows directly as $\sin\theta(X,0,\infty) = \dfrac{1}{\cosh d_{hyp}(X,\gamma_{0,\infty})}$ by Proposition 4.2. Before proving Theorem 7.1, we show how to deduce Corollary 1.2.

Proof of Corollary 1.2. Since $\mathrm{Vol}(S_0) = \frac{n}{2}\cos\frac{\pi}{n}$ by 2 and the furthest point of $\mathcal{D}$ from $\gamma_{0,\infty}$ is X_0, the corresponding angle $\sin\theta(X_0,0,\infty)$ being equal to $\sin\frac{\pi}{n}$, Equation (7) implies

$$\frac{n}{2}\cos\frac{\pi}{n}\cdot K(0,\infty)\cdot\sin\frac{\pi}{n} \leq \mathrm{KVol}(X) \leq \frac{n}{2}\cos\frac{\pi}{n}\cdot K(0,\infty).$$

We conclude with Proposition 5.2 and Equation (2): $K(0,\infty) = \frac{1}{l(\alpha_m)^2} = \frac{1}{\sin^2\frac{\pi}{n}}$.

The maximum is achieved precisely when $\sin\theta(X,0,\infty) = 1$ *i.e.* X belongs to the geodesic $\gamma_{0,\infty}$, namely X is the image of S_0 by a diagonal matrix of $\mathrm{SL}_2(\mathbb{R})$. As we have seen the minimum is achieved uniquely at X_0. Finally by Proposition 6.1, the supremum is achieved by pairs of curves that are (images of) pairs of sides of X_0. □

7.1. **Interpolation between the regular n-gon and the staircase model.** Recall that Proposition 5.1 provides another expression of KVol:

$$K(X) = \sup_{(d,d')} K(d,d') \sin\theta(X,d,d'), \tag{8}$$

where the supremum is taken over all pairs (d,d') of distinct periodic directions. The quantity $K(d,d')$ is invariant under the diagonal action of the Veech group. Moreover, we know that Equation (7) holds:

- for X in the geodesic $\gamma_{0,\infty}$ by Proposition 5.2
- for $X = X_0$ the double $(2m+1)$-gon by Corollary 6.2.

The main idea of the proof of Theorem 7.1 is to use these two results and interpolate between them to show that Equation (7) holds in fact for the whole Teichmüller disc. By symmetry, we can restrict to the surfaces X on the right half of the fundamental domain, that is on $\mathcal{D}_+ = \{x+iy \mid 0 \leq x \leq \frac{\Phi}{2} \text{ and } x^2+y^2 \geq 1\}$. Using Equation (8), it suffices to show that for any pair of distinct periodic directions (d,d') one has:

$$(\clubsuit) \qquad \forall X \in \mathcal{D}_+,\ K(d,d')\sin\theta(X,d,d') \leq K(0,\infty)\sin\theta(X,0,\infty)$$

The proof is divided in two steps:

(1) Show that it suffices to prove ($\clubsuit$) for $0 \leq d < \frac{\Phi}{2} < d'$.
(2) Show that ($\clubsuit$) holds under the assumption $0 \leq d < \frac{\Phi}{2} < d'$.

The proof of the first step (Section 7.2) involves hyperbolic geometry and Veech group action, while the second step (Section 7.3) will be deduced from the study of the function

$$X \mapsto \frac{\sin\theta(X,0,\infty)}{\sin\theta(X,d,d')}.$$

7.2. **Reduction to convenient geodesics.** In this section, we prove that it suffices to verify ($\clubsuit$) for pairs (d,d') with $0 \leq d < \frac{\Phi}{2} < d'$. The main step of the proof is Lemma 7.6.

Definition 7.2. Given a pair of distinct periodic directions (d,d') and its associated geodesic $\gamma_{d,d'}$ on $\mathbb{H}^2$, we denote by $V(d,d')$ be the connected component of $\mathbb{H}^2 \backslash (\Gamma_n.\gamma_{d,d'})$ containing X_0.

Remark 7.3. If one of the images of $\gamma_{d,d'}$ by the action of the Veech group Γ_n passes through X_0, then $V(d,d')$ is not well defined. It is convenient, in this case, to set $V(d,d') = \{X_0\}$. Note that in this case there exists $G \in \Gamma_n$ such that $\sin\theta(X_0, G.d, G.d') = 1$, so by Equation ($\clubsuit$) for $X = X_0$ we have

$$\begin{aligned} K(d,d')\sin\theta(X,d,d') \leq K(d,d') &= K(G.d,G.d')\sin\theta(X_0,G.d,G.d') \leq \\ &\leq K(0,\infty)\sin\theta(X_0,0,\infty) \leq K(0,\infty)\sin\theta(X,0,\infty), \end{aligned}$$

therefore, ($\clubsuit$) holds for any $X \in \mathcal{D}_+$.

Remark 7.4. Notice that, by definition, the boundary of $V(d,d')$ is made of geodesic segments in the Veech group orbit of $\gamma_{d,d'}$. Since d and d' correspond to directions of cusps, there is a finite number of such segments.

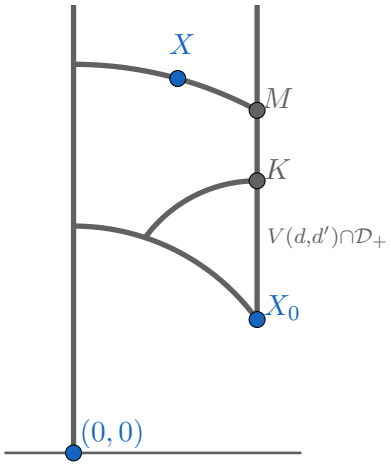

FIGURE 13. The highest K point of $V(d,d') \cap \gamma_{\Phi/2,\infty}$ is further away from $\gamma_{0,\infty}$ than M, which is itself further away from $\gamma_{0,\infty}$ than X.

Lemma 7.5. *For any pair of distinct periodic directions (d,d'), the furthest point X_1 from $\gamma_{0,\infty}$ in the boundary of $V(d,d') \cap \mathcal{D}_+$ is further away from $\gamma_{0,\infty}$ than any point $X \in \mathcal{D}_+$ outside $V(d,d')$. Equivalently*

$$\sin\theta(X_1, 0, \infty) \leq \sin\theta(X, 0, \infty).$$

Proof. Take $X \in \mathcal{D}_+ \setminus V(d,d')$ and call g the perpendicular to $\gamma_{0,\infty}$ which contains X. If g intersects $V(d,d')$ then there is an intersection point in the boundary of $V(d,d')$, and this point is further away from $\gamma_{0,\infty}$ than X (see Figure 13). If g does not meet $V(d,d')$, then g intersects the geodesic $\gamma_{\Phi/2,\infty}$ above $V(d,d')$ at M. We claim that the highest point K of

$$V(d,d') \cap \gamma_{\Phi/2,\infty}$$

is further away from $\gamma_{0,\infty}$ than M. Indeed by construction we have the inequality

$$\sin\theta(M, 0, \infty) \geq \sin\theta(K, 0, \infty).$$

By Proposition 4.2, one has $\cosh d_{\mathrm{hyp}}(M, \gamma_{0,\infty}) = \sin^{-1}\theta(M, 0, \infty)$. Since cosh is an increasing function, we deduce $d_{\mathrm{hyp}}(M, \gamma_{0,\infty}) \leq d_{\mathrm{hyp}}(K, \gamma_{0,\infty})$. Now since M is by construction further away from $\gamma_{0,\infty}$ than X, this proves the lemma. □

Lemma 7.6. *Let (d_1, d_1') and (d_2, d_2') be two pairs of directions such that the associated geodesics $\gamma_{d_1,d_1'}$ and $\gamma_{d_2,d_2'}$ cross the half fundamental domain $\mathcal{D}_+$. We assume that:*

- *(i) $K(d_1, d_1') \geq K(d_2, d_2')$.*
- *(ii) The geodesic $\gamma_{d_2,d_2'}$ lies outside $V(d_1, d_1')$.*
- *(iii) (♣) holds for any pair of directions whose associated geodesic is in the boundary of $V(d_1, d_1')$.*

Then (♣) holds for (d_2, d_2').

Proof. Pick a point $X \in \mathcal{D}_+$. We subdivide the proof in two cases.
First case: $X \notin V(d_1, d_1')$. Then, Lemma 7.5 gives us a point X_1 on the boundary of $V(d_1, d_1')$ such that

$$\sin\theta(X_1, 0, \infty) \leq \sin\theta(X, 0, \infty). \tag{9}$$

Note that up to acting by the Veech group, which does not change the conclusion, we may assume that X_1 lies on $\gamma_{d_1,d_1'}$ itself, so $\sin\theta(X_1, d_1, d_1') = 1$. Then

$$\begin{aligned} K(d_2, d_2')\sin\theta(X, d_2, d_2') &\leq K(d_2, d_2') \\ &\leq K(d_1, d_1') \text{ by assumption (i)} \\ &= K(d_1, d_1')\sin\theta(X_1, d_1, d_1') \text{ because } \sin\theta(X_1, d_1, d_1') = 1 \\ &\leq K(0, \infty)\cdot\sin\theta(X_1, 0, \infty) \text{ by assumption (iii)} \\ &\leq K(0, \infty)\cdot\sin\theta(X, 0, \infty) \text{ by (9).} \end{aligned}$$

Second case: $X \in V(d_1, d_1')$. Then, by assumption (ii), the perpendicular to $\gamma_{d_2,d_2'}$ through X crosses the boundary of $V(d_1, d_1')$ before it reaches $\gamma_{d_2,d_2'}$, and again, up to acting by the Veech group we may assume the crossing occurs at $\gamma_{d_1,d_1'}$ so that $\sin\theta(X, d_1, d_1') \geq \sin\theta(X, d_2, d_2')$. Therefore

$$\begin{aligned} K(d_2, d_2')\sin\theta(X, d_2, d_2') &\leq K(d_1, d_1')\sin\theta(X, d_2, d_2') \text{ by assumption (i)} \\ &\leq K(d_1, d_1')\sin\theta(X, d_1, d_1') \\ &\leq K(0, \infty)\cdot\sin\theta(X, 0, \infty) \text{ by assumption (iii),} \end{aligned}$$

which finishes the proof. □

In particular, since we can apply Lemma 7.6 when (d_2, d_2') is in the orbit of (d_1, d_1') under the diagonal action of the Veech group, it suffices to prove (♣) for pairs of directions (d, d') such that some segment of $\gamma_{d,d'}$ is in the boundary of $V(d_1, d_1')$. Since $V(d_1, d_1')$ is invariant under the dihedral group preserving X_0, it suffices to consider segments of the boundary which are contained in $\mathcal{D}_+$. These geodesics satisfy the following property.

Lemma 7.7. *If $\gamma_{d,d'}$ is a geodesic whose closest point to X_0 lies in $\mathcal{D}_+$, then $\gamma_{d,d'}$ intersects the geodesic $\gamma_{\Phi/2,\infty}$. In particular, we can assume $d < \frac{\Phi}{2} < d'$. Moreover, the direction of the tangent vector of $\gamma_{d,d'}$ at the intersection point lies in the first quadrant, in particular $d + d' > \Phi$.*

Proof. If $\gamma_{d,d'}$ does not intersect the geodesic $\gamma_{\Phi/2,\infty}$, then the perpendicular projection of X_0 to $\gamma_{d,d'}$ lies below X_0, hence not in $\mathcal{D}$, see Figure 14 (left part). The statement about the tangent vector at the intersection follows from the convexity of $V(d, d')$ and its symmetry with respect to $\gamma_{\Phi/2,\infty}$. See Figure 14 (right part). □

In particular, to prove Theorem 7.1 it suffices to show that (♣) holds for pairs (d, d') with $d < \frac{\Phi}{2} < d'$ and $d + d' > \Phi$. We distinguish two cases:

(1) $d \geq 0$
(2) $d < 0$

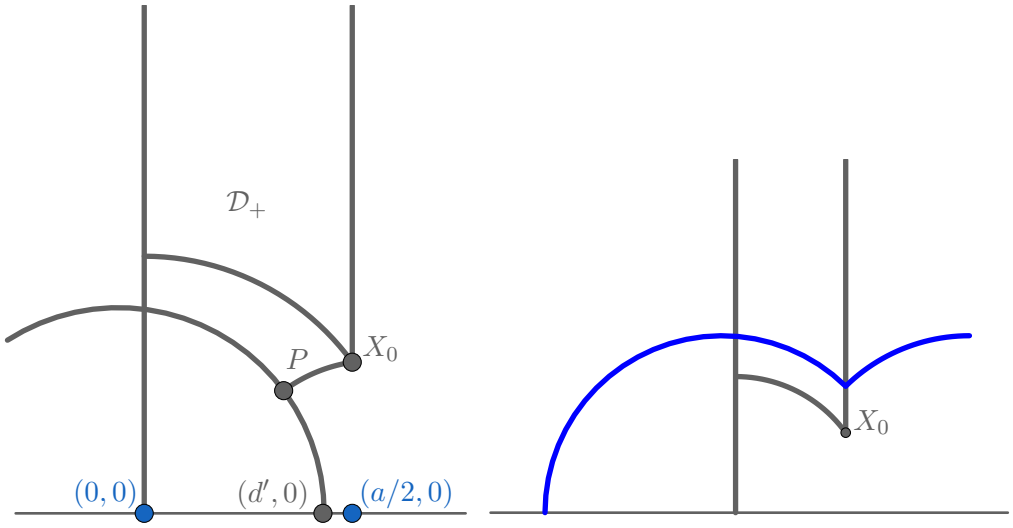

FIGURE 14. Left: when $d' < \Phi/2$, the orthogonal projection of X_0 to $\gamma_{d,d'}$ does not lie in $\mathcal{D}$. Right: when the tangent vector to $\gamma_{d,d'}$ at the intersection with the right boundary of $\mathcal{D}$ does not lie in the first quadrant, $V(X_0, d, d')$ is not convex.

In fact, case 1 is more difficult and will be proven in the next section. However, case 2 can be directly deduced from case 1. Indeed, by Lemma 7.7, if $d < 0$ then $d' \geq \Phi - d > \Phi$. In particular, $\gamma_{d,d'}$ lies outside $V(0,\Phi)$, whose boundary is made of the geodesic segments that are images of $\gamma_{0,\Phi}$ by the rotation around X_0, in particular $\gamma_{0,\Phi} \cap \mathcal{D}$ is the only boundary of $V(0,\Phi)$ intersecting $\mathcal{D}_+$; see Figure 15 for the double pentagon. Since $K(d,d') \leq K(0,\Phi)$ (by Proposition 5.2) and the pair $(0,\Phi)$ satisfies (♣) by case 1, we conclude by Lemma 7.6 that (d,d') satisfies (♣). This shows that case 1 implies case 2.

7.3. **Study of the ratio of sines.** In this section we show that any pair of periodic directions (d,d') in case 1 (i.e $0 \leq d < \frac{\Phi}{2} < d'$) satisfies (♣). Our proof relies on the study of the function

$$F_{(d,d')} : X \mapsto \frac{\sin\theta(X,0,\infty)}{\sin\theta(X,d,d')}.$$

More precisely:

Proposition 7.8. *Under the assumption $0 \leq d < \frac{\Phi}{2} < d'$, the function $F_{(d,d')}$ on $\mathcal{D}_+$ is minimal at X_0.*

Before giving the proof of this proposition, let us first state and prove the following corollary, which concludes the proof of Theorem 7.1:

Corollary 7.9. *For any (d,d') such that $0 \leq d < \frac{\Phi}{2} < d'$, (♣) holds.*

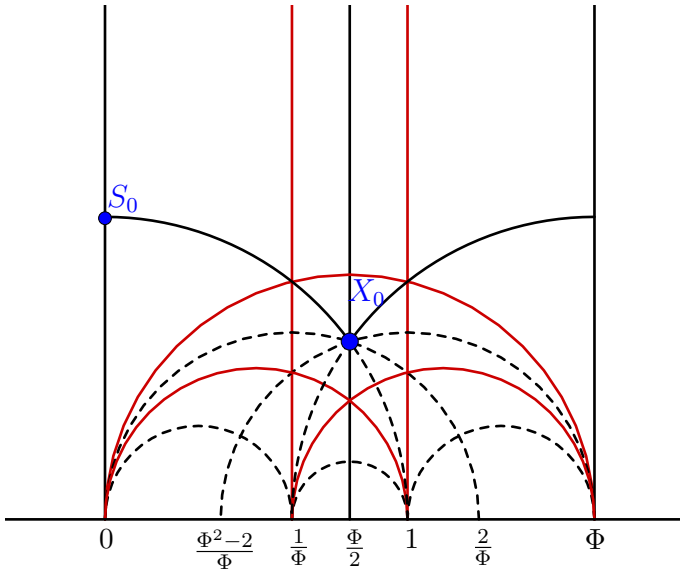

FIGURE 15. The domain $V(0,\Phi)$ for the double pentagon.

Proof of Corollary 7.9. Let (d,d') be such that $0 \leq d < \frac{\Phi}{2} < d'$, and $X \in \mathcal{D}_+$. We know from Corollary 6.2 that

$$K(d,d')\sin\theta(X_0,d,d') \leq K(0,\infty)\sin\theta(X_0,0,\infty).$$

In particular, by minimality of $F_{(d,d')}$ at X_0

$$K(d,d') \leq K(0,\infty)F_{(d,d')}(X_0) \leq K(0,\infty)F_{(d,d')}(X)$$

Hence

$$K(d,d')\sin\theta(X,d,d') \leq K(0,\infty)\sin\theta(X,0,\infty)$$

This concludes the proof. □

Proof of Proposition 7.8. We divide the proof in 5 steps:

(1) We remark that $F_{(d,d')}$ is well defined and differentiable on $\mathbb{H}^2$, and has a well defined minimum on $\mathcal{D}_+$.
(2) We study the gradient of $F_{(d,d')}$ in $\mathcal{D}_+$ and show that it doesn't vanish inside $\mathcal{D}_+$.
(3) We remark that $F_{(d,d')}$ is not minimal at the left boundary of $\mathcal{D}_+$.
(4) We study the variations of $F_{(d,d')}$ on the lower boundary of $\mathcal{D}_+$, which we parametrize as $\left\{(\cos\theta,\sin\theta) : \theta \in \left[\frac{\pi}{n},\frac{\pi}{2}\right]\right\}$, and show that $F_{(d,d')}$ increases with θ.
(5) We study the variations of $F_{(d,d')}$ on the line $x = \frac{\Phi}{2}$ and show that it increases strictly with y.

Proof of step 1.
Note that by Proposition 4.2

$$F_{(d,d')}(X) = \frac{\cosh \mathrm{d}_{hyp}(X,\gamma_{d,d'})}{\cosh \mathrm{d}_{hyp}(X,\gamma_{0,\infty})}$$

where $\mathrm{d}_{hyp}(X, \gamma_{d,d'})$ is the hyperbolic distance from X to the geodesic $\gamma_{d,d'}$. Distance functions are not differentiable, but their cosh's are.

Moreover, $F_{(d,d')}(x+iy) \to +\infty$ when $y \to +\infty$ (and $x \in [0, \frac{\Phi}{2}]$), so if $A > 0$ is sufficiently big, we have $F_{(d,d')}(X) > F_{(d,d')}(X_0)$ for any $X = x + iy \in \mathcal{D}_+$ with $y > A$. In particular, $F_{(d,d')}$ reaches its minimum on the compact set $\mathcal{K} = \mathcal{D}_+ \cap \{x + iy | y \leq A\}$. This finishes the proof of step 1.

Proof of step 2.
Note that since the natural logarithm is an increasing diffeomorphism, we may as well look for the minimum of $\log F_{(d,d')}(X)$ over $\mathcal{D}_+$. Now

$$\begin{aligned}\nabla \log F_{(d,d')}(X) &= \frac{\nabla \cosh \mathrm{d}_{hyp}(X, \gamma_{d,d'})}{\cosh \mathrm{d}_{hyp}(X, \gamma_{d,d'})} - \frac{\nabla \cosh \mathrm{d}_{hyp}(X, \gamma_{0,\infty})}{\cosh \mathrm{d}_{hyp}(X, \gamma_{0,\infty})} \\ &= \tanh \mathrm{d}_{hyp}(X, \gamma_{d,d'}) \nabla \mathrm{d}_{hyp}(X, \gamma_{d,d'}) - \tanh \mathrm{d}_{hyp}(X, \gamma_{0,\infty}) \nabla \mathrm{d}_{hyp}(X, \gamma_{0,\infty}).\end{aligned}$$

Now the distance gradients are unit vectors, and they are parallel only along the common perpendicular (if it exists) to $\gamma_{0,\infty}$ and $\gamma_{d,d'}$, or never (otherwise), so the gradient of $F_{(d,d')}$ cannot vanish outside of the common perpendicular. Along the common perpendicular, the numbers $\tanh \mathrm{d}_{hyp}(X, \gamma_{d,d'})$ and $\tanh \mathrm{d}_{hyp}(X, \gamma_{0,\infty})$ are equal only at the middle of the common perpendicular segment between the two lines, and there the distance gradients point in opposite directions. So the gradient of $F_{(d,d')}$ cannot vanish at all. Thus $F_{(d,d')}$ does not have a minimum in the interior of $\mathcal{D}_+$.

Proof of step 3.
On the left boundary of $\mathcal{D}_+$, which is contained in $\gamma_{0,\infty}$, we have $\nabla \mathrm{d}_{hyp}(X, \gamma_{0,\infty}) = 0$, and $\nabla \mathrm{d}_{hyp}(X, \gamma_{d,d'})$ points to the left because $d \geq 0$. Therefore no point on the left boundary is a local minimum for $F_{(d,d')}$.

Proof of step 4.
Now let us study the function $F_{(d,d')}(X)$ restricted to the lower boundary of $\mathcal{D}_+$.

We first give a more convenient expression of $F_{(d,d')}$. Let $X = x + iy$ be a point in the domain $\mathcal{D}_+$. We have:

$$\sin \theta(X, 0, \infty) = \frac{y}{\sqrt{x^2 + y^2}}$$

And since the matrix $\begin{pmatrix} -1 & d \\ \frac{1}{d'-d} & \frac{-d'}{d'-d} \end{pmatrix} \in SL_2(\mathbb{R})$ acts on $\mathbb{H}^2$ by isometry and sends the geodesic $\gamma_{d,d'}$ to $\gamma_{0,\infty}$ and $x + iy$ to

$$\tilde{x} + i\tilde{y} = \frac{(-x - iy + d)(d' - d)}{x + iy - d'} = \frac{d - d'}{(x - d')^2 + y^2} \cdot (-(x-d)(x-d') - y^2 + iy(d'-d))$$

we have:

$$\sin \theta(X, d, d') = \frac{\tilde{y}}{\sqrt{\tilde{x}^2 + \tilde{y}^2}} = \frac{y(d' - d)}{\sqrt{((x-d)(x-d') + y^2)^2 + y^2(d'-d)^2}}$$

Hence:

$$F_{(d,d')}(X) = \frac{1}{d'-d}\sqrt{\frac{((x-d)(x-d')+y^2)^2+y^2(d'-d)^2}{x^2+y^2}} \tag{10}$$

To study the variations of $F_{(d,d')}(X)$, it suffices to consider what is inside the square root in (10):

$$G : (x,y) \mapsto \frac{((x-d)(x-d')+y^2)^2+y^2(d'-d)^2}{x^2+y^2}$$

On the lower boundary of $\mathcal{D}_+$, this reduces to

$$(1+dd'-(d+d')\cos\theta)^2+(d'-d)^2\sin^2\theta = (1+dd')^2-2(1+dd')(d+d')\cos\theta+2dd'\cos 2\theta-1$$

whose derivative with respect to θ is

$$-4dd'\sin 2\theta + 2(1+dd')(d+d')\sin\theta = 2\sin\theta\left[(1+dd')(d+d')-4dd'\cos\theta\right].$$

We want to prove that G is an increasing function of θ. This follows from $(1+dd')(d+d') \geq 4dd'$, which in turn follows from $d+d' \geq 2\sqrt{dd'}$, and the fact that $x^2-2x+1 \geq 0$ for any real number x, in particular for $x=\sqrt{dd'}$.

Proof of step 5.
We compute the differential of G with respect to y. It gives

$$\frac{\partial G}{\partial y}(x,y) = \frac{2y}{(x^2+y^2)^2}\cdot(y^4+2x^2y^2+x^4-dd'(2x-d)(2x-d')).$$

The sign of $\frac{\partial G}{\partial y}(x,y)$ is the sign of the polynomial $P(X) = X^2+2x^2X+x^4-dd'(2x-d)(2x-d')$, which has discriminant

$$\Delta = 4dd'(2x-d)(2x-d').$$

Setting $x=\frac{\Phi}{2}$ yields:

$$\Delta = 4dd'(\Phi-d)(\Phi-d').$$

In particular:

- If $d'>\Phi$, then $\Delta<0$ and P has no real roots.
- If $d'=\Phi$ then $\Delta=0$ and the only real root of P is $-\frac{\Phi^2}{4}<0$.
- Else, $\frac{\Phi}{2}<d'<\Phi$ and P has two real roots:

$$\lambda_- = -\frac{\Phi^2}{4}-\sqrt{dd'(\Phi-d)(\Phi-d')} < 0 \text{ and } \lambda_+ = -\frac{\Phi^2}{4}+\sqrt{dd'(\Phi-d)(\Phi-d')}.$$

But $d(\Phi-d) \leq \frac{\Phi^2}{4}$ and $d'(\Phi-d') \leq \frac{\Phi^2}{4}$ so $\sqrt{dd'(\Phi-d)(\Phi-d')} \leq \frac{\Phi^2}{4}$ and $\lambda_+ \leq 0$.

In conclusion, P has no real positive roots, in particular it is positive on $\mathbb{R}_+^*$, and so is $\frac{\partial G}{\partial y}(\frac{\Phi}{2},y)$. This finishes the proof of the last step.

In particular, the only possible minimum for $F_{(d,d')}$ on $\mathcal{D}_+$ is X_0. This proves Proposition 7.8. □

References

[AH22] Francisco Arana-Herrera. Effective mapping class group dynamics 1: Counting lattice points in Teichmüller space. *Duke Math. J.*, 2022.

[CKM21a] Smail Cheboui, Arezki Kessi, and Daniel Massart. Algebraic intersection for translation surfaces in a family of Teichmüller disks. *Bull. Soc. Math. France*, 149(4):613–640, 2021.

[CKM21b] Smail Cheboui, Arezki Kessi, and Daniel Massart. Algebraic intersection for translation surfaces in the stratum $H(2)$. *C. R. Math. Acad. Sci. Paris*, 359:65–70, 2021.

[DFT11] Diana Davis, Dmitry Fuchs, and Serge Tabachnikov. Periodic trajectories in the regular pentagon. *Mosc. Math. J.*, 11(3):439–461, 2011.

[DL19] Diana Davis and Samuel Lelièvre. Periodic paths on the pentagon, double pentagon and golden l. *Preprint*, 2019.

[KW22] Jeremy Kahn and Alex Wright. Hodge and Teichmüller. *J. Mod. Dyn.*, 18:149–160, 2022.

[LN14] Erwan Lanneau and Duc-Manh Nguyen. Teichmüller curves generated by Weierstrass Prym eigenforms in genus 3 and genus 4. *J. Topol.*, 7(2):475–522, 2014.

[Mas97] Daniel Massart. Normes stables des surfaces. *Comptes Rendus de l'Académie des Sciences - Series I - Mathematics*, 324(2):221–224, 1997.

[Mas22] Daniel Massart. A short introduction to translation surfaces, Veech surfaces, and Teichmüller dynamics. In *Surveys in geometry I*, pages 343–388. Springer, Cham, [2022] ©2022.

[McM05] Curtis T. McMullen. Teichmüller curves in genus two: Discriminant and spin. *Math. Ann.*, 333(1):87–130, 2005.

[McM07] Curtis T. McMullen. Dynamics of $\mathrm{SL}_2(\mathbb{R})$ over moduli space in genus two. *Ann. Math. (2)*, 165(2):397–456, 2007.

[MM14] Daniel Massart and Bjoern Muetzel. On the intersection form of surfaces. *Manuscr. Math.*, 143(1-2):19–49, 2014.

[Mon05] Thierry Monteil. On the finite blocking property. *Ann. Inst. Fourier*, 55(4):1195–1217, 2005.

[SW10] John Smillie and Barak Weiss. Characterizations of lattice surfaces. *Invent. Math.*, 180(3):535–557, 2010.

[Vee89] W. A. Veech. Teichmüller curves in moduli space, Eisenstein series and an application to triangular billiards. *Invent. Math.*, 97(3):553–583, 1989.

[Vor96] Ya. B. Vorobets. Planar structures and billiards in rational polygons. *Russ. Math. Surv.*, 51(1):177–178, 1996.

[Wri16] Alex Wright. From rational billiards to dynamics on moduli spaces. *Bull. Amer. Math. Soc. (N.S.)*, 53(1):41–56, 2016.

[ZK76] A. N. Zemlyakov and A. B. Katok. Topological transitivity of billiards in polygons. *Math. Notes*, 18:760–764, 1976.

[Zor06] Anton Zorich. Flat surfaces. In *Frontiers in number theory, physics, and geometry. I*, pages 437–583. Springer, Berlin, 2006.

UMR CNRS 5582, Univ. Grenoble Alpes, CNRS, Institut Fourier, F-38000 Grenoble, France

Email address: julien.boulanger@univ-grenoble-alpes.fr

UMR CNRS 5582, Univ. Grenoble Alpes, CNRS, Institut Fourier, F-38000 Grenoble, France

Email address: erwan.lanneau@univ-grenoble-alpes.fr

IMAG, CNRS, Univ Montpellier, France

Email address: daniel.massart@umontpellier.fr

Chapitre 3

KVol on regular n-gons

Résumé en français. Ce chapitre correspond à l'article [Bou23a] (soumis pour publication), dans lequel nous étendons les méthodes du chapitre précédent pour calculer KVol sur le n-gone régulier. Bien que les idées soient identiques, trois spécificités du n-gone régulier rendent ce cas plus difficile. En premier, les côtés du n-gone régulier sont identifiés deux à deux, de sorte que deux segments adjacents consécutifs peuvent intersecter deux fois un segment non-adjacent, ce qui nécessite de raffiner l'estimation sur les longueurs dans certains cas. Par ailleurs, lorsque $n \equiv 2 \mod 4$, le n-gone régulier possède deux singularités distinctes : dans ce cas, la méthode de découpage, adaptée aux connexions de selles, ne permet pas de calculer précisément KVol mais seulement d'obtenir une borne supérieure. Pour cette même raison, l'argument d'extension au disque de Teichmüller ne se généralise pas lorsque $n \equiv 2 \mod 4$ et on peut seulement obtenir une borne supérieure sur KVol pour tout le disque de Teichmüller du n-gone régulier en regardant les décompositions en cylindres. Enfin, alors que KVol était réalisé par une paire de systoles pour le modèle en escalier du double n-gone, ce n'est pas le cas pour le modèle en escalier du n-gone régulier ($n \equiv 0 \mod 4$). Cela a pour conséquence que, à la place d'avoir une seule géodésique maximisant KVol sur le disque de Teichmüller, il y en a une infinité et il faut être beaucoup plus fin dans les calculs. Cela constitue la principale difficulté de ce chapitre, et correspond à la Section 6.

Nous démontrons les Théorèmes 1.3.3 et 1.3.4 dans la Section 3, puis le Théorème 1.3.9 dans la Section 6. Enfin, nous démontrons les Théorèmes D et 1.3.11 dans la Section 7.

ALGEBRAIC INTERSECTION, LENGTHS AND VEECH SURFACES

JULIEN BOULANGER

ABSTRACT. In this paper, we continue the study of intersections of closed curves on translation surfaces, initiated in [2] and [3] for a family of arithmetic Veech surfaces and [1] for a family of non-arithmetic Veech surfaces. Namely, we investigate the question of maximizing the algebraic intersection between two curves of given lengths, and we focus on the case of translation surfaces in the Teichmüller disk of the regular n-gons for even n.

1. INTRODUCTION

We study the question of maximizing the algebraic intersection between two closed curves of given lengths on translation surfaces. A suitable way of quantifying this is to consider the following quantity, which is in fact defined for any closed oriented surface X with a Riemannian metric g (possibly with singularities):

$$\mathrm{KVol}(X) := \mathrm{Vol}(X,g) \cdot \sup_{\alpha,\beta} \frac{\mathrm{Int}(\alpha,\beta)}{l_g(\alpha) l_g(\beta)}, \tag{1}$$

where the supremum ranges over all piecewise smooth closed curves α and β in X, Int denotes the algebraic intersection, and $l_g(\cdot)$ denotes the length with respect to the Riemannian metric (it is readily seen that multiplying by the volume $\mathrm{Vol}(X,g)$ makes the quantity invariant by rescaling the metric g). As shown by Massart-Müetzel [5], this function is well defined and finite.

Though KVol is a close cousin of the systolic volume $\mathrm{SysVol}(X) = \sup_\alpha \frac{\mathrm{Vol}(X)}{l_g(\alpha)^2}$, it is difficult to compute on a given surface outside the case of a flat torus (where $\mathrm{KVol} = 1$). In this context, Cheboui, Kessi and Massart [2, 3] initiated the study of KVol on translation surfaces, which are instances of flat surfaces with conical singularities. More precisely, [2] provides estimates of KVol on the Teichmüller curves associated with a family of arithmetic translation surfaces (X,ω). In Boulanger–Lanneau–Massart [1], we give a closed formula for KVol on the Teichmüller disk of the double regular n-gon translation surface for $n \geq 5$ odd. In this paper, we continue the study of KVol in the Teichmüller disk of translation surfaces coming from regular polygons. Namely, we deal with the case of the regular n-gon for $n \geq 8$ even. Although similar to the case of the double regular n-gon for odd n, the case of the regular n-gon for even n requires a more careful study.

Given an even integer $n \geq 8$, we denote by X_n the translation surface made from a regular n-gon by identifying its parallel opposite sides by translations. The resulting surface has a unique conical singularity if $n \equiv 0 \mod 4$ and two distinct conical singularities if $n \equiv 2 \mod 4$. This surface can also be obtained by the unfolding construction of Katok–Zemlyakov [12] from a triangle of angles $(\frac{\pi}{2}, \frac{\pi}{n}, \frac{(n/2-1)\pi}{n})$ and is one of the original Veech surfaces (see [9]). As it will be recalled in Section 2, the Veech group of X_n has a *staircase model* $\mathcal{S}$ in its Teichmüller disk whose Veech group Γ_n is an index two subgroup of the Hecke group of order n. In particular, the Teichmüller curve associated to X_n can be identified with $\mathbb{H}^2/\Gamma_n$ and has a fundamental domain $\mathcal{T}_n$ depicted in Figure 1, where $\Phi := \Phi_n = 2\cos(\frac{\pi}{n})$.

In this paper, we study KVol in the Teichmüller disk of X_n, and we give a formula to compute KVol on any surface of $\mathcal{T}_n$ for $n \equiv 0 \mod 4$. If $n \equiv 2 \mod 4$, the fact that X_n has two singularities makes it more difficult to compute KVol. In this latter case, our methods provide upper bounds on KVol in the Teichmüller disk of X_n.

The case $n \equiv 0 \mod 4$. Our main result holds in the case where $n \equiv 0 \mod 4$, so that the regular n-gon as a single singularity, and can be stated as:

Theorem 1.1. *Let $n \geq 8$ such that $n \equiv 0 \mod 4$. Given $d, d' \in \mathbb{R} \cup \{\infty\} \simeq \partial\mathbb{H}^2$, let $\gamma_{d,d'}$ denote the geodesic in the hyperbolic plane $\mathbb{H}^2$ having d and d' as endpoints, and define:*

$$\mathcal{G}_{max} = \bigcup_{k \in \mathbb{N}^* \cup \{\infty\}} \gamma_{\infty, \pm\frac{1}{k\Phi}}$$

(with the convention $\frac{1}{\infty} = 0$).

Let $X = M \cdot \mathcal{S}_n$ be a surface in the Teichmüller disk of X_n, obtained from the staircase model $\mathcal{S}$ by applying a matrix $M = \begin{pmatrix} a & b \\ c & d \end{pmatrix} \in SL_2(\mathbb{R})$. Then, we have:

$$\mathrm{KVol}(X) = K_0 \cdot \frac{1}{\cosh(\mathrm{dist}_{\mathbb{H}^2}(\frac{di+b}{ci+a}, \Gamma_n \cdot \mathcal{G}_{max}))} \tag{2}$$

Where $K_0 > 0$ is an explicit constrant which only depends on n and $\mathrm{dist}_{\mathbb{H}^2}$ denotes the hyperbolic distance.

In particular, KVol is bounded on the Teichmüller disk of the regular n-gon, and

- *(i) the maximum of KVol is achieved for surfaces represented by images of elements of $\mathcal{G}_{max}$ under the group Γ_n,*
- *(ii) the minimum of KVol is achieved, uniquely, at X_n.*

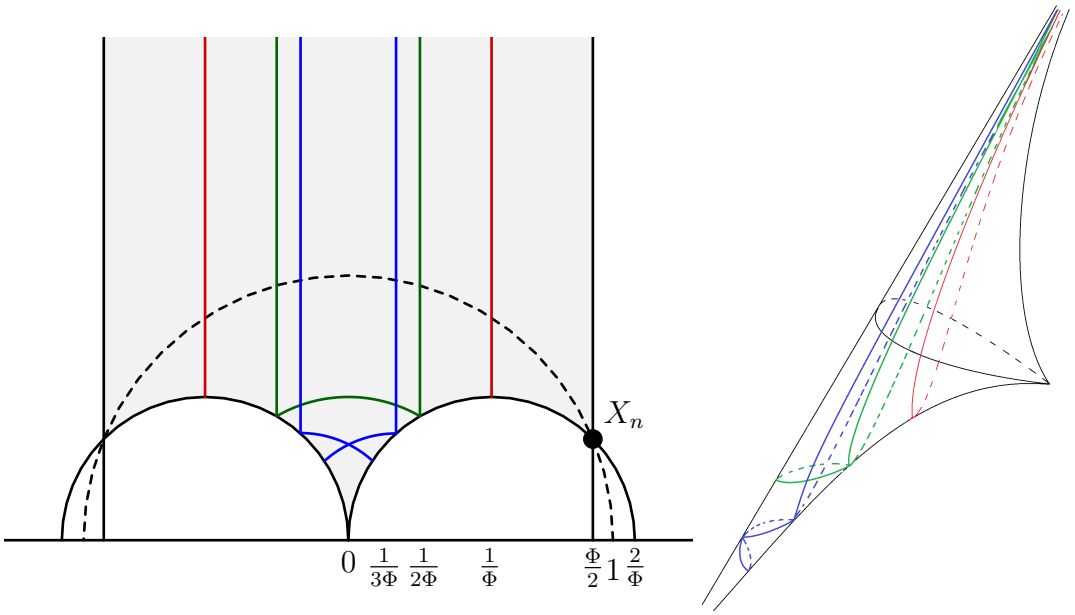

FIGURE 1. The geodesics $\gamma_{\infty,\frac{1}{k\Phi}}$ for $k = 1, 2, 3$ and their images by the Veech group intersecting the fundamental domain $\mathcal{T}_{nn}$. On the right, the same geodesics on the surface $\mathbb{H}^2/\Gamma_n$.

Specifically when $X = X_n$ is the regular n-gon, the result of Theorem 1.1 can be stated as follows[1]:

Theorem 1.2. *Let $n \geq 8$, $n \equiv 0 \mod 4$. Let l_0 be the length of the side of the n-gon[2]. For any pair of saddle connections α, β, we have*

$$\frac{\mathrm{Int}(\alpha, \beta)}{l(\alpha)l(\beta)} \leq \frac{1}{l_0^2}. \tag{3}$$

Moreover, equality is achieved if and only if α and β are distinct sides of the n-gon.

Using that the volume of a regular n-gon of unit side is $\frac{n}{4\tan\frac{\pi}{n}}$, we get:

Corollary 1.3. *For any $n \geq 8$ such that $n \equiv 0 \mod 4$, we have:*

$$\mathrm{KVol}(X_n) = \frac{n}{4\tan(\frac{\pi}{n})}.$$

Notice that although X_n has minimal KVol in its Teichmüller disk, it is not a local minimum for KVol in its stratum $\mathcal{H}(2g-2)$. Indeed, the regular n-gon is the polygon with n sides of the same length that have maximal volume. In

[1]Although stated in this order, we first prove Theorem 1.2 and then use it to prove Theorem 1.1

[2]Which is also the systolic length of the resulting surface X_n.

particular, any other such polygon close to the regular n-gon will have a smaller volume, and KVol will still be realized by pairs of sides of the corresponding n-gon, hence will be smaller.

The case $n \equiv 2 \mod 4$. If $n \equiv 2 \mod 4$, the resulting translation surface X_n has two conical singularities, so that saddle connections may not be closed curves anymore, and simple closed geodesics could be homologous to the union of several non-closed saddle connections in different directions. For this reason, we do not have a closed formula for KVol in the Teichmüller disk of the regular n-gon. However, we show:

Theorem 1.4. *For $n \geq 10$ with $n \equiv 2 \mod 4$, KVol is bounded on the Teichmüller disk of the regular n-gon.*

An explicit bound is given in Corollary 6.3. This result contrasts with examples of squared tiled translation surfaces with multiple singularities having unbounded KVol on their Teichmüller disk. It is the first example of a translation surface with more than one singularity where we can show boundedness on the Teichmüller disk. In fact, we give an explicit boundedness criterion in the Teichmüller disk of a Veech surface:

Theorem 1.5. KVol *is bounded on the Teichmüller disk of a Veech surface X if and only if there are no intersecting closed curves η and ξ on X such that $\eta = \eta_1 \cup \cdots \cup \eta_k$ and $\xi = \xi_1 \cup \cdots \cup \xi_l$ are unions of parallel saddle connections (that is all saddle connections $\eta_1, \ldots, \eta_k, \xi_1, \ldots, \xi_l$ have the same direction).*

This criterion generalises Proposition 3.2 of [1] to the case of translation surfaces with several singularities.

Finally, concerning the regular n-gon itself, the proof of Theorem 1.2 extends and gives:

Theorem 1.6. *Let $n \geq 10$ with $n \equiv 2 \mod 4$. Let l_0 be the length of the side of the n-gon. For any pair of closed curves α, β on X_n, we have*

$$\frac{Int(\alpha, \beta)}{l(\alpha) l(\beta)} < \frac{1}{l_0^2}.$$

Notice that in this case, we show that the inequality is strict. In fact, it is unclear whether the best possible ratio is achieved and, if so, by which closed curves. Our guess would be the following:

Conjecture 1.7. *Let $n \geq 10$ with $n \equiv 2 \mod 4$. For any pair of closed curves α, β on X_n, we have*

$$\frac{Int(\alpha, \beta)}{l(\alpha) l(\beta)} \leq \frac{1}{2l_0^2},$$

where l_0 is the length of the side of the n-gon. Moreover, equality is achieved if and only if α and β are twice intersecting pairs of sides of the n-gon, as in Figure

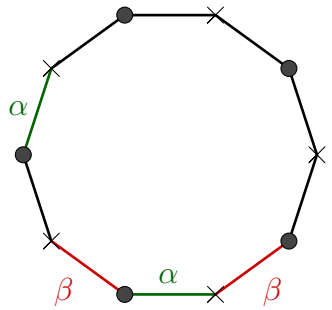

FIGURE 2. In this example, the curves α and β (oriented such that the resulting curve has a well defined orientation) intersect twice.

2 for the decagon. In particular:

$$\mathrm{KVol}(X_n) = \frac{n}{8\tan(\frac{\pi}{n})}$$

Strategy of proof. Although stated in the reversed order, the proof of Theorem 1.1 rely on Theorem 1.2. The proof of both Theorem 1.2 and Theorem 1.6 uses a subdivision method developped in [1] in the case of the double n-gon for odd n, which we extend to the case of the regular n-gons for even n: given two saddle connections, we can estimate simulteneously their lengths and their intersection by subdivising each saddle connection into smaller well-chosen segments.

Then, we prove Theorem 1.1 by studying how the ratio $\frac{\mathrm{Int}(\alpha,\beta)}{l(\alpha)l(\beta)}$ varies as the surface X and the saddle connections α and β moves under the action of a matrix of $SL_2(\mathbb{R})$. The proof of both Theorem 1.1 and Theorem 1.4 uses the fact that there are only two cylinder decompositions up to the action of $SL_2(\mathbb{R})$ on each surface of the Teichmüller disk of the regular n-gon.

Further, although Theorem 1.1 is similar to Theorem 1.1 of [1] stated for the double n-gon when n is odd, the main difference is that the maximum of KVol on the Teichmüller disk of the regular n-gon is achieved along an infinite set of geodesics instead of a single geodesic for the Teichmüller disk of the double regular n-gon. This has to do with the fact that the staircase model associated with the double regular n-gon has a pair of intersecting systoles, giving a big KVol, while there is only one systole for the staircase model associated with the regular n-gon. In particular, the supremum in the definition of KVol on the staircase model associated with the regular n-gon ($n \geq 8$, $n \equiv 0 \mod 4$) is achieved when α and β are respectively the systole and the second shortest closed curve (which is perpendicular to the systole, see Figure 4), but it is also realised as the limit when k goes to infinity of the ratio $\frac{\mathrm{Int}(\alpha,\beta_k)}{l(\alpha)l(\beta_k)}$, where α is the systole and β_k is a saddle connection winding k times around the smallest vertical cylinder of $\mathcal{S}_n$ (and hence intersecting $k+1$ times α, counting one singular intersection).

Organization of the paper. We recall in Section 2 useful results about translation surfaces and their Veech groups, and we describe the staircase model associated with the regular n-gon. In Section 3, we compute explicitly KVol on the regular n-gon using elementary geometry, showing both Theorem 1.2 and Theorem 1.6. Next, we provide in Section 4 key estimates that allows to understand the function KVol on the Teichmüller disk. Using the knowledge of KVol on the regular n-gon ($n \equiv 0 \mod 4$), we prove Theorem 1.1 in Section 5. Finally, we show the boundedness criterion for KVol on Teichmüller disks (Theorem 1.5) in Section 6 and we apply this criterion to the regular n-gon ($n \equiv 2 \mod 4$) in order to deduce Theorem 1.4.

Ackowledgements. I would like to thank Erwan Lanneau and Daniel Massart for their constant support and for enlightening discussions, as well as helpful comments on preliminary versions of this document.

2. Background

2.1. **Translation surfaces and their Veech groups.** We start with a quick review of useful notions. We encourage the reader to check out the surveys [13], [11] and [4] for a general introduction to translation surfaces.

A *translation surface* (X, ω) is a real compact genus g surface X with an atlas ω such that all transition functions are translations except on a finite set of singularities Σ, along with a distinguished direction. In fact, it can also be seen as a surface obtained from a finite collection of polygons embedded in $\mathbb{C}$ by gluing pairs of parallel opposite sides by translation. The resulting surface has a flat metric and a finite number of conical singularities. With this description, the moduli space of translation surfaces can be thought of as the space of all translation surfaces up to cut and paste.

The action of $GL_2^+(\mathbb{R})$ on polygons induces an action on the moduli space of translation surfaces. The orbit of a given translation surface is called its *Teichmüller disk* and its stabilizer is called the *Veech group* and is often denoted $SL(X)$. W.A. Veech showed in [9] that the latter are discrete subgroups of $SL_2(\mathbb{R})$. In particular, the Teichmüller disk of a translation surface can be identified with $\mathbb{H}^2/SL(X)$.

2.2. **The regular n-gon and its staircase model.** Given $n \geq 4$ even, one can contruct a translation surface by identifying parallel opposite sides of a regular n-gon. If $n \equiv 0 \mod 4$ (and $n \geq 8$), the resulting surface has a single singularity, and in particular, every edge corresponds to a closed curve on the surface. However, if $n \equiv 2 \mod 4$ (and $n \geq 10$), the resulting surface has two singularities, so that sides are no longer closed curves.

As described in [6] and depicted in Figures 3 and 4, the regular n-gon X_n has a staircase shaped model $\mathcal{S}_n$ in its Teichmüller disk.

With the notations of Figure 4, the lengths of the sides are given by:

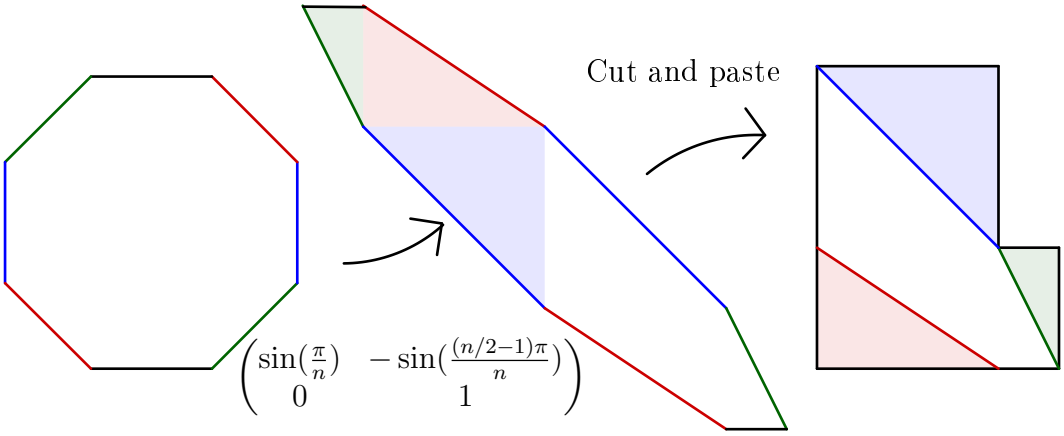

FIGURE 3. From the regular octagon to its staircase model.

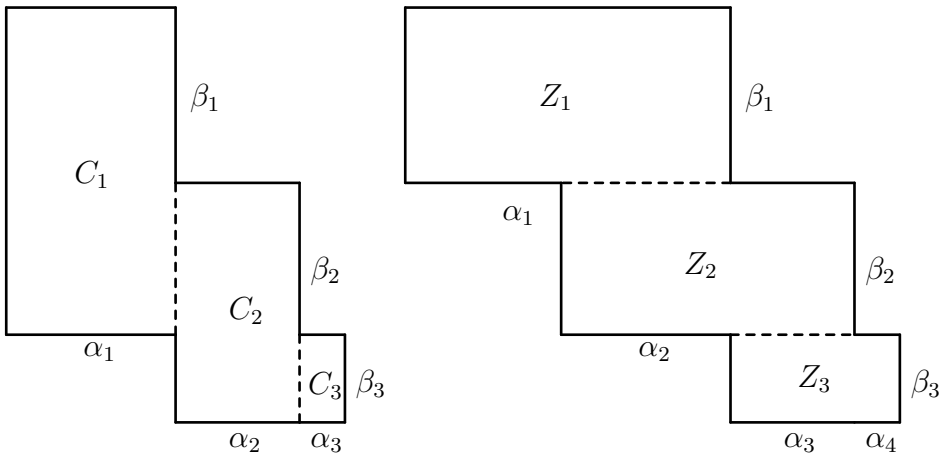

FIGURE 4. The staircase model associated with the regular n-gon for $n = 12$ on the left and $n = 14$ on the right.

$$l(\alpha_i) = \sin(\frac{(n/2 - 2i + 1)\pi}{n}) \text{ and } l(\beta_j) = \sin(\frac{(n/2 - 2j + 2)\pi}{n})$$

Where $i, j \in [\![1, \frac{n}{4}]\!]$ for $n \equiv 0 \mod 4$, and $i \in [\![1, \frac{n-2}{4} + 1]\!]$ while $j \in [\![1, \frac{n-2}{4}]\!]$ for $n \equiv 2 \mod 4$. In particular, the modulus of each vertical cylinder C_i is $\Phi = 2\cos(\frac{\pi}{n})$ as well as the modulus of each horizontal cylinder Z_j, except the horizontal cylinder Z_1 if $n \equiv 0 \mod 4$ (resp. the vertical cylinder C_1 if $n \equiv 2 \mod 4$) having a modulus of $\Phi/2$.

In both cases, the Veech group Γ_n associated with the staircase model contains the horizontal twist $T_H = \begin{pmatrix} 1 & \Phi \\ 0 & 1 \end{pmatrix}$ and the vertical twist $T_V = \begin{pmatrix} 1 & 0 \\ \Phi & 1 \end{pmatrix}$. In fact, it is shown in [9] that Γ_n is generated by T_H and T_V. In particular, the Teichmüller disk of the regular n-gon, identified with $\mathbb{H}^2/\Gamma_n$ has a fundamental domain $\mathcal{T}_n$ as depicted in Figure 5.

It will sometimes be convenient to include orientation-reversing elements in the definition of the Veech group. The matrix $R = \begin{pmatrix} 1 & 0 \\ 0 & -1 \end{pmatrix}$ gives an affine orientation-reversing diffeomorphism of the staircase model, and in fact T_H, T_V and R generate the "non-oriented" Veech group, which we will denote by $\Gamma_n^{\pm}$.

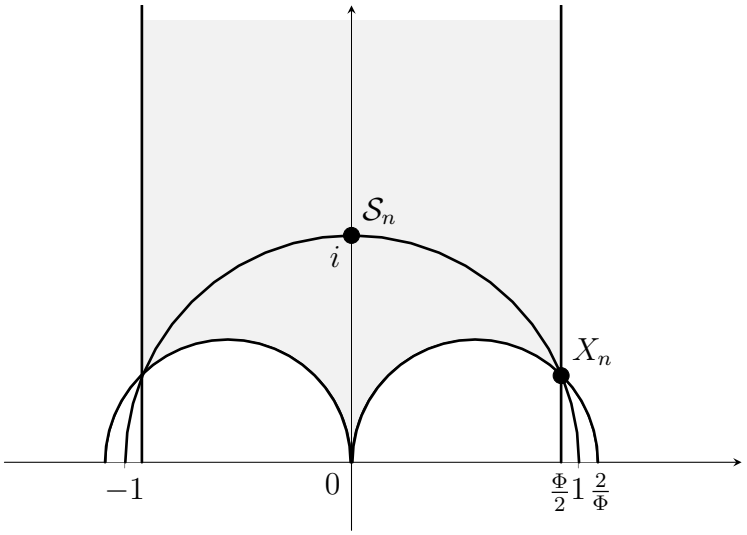

FIGURE 5. The fundamental domain of the Teichmüller disk of X_n.

3. KVOL ON THE REGULAR n-GON, $n \equiv 0 \mod 4$.

In this section, we give an elementary proof of Theorem 1.2 and Theorem 1.6. The main idea of the proof is to subdivide saddle connections α and β into smaller (non-closed) segments where we can control both the lengths and the intersections.

Given saddle connections α and β, we start by defining a notion of sector for the direction of α (resp. β) which tells how to subdivide the saddle connection α (resp. β) into segments (§§3.1 & 3.2). Then, we study these segments separately and show that they are all longer than the side of the regular n-gon (§3.2). Finally, we study the possible intersection for each pair of segments (§3.3). Setting aside two particular cases that are studied separately, each pair of segments (α_i, β_j) intersect at most once, giving the desired ratio. To conclude the proof, it remains

to take into account the possible singular intersections. This can be acomplished by paying closer attention to the intersections and the lengths.

3.1. **Sectors and separatrix diagrams.** The directions of the diagonals of the regular n-gon subdivide the set of possible directions into n sectors of angle $\frac{\pi}{n}$, as in Figure 6 for the octagon.

In each sector there is an associated *transition diagram* which encodes the possible sequence of intersections of sides for a line whose direction lies in this sector. For example, a geodesic with direction in the sector Σ_0 of Figure 6 has to intersect e_2 before and after each intersection with e_1 while it can intersect either e_2 or e_3 before and after each intersection with e_0. In this example, the sector Σ_0 gives the following transition diagram:

$$e_1 \leftrightarrows e_2 \leftrightarrows e_0 \leftrightarrows e_3 \circlearrowleft$$

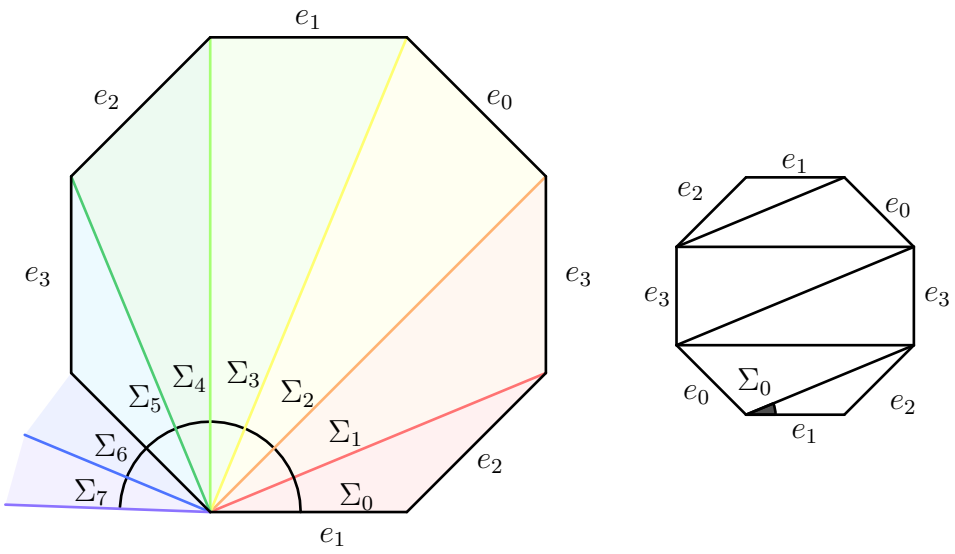

FIGURE 6. The directions of the diagonals of the octagon divide the set of directions into 8 sectors. On the right, diagonals corresponding to the sector Σ_0.

In this configuration we say that e_1 is *sandwiched*. The side e_1 can only be preceded and followed by the (adjacent) side e_2. More generally, for a given sector Σ on the regular n-gon we have a separatrix diagram of the form

$$e_{\sigma(0)} \leftrightarrows e_{\sigma(1)} \leftrightarrows \cdots \leftrightarrows e_{\sigma(n/2-2)} \leftrightarrows e_{\sigma(n/2-1)} \circlearrowleft$$

where $\sigma = \sigma_\Sigma \in \mathfrak{S}_{n/2}$ is a given permutation. We say that the side $e_{\sigma(0)}$ is sandwiched by the side $e_{\sigma(1)}$ in sector Σ. Note that it is sufficient to know $\sigma(0)$ and $\sigma(1)$ to tell the sector, as the sector is defined by the directions of the side $e_{\sigma(0)}$ and the diagonal $e_{\sigma(0)} + e_{\sigma(1)}$. See [7] for further details on transition diagrams of regular n-gons.

3.2. **Construction of the subdivision.** Let α be an oriented saddle connections on the regular n-gon. Assume α is not a diagonal of the n-gon, so that it has a well defined sector Σ_α which corresponds to a transition diagram given by the permutation σ_α. We cut α each time it intersects a non-sandwiched side of the n-gon. This gives a decomposition into non-closed segments $\alpha = \alpha_1 \cup \cdots \cup \alpha_k$ where each segment is either (see Figure 7):

- A non-sandwiched segment which goes from a side of the n-gon to another non-adjacent side of the n-gon.
- A sandwiched segment, with extremities on the side $e' = e_{\sigma_\alpha(1)}$, intersecting the sandwiched side $e = e_{\sigma_\alpha(0)}$ on its interior. Such segments are made of one piece going from e' to e and another piece going from e to e'. We say that such a sandwiched segment has type $e' \to e \to e'$.
- An initial or terminal segment α_1 or α_k. Such segments will be considered as non-sandwiched segments.

If α is a diagonal or a side of the n-gon, we set $k = 1$ and $\alpha = \alpha_1$.

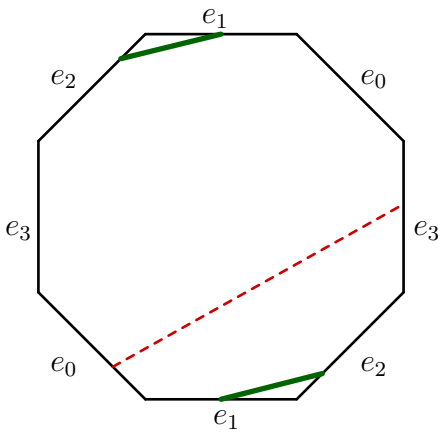

FIGURE 7. Example of a non-sandwiched segment (in dashed red) and a sandwiched segment (in bold green). The sandwiched segment is of type $e_2 \to e_1 \to e_2$.

By construction, we have:

Lemma 3.1. *For every i, we have $l(\alpha_i) \geq l_0$ and equality holds if and only if $k = 1$ and α is a side of the regular n-gon.*

Proof. A non-sandwiched segment has length at least l_0 since each segment going from a side to another non-adjacent side has length at least l_0 in the regular n-gon.
Now, take a sandwiched segment and assume up to a rotation that it is of type $e_2 \to e_1 \to e_2$, as in Figure 7. Since angles between the sides e_1 and e_2 are obtuse, the sandwiched segment has a length bigger than the length of e_1, that is l_0. □

3.3. **Study of the intersections.** In this section, we investigate the possible intersections between two distinct saddle connections α and β, and show:

$$\frac{|\alpha \cap \beta| + 1}{l(\alpha)l(\beta)} \leq \frac{1}{l_0^2} \tag{4}$$

where $|\alpha \cap \beta|$ is the cardinal of the set of intersection points without counting the singularities. This set is finite as α and β are distinct saddle connections.

As before, we decompose both $\alpha = \alpha_1 \cup \cdots \cup \alpha_k$ and $\beta = \beta_1 \cup \cdots \cup \beta_l$ into sandwiched and non-sandwiched segments. We start with the case where either α or β are sides of the n-gon.

If α (resp. β) is a side of the n-gon. In this case, notice that:

(1) Between each non-singular intersection with α, there is at least one sandwiched segment or one non-sandwiched segment of β, giving a length greater than l_0.
(2) Further, after the last non singular intersection with α, there is a least one non-sandwiched segment, giving a length greater than l_0.
(3) If there are no non-singular intersection with α, then β has length at least l_0 anyway (with equality if and only if β is another side of the regular n-gon).

In particular, $l(\beta) \geq (|\alpha \cap \beta| + 1)l_0$ and hence:

$$\frac{|\alpha \cap \beta| + 1}{l(\alpha)l(\beta)} \leq \frac{1}{l_0^2}$$

with equality if and only if both α and β are sides of the regular n-gon.

The other cases. In the rest of this section, we assume that α and β are not both sides of the regular n-gon. As such, there is at least one segment α_i of α for which the inequaltity $l(\alpha_i) > l_0$ is strict, and hence $l(\alpha)l(\beta) > kl \cdot l_0^2$. Further, up to a small deformation of α, we can assume there are no intersection on the sides of the n-gon (it is possible to do it while keeping each α_i straight and in the same sector). In this setting, all non-singular intersections between α and β correspond to an intersection of two segments α_i and β_j and we have:

$$|\alpha \cap \beta| \leq \sum_{i,j} |\alpha_i \cap \beta_j|$$

where $|\alpha_i \cap \beta_j|$ is the number of intersection points between the (non-closed) curves α_i and β_j. The latter quantity is finite as long as α and β are assumed to be distinct. Notice that if $n \equiv 0 \mod 4$, there is a single singularity so that α and β are automatically closed curves and we can define their algebraic intersection, and hence:

$$\mathrm{Int}(\alpha, \beta) \leq (\sum_{i,j} |\alpha_i \cap \beta_j|) + 1 \tag{5}$$

where the added $+1$ corresponds to the possible singular intersection.

Now, remark that if both α_i and β_j are not sandwiched, then $|\alpha_i \cap \beta_j| \leq 1$. More generally, we have:

Lemma 3.2. *For any i, j, $|\alpha_i \cap \beta_j| \leq 2$. Further, the case $|\alpha_i \cap \beta_j| = 2$ is possible only if:*

(i) Either α_i is a sandwiched segment of type $e' \to e \to e'$ and β_j is a sandwiched segment of type $e \to e' \to e$.

(ii) Or, up to permutation of α and β, α_i is a sandwiched segment of type $e' \to e \to e'$, and β_j is a long segment, that is the endpoints of β_j lie in $e_{\sigma_\beta(2m-1)}$ or $e_{\sigma_\beta(2m-2)}$ or at the two vertices contained in both $e_{\sigma_\beta(n/2-1)}$ and $e_{\sigma_\beta(n/2-2)}$. Further, $\{e, e'\} = \{e_{\sigma_\beta(n/2-1)}, e_{\sigma_\beta(n/2-2)}\}$.

These two configurations are depicted in Figure 8.

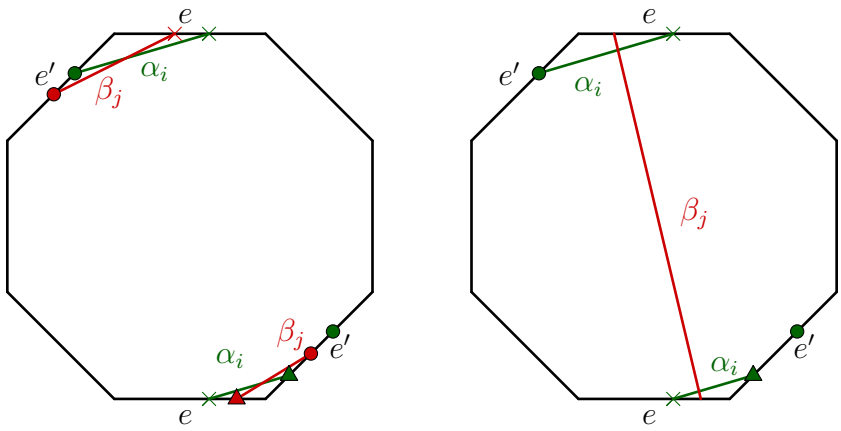

FIGURE 8. The two cases where $|\alpha_i \cap \beta_j| = 2$.

Remark 3.3. Notice that the two cases cannot happen simultaneously since in case (i) we have $\{e, e'\} = \{e_{\sigma_\beta(1)}, e_{\sigma_\beta(0)}\}$ while in case (ii) we have $\{e, e'\} = \{e_{\sigma_\beta(n/2-1)}, e_{\sigma_\beta(n/2-2)}\}$.

Proof of Lemma 3.2. 1^{st} **case:** Assume that both α_i and β_j are sandwiched segments. Then, the study of the intersections is exactly the same as the study of the intersections of pairs of sandwiched segments in the double n-gon for odd n, see [1, §6.3]. Up to a rotation or a symmetry, we can assume α_i is sandwiched of type $e_2 \to e_1 \to e_2$.

In particular, $|\alpha_i \cap \beta_j| = 0$ unless β_j has one of the following type:

$$\begin{array}{ll} (1) \quad e_0 \to e_1 \to e_0 & (2) \quad e_1 \to e_0 \to e_1 \\ (3) \quad e_1 \to e_2 \to e_1 & (4) \quad e_2 \to e_1 \to e_2 \\ (5) \quad e_2 \to e_3 \to e_2 & (6) \quad e_3 \to e_2 \to e_3 \end{array}$$

(This is because α_i and β_j have to share at least a common side of the n-gon to intersect).

Similarly to the case of the double n-gon for odd n, we can show (see Figure 9) that in all cases but (3) we have $|\alpha_i \cap \beta_j| \leq 1$. In particular, the case (3) is the only case where we possibly have $|\alpha_i \cap \beta_j| = 2$ (as in the left of Figure 8).
2^{nd} **case:** Up to permutation of α and β, α_i is sandwiched (say of type $e' \to e \to e'$) while β_j is not. In this case, we see easily that β_j has to be a long segment whose extremities lie on the sides e or e' in order to get two intersections, as in the right of Figure 8. □

In light of Lemma 3.2 and Remark 3.3, we distinguish three mutually exclusive cases:

(0) There is no configuration of type (i) or (ii).
(i) There exists i, j such that α_i and β_j are in a configuration of type (i).
(ii) There exists i, j such that α_i and β_j are in a configuration of type (ii).

Case (0)**: There is no configuration of type** (i) **or** (ii)**.** In this case, we deduce from Equation (5) and Lemma 3.2 that:

$$|\alpha \cap \beta| \leq kl. \tag{6}$$

In order to get Equation (4), we either improve the inequality on the intersections (Equation (6)) or the inequality on the lengths $l(\alpha)l(\beta) > kl \cdot l_0^2$. For this purpose, we distinguish two cases:

(1) If α is not contained in the cylinder defined by $e_{\sigma_\alpha(0)}, e_{\sigma_\alpha(1)}$ as in Figure 10 (in the example of the octagon), then we can find two consecutive segments α_i and α_{i+1} which are not contained in the cylinder. As explained in Figure 10, the length $l(\alpha_i) + l(\alpha_{i+1})$ should be at least $\Phi^2 l_0$. Since $\Phi^2 > 3$, we have $l(\alpha_i) + l(\alpha_{i+1}) > 3l_0$, so that $l(\alpha) > (k+1)l_0$, and

$$l(\alpha)l(\beta) > (kl+1)l_0^2.$$

Using Equation (6) we have directly that Equation (4) holds (the inequality being strict in this case). By symmetry, the same argument holds if β is not contained in the cylinder defined by $e_{\sigma_\beta(0)}, e_{\sigma_\beta(1)}$.

(2) Otherwise, we can assume that α is contained in the cylinder defined by $e_{\sigma_\alpha(0)}$ and $e_{\sigma_\alpha(1)}$ while β is contained in the cylinder defined by $e_{\sigma_\beta(0)}$ and $e_{\sigma_\beta(1)}$. In this case, unless β is a diagonal, we see that α_1 cannot intersect both β_1 (which lies in a region S_0 as in Figure 11) and β_l (which lie in a

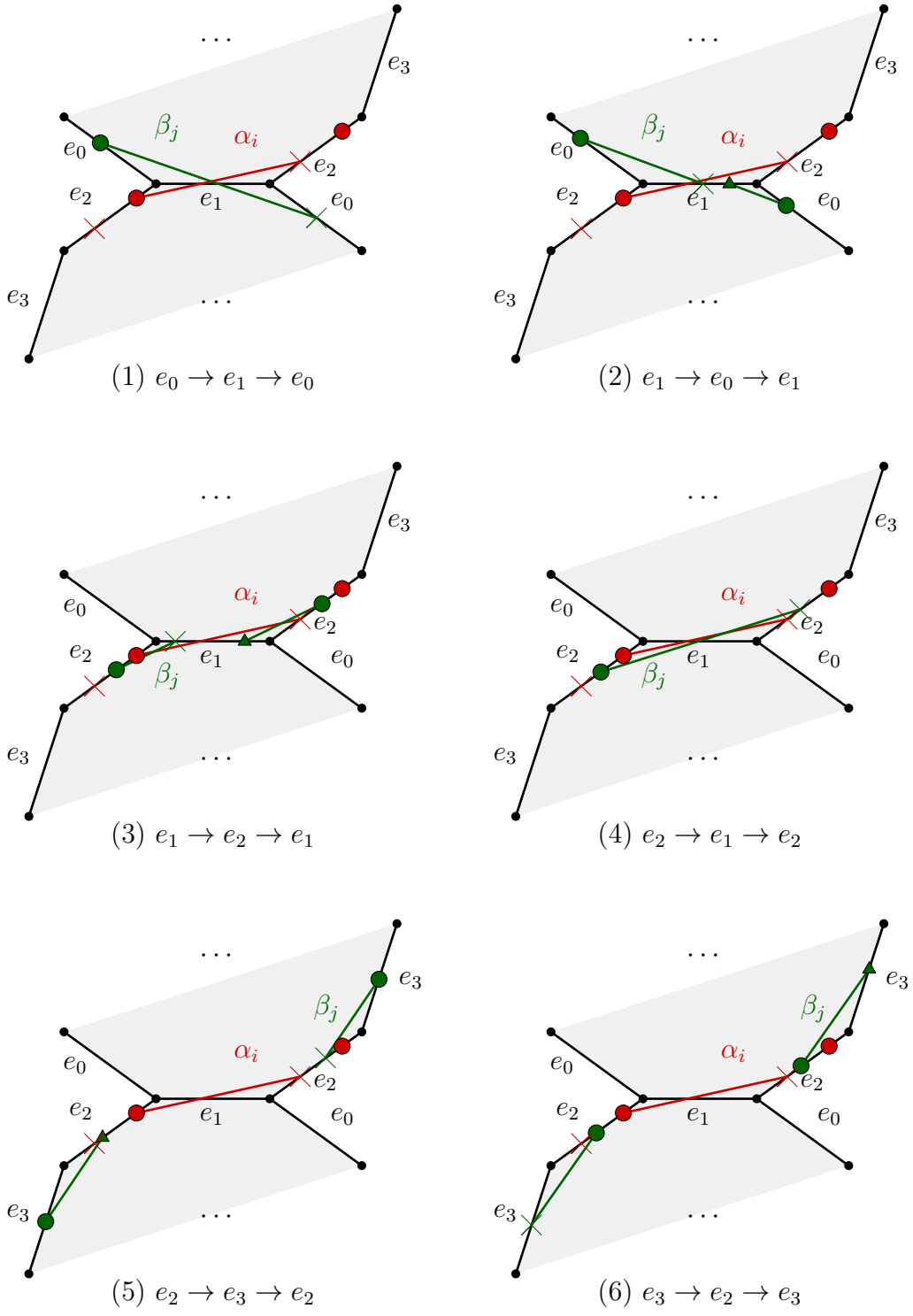

FIGURE 9. The six cases in Lemma 3.2, (i).

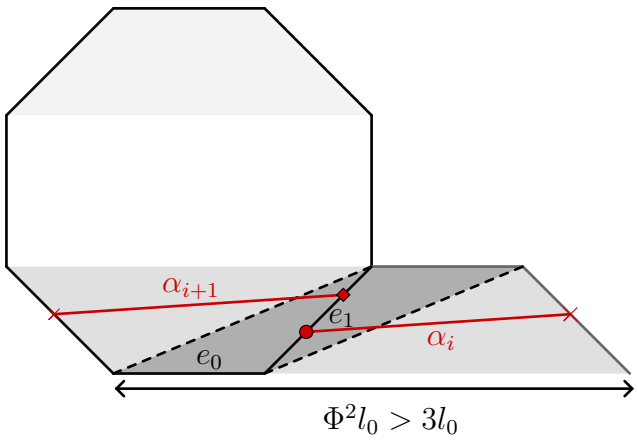

FIGURE 10. If α is not contained in the cylinder defined by e_0 and e_1, then there are two consecutive segments α_i and α_{i+1} with $l(\alpha_i) + l(\alpha_{i+1}) > 3l_0$.

symmetric region S_1), so that

$$|\alpha \cap \beta| \leq kl - 1.$$

In particular $|\alpha \cap \beta| + 1 \leq kl$ and using that $l(\alpha)l(\beta) > kl \cdot l_0^2$, we deduce that Equation (4) holds (and the inequality is strict in this case).

(3) Finally, if both α and β are diagonals, we have $l(\alpha), l(\beta) \geq \Phi l_0$ and hence $l(\alpha)l(\beta) \geq \Phi^2 l_0^2 > 2l_0^2$, so that Equation (4) holds as well and the inequality is strict.

It remains to investigate cases (i) and (ii).

Case (i): $\exists i, j$, α_i and β_j are in a configuration of type (i), that is α_i is a sandwiched segment of type $e' \to e \to e'$ and β_j is a sandwiched segment of type $e \to e' \to e$. This case corresponds to case (3) of [1, §6.3]. Similarly, we consider the maximal sequence of sandwiched segments $\alpha_{i_0} \cup \cdots \cup \alpha_{i_0+p}$ (resp. $\beta_{j_0} \cup \cdots \cup \beta_{j_0+q}$) containing α_i (resp. β_j), which is maximal in the sense that both α_{i_0-1} and α_{i_0+p+1} (resp. β_{j_0-1} and β_{j_0+q+1}) are non-sandwiched, and we can show:

Lemma 3.4. *$\alpha_{i_0} \cup \cdots \cup \alpha_{i_0+p} \cup \alpha_{i_0+p+1}$ and $\beta_{j_0} \cup \cdots \cup \beta_{j_0+q} \cup \beta_{j_0+q+1}$ intersect at most $(p+3)(q+2)$ times while there are $(p+3)(q+3)$ pairs of segments.*

In particular, summing the intersections of pairs of maximal sequences of sandwiched segments and intersections of pairs of segments which are not already counted in such maximal sequences (and as such intersect at most once), we get:

$$\sum_{i,j} |\alpha_i \cap \beta_j| < kl$$

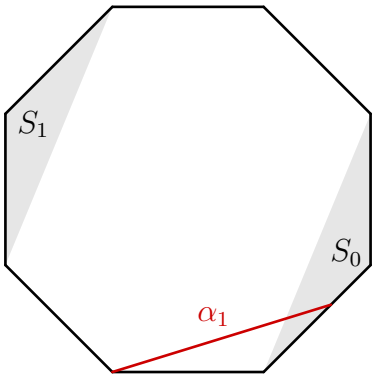

FIGURE 11. In case 2, α_1 cannot intersect both β_1 (which lies in a region S_0) and β_l (which lies in the symetric region S_1). In this example β has direction in Σ_2.

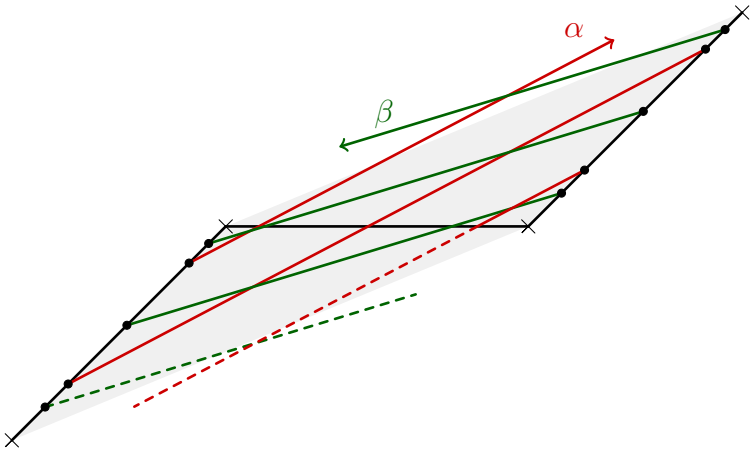

FIGURE 12. Exemple of maximal sequences of sandwiched segments. In this example, $p = 1$ and $q = 1$. There are 5 intersections.

so that $|\alpha \cap \beta| + 1 \leq kl$ and $\dfrac{|\alpha \cap \beta| + 1}{l(\alpha)l(\beta)} < \dfrac{1}{l_0^2}$, as required.

Case (ii)**:** $\exists i, j$**,** α_i **and** β_j **are in a configuration of type** (ii)**.** In this case, we count the intersection of α with the maximal sequence of non-adjacent segments β_j contained in the big cylinder spanned by $e_{\sigma_\beta(n/2-1)}$ and $e_{\sigma_\beta(n/2-2)}$. Examples are depicted in Figure 13 and Figure 14 in the case of the octagon.

We distinguish two cases: one where we can get a better estimation of the length of β while in the other we can get a better lower bound on the number of intersections between α and β.

(1) If β contains only non-sandwiched segments contained in the big cylinder, then in particular β start and end at the vertices which are the common endpoints to the sides of label $e_{\sigma_\beta(n/2-1)}$ and $e_{\sigma_\beta(n/2-2)}$, see Figure 13). In this case, $\beta = \beta_1 \cup \cdots \cup \beta_l$ could have $l+1$ intersections with α_i (instead of l). However, we can compensate with a better estimation of the lengths. A convenient way to estimate the length is to unfold the big cylinder as in Figure 13 and get:
   - If l is odd, then $l(\beta) \geq (\frac{l+1}{2}\Phi^2 - 1)l_0$.
   - If l is even, then $l(\beta) \geq \frac{l}{2}\Phi^2 l_0$.

   Hence, in both cases, we have $\dfrac{|\alpha_i \cap \beta|}{l(\alpha_i)l(\beta)} < \dfrac{1}{l_0^2}$. Further, the same holds if α_i is a non-sandwiched segment: in this case α_i intersect β at most l times, so that $\dfrac{|\alpha_i \cap \beta| + 1}{l(\alpha_i)l(\beta)} < \dfrac{1}{l_0^2}$. Since α_1 is non-sandwiched, this allows to count the singular intersection, so that:

$$\frac{(\sum_i |\alpha_i \cap \beta|) + 1}{(\sum_i l(\alpha_i))l(\beta)} < \frac{1}{l_0^2}.$$

   As required.

(2) Else, the maximal sequence $B = \beta_{j_0} \cup \cdots \cup \beta_{j_0+p-1}$ of non-sandwiched segments in the big cylinder containing β_j is not contained big cylinder, as in Figure 14. In this case, given that p is the number of non-sandwiched segments in the maximal sequence, there are at most
   - p intersections, if β either start or end at the central singularity. That is we can assume up to changing the orientation of β that the maximal sequence of non-sandwiched segments containing β_j is $\beta_1 \cup \cdots \cup \beta_p$, and hence we have

$$\frac{|\alpha_i \cap B|}{l(\alpha_i)l(B)} < \frac{p}{pl_0^2} = \frac{1}{l_0^2}.$$

     Further, using that in this case, $l(\beta_1) \geq (\Phi^2 - 1)l_0 > 2l_0$, we deduce that in fact $l(B) = l(\beta_1) + \cdots + l(\beta_p) > 2l_0 + (p-1)l_0 = (p+1)l_0$, so that

$$\frac{|\alpha_i \cap B| + 1}{l(\alpha_1)l(B)} < \frac{p+1}{(p+1)l_0^2} = \frac{1}{l_0^2}.$$

     Summing all intersections of this kind with the other intersections, we finally get $\dfrac{\mathrm{Int}(\alpha, \beta)}{l(\alpha)l(\beta)} < \dfrac{1}{l_0^2}$ as required.

- $(p-1)$ intersections, if β does not start and does not end at the central singularity, so that

$$\frac{|\alpha_i \cap B| + 1}{l(\alpha_i) l(B)} < \frac{(p-1)+1}{p l_0^2} = \frac{1}{l_0^2}.$$

Similarly, we conclude that $\dfrac{\mathrm{Int}(\alpha, \beta)}{l(\alpha) l(\beta)} < \dfrac{1}{l_0^2}$ as required.

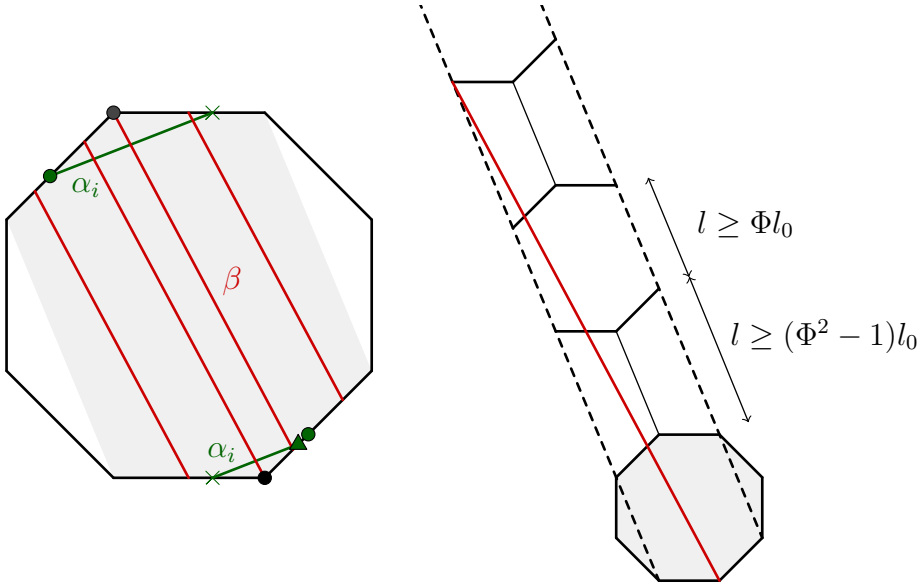

FIGURE 13. In the case where the curve β stays in the big cylinder, there could be one intersection more (here 5) than non sandwiched segments in β (here 4). However, unfolding the trajectory of the curve β allows to estimate precisely its length, given the lengths of the long diagonals which can be expressed using Φ.

3.4. **Conclusion.** As shown in the previous section, for any two distinct saddle connections α and β, we have

$$\frac{|\alpha \cap \beta| + 1}{l(\alpha) l(\beta)} \leq \frac{1}{l_0^2} \tag{4}$$

and equality occurs if and only if α and β are sides of the regular n-gon.

Now, any closed curve η (resp. ξ) on the regular n-gon is homologous to a union of saddle connections $\eta = \eta_1 \cup \cdots \cup \eta_k$ (resp. $\xi = \xi_1 \cup \cdots \cup \xi_l$). In this case, we have

$$\mathrm{Int}(\eta, \xi) \leq (\sum_{i,j} |\eta_i \cap \xi_j|) + s$$

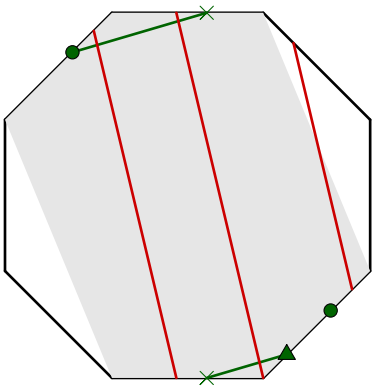

FIGURE 14. In the case where the curve β leaves the big cylinder, there are at most as many non-sandwiched segments as intersections with the segment α_i.

where s is the number singular intersection points. It should be noted that we set $|\eta_i \cap \xi_j| = 0$ if $\eta_i = \xi_j$. Further, we can assume without loss of generality that η and ξ are simple closed curves (see Lemma 3.1 of [5]) so that there are no multiple intersections at the singularities, and hence $s \leq \min(k, l)$. Further, $s \leq 1$ for $n \equiv 0 \mod 4$ and $s \leq 2$ for $n \equiv 2 \mod 4$. Using Equation (4), we get:

$$\mathrm{Int}(\eta, \xi) \leq (\sum_{i,j} l(\eta_i) l(\xi_j)) \times \frac{1}{l_0^2} + s - kl = \frac{l(\eta) l(\xi)}{l_0^2} + s - kl$$

with equality if and only if each η_i (resp. ξ_j) is a side of the regular n-gon. In particular:

- For $n \equiv 0 \mod 4$, $s \leq 1$ and we get directly Theorem 1.2, by noticing that distinct sides of the n-gon are indeed intersecting once at the singularity.
- For $n \equiv 2 \mod 4$, if $s \leq 1$ then at least one of the η_i (or ξ_j) is not a side of the n-gon so that $l(\eta_i) > l_0$ (or $l(\xi_j) > l_0$) and

$$\mathrm{Int}(\eta, \xi) < \frac{l(\eta) l(\xi)}{l_0^2}$$

Else, if $s = 2$ then $k, l \geq 2$ so that $kl \geq 4$ and

$$\mathrm{Int}(\eta, \xi) \leq \frac{l(\eta) l(\xi)}{l_0^2} - 2 < \frac{l(\eta) l(\xi)}{l_0^2}$$

This gives Theorem 1.6.

4. KVol as a supremum over pairs of directions

In this section, we extend the study of KVol as a function over the Teichmüller disk. We assume $n \equiv 0 \mod 4$ so that X_n has a single singularity (as well as all

the translation surfaces in its Teichmüller disk). The study follows the method of [1], but the case of the regular n-gon requires more precise estimates.

We first give a consistent name for saddle connections as the surface varies in the Teichmüller disk, as well as the direction of such saddle connections. This is done in §4.1 by choosing a base surface in the Teichmüller disk, namely $\mathcal{S}_n$, the staircase model. Next, for each pair of distinct periodic directions we define a quantity $K(d, d')$ which can be computed on the base surface $\mathcal{S}_n$, and allows for a more convenient expression of KVol (see Proposition 4.4). Finally, we provide in Proposition 4.7 precise estimates on $K(d, d')$. These estimates are one of the main ingredients in the proof of Theorem 1.1, and they differ from the case of the double n-gon.

4.1. **Directions in the Teichmüller disk.** Following [1, §4], we consider the plane template of $\mathcal{S}_n$ as our base surface and define the direction of a saddle connection α in $X = M \cdot \mathcal{S}_n$ as the direction (in $\mathbb{R}P^1$) of the preimage saddle connection $M^{-1} \cdot \alpha$ in $\mathcal{S}_n$ it corresponds to. More precisely:

Definition 4.1. For $d \in \mathbb{R}P^1$, we say that a saddle connection in $\mathcal{S}_n$ has direction d if it has direction d in the plane template of Figure 15. For $M \in \mathrm{GL}_2^+(\mathbb{R})$ we say that a saddle connection α in $M \cdot \mathcal{S}_n$ has direction d if $M^{-1} \cdot \alpha$ has direction d in $\mathcal{S}_n$.

This is a bit counter-intuitive because α may not have direction d in a plane template for $M \cdot \mathcal{S}_n$, but it allows for a consistent choice of the notion of direction along the Teichmüller space. Moreover, we have:

Proposition 4.2. [1, §4] *Using the identifications*

$$d = [x : y] \in \mathbb{R}P^1 \mapsto -\frac{x}{y} \in \mathbb{R} \cup \{\infty\} \equiv \partial\mathbb{H}^2$$

and for $M = \begin{pmatrix} a & b \\ c & d \end{pmatrix} \in SL_2(\mathbb{R})$

$$M \cdot \mathcal{S}_n \in \mathcal{T}_n \mapsto \frac{di + b}{ci + a} \in \mathbb{H}^2,$$

the locus of surfaces in $\mathcal{T}_n$ *where the directions* d *and* d' *make an (unoriented) angle* $\theta \in]0, \frac{\pi}{2}]$ *is the banana neighborood*

$$\gamma_{d,d',r} = \{z \in \mathbb{H}^2 : \mathrm{dist}_{\mathbb{H}^2}(z, \gamma_{d,d'}) = r\}$$

where $\cosh r = \dfrac{1}{\sin\theta}$.

In particular, the locus of surfaces in $\mathcal{T}_n$ *where the directions* d *and* d' *are orthogonal is the hyperbolic geodesic with endpoints* d *and* d'.

In the rest of the paper, we use the following

Notation 4.3. Given $X = M \cdot \mathcal{S}_n \in \mathcal{T}_n$, and d, d' distinct periodic directions, we define $\theta(X, d, d') \in]0, \frac{\pi}{2}]$ as the (unoriented) angle between the directions d and d' in the surface X. With this notation, we have by Proposition 4.2:

$$\sin\theta(X, d, d') = \frac{1}{\cosh(\mathrm{dist}_{\mathbb{H}^2}(X, \gamma_{d,d'}))}. \tag{7}$$

4.2. **KVol as a supremum over pairs of directions.** With the above choice of a consistent name for saddle connections and directions along the Teichmüller disk, we have the following proposition, which is already stated in [1] in the case of the double n-gon but can be extended with the same proof to the case of translation surfaces S for which saddle connections in the same direction do not intersect.

Proposition 4.4. [1, Proposition 5.1] *Let S be a translation surface with a single singularity such that saddle connections in the same direction are non-intersecting. Let $\mathcal{P}$ be the set of directions of saddle connections of S. Define the notion of direction for X in the Teichmüller disk of S using Definition 4.1. Then, for any surface X in the Teichmüller disk of S, we have:*

$$\mathrm{KVol}(X) = \mathrm{Vol}(X) \cdot \sup_{\substack{d, d' \in \mathcal{P} \\ d \neq d'}} K(d, d') \cdot \sin\theta(X, d, d'), \tag{8}$$

where $K(d, d') = \sup_{\substack{\alpha \subset \mathcal{S}_n \text{ saddle connection in direction } d \\ \beta \subset \mathcal{S}_n \text{ saddle connection in direction } d'}} \frac{\mathrm{Int}(\alpha,\beta)}{\alpha \wedge \beta}$ and $\theta(X, d, d')$ is the angle given by Notation 4.3.

The fact that saddle connections in the same direction on the regular n-gon are non-intersecting can be checked using the horizontal and vertical cylinder decomposition of the staircase model.

Remark 4.5. Notice that the Veech group $\Gamma_n^{\pm}$ of the staircase model $\mathcal{S}_n$ acts on $\mathcal{S}_n$ while preserving the intersection form, and acts linearly on $\mathbb{R}^2$, hence preserving the wedge product. In particular, $K(d, d') = K(g \cdot d, g \cdot d')$ for any element $g \in \Gamma_n^{\pm}$.

From this result and Theorem 1.2, we deduce

Corollary 4.6. *For $n \geq 8, n \equiv 0 \mod 4$, we have:*

$$\mathrm{KVol}(X_n) = \mathrm{Vol}(X) \cdot K(\infty, \frac{1}{\Phi}) \cdot \sin\theta(X_n, \infty, \frac{1}{\Phi})$$

In particular,

$$\forall (d, d'),\ K(d, d') \cdot \sin\theta(X_n, d, d') \leq K(\infty, \frac{1}{\Phi}) \cdot \sin\theta(X_n, \infty, \frac{1}{\Phi}).$$

Proof. By Theorem 1.2, KVol is achieved on the regular n-gon by pairs of distinct sides. In particular, the sides of the n-gon α and β corresponding to directions ∞ and $\frac{1}{\Phi}$ achieve the supremum:

$$\begin{aligned}\mathrm{KVol}(X_n) &= \frac{\mathrm{Int}(\alpha,\beta)}{l(\alpha)l(\beta)} \text{ by Theorem 1.2.}\\ &= \frac{\mathrm{Int}(\alpha,\beta)}{\alpha\wedge\beta}\sin angle(\alpha,\beta)\\ &= K(\infty,\frac{1}{\Phi})\sin\theta(X_n,\infty,\frac{1}{\Phi}) \text{ by definition of } K(d,d') \text{ and } \theta(X,d,d').\end{aligned}$$

□

Next, we provide precise estimates on $K(d,d')$ using its invariance under the diagonal action of the Veech group. These estimates are one of the main ingredients in the proof of Theorem 1.1.

Proposition 4.7. *For any pair of distinct periodic directions (d,d'), we have, with the notations of Figure 15:*

- ♠ *If there exist $k\in\mathbb{N}^*\cup\{\infty\}$ and $g\in\Gamma_n^{\pm}$ such that $(d,d')=(g\cdot\infty,\pm g\cdot\frac{1}{k\Phi})$, we have*
$$K(d,d')=\frac{1}{l(\alpha_1)l(\alpha_m)}=\frac{1}{\Phi l_m^2}$$
with $l_m:=l(\alpha_m)$.
- ♦ *If there exist $g\in\Gamma_n^{\pm}$ such that $(d,d')=(g\cdot\infty,\pm g\cdot\frac{\Phi^2-1}{\Phi^3-2\Phi})$, then*
$$K(d,d')=\frac{1}{(\Phi^3-2\Phi)l_m^2}=\frac{1}{\Phi^2-2}K(\infty,\frac{1}{\Phi}).$$
This is the case of $(d,d')=(\frac{1}{\Phi},\Phi-\frac{1}{\Phi})$, image of $(\infty,\frac{\Phi^2-1}{\Phi^3-2\Phi})$ by the element $g=T_VR\in\Gamma^{\pm}$.
- *In the other cases,*
$$K(d,d')<\frac{1}{(\Phi^3-2\Phi)l_m^2}.$$

Recall that the α_i (resp. β_j) are the horizontal (resp. vertical) saddle connection sorted by decreasing length, and define $l_i:=l(\alpha_i)$ and $h_j:=l(\beta_j)$ for $1\le i,j\le m$. Further, we denote $C_1,\dots,C_m$ (resp. $Z_1,\dots,Z_m$) the vertical (resp. horizontal) cylinders, as in Figure 15. Using that the moduli of both horizontal and vertical cylinders are all $1/\Phi$ (except the horizontal cylinder Z_1), one can compare the lengths h_m,h_{m-1} and l_{m-1} to l_m, as in Figure 16.

Proof. The proof goes as follow: given a pair of distinct periodic directions (d,d') and a pair of saddle connections (α,β) in respective directions d,d', we first notice that it is possible to assume that α is either horizontal ($d=\infty$, i.e $\alpha=\alpha_i$ for $i\in[\![1,m]\!]$) or vertical ($d=0$, i.e $\alpha=\beta_j$ for $j\in[\![1,m]\!]$). This is because

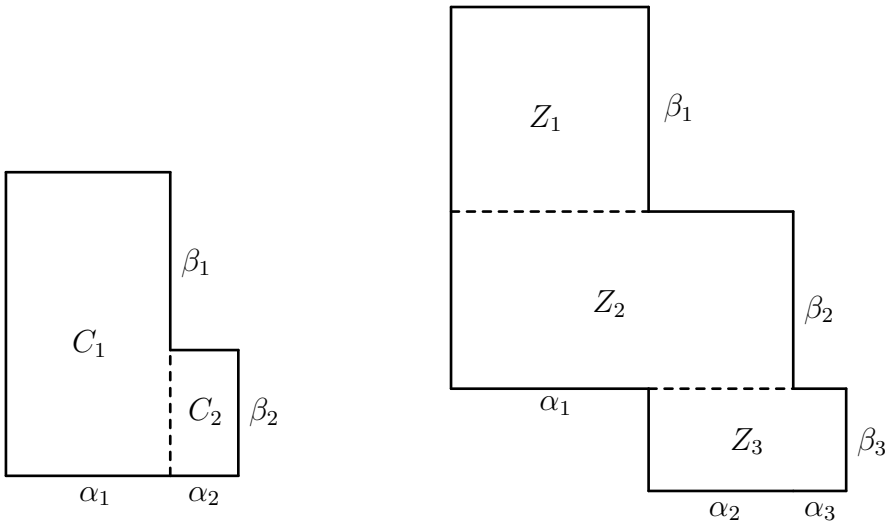

FIGURE 15. The staircase models associated to the n-gon for $n = 8$ on the left and $n = 12$ on the right, and the cylinders.

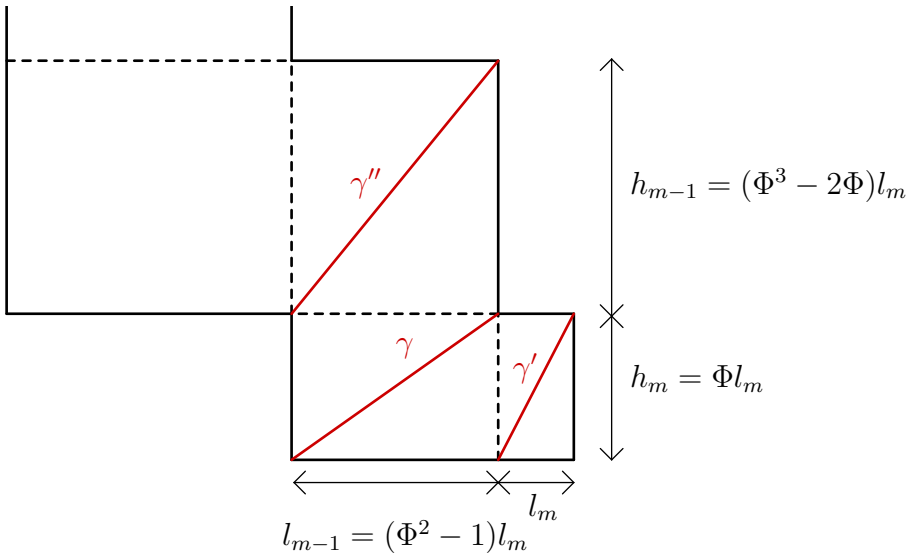

FIGURE 16. The lengths h_m, h_{m-1} and l_{m-1} expressed using l_m. The diagonal curves γ, γ' and γ'' have respective co-slope $\Phi - \frac{1}{\Phi}$, $\frac{1}{\Phi}$, and $\frac{\Phi^2-1}{\Phi^3-2\Phi}$.

$K(d, d')$ is by invariant under the action of the Veech group and any periodic direction is either the image of the horizontal or the vertical by an element of the Veech group. We study the cases $d = \infty$ and $d = 0$ separately, identify the

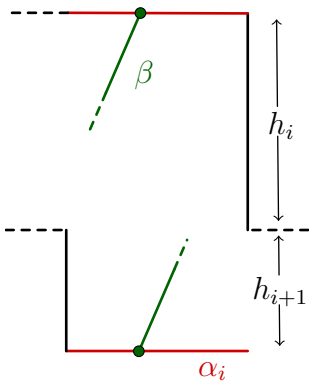

FIGURE 17. A non singular intersection with α_i, $i < m$, requires a vertical length at least $h_i + h_{i+1}$.

configurations ♠ and ♦ and show that $K(d, d')$ is smaller in the other cases.

Case 1: d represents the horizontal cusp. Up to the action by an element of the Veech group, we can assume α is one of the α_i. Let us first study the intersection with α_i for $i < m$. **Case 1.1: $\alpha = \alpha_i$ for $i < m$.**

Lemma 4.8. *For any $i < m$, and any saddle connection β, we have*

$$\frac{\mathrm{Int}(\alpha_i, \beta)}{\alpha_i \wedge \beta} < \frac{1}{\Phi^3 - 2\Phi} \cdot \frac{1}{l_m^2}.$$

Proof. First notice that if a saddle connection β does not intersect the core curves of the cylinders $Z_1, \dots, Z_m$, we have $\mathrm{Int}(\alpha_i, \beta) = 0$ since the core curves are respectively homologous to $\alpha_1, \alpha_1 + \alpha_2, \cdots, \alpha_{i-1} + \alpha_i$. In particular, a saddle connection β having non-zero intersection with α has a vertical length at least h_i. Further, any non singular intersection of β with α_i for $i < m$ requires a vertical length at least $h_i + h_{i+1}$ (see Figure 17). This gives:

$$\alpha_i \wedge \beta \geq l_i \max((h_i + h_{i+1})(\mathrm{Int}(\alpha_i, \beta) - 1), h_i)$$

In particular,

(i) If $\mathrm{Int}(\alpha_i, \beta) \leq 1$, we use $\alpha_i \wedge \beta \geq l_i h_i$ to get

$$\frac{\mathrm{Int}(\alpha_i, \beta)}{\alpha_i \wedge \beta} \leq \frac{1}{l_i h_i},$$

and, since $i < m$, we get

$$\frac{1}{l_i h_i} \leq \frac{1}{l_{m-1} h_{m-1}} \leq \frac{1}{(\Phi^2 - 1)(\Phi^3 - 2\Phi) l_m^2} < \frac{1}{(\Phi^3 - 2\Phi) l_m^2}.$$

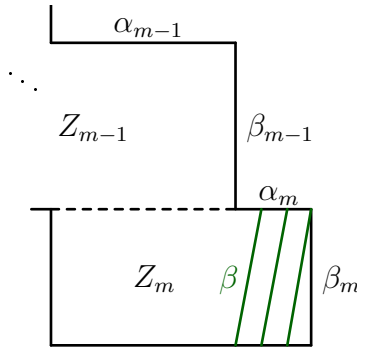

FIGURE 18. Example of β with co-slope $\frac{1}{3\Phi}$. Here, $\mathrm{Int}(\alpha_m, \beta) = 3$ with an intersection at the singularity.

(ii) Otherwise, we use $\alpha_i \wedge \beta \geq l_i(h_i + h_{i+1})(\mathrm{Int}(\alpha_i, \beta) - 1)$ and obtain

$$\frac{\mathrm{Int}(\alpha_i, \beta)}{\alpha_i \wedge \beta} \leq \frac{2}{l_i(h_i + h_{i+1})}.$$

But, since $i < m$, we have $l_i \geq l_{m-1} = (\Phi^2 - 1)l_m$ and $h_i + h_{i+1} \geq h_{m-1} + h_m = (\Phi^3 - \Phi)l_m$ and in particular

$$\frac{2}{l_i(h_i + h_{i+1})} \leq \frac{2}{(\Phi^3 - \Phi)(\Phi^2 - 1)l_m^2} < \frac{1}{(\Phi^3 - 2\Phi)l_m^2},$$

where the last inequality comes from $\Phi^3 - \Phi > \Phi^3 - 2\Phi$ and $\Phi^2 - 1 > 2$. □

Case 1.2: $\alpha = \alpha_m$. In this case, notice that either β is contained in the horizontal cylinder Z_m (see Figure 15) and, up to a horizontal twist, its co-slope is $\pm\frac{1}{k\Phi}$ for $k \in \mathbb{N}^* \cup \{\infty\}$ so that it corresponds to a geodesic of case ♠, or β is not contained in Z_m.

Case 1.2.i. If the direction of β is, up to an horizontal twist, $d' = \pm\frac{1}{k\Phi}$ as in ♠, and β is contained in Z_m, we see that α and β intersect $k+1$ times and $\alpha \wedge \beta = (k+1)l(\beta_m)l(\alpha_m) = (k+1)\Phi l_m^2$ (see Figure 18 for the case $k = 3$). This gives directly that

$$\frac{\mathrm{Int}(\alpha_m, \beta)}{l(\alpha)l(\beta)} = \frac{k+1}{(k+1)\Phi l_m^2} = \frac{1}{\Phi l_m^2}.$$

In particular, $K(\infty, \frac{1}{k\Phi}) \geq \frac{1}{\Phi l_m^2}$, and the reversed inequality holds since the other saddle connections of direction $d' = \frac{1}{k\Phi}$ do not intersect α_m, and as seen in Case 1.1 the intersection of any β with α_i, $i < m$, gives a lower ratio. Consequently,

$$(\spadesuit)\ \forall k \in \mathbb{N}^* \cup \{\infty\},\ K(\infty, \frac{1}{k\Phi}) = \frac{1}{\Phi l_m^2}.$$

Case 1.2.ii. In the second case, the geodesic β is not contained in the horizontal cylinder Z_m. As such, β has a vertical length at least the length of β_{m-1}, that is $h_{m-1} = (\Phi^3 - 2\Phi)l_m$.

(1.2.ii.a) If $\mathrm{Int}(\alpha_m, \beta) = 0$ or 1, we directly have

$$\frac{\mathrm{Int}(\alpha_m, \beta)}{\alpha_m \wedge \beta} \leq \frac{1}{(\Phi^3 - 2\Phi)l_m^2},$$

with equality if and only if $\mathrm{Int}(\alpha_m, \beta) = 1$ and the vertical length of β is exactly h_{m-1}. In particular, β is contained in the horizontal cylinder Z_{m-1} and up to an horizontal twist, its direction is $d' = 0$ or $d' = \pm\frac{\Phi^2-1}{\Phi^3-2\Phi}$ (see Figure 16). The case $d' = 0$ is an instance of case ♠ and has already been dealt with. The case $d' = \pm\frac{\Phi^2-1}{\Phi^3-2\Phi}$ is exactly case ♦. Further, taking the diagonal saddle connections γ and γ' of Figure 16 of respective holonomy vectors $\begin{pmatrix}\Phi^2-1\\ \Phi\end{pmatrix} l_m$ and $\begin{pmatrix}1\\ \Phi\end{pmatrix} l_m$ which intersect once at the singularity, we get:

$$\frac{\mathrm{Int}(\gamma, \gamma')}{\gamma \wedge \gamma'} = \frac{1}{(\Phi^3 - 2\Phi)l_m^2} = K(\infty, \frac{\Phi^2 - 1}{\Phi^3 - 2\Phi}),$$

This is due to the fact that the pair of directions $(\frac{1}{\Phi}, \Phi - \frac{1}{\Phi})$ is the image of the pair $(\infty, \frac{\Phi^2-1}{\Phi^3-2\Phi})$ by the diagonal action of the matrix $T_V R$ which belongs to the (unoriented) Veech group. In particular:

$$K(\frac{1}{\Phi}, \Phi - \frac{1}{\Phi}) = K(\infty, \frac{\Phi^2 - 1}{\Phi^3 - 2\Phi}).$$

(1.2.ii.b) Otherwise, β intersects α_m outside the singularity and is not contained in the horizontal cylinder Z_m. In this case, we show:

Lemma 4.9. *Assume β intersects α_m outside the singularity and is not contained in the horizontal cylinder Z_m. Then*

$$\frac{\mathrm{Int}(\alpha_m, \beta)}{\alpha_m \wedge \beta} < \frac{1}{(\Phi^3 - 2\Phi)l_m^2}.$$

Proof. Let c denote the co-slope of β. The assumption ensures that $c \neq \frac{1}{k\Phi}$. Up to an horizontal twist, we can also assume that $c \in]-\frac{1}{\Phi}, \Phi - \frac{1}{\Phi}[$. Finally, up to a symmetry with respect to the vertical axis, we can further assume $c > 0$, giving:

$$c \in]0, \Phi - \frac{1}{\Phi}[\setminus \{\frac{1}{k\Phi}, k \in \mathbb{N}^* \cup \{\infty\}\}$$

(1) Let us first study the case $\frac{1}{\Phi} < c < \Phi - \frac{1}{\Phi}$. Under this assumption, β has to vertically go through the small horizontal cylinder Z_m before any non singular intersection with α_m and vertically go through Z_{m-1} after each

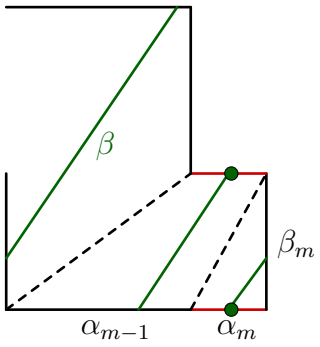

FIGURE 19. If the co-slope of β lies between $\frac{1}{\Phi}$ and $\Phi - \frac{1}{\Phi}$, then a non-singular intersection with α_m requires a vertical length at least $h_m + (h_m + h_{m-1})$.

non-singular intersection with α_m (see Figure 19), so that if we denote by p the number of non singular intersections between α_m and β we get

$$l(\beta)\sin\theta \geq p(h_m + (h_m + h_{m-1}))$$

where θ is the angle between the horizontal and the direction of β, so that $l(\beta)\sin\theta$ is the vertical length of β.
Now, adding the possible singular intersection, we deduce that

$$\begin{aligned}\frac{\mathrm{Int}(\alpha_m,\beta)}{\alpha_m \wedge \beta} &\leq \frac{p+1}{p(h_m + (h_m + h_{m-1}))l_m} \\ &= \frac{p+1}{p\Phi^3}\cdot\frac{1}{l_m^2}.\end{aligned}$$

(Recall that $h_m = \Phi l_m$ and $h_{m-1} = (\Phi^3 - 2\Phi)l_m$.)
The last quantity is maximal for $p = 1$, so that

$$\frac{\mathrm{Int}(\alpha_m,\beta)}{\alpha_m \wedge \beta} \leq \frac{2}{\Phi^3}\cdot\frac{1}{l_m^2} < \frac{1}{\Phi^3 - 2\Phi}\cdot\frac{1}{l_m^2}$$

where the last inequality comes from $\Phi < 2$.

(2) Now, assume $0 < c < \frac{1}{\Phi}$ and let $k \geq 0$ be such that $\frac{1}{(k+1)\Phi} < c < \frac{1}{k\Phi}$. Let $p \geq 1$ denote the number of times the curve β crosses the small vertical cylinder C_m, that is the number of connected components of $\beta \cap C_m$. Then β crosses C_{m-1} at most once fewer, say $p' \geq 1$ times with $p' \geq p-1$. Moreover, the assumption on the co-slope gives that for each crossing of C_m the curve β intersects at most $k+1$ times α_m and for each crossing of C_{m-1} it intersects at least k times α_{m-1} (see Figure 20). This gives that :

$$\mathrm{Int}(\alpha_m,\beta) \leq s^{\circ}_{max} := p(k+1) + 1$$

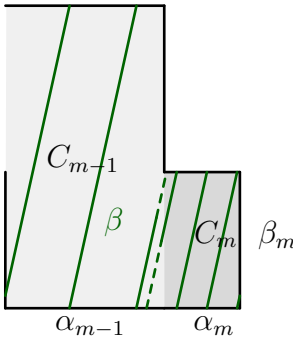

FIGURE 20. A portion of the curve β with co-slope $\frac{1}{3\Phi} < c < \frac{1}{2\Phi}$. Each time β crosses the cylinder C_m, it gives at most $k+1=3$ intersections with α_m and it is followed by a crossing of C_{m-1}, giving at least $k=2$ intersections with α_{m-1}.

(where the added intersection stands for the possible singular intersection). In fact, this estimate can be improved in the cases $p' = p$ and $p' = p-1$ as follows:

★ If $p' = p$, the curve β has to either start or end at a vertex of C_m, so that either the first or the last crossing of C_m has only k intersections with α_m instead of $k+1$. Hence,

$$\mathrm{Int}(\alpha_m, \beta) \leq s^{\star}_{max} := k(p+1) = (k+1)p - 1 + 1.$$

▲ If $p' = p-1$ (so that $p \geq 2$), the curve β has to both start and end at a vertex of C_m. The same argument shows:

$$\mathrm{Int}(\alpha_m, \beta) \leq s^{\Delta}_{max} := (k+1)p - 1 = (k+1)p - 2 + 1.$$

Concerning the lengths, cutting β at each intersection with α_m and α_{m-1} helps us notice that:

(*i*) Before any non-singular intersection with α_m, there is a vertical length at least h_m.

(*ii*) Before any non-singular intersection with α_{m-1}, there is a vertical length at least $h_m + h_{m-1}$, except maybe the first intersection with α_{m-1} for which there is a vertical length a least h_{m-1} (but note that this case arises only if α starts at a bottom vertex of Z_{m-1}, in particular this cannot happen for $p' = p-1$).

(*iii*) We further have to count a vertical length h_m for β to reach the singularity after the last intersection with either α_m or α_{m-1}.

In particular, letting $s := Int(\alpha_m, \beta) \geq 2$ (so that there are at least $s-1$ non-singular intersections), we have :

$$\begin{aligned} l(\beta)\sin\theta &\geq (s-1)h_m + (kp'-1)(h_m + h_{m-1}) + h_{m-1} + h_m \\ &= kp'(h_m + h_{m-1}) + (s-1)h_m, \end{aligned}$$

and for $p' = p-1$, we can replace $kp'-1$ by kp' as remarked in (ii).

$$\begin{aligned} l(\beta)\sin\theta &\geq (s-1)h_m + kp'(h_m + h_{m-1}) + h_m \\ &= k(p-1)(h_m + h_{m-1}) + sh_m. \end{aligned}$$

In particular, the following inequalities holds:

$$\text{If } p' \geq p, \text{ then } \frac{\mathrm{Int}(\alpha_m, \beta)}{\alpha_m \wedge \beta} \leq \frac{s}{p'k(h_m + h_{m-1}) + (s-1)h_m} \cdot \frac{1}{l_m}$$

$$(\blacktriangle) \text{ If } p' = p-1, \text{ then } \frac{\mathrm{Int}(\alpha_m, \beta)}{\alpha_m \wedge \beta} \leq \frac{s}{(p-1)k(h_m + h_{m-1}) + sh_m} \cdot \frac{1}{l_m}.$$

Now, since $k(h_m + h_{m-1}) > h_m$, for fixed k and p, the right part is maximal when s is maximal. Distinguishing cases ● ($p' \geq p+1$), ★ ($p' = p$) and ▲ ($p' = p-1$), we have:

● If $p' \geq p+1$, then $s_{max} = s^{\circ}_{max} = p(k+1)+1$ and

$$\begin{aligned} \frac{\mathrm{Int}(\alpha_m, \beta)}{\alpha_m \wedge \beta} &\leq \frac{p(k+1)+1}{p'k(\Phi^3 - \Phi) + p(k+1)\Phi} \cdot \frac{1}{l_m^2} \\ &\leq \frac{p(k+1)+1}{(p+1)k(\Phi^3 - \Phi) + p(k+1)\Phi} \cdot \frac{1}{l_m^2} \\ &= \frac{pk+p+1}{k((p+1)\Phi^3 - \Phi) + p\Phi} \cdot \frac{1}{l_m^2} \end{aligned}$$

(given that $h_m = \Phi l_m$ and $h_{m-1} = (\Phi^3 - 2\Phi)l_m$.)

To give an upper bound for this last quantity, it is convenient to use the following lemma which will be used several times along the proof:

Lemma 4.10. *Let $a, b, c, d \in \mathbb{R}$. Assume the möbius transformation $f : x \mapsto \frac{ax+b}{cx+d}$ is defined for any $x \geq 1$. Then,*
- *if $ad - bc \geq 0$, then $\forall x \geq 1$, $f(x) \leq \lim_{x\to\infty} f(x) = \frac{a}{c}$.*
- *Otherwise, $\forall x \geq 1$, $f(x) \leq f(1) = \frac{a+b}{c+d}$.*

Proof. f is differentiable of derivative map $f'(x) = \frac{ad-bc}{(cx+d)^2}$. □

Since for any fixed $p \geq 1$ we have $p^2\Phi - (p+1)((p+1)\Phi^3 - \Phi) < (p+1)^2(\Phi - \Phi^3) < 0$, we can use Lemma 4.10 to conclude that the

last quantity is maximal for $k=1$, and it gives

$$\begin{aligned}\frac{\mathrm{Int}(\alpha_m,\beta)}{\alpha_m\wedge\beta} &\leq \frac{2p+1}{(p+1)(\Phi^3-\Phi)+2p\Phi}\cdot\frac{1}{l_m^2}\\ &= \frac{2p+1}{p(\Phi^3+\Phi)+(\Phi^3-\Phi)}\cdot\frac{1}{l_m^2}\end{aligned}$$

Similarly, given the inequality $2(\Phi^3-\Phi)-(\Phi^3+\Phi)<0$, coming from $\Phi>2\cos(\frac{\pi}{6})=\sqrt{3}$, Lemma 4.10 shows that the last quantity is maximal for $p\to\infty$, and we have

$$\frac{\mathrm{Int}(\alpha_m,\beta)}{\alpha_m\wedge\beta} = \frac{2}{\Phi^3+\Phi}\cdot\frac{1}{l_m^2} < \frac{1}{\Phi^3-2\Phi}\cdot\frac{1}{l_m^2},$$

where the last inequality comes from $\Phi<2$.

★ If $p'=p$, then $s_{max}=s^\star_{max}=p(k+1)$ and:

$$\begin{aligned}\frac{\mathrm{Int}(\alpha_m,\beta)}{\alpha_m\wedge\beta} &\leq \frac{p(k+1)}{pk(\Phi^3-\Phi)+(p(k+1)-1)\Phi}\cdot\frac{1}{l_m^2}\\ &= \frac{p(k+1)}{p(k\Phi^3+\Phi)-\Phi}\cdot\frac{1}{l_m^2}\end{aligned}$$

Similarly, for fixed k the last quantity is maximal for $p=1$, giving

$$\begin{aligned}\frac{\mathrm{Int}(\alpha_m,\beta)}{\alpha_m\wedge\beta} &\leq \frac{k+1}{k(\Phi^3-\Phi)+k\Phi}\cdot\frac{1}{l_m^2}\\ &= \frac{k+1}{k\Phi^3}\cdot\frac{1}{l_m^2} < \frac{2}{\Phi^3}\cdot\frac{1}{l_m^2} < \frac{1}{\Phi^3-2\Phi}\cdot\frac{1}{l_m^2}.\end{aligned}$$

▲ Finally, if $p'=p-1$, we have $s_{max}=s^\Delta_{max}=p(k+1)-1$ and:

$$\begin{aligned}\frac{\mathrm{Int}(\alpha_m,\beta)}{\alpha_m\wedge\beta} &\leq \frac{p(k+1)-1}{(p-1)k(\Phi^3-\Phi)+(p(k+1)-1)\Phi}\cdot\frac{1}{l_m^2}\\ &= \frac{p(k+1)-1}{p(k\Phi^3+\Phi)-k\Phi^3+(k-1)\Phi}\cdot\frac{1}{l_m^2}\end{aligned}$$

Using the inequality $(k+1)((k-1)\Phi-k\Phi^3)+k\Phi^3+\Phi=k^2(\Phi-\Phi^3)<0$ and Lemma 4.10, we see that for fixed $k\geq 1$, the last quantity is maximal for p minimal, that is $p=2$ since $p'=p-1$ should be at least one. In particular

$$\begin{aligned}\frac{\mathrm{Int}(\alpha_m,\beta)}{\alpha_m\wedge\beta} &\leq \frac{2k+1}{k(\Phi^3-\Phi)+(2k+1)\Phi}\cdot\frac{1}{l_m^2}\\ &= \frac{2k+1}{k(\Phi^3+\Phi)+\Phi}\cdot\frac{1}{l_m^2}\end{aligned}$$

which, using again Lemma 4.10, is shown to be minimal for $k = 1$, so that

$$\frac{\mathrm{Int}(\alpha_m, \beta)}{\alpha_m \wedge \beta} < \frac{3}{\Phi^3 + 2\Phi} \cdot \frac{1}{l_m^2} < \frac{1}{\Phi^3 - 2\Phi} \cdot \frac{1}{l_m^2},$$

where the last inequality comes from $\Phi < 2$.

This concludes the proof of Lemma 4.9. □

Case 2: d represents the vertical cusp. Up to the action by an element of the Veech group, we can assume that α is one of the β_j, $j \in [\![1, m]\!]$. We first study the case $\alpha = \beta_j$ for $j < m$. **Case 2.1: $\alpha = \beta_j$ for $j < m$.**

Lemma 4.11. *Assume $d' \notin \{\frac{1}{k\Phi}, k \in \mathbb{N} \cup \{\infty\}\}$. For any $j < m$,*

$$\frac{\mathrm{Int}(\beta_j, \beta)}{\beta_j \wedge \beta} < \frac{1}{(\Phi^3 - 2\Phi)} \cdot \frac{1}{l_m^2}$$

Proof. First notice that if β has horizontal length l_m, then its direction is $\frac{1}{k\Phi}$ for a given k. In particular the assumption on d' ensures that β has horizontal length at least than l_{m-1}. Further, any non-singular intersection with β_j for $j < m$ requires an horizontal length $l_j + l_{j-1}$ (see Figure 21). This gives, for $j < m$,

$$\beta_j \wedge \beta \geq h_j \max((l_j + l_{j-1})(\mathrm{Int}(\beta_j, \beta) - 1), l_{m-1}).$$

In particular,

(i) If $\mathrm{Int}(\beta_j, \beta) \leq 1$, we use $\beta_j \wedge \beta \geq h_j l_{m-1}$ to get

$$\frac{\mathrm{Int}(\beta_j, \beta)}{\beta_j \wedge \beta} \leq \frac{1}{l_{m-1} h_j} \leq \frac{1}{l_{m-1} h_{m-1}}.$$

Then, given that $l_{m-1} = (\Phi^2 - 1) l_m$ and $h_{m-1} = (\Phi^3 - 2\Phi) l_m$, we draw:

$$\frac{\mathrm{Int}(\beta_j, \beta)}{\beta_j \wedge \beta} \leq \frac{1}{(\Phi^3 - 2\Phi)(\Phi^2 - 1) l_m^2} < \frac{1}{(\Phi^3 - 2\Phi)} \cdot \frac{1}{l_m^2}$$

(ii) Otherwise, we use $\beta_j \wedge \beta \geq h_j (l_j + l_{j-1})(\mathrm{Int}(\beta_j, \beta) - 1)$ to obtain:

$$\frac{\mathrm{Int}(\beta_j, \beta)}{\beta_j \wedge \beta} \leq \frac{2}{h_j (l_j + l_{j-1})}.$$

Since $2 l_{m-1} \leq 2 l_j < (\Phi^2 - 1) l_j = l_{j-1}$, we deduce that

$$\frac{\mathrm{Int}(\beta_j, \beta)}{\beta_j \wedge \beta} \leq \frac{1}{h_j l_{m-1}} \leq \frac{1}{l_{m-1} h_{m-1}} < \frac{1}{(\Phi^3 - 2\Phi)} \cdot \frac{1}{l_m^2}.$$

□

Case 2.2: $\alpha = \beta_m$. In this case α is homologous to a non singular geodesic so there is no non singular intersection. The first intersection with β_m requires a horizontal length at least l_m while all the following intersections require a length

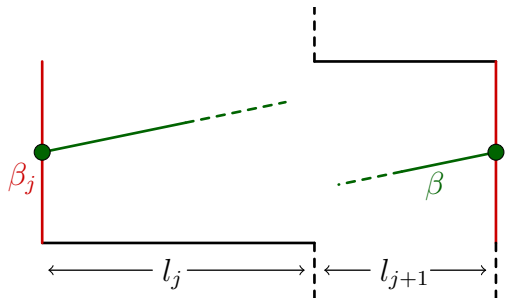

FIGURE 21. Any non-singular intersection with β_j requires a horizontal length at least $l_j + l_{j+1}$.

$l_{m-1}+l_m$. In particular, either β stays in the vertical cylinder C_m and the co-slope is $\frac{1}{k\Phi}$ for $k \in \mathbb{N} \cup \{\infty\}$ (case ♠), or there are at least two intersections and

$$\frac{\mathrm{Int}(\beta_m, \beta)}{\beta_m \wedge \beta} \leq \frac{2}{h_m(2l_m + l_{m-1})} = \frac{2}{\Phi(\Phi^2+1)} \cdot \frac{1}{l_m^2} < \frac{1}{\Phi^3 - 2\Phi} \cdot \frac{1}{l_m^2}.$$

where the last inequality comes from $\Phi < 2$. This concludes the proof of Proposition 4.7.

□

5. Proof of Theorem 1.1

In this section, we finally prove our main result. More precisely, we show

Theorem 5.1. *For any $X \in \mathcal{T}_n$, we have*

$$\mathrm{KVol}(X) = \mathrm{Vol}(X) K(\infty, \frac{1}{\Phi}) \cdot \frac{1}{\cosh(\mathrm{dist}_{\mathbb{H}^2}(X, \Gamma_n \cdot \mathcal{G}_{max}))} \tag{9}$$

Recall that $\mathcal{G}_{max} = \bigcup_{k \in \mathbb{N}^* \cup \{\infty\}} \gamma_{\infty, \pm\frac{1}{k\Phi}}$, and notice that the constant K_0 given in the statement of Theorem 1.1 is now explicitely determined by $K_0 = \mathrm{Vol}(X) K(\infty, \frac{1}{\Phi})$.

We begin this section by giving an overview of the geometric ideas behind the proof.

5.1. Geometric interpretation of Proposition 4.4.

Following §7.2 of [1], we first give a geometric interpretation of Equation (8) (see Proposition 4.4), which we restate here for the reader's convenience:

$$\mathrm{KVol}(X) = \mathrm{Vol}(X) \cdot \sup_{\substack{d, d' \in \mathcal{P} \\ d \neq d'}} K(d, d') \cdot \sin\theta(X, d, d').$$

Recall that $\mathcal{P}$ is the set of periodic directions on the staircase model $\mathcal{S}_n$.

Given a pair of distinct periodic directions (d, d'), its associated geodesic $\gamma_{d,d'}$ on $\mathbb{H}^2$ gives a projected geodesic on the hyperbolic surface $\mathbb{H}^2/\Gamma_n$. In the fundamental domain $\mathcal{T}_n$, it gives a set of geodesics formed by all the images of $\gamma_{d,d'}$ by an element of Γ_n. By Remark 4.5, all pairs of directions in $\Gamma_n^{\pm} \cdot (d, d')$ give the same value for $K(\cdot, \cdot)$. This amounts to saying that the corresponding geodesic trajectory on the surface $\mathbb{H}^2/\Gamma_n$ has a well defined associated constant, $K(d, d')$. Now, given a point $X \in \mathbb{H}^2/\Gamma_n$, we can look at the minimal distance r from X to the geodesic trajectory associated with (d, d'). Proposition 4.2 gives that for a pair of saddle connections α and β on X of respective directions d and d' (in the sense of Definition 4.1), we have the sharp inequality:

$$\frac{\mathrm{Int}(\alpha, \beta)}{l(\alpha) l(\beta)} \leq K(d, d') \times \frac{1}{\cosh r}.$$

Examples of geodesic trajectories for $d = \infty$ and $d' = \frac{1}{\Phi}, \frac{1}{2\Phi}$ and $\frac{1}{3\Phi}$ are depicted in Figure 1 of the introduction, as well as in Figure 22 for $d' = \frac{\Phi}{2\Phi^2 - 1}$.

Using this interpretation, we can prove Theorem 5.1 by showing that for every pair of distinct periodic directions (d, d') and any $X \in \mathcal{T}_n$ (or, by symmetry, for any $X \in \mathcal{T}_{n+} = \{X = x + iy \in \mathcal{T}_n, x \geq 0\}$) we have:

$$(\clubsuit) \qquad K(d, d') \sin \theta(X, d, d') \leq \max_{k \in \mathbb{N}^*} \{K(\infty, \frac{1}{k\Phi}) \sin \theta(X, \infty, \frac{1}{k\Phi})\}$$

The constant $K(\infty, \frac{1}{k\Phi})$ being maximal among all possible constants $K(d, d')$, Equation $(\clubsuit)$ holds for surfaces X close to $\Gamma_n \cdot \mathcal{G}_{max}$. More precisely, in §5.2, we use Proposition 4.7 to show that $(\clubsuit)$ holds in the domain $\mathcal{R}_+ = \{X = x + iy \in \mathcal{T}_{n+}, y \geq x - \frac{1}{\Phi}\}$ (Lemma 5.2 and Figure 23).

Then, it remains to deal with surfaces outside $\mathcal{R}_+$ (which are, in some sense, surfaces close to the regular n-gon X_n). This latter case is explained in §5.3 and requires use of the machinery of [1, §7], along with Corollary 4.6 and Proposition 4.7.

5.2. **The case of surfaces close to $\Gamma_n \cdot \mathcal{G}_{max}$.** With the above geometric interpretation, we deduce that for surfaces close to the geodesic trajectories associated to the directions $(\infty, \frac{1}{k\Phi})$, $k \in \mathbb{N}^* \cup \{\infty\}$ (having maximal $K(\cdot, \cdot)$), KVol is achieved by pairs of saddle connections in directions $d = \infty$ and $d' = \frac{1}{k\Phi}$, and Equation $(\clubsuit)$ holds. More precisely, we have:

Lemma 5.2. *For any $X \in \mathcal{R}_+ = \{X = x + iy \in \mathcal{T}_{n+}$ with $y \geq x - \frac{1}{\Phi}\}$, Equation $(\clubsuit)$ holds.*

Recall that because of the symmetry of KVol with respect to the reflection on the vertical axis, we can assume $X \in \mathcal{T}_{n+} := \{X = x + iy \in \mathcal{T}_n, x \geq 0\}$.

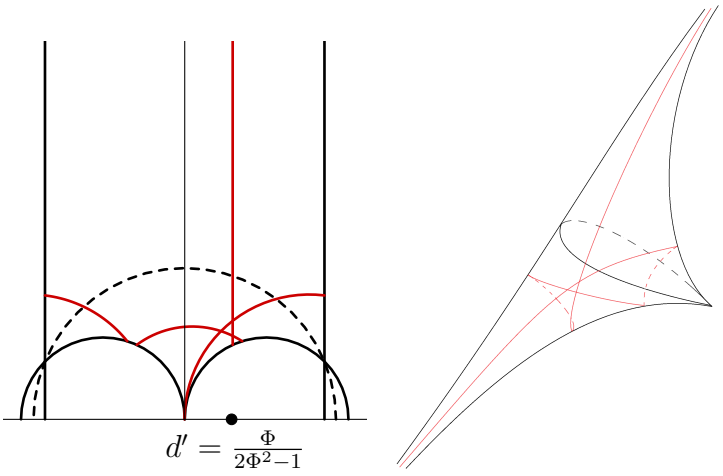

FIGURE 22. The geodesic $\gamma_{\infty,\frac{\Phi}{2\Phi^2-1}}$ its images by the Veech group intersecting the fundamental domain $\mathcal{T}_n$. On the right, the same geodesics on the surface $\mathbb{H}^2/\Gamma_n$.

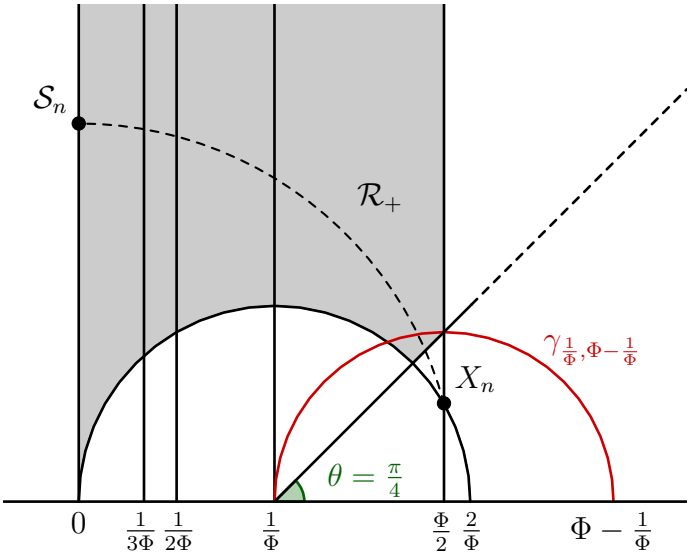

FIGURE 23. The region $\mathcal{R}_+$ in the right part of the fundamental domain ${\mathcal{T}_n}^+$ and the geodesic $(\frac{1}{\Phi}, \Phi - \frac{1}{\Phi})$ for the case $n = 12$.

Proof. By Proposition 4.7, Equation (♣) holds for any $X \in {\mathcal{T}_n}^+$ such that there is a $k \in \mathbb{N}^* \cup \{\infty\}$ with

$$\sin\theta(X, \infty, \frac{1}{k\Phi}) \geq \frac{1}{\Phi^2 - 2}. \tag{10}$$

Since $\frac{1}{\Phi^2-2} \leq \frac{1}{\Phi_8^2-2} = \frac{\sqrt{2}}{2} = \sin\frac{\pi}{4}$, we directly have that the above condition is verified for $X \in \{Y \in {\mathcal{T}_n}^+, \exists k \in \mathbb{N}^* \cup \{\infty\}, \theta(Y, \infty, \frac{1}{k\Phi}) \geq \frac{\pi}{4}\}$. One verifies that this set is exactly $\mathcal{R}_+$. □

Remark 5.3. In fact, $\mathcal{R}_+ = {\mathcal{T}_n}^+$ for $m = 2$, which finishes the proof in the case of the octagon. However, this is no longer the case for $m \geq 3$.

5.3. **The case of surfaces close to X_n.** It remains to deal with surfaces away from geodesics associated with directions ∞ and $\frac{1}{k\Phi}$. In a way, these surfaces are close to the regular n-gon X_n. To this end we make the following definition (which can also be found in [1, §7.2]):

Definition 5.4. Given a pair of distinct periodic directions (d, d') and its associated geodesic $\gamma_{d,d'}$ on $\mathbb{H}^2$, we denote by $V(d, d')$ the connected component of $\mathbb{H}^2 \backslash (\Gamma_n^{\pm} \cdot \gamma_{d,d'})$ containing X_n.

As an example, the domain $V(\infty, d')$ with $d' = \frac{\Phi}{2\Phi^2-1}$ is drawn in Figure 24.

Remark 5.5. If a geodesic of $\Gamma_n^{\pm} \cdot \gamma_{d,d'}$ passes through X_n, then $V(d, d')$ is not well defined. For convenience, we set $V(d, d') = \{X_n\}$ as in this case we automatically have:

$$K(d, d') \leq K(\infty, \frac{1}{\Phi}) \sin\theta(X_n, \infty, \frac{1}{\Phi})$$

and since X_n is the furthest point away from the set of geodesics $\mathcal{G}_{max}$, we have for any surface $X \in \mathcal{T}_n$:

$$K(d, d') \sin\theta(X, d, d') \leq K(d, d') \leq K(\infty, \frac{1}{\Phi}) \sin\theta(X_n, \infty, \frac{1}{\Phi}).$$

With this definition, the proof of Lemmas 7.6 and 7.7 of [1, §7.2] generalizes to our setting and gives:

Lemma 5.6. *Let (d_0, d_0') be a pair of distinct periodic directions. Assume that Equation (♣) holds for any pair of directions (d, d') whose associated geodesic lie in the boundary of the domain $V(d_0, d_0')$. Then the same inequality is true for (d_0, d_0').*
Furthermore, a pair of directions (d, d'), $d < d'$ whose associated geodesic lies in the boundary of the domain $V(d_0, d_0') \cap \mathcal{T}_{n+}$ has to satisfy $d' + d \geq \Phi$.

In particular, it suffices to prove Equation (♣) for pairs of directions (d, d') with $d + d' \geq \Phi$. This relies on the sinus comparison techniques of [1, §7.3].

Proposition 5.7. *Let (d, d') with $d + d' \geq \Phi$ and $X = x + iy \in \mathcal{T}_n$ inside the half disk defined by the geodesic $\gamma_{\frac{1}{\Phi}, \Phi - \frac{1}{\Phi}}$. We have*

$$K(d, d') \sin\theta(X, d, d') \leq K(\infty, \frac{1}{\Phi}) \sin\theta(X, \infty, \frac{1}{\Phi}).$$

This condition is verified in particular for $X \in \mathcal{T}_n \backslash \mathcal{R}_+$.

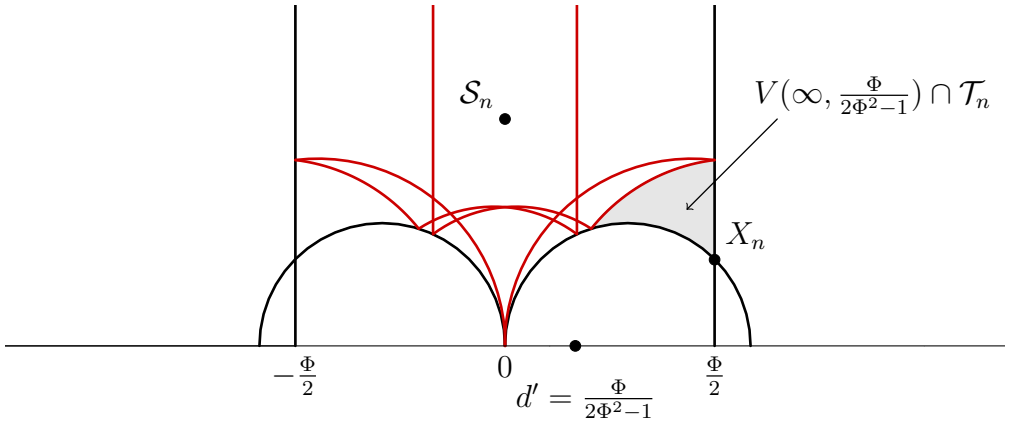

FIGURE 24. The geodesics of $\Gamma_n^{\pm} \cdot \gamma_{\infty, \frac{\Phi}{2\Phi^2-1}}$ intersecting the fundamental domain $\mathcal{T}_n$, and the domain $V(\infty, \frac{\Phi}{2\Phi^2-1}) \cap \mathcal{T}_n$.

Proof of Proposition 5.7. We distinguish two cases:

(1) In the case $d \geq \frac{1}{\Phi}$, we use Proposition 7.8 of [1] which can be stated more generally as:

Proposition 5.8. *Let $a \in \mathbb{R}$, $b > 0$, and $c \geq b$. Let $\mathcal{D} \subset \mathbb{H}^2$ be the domain enclosed by the geodesics $\gamma_{a,\infty}$, $\gamma_{a+b,\infty}$ and $\gamma_{a-c,a+c}$, and X_0 be the right corner of the domain $\mathcal{D}$, as in Figure 25. Then for any (d, d') with $a \leq d \leq a+b \leq d'$ such that $\gamma_{d,d'}$ intersect the domain $\mathcal{D}$, the function*

$$F_{(d,d')} : X \in \mathcal{D} \mapsto \frac{\sin\theta(X, \infty, a)}{\sin\theta(X, d, d')}$$

is minimal at X_0 on the domain $\mathcal{D}$.

In our setting, we set $a = \frac{1}{\Phi}$, $b = \frac{\Phi}{2} - \frac{1}{\Phi}$ and $c = \frac{1}{\Phi}$ and it gives that for any (d, d') with $\frac{1}{\Phi} \leq d \leq \frac{\Phi}{2} \leq d'$, the function

$$F_{(d,d')} : X \mapsto \frac{\sin\theta(X, \infty, \frac{1}{\Phi})}{\sin\theta(X, d, d')}$$

is minimal at X_n on the domain $\mathcal{D} = \{X = x + iy \in \mathcal{T}_n \text{ with } x \geq \frac{1}{\Phi}\}$. In particular, since by Corollary 4.6

$$\forall (d, d'),\ K(d, d') \sin\theta(X_n, d, d') \leq K(\infty, \frac{1}{\Phi}) \sin\theta(X_n, \infty, \frac{1}{\Phi})$$

we deduce that for all $X \in \{X = x + iy \in \mathcal{T}_n \text{ with } x \geq \frac{1}{\Phi}\}$ and (d, d') with $\frac{1}{\Phi} \leq d \leq \frac{\Phi}{2} \leq d'$, we have

$$K(d, d') \sin\theta(X, d, d') \leq K(\infty, \frac{1}{\Phi}) \sin\theta(X, d, d').$$

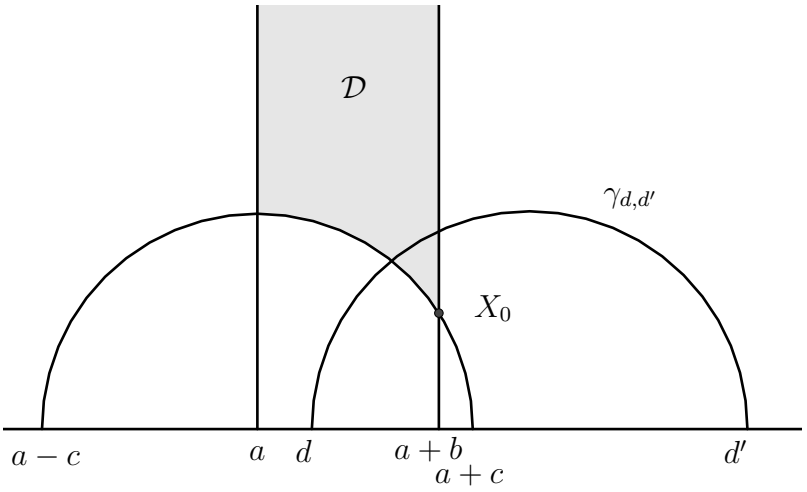

FIGURE 25. The domain $\mathcal{D}$ of Proposition 5.8.

(2) Else, $d < \frac{1}{\Phi}$ so that $d' > \Phi - \frac{1}{\Phi}$. In this case, for any pair of directions (d, d') not in $\Gamma \cdot \mathcal{G}_{max}$ and such that $d \leq \frac{1}{\Phi}$ and $d' \geq \Phi - \frac{1}{\Phi}$, and for all $X \in \mathcal{R}_+$, we have $\sin\theta(X, d, d') \leq \sin\theta(X, \frac{1}{\Phi}, \Phi - \frac{1}{\Phi})$ so that

$$\begin{aligned} K(d,d')\sin\theta(X,d,d') &\leq K(d,d')\sin\theta(X,\frac{1}{\Phi},\Phi-\frac{1}{\Phi}) \\ &\leq K(\frac{1}{\Phi},\Phi-\frac{1}{\Phi})\sin\theta(X,\frac{1}{\Phi},\Phi-\frac{1}{\Phi}) \quad \text{(by Proposition 4.7)} \\ &\leq K(\infty,\frac{1}{\Phi})\sin\theta(X,\infty,\frac{1}{\Phi}) \quad \text{(by case 1.)} \end{aligned}$$

This concludes the proof.

□

6. Proof of Theorem 1.4

In the case where $n \equiv 2 \mod 4$, saddle connections are not necessarily closed anymore, and it is no longer possible to use techniques from Sections 4 and 5. However, we can still show that KVol is bounded on the Teichmüller disk of X_n. In §6.1, we extend a boundedness criterion of [1, §3] to the case of multiple singularities. In §6.2, we use this criterion to show that KVol is bounded on the Teichmüller disk of the regular n-gon.

6.1. Boundedness criterion for multiple singularities.

In this paragraph, we show Theorem 1.5 which extends the boundedness criterion of [1] to the case of translation surfaces with multiple singularities.

Theorem 1.5. KVol is bounded on the Teichmüller disk of a Veech surface X if and only if there are no intersecting closed curves α and β on X such that

$\alpha = \alpha_1 \cup \cdots \cup \alpha_k$ and $\beta = \beta_1 \cup \cdots \cup \beta_l$ are unions of parallel saddle connections (that is all saddle connections $\alpha_1, \ldots, \alpha_k, \beta_1, \ldots, \beta_l$ have the same direction).

Proof. First, notice that if there exist a pair (α, β) of parralel closed curves, then applying the Teichmüller geodesic flow in their common direction make the length of both α and β go to zero, while the interserction remain unchanged. In particular

$$\mathrm{KVol}(g_t \cdot X) \to +\infty \text{ as } t \to +\infty.$$

Conversely, let X be a Veech surface, which we assume to be of unit area. Recall that for such a surface, the "no small triangle condition" of [10] (see also [8]) gives a constant $A > 0$ such that for any two saddle connections α and β, the inequality $|\alpha \wedge \beta| \geq A$ holds. Further, the constant A does not depend on the choice of the surface in the Teichmüller disk of X.

Now, let α be a saddle connection in a periodic direction. The Veech surface X decomposes into cylinders in the direction of α. Let h be the smallest height of the cylinders. For any saddle connection β which is not parallel to α, β has at least a vertical length h between each non-singular intersection with α, plus a vertical length at least h before the first non-singular intersection, and after the last non-singular intersection with α. In particular, for any saddle connection β having at least one non-singular intersection with α, we have:

$$h(\beta) \geq h(|\alpha \cap \beta| + 1)$$

where $h(\beta) = l(\beta) \sin angle(\alpha, \beta)$. In fact, if β does not intersect α non-singularly then the above inequality still holds, as it becomes $h(\beta) \geq h$ which is true as long as β is not parallel to α. Finally, since $h(\beta) \leq l(\beta)$, we conclude that :

$$\frac{|\alpha \cap \beta| + 1}{l(\alpha) l(\beta)} \leq \frac{1}{l(\alpha) h} \leq \frac{1}{A}.$$

The last inequalty comes from the fact that $l(\alpha)h = \alpha \wedge \beta_0 \geq A$ for a saddle connection β_0 which stays inside the cylinder of height h.

Next, take α and β two simple closed curves decomposed as an union of saddle connections $\alpha = \alpha_1 \cup \cdots \cup \alpha_k$ and $\beta = \beta_1 \cup \cdots \cup \beta_l$, and assume that $\alpha_1, \ldots, \alpha_k, \beta_1, \ldots, \beta_l$ are not all parallel. Then,

$$\mathrm{Int}(\alpha, \beta) \leq \Big(\sum_{\substack{1 \leq i \leq k \\ 1 \leq j \leq l}} |\alpha_i \cap \beta_j| \Big) + s$$

where $s \leq \min(k, l)$ denotes the number of common singularities between α and β. It should be noted that if $\alpha_i = \beta_j$, we set $|\alpha_i \cap \beta_j| = 0$.
Now, since saddle connections are not all parallel, there is at least $\min(k, l)$ pairs

(i,j) such that α_i and β_j are not parallel, and we get

$$\begin{aligned}\mathrm{Int}(\alpha,\beta) &\leq \Big(\sum_{\substack{1\leq i\leq k\\ 1\leq j\leq l}} |\alpha_i\cap\beta_j|\Big)+s\\ &\leq \sum_{\substack{i,j\\ \alpha_i \text{ and } \beta_j \text{ non-parallel}}} (|\alpha_i\cap\beta_j|+1)\\ &\leq \sum_{\substack{i,j\\ \alpha_i \text{ and } \beta_j \text{ non-parallel}}} \frac{1}{A}\times l(\alpha_i)l(\beta_j)\\ &\leq \frac{1}{A}l(\alpha)l(\beta).\end{aligned}$$

This gives the required boundedness result

$$\mathrm{KVol}(X)\leq\frac{1}{A}.$$

□

6.2. **Intersection of parallel curves on X_n, $n\equiv 2 \mod 4$.** In this paragraph, we go back to the regular n-gon for $n\equiv 2 \mod 4$ and we study the intersection $\mathrm{Int}(\alpha,\beta)$ in the case where α and β are union of parallel saddle connections. Up to the action of the Veech group, we can assume that α and β are either both horizontal or both vertical. We will work in the staircase model $\mathcal{S}$, as in Figure 26. Notice that in the horizontal direction, saddle connections go from one singularity to the other while saddle connections are closed curves in the vertical direction. In this latter case, it is easy to show:

Lemma 6.1 (Vertical curves)**.** *For every i,j, $\mathrm{Int}(\beta_i,\beta_j)=0$*

Proof. First, since β_m is homologous to a non-singular curve which do not intersect any of the β_j for $j<m$, we have $\mathrm{Int}(\beta_m,\beta_j)=0$.
Next, for any $j<m$ the curve $\beta_j+\beta_{j+1}$ is homologous to a non-singular curve and for all i, $\mathrm{Int}(\beta_j+\beta_{j+1},\beta_i)=0$ and hence $\mathrm{Int}(\beta_j,\beta_i)=-\mathrm{Int}(\beta_{j+1},\beta_i)$ and by induction $\mathrm{Int}(\beta_j,\beta_i)=\pm\mathrm{Int}(\beta_m,\beta_i)=0$. □

In the case where α (resp. β) is an horizontal curve made of two horizontal saddle connections α_{i_1} and α_{i_2} (resp. α_{j_1} and α_{j_2}) going from one singularity to the other and oriented such that the resulting curve $\alpha=\alpha_{i_1}\pm\alpha_{i_2}$ has a well defined orientation, we have:

Lemma 6.2 (Horizontal curves)**.** *In this setting,* $\mathrm{Int}(\alpha,\beta)=0$.

Proof. First notice that, given the orientation of the saddle connections α_i is from left to right as in Figure 26, the curve α has a well defined orientation if and only

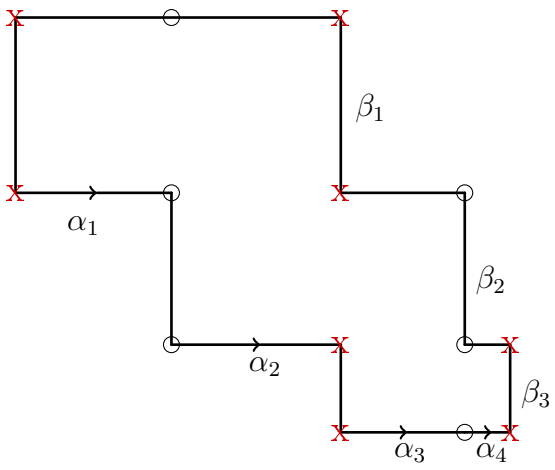

FIGURE 26. The staircase model associated with the 14-gon. The horizontal and the vertical direction represent the two cuspidal directions. Notice that vertical saddle connections are closed while horizontal saddle connections are not.

if $\alpha = \pm[\alpha_{i_1} + (-1)^{i_2-i_1-1}\alpha_{i_2}]$. In this case, we can write (assuming $i_1 < i_2$ for convenience)

$$\begin{aligned}\alpha &= \pm[(\alpha_{i_1} + \alpha_{i_1+1}) - (\alpha_{i_1+1} + \alpha_{i_1+2}) + \cdots + (-1)^{i_2-i_1-1}(\alpha_{i_2-1} + \alpha_{i_2})] \\ &= \pm \sum_{k=0}^{i_2-i_1-1} (-1)^k(\alpha_{i_1+k} + \alpha_{i_1+k+1}).\end{aligned}$$

Now, since the curves $\alpha_i + \alpha_{i+1}$ are closed curves homologous to core curve of horizontal cylinder, they are pairwise non-intersecting. Making the same decomposition for β gives directly $\mathrm{Int}(\alpha, \beta) = 0$. □

As a corollary, we can apply the criterion of Theorem 1.5 to deduce that KVol is bounded on the Teichmüller disk of the regular n-gon. In fact, a closer look at the proof of Theorem 1.5 gives the following explicit bound:

Corollary 6.3. *Let $n \geq 10$, $n \equiv 2 \mod 4$. For any surface X in the Teichmüller disk of the regular n-gon, and any closed curves α and β on X, we have:*

$$\frac{\mathrm{Int}(\alpha, \beta)}{l(\alpha)l(\beta)} \leq \frac{1}{\Phi l_m^2}.$$

REFERENCES

[1] Julien Boulanger, Erwan Lanneau, and Daniel Massart. Algebraic intersection in a family of veech surfaces. *arXiv:2110.14235*, 2022.

[2] Smail Cheboui, Arezki Kessi, and Daniel Massart. Algebraic intersection for translation surfaces in a family of Teichmüller disks. *Bull. Soc. Math. France*, 149(4):613–640, 2021.

[3] Smail Cheboui, Arezki Kessi, and Daniel Massart. Algebraic intersection for translation surfaces in the stratum $H(2)$. *C. R. Math. Acad. Sci. Paris*, 359:65–70, 2021.
[4] Daniel Massart. A short introduction to translation surfaces, Veech surfaces, and Teichmüller dynamics. In *Surveys in geometry I*, pages 343–388. Springer, Cham, [2022] ©2022.
[5] Daniel Massart and Bjoern Muetzel. On the intersection form of surfaces. *Manuscr. Math.*, 143(1-2):19–49, 2014.
[6] Thierry Monteil. On the finite blocking property. *Ann. Inst. Fourier*, 55(4):1195–1217, 2005.
[7] John Smillie and Corinna Ulcigrai. Geodesic flow on the Teichmüller disk of the regular octagon cutting sequences and octagon continued fractions maps. In *Dynamical numbers. Interplay between dynamical systems and number theory.*
[8] John Smillie and Barak Weiss. Characterizations of lattice surfaces. *Invent. Math.*, 180(3):535–557, 2010.
[9] W. A. Veech. Teichmüller curves in moduli space, Eisenstein series and an application to triangular billiards. *Invent. Math.*, 97(3):553–583, 1989.
[10] Ya. B. Vorobets. Planar structures and billiards in rational polygons. *Russ. Math. Surv.*, 51(1):177–178, 1996.
[11] Alex Wright. From rational billiards to dynamics on moduli spaces. *Bull. Amer. Math. Soc. (N.S.)*, 53(1):41–56, 2016.
[12] A. N. Zemlyakov and A. B. Katok. Topological transitivity of billiards in polygons. *Math. Notes*, 18:760–764, 1976.
[13] Anton Zorich. Flat surfaces. In *Frontiers in number theory, physics, and geometry. I*, pages 437–583. Springer, Berlin, 2006.

Institut Fourier. 100 rue des Mathématiques, 38000 Grenoble, France.
Email address: julien.boulanger@univ-grenoble-alpes.fr

Chapitre 4

Surfaces made with convex polygons having obtuse or right angles

Résumé en français. Dans ce chapitre ainsi que le chapitre suivant, nous exposons un travail réalisé en collaboration avec I. Pasquinelli, et dans lequel nous étendons les méthodes développées au Chapitre 2 à une famille plus générale de surfaces plates, construites à partir de polygones convexes à angles obtus ou droits. On commence par généraliser la méthode de découpage à l'aide d'arguments combinatoires et géométriques qui permettent de compter assez finement les intersections, et nous démontrons le Théorème A. Dans le chapitre suivant, nous utiliserons ces résultats dans le cadre sprécifique des surfaces de Bouw-Möller.

In this Chapter and the following chapter, we present a work carried out in collaboration with I. Pasquinelli, in which we extend the methods developed in Chapter 2 to a large class of flat surfaces, built from convex polygons with obtuse angles. We begin by generalizing the subdivision method using combinatorial and geometric arguments that allow to count finely the intersections, and we prove Theorem A. In the next chapter, we will use these results in the specific framework of Bouw-Möller surfaces.

In this chapter and the following chapter, we present a work carried out in collaboration with I. Pasquinelli, in which we extend the methods developed in Chapter 2. to a large class of flat surfaces, built from convex polygons with obtuse angles. We begin by generalizing the subdivision method using combinatorial and geometric arguments that allow to count finely the intersections, and we prove Theorem A. In the next chapter, we will use these results in the specific framework of Bouw-Möller surfaces.

4.1 Introduction

Let X be a translation surface constructed from a (finite) collection $(P_i)_{i\in I}$ whose pairs of parallel sides of the same length are glued together by translations. We assume that:

(H1) Each polygon is convex with obtuse or right angles,

(H2) Sides of the same polygon are not identified together.

We denote by l_0 the length of the smallest sides of the polygons. We show:

Theorem 4.1.1. *Under the hypotheses (H1) and (H2), for any two closed curves γ and δ on X, we have:*

$$\frac{\mathrm{Int}(\gamma,\delta)}{l(\gamma)l(\delta)} \leq \frac{1}{l_0^2}.$$

Further, if the angles are all strictly obtuse, equality holds if and only if γ and δ are sides of the polygons of length l_0 intersecting once. If there are right angles, equality may also hold only in the following cases:

- *γ and δ are sides or also diagonals of the polygons, both of length l_0 and intersecting once at a singularity,*
- *γ and δ are both diagonals of length $\sqrt{2}l_0$ intersecting twice (once at a singularity and once outside the singularities, with the same sign),*
- *up to symmetry, γ is a side or a diagonal of length l_0 and δ is a geodesic of length $2l_0$, contained the union of exactly two polygons, and intersecting twice.*

The initial motivation for proving this result was to be able to deal with the case of Bouw-Möller surfaces. The Bouw-Möller surface $S_{m,n}$ satisfies hypotheses (H1) and (H2) as soon as $n \geq 4$. For $n = 2$ and $m \geq 3$, the Bouw-Möller surface $S_{m,2}$, which is also called the staircase model associated to the regular m-gon does not satisfy (H2), but similar techniques allow to show that Theorem 4.1.1 still holds (see [BLM22]).

Finally, if $n = 3$ and $m \geq 3$, the surface $S_{m,n}$ does not satisfy (H1). We can still show that the same result holds and it uses a similar proof, but it requires more precise estimates on the length of saddle connections which we will give in the next chapter.

Before going on any further, let us make several comments on this result.

KVol and the systolic volume. Recall that the (homological) systolic length of a Riemannian surface X is the length of a shortest non-homotopically trivial loop on X. The systolic volume is then the volume of X divided by the square of the systolic length. In other words:

$$\mathrm{SysVol}(X) := \mathrm{Vol}(X) \cdot \sup_{\substack{\alpha \text{ closed curve,} \\ [\alpha] \neq 0}} \frac{1}{l(\alpha)^2}.$$

In particular, KVol can be thought of as a cousin of the systolic volume, twisted by the algebraic intersection, and it is natural to compare them.

An interesting corollary of Theorem 4.1.1 is when all the vertices of the polygons are identified to the same point. It is for example the case on the Bouw-Möller surface $S_{m,n}$ when m and n are coprime. In this case there is only one singularity and the sides of the polygons represent closed curves on the surface. In particular, l_0 is also the systolic length and we have (if the surface has finite volume):

$$\mathrm{KVol}(X) \leq \mathrm{SysVol}(X).$$

This result can be compared with Theorem 1.1 of [MM14], which states that in the general setting of Riemannian surfaces, one has $\mathrm{KVol}(X) \leq 9\mathrm{Volsys}(X)$. In fact, we conjecture that:

Conjecture 4.1.2. *For any translation surface X,*

$$KVol(X) \leq \frac{2}{\sqrt{3}}\mathrm{SysVol}(X).$$

Notice that equality holds for equilateral staircases (see [BLM22]), but these should not be the only equality cases.

General flat surfaces. Although Theorem 4.1.1 is stated for translation surfaces, the proof should extend to any surface constructed from flat polygons satisfying (H1) and (H2) and such that the resulting surface is flat with finitely many conical singularities, but is not necessarily a translation surface. This is discussed in Section 4.5.4.

What about polygons having acute angles? In light of Theorem 4.1.1, one may wonder what happens if we remove hypothesis (H1), that is we allow some of the angles to be acute. In this case, we will see that our methods have no chance to extend unless we assume:

(H1') The sum of two consecutive angles at a vertex is at least π.

Assuming both (H1') and (H2), the result of Theorem 4.1.1 hold if we replace l_0 by $l_0 \sin\theta_0$, where θ_0 is the minimal angle of all the polygons. Namely:

Theorem 4.1.3. *Let X be a flat surface constructed from a collection of convex polygons by gluing pairs of sides satisfying (H1') and (H2). Let θ_0 be the smallest angle of the polygons, and l_0 be the length of the smallest side of the polygons. Assume $\theta_0 \geq \frac{1}{2}\arccos\frac{8}{9}$. We have:*

$$\frac{\mathrm{Int}(\alpha,\beta)}{l(\alpha)l(\beta)} \leq \frac{1}{(l_0\sin\theta_0)^2}.$$

At the moment, we are only able to prove this result if $\theta_0 \geq \frac{1}{2}\arccos\frac{8}{9} \simeq 0,076\pi$, but it should hold for any $\theta_0 > 0$.

What if we remove hypothesis (H2)? For surfaces satisfying (H1) but not (H2), we will see that our methods allows to prove:

Theorem 4.1.4. *Let X be a surface constructed from a collection of euclidean polygons by identifying pairs of sides of the polygons satisfying hypothesis (H1). Then, for any two closed curves γ and δ on X, we have*

$$\frac{\mathrm{Int}(\alpha,\beta)}{l(\alpha)l(\beta)} \leq \frac{4}{l_0^2}.$$

In fact, we believe that Theorem 4.1.1 holds without hypothesis (H2), as it is the case for example for the regular n-gon (see Chapter 3). However, proving this would require much more precise estimates on both the intersections and the lengths of the segments, as we have seen in Chapter 3.

Outline of the proof. Our proof of Theorem 4.1.1 relies on a *subdivision* method which generalises that of [BLM22] (Chapter 2) and [Bou23] (Chapter 3). More precisely, given two closed *geodesics* γ and δ on X (which are then piecewise straight lines), we define the *polygonal decomposition* of γ (resp. δ) by cutting γ (resp. δ) each time it goes from a polygon to another. This gives a decomposition $\gamma = \gamma_1 \cup \cdots \cup \gamma_k$ (resp. $\delta = \delta_1 \cup \cdots \cup \delta_l$) into smaller (non-closed) segments, which are chords of the polygons. We will see that this decomposition allows to estimate simultaneously the intersections and the lengths of the segments.

Notice that the case of closed curves which are union of saddle connections (i.e vertex-to-vertex trajectories) should be treated as a particular case, as then there could be singular intersections. In fact, on a translation surface any closed curve is homologous to a union of saddle connections. More precisely, any homology class has a representative which is a union of saddle connections and such that this representative minimizes the length among closed curves in the same homology class. In particular, it is easy to see that in the definition of KVol we can assume that the curves γ and δ are union of saddle connections. In the following, we show:

Theorem 4.1.5. *Under the hypotheses (H1) and (H2), for any two saddle connections α and β on X, we have:*

$$\frac{|\alpha \cap \beta| + 1}{l(\alpha) l(\beta)} \leq \frac{1}{l_0^2}$$

where $|\alpha \cap \beta|$ denotes the number of non-singular intersections points if $\alpha \neq \beta$, and is set as 0 if $\alpha = \beta$.

Further, if the angles are all strictly obtuse, equality holds if and only if α and β are sides of the polygons both having length l_0. If there are right angles, equality holds if and only if:

- *α and β are sides or also diagonals of the polygons, having both length l_0,*
- *α and β are both diagonals of length $\sqrt{2} l_0$ and such that $\alpha \cap \beta| = 1$,*
- *up to symmetry, α is a side or a diagonal of length l_0 and β is a geodesic of length $2l_0$, contained the union of exactly two polygons, and $|\alpha \cap \beta| = 2$.*

Proof of Theorem 4.1.1 using Theorem 4.1.5. Let $\gamma = \gamma_1 \cup \cdots \cup \gamma_k$ and $\delta = \delta_1 \cup \cdots \cup \delta_l$ be two closed curves decomposed as a union of saddle connections. Note that k (resp. l) is also the number of singularities that γ (resp. δ) crosses. Denote by $|\gamma_i \cap \delta_j|$ the number of intersections of the two saddle connections γ_i and δ_j outside of the singularity. Then the intersection number of γ and δ at the singularities can be at most $\min(k, l)$ and

$$\begin{aligned} \mathrm{Int}(\gamma, \delta) &\leq \sum_{\substack{1 \leq i \leq k \\ 1 \leq j \leq l}} |\gamma_i \cap \delta_j| + \min(k, l) && (4.1) \\ &\leq \sum_{\substack{1 \leq i \leq k \\ 1 \leq j \leq l}} |\gamma_i \cap \delta_j| + kl = \sum_{\substack{1 \leq i \leq k \\ 1 \leq j \leq l}} \left(|\gamma_i \cap \delta_j| + 1 \right). && (4.2) \end{aligned}$$

with equality only if $k = l = 1$. Hence, by Theorem 4.1.5,

$$\mathrm{Int}(\gamma, \delta) \leq \sum_{\substack{1 \leq i \leq k \\ 1 \leq j \leq l}} \frac{l(\gamma_i) l(\delta_j)}{l_0^2} = \frac{1}{l_0^2} \left(\sum_{1 \leq i \leq k} l(\gamma_i) \right) \left(\sum_{1 \leq j \leq l} l(\delta_j) \right) = \frac{l(\gamma) l(\delta)}{l_0^2}.$$

Further, equality holds only if we have equality in both (4.2) and in Theorem 4.1.5. The condition $k = l = 1$ just tells us that γ and δ need to be saddle connections. Moreover, γ and δ both must have length l_0 and intersect once at a singularity, or be two diagonals of the polygons, both of length $\sqrt{2}l_0$ and intersecting twice. □

We are now left to prove Theorem 4.1.5. Given two saddle connections α and β on X, we define the *polygonal decomposition* of α (resp. β) by cutting α (resp. β) each time it goes from a polygon to another. This gives a decomposition $\alpha = \alpha_1 \cup \cdots \cup \alpha_k$ (resp. $\beta = \beta_1 \cup \cdots \cup \beta_l$) into smaller (non-closed) segments. We will see that this decomposition allows to estimate simultaneously the number of intersections and the lengths of the segments. To estimate the length of the segments we will distinguish two kinds of segments in the polygonal decomposition:

Definition 4.1.6. (i) a *non-adjacent segment* is a segment going from a side of a polygon P to a non-adjacent side of P, or a segment having one of its endpoints as a vertex of a polygon.

(ii) an *adjacent segment* is a segment going from the interior of a side e of a polygon P to the interior of a side of P adjacent to e.

Remark that, by definition, the segments α_1 and α_k (resp. β_1 and β_l) are non-adjacent segments. Let us also notice that if $k = 1$, then α is either a side or a diagonal of a polygon: in this case we have a single non-adjacent segment according to the definition, and we will deal with this case separately.

Organisation of the chapter. In Section 4.2, we give a lower bound on the length of a saddle connection using its polygonal decomposition, and as an application we prove Theorem 4.1.4. Then, in Section 4.3 we study some properties of sequences of consecutive adjacent segments, as this will allow us to study the intersections of pieces of saddle connections using its polygonal decomposition in Section 4.4. Finally, in Section 4.5 we conclude the proof of Theorem 4.1.5 and we deal with the case where one of the saddle connections is a side or a diagonal of a polygon (Section 4.5.3).

From now on and until Section 4.5.4, we consider a translation surface X satisfying hypotheses (H1) and (H2). We consider two saddle connections α and β on X and denote by $\alpha_1 \cup \cdots \cup \alpha_k$ (resp. $\beta_1 \cup \cdot \cup \beta_l$) the polygonal decomposition of α (resp. β).

We use the following:

Notation 4.1.7. Given a segment α_i in the polygonal decomposition of the (oriented) saddle connection α, we will denote α_i^- and α_i^+ the endpoints of α_i, so that the orientation of α takes us from α_i^- to α_i^+.

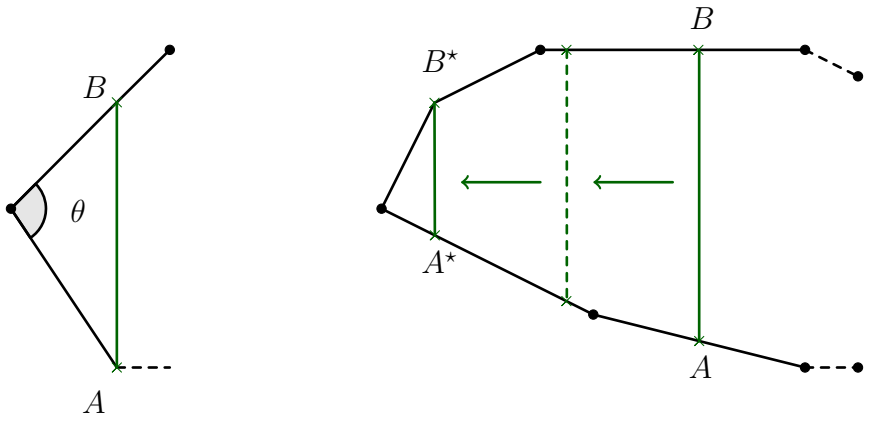

Figure 4.1: The pushing process of Lemma 4.2.2.

4.2 Study of the lengths

4.2.1 Length of adjacent and non-adjacent segments

In this paragraph, we use the hypothesis on the polygons (which are convex with obtuse or right angles) to obtain a first estimate on the length of the segments, namely:

Lemma 4.2.1 (Length of adjacent and non-adjacent segments)**.** *We have:*

1. *The length of a non-adjacent segment is at least l_0.*

2. *The length of a pair of consecutive adjacent segments is greater than l_0.*

The Lemma will follow from elementary convex geometry. More precisely, we start by showing:

Lemma 4.2.2. *Let P be a convex polygon whose angles are all obtuse or right and denote by l_0 the length of the smallest side of P. Let A and B be two points on the boundary of the polygon which do not lie on the same side of the polygon or on adjacent sides. Then the distance between A and B is at least l_0.*

Proof of Lemma 4.2.2. (i) Let us start with the case where one of the points (say A) is a vertex of the polygon and the other point B lies on one of the sides adjacent to the sides containing A. This means that there is a side e which has A as an endpoint and is adjacent to the side e' containing B in its interior (see the left hand side of Figure 4.1). As the angle θ between e and e' is obtuse or right, the distance between A and B is at least the length of the side e. By definition, that is at least l_0.

(ii) In the general case, given two points A and B on the boundary of the polygon which do not lie in the same side of the polygon or in adjacent sides, we get back to case (i) by "pushing" the points while decreasing the length. One way to do this is to draw the parallel lines to AB. Since the polygon is convex, there is at least one "pushing" direction for which we decrease the length, as in the right of Figure 4.1. This process allows to get points $A^\star$ and $B^\star$ in the configuration of case (i) such that:

$$d(A, B) \geq d(A^\star, B^\star) \geq l_0.$$

□

Proof of Lemma 4.2.1. The first part of the Lemma follows directly from Lemma 4.2.2 applied to the polygon containing the non-adjacent segment.

For the second part of Lemma 4.2.1, consider two consecutive adjacent segments α_i and α_{i+1} connected on a side e shared by two polygons P and P'. Since all the internal angles of polygons forming the surface X are obtuse or right by hypothesis, we are in a configuration as in Figure 4.2, and hence the length $l(\alpha_i \cup \alpha_{i+1})$ will be greater than the length of the side e, which must be at least l_0. □

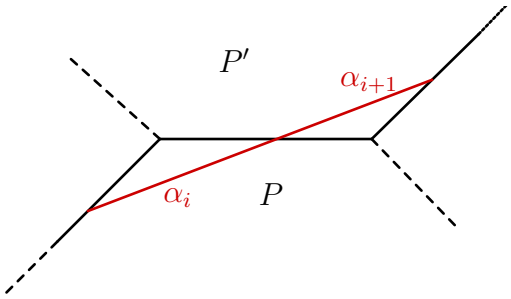

Figure 4.2: Two consecutive adjacent segment have length at least l_0.

4.2.2 Lengths of saddle connections

Now that, in the previous section, we studied the length of pieces of the polygonal decomposition, we want to use these results to estimate the length of the whole saddle connection. As suggested by Lemma 4.2.1, we will do this by grouping consecutive adjacent segment by pairs. This motivates the following

Notation 4.2.3. Given a saddle connection α, we denote by p_α the number of non-adjacent segments in the decomposition of α and q_α the maximal number of *pairs* of consecutive adjacent segments we can form in the decomposition of α (see Figure 4.3)

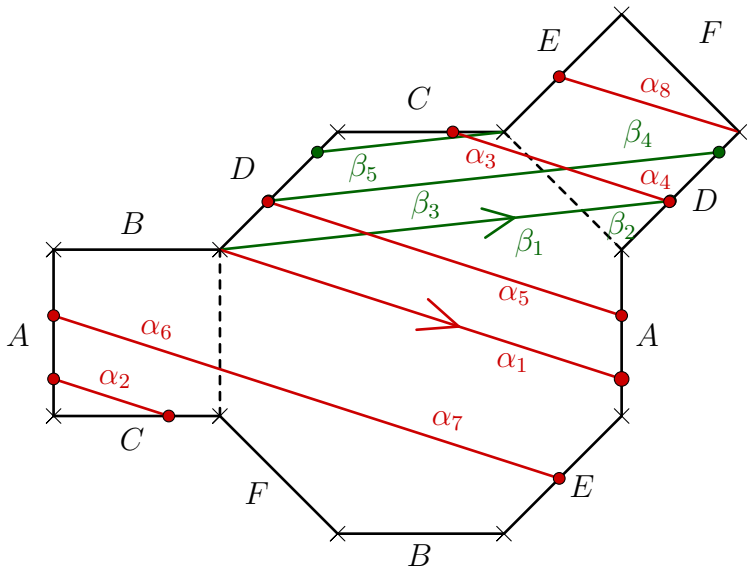

Figure 4.3: Examples of saddle connections and their polygonal decomposition. Here, the segments $\alpha_2, \alpha_3, \alpha_4, \beta_2$ and β_4 are adjacent segments while all other segments are non-adjacent, and hence $p_\alpha = 5, q_\alpha = 1$, $p_\beta = 3$ and $q_\beta = 0$.

Using this notation, it follows directly from Lemma 4.2.1 that

$$l(\alpha) \geq (p_\alpha + q_\alpha) l_0. \tag{4.3}$$

Further, one notices that the cases where this estimate is far from being sharp are the cases where there are odd sequences of consecutive adjacent segments, as then it is not possible to group all adjacent segments by pairs.

In fact, we can slightly improve the estimate of the length in this case:

Lemma 4.2.4. *1. The total length of three consecutive adjacent segments is more than* $\sqrt{2} l_0 = (1 + (\sqrt{2} - 1)) l_0$.

2. The total length of three consecutive segments α_{i-1}, α_i *and* α_{i+1}*, being respectively non-adjacent, adjacent and non-adjacent, is more than* $(1+\sqrt{2}) l_0$.

We will need the following elementary geometry lemma:

Lemma 4.2.5. *Let* Δ *and* Δ' *be two half lines from a point* S *and making an angle* $\theta \in]0, \pi[$*. Let* B *be the point at distance* $l_0 > 0$ *from both* Δ *and* Δ'*. Then, for any* $P \in \Delta$ *and* $Q \in \Delta'$ *such that the segment* $[PQ]$ *passes through* B*, we have* $l(PQ) \geq 2 l_0 \sin \frac{\theta}{2}$.

Proof. Let H_Δ (resp. $H_{\Delta'}$) be the orthogonal projection of B on Δ (resp. Δ') and let θ_1 (resp. θ_2) be the angle at B between the segments $[PB]$ and $[BH_\Delta]$ (resp. $[QB]$ and $[BH_{\Delta'}]$), see Figure 4.2.5.

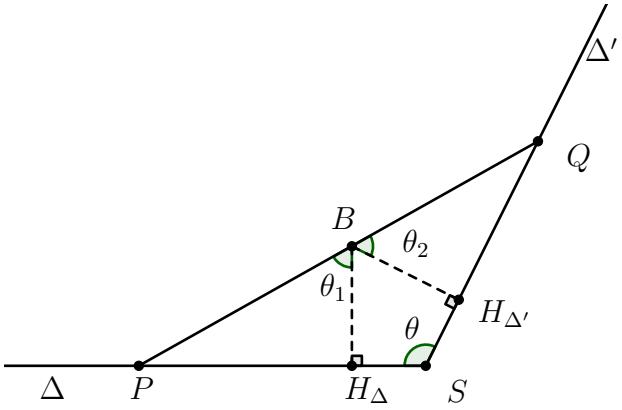

Figure 4.4: The setting of Lemma 4.2.5.

Elementary geometry entails $\theta_1 + \theta_2 = \theta$. Further, $l(PQ) = l(PB) + l(BQ) = l_0 \sin\theta_1 + l_0 \sin\theta_2$. Given that $\theta_2 = \theta - \theta_1$, one easily checks that this quantity is minimal for $\theta_1 = \theta_2 = \frac{\theta}{2}$. □

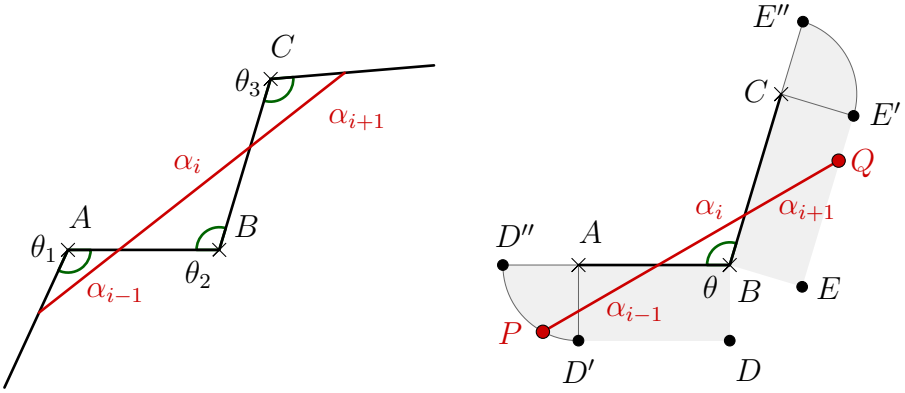

Figure 4.5: The two cases in Lemma 4.2.4.

Proof. 1. Given three consecutive adjacent segments α_{i-1}, α_i and α_{i+1}, we can unfold the trajectory to get a picture like Figure 4.5. Since the angles θ_1, θ_2 and θ_3 are comprised between $\frac{\pi}{2}$ and π, we directly deduce that the length of $\alpha_{i-1} \cup \alpha_i \cup \alpha_{i+1}$ is greater than the length of the segment AC, which is at least $\sqrt{2} l_0$.

2. Similarly, we can draw a picture like the right part of Figure 4.5. By Lemma 4.2.2, any point on a side which is non-adjacent to the segment AB (resp. BC) must be at a distance at least l_0 away from the side AB (resp. BC). In particular, the endpoints α_{i-1}^- and α_{i+1}^+ are outside the gray zone of Figure

4.5, which is the set of points of the polygon containing α_{i-1} (resp. α_{i+1}) at distance less than l_0 from AC (resp. BC). The boundary of this region is made of a segment $[D, D']$ (resp. $[E, E']$) parallel to AB (resp. BC) at a distance l_0, and and two arcs of circles at B and A (resp. B and C). Specifically, we denote by D'' (resp. E'') the point on the side adjacent to AB having A as an endpoint (resp. the side adjacent to BC having C as an endpoint), which is at distance l_0 of AB (resp. BC).

Now, let P (resp. Q) be the point of α_{i-1} (resp. α_{i+1}) at the boundary of the gray zone. We have $l(\alpha_{i-1} \cup \alpha_i \cup \alpha_{i+1}) \geq l(PQ)$. Further, we can push the segment PQ while keeping it in the same direction until it passes through B. It is easily checked that the length of PQ decreases by this process, and hence we can assume that PQ passes through B. Now,

(a) If P lies in the arc of circle $[D', D'']$, then the length of the segment PB is at least $\sqrt{2}l_0$. Since the length of BQ is by construction at least l_0, we conclude that

$$l(PQ) = l(PB) + l(BQ) \geq (\sqrt{2} + 1)l_0.$$

By symmetry, the same holds if Q lies in the arc of circle $[E', E'']$. (In fact, we can even show that $l(PQ) \geq 2\sqrt{2}l_0$ but it won't be needed here.)

(b) Else, $P \in [D, D']$ and $Q \in [E, E']$, then PQ has minimal length when it goes through B, and we can use Lemma 4.2.5 to conclude that $l(PQ) \geq 2\sqrt{2}l_0$.

□

Remark 4.2.6. In fact, we can combine the proofs of 1. and 2. in Lemma 4.2.4 to show that the total length of $2q + 1$ consecutive segments such that the first and the last are non-adjacent while all the other are adjacent is at least $(q + 2)\sqrt{2}l_0$.

In the remaining part of this section, we will use the following

Definition 4.2.7 (Odd saddle connection)**.** Given a finite sequence of elements of $\{1, 2\}$, we will say that the sequence is *odd* if it starts and ends with 1, the 1s are isolated and the blocks of 2s contain an odd number of elements. Similarly, given a saddle connection with its polygonal decomposition, we will say that α is *odd* if the non-adjacent segments are isolated (i.e. there are no consecutive pairs of pieces of non-adjacent segments) and between two isolated non-adjacent segments there is an odd number of adjacent segments. In other words, α is *odd* if the sequence given by the types of the pieces of its polygonal decomposition is *odd* with the rule 1 = non-adjacent and 2 = adjacent. Note also that the number of pieces in the polygonal decomposition of an odd saddle connection is odd.

The first reason for this definition is that for an odd saddle connection (recall that we are excluding sides and diagonals), there is always either three consecutive adjacent segments or a sequence of three consecutive segment being respectively non-adjacent, adjacent and non-adjacent, so that we deduce from Lemma 4.2.4 that:

Lemma 4.2.8. *If α is an odd saddle connection, then:*

$$l(\alpha) \geq (p_\alpha + q_\alpha + \sqrt{2} - 1)l_0.$$

In fact, the notion of odd saddle connection will also turn out to be particularly useful in the study of the intersections. The main reason for this is because they form the equality case in the following

Lemma 4.2.9. *Given a saddle connection with its polygonal decomposition $\alpha = \alpha_1 \cup \cdots \cup \alpha_k$, we have*

$$\left\lceil \frac{k}{2} \right\rceil \leq p_\alpha + q_\alpha$$

with equality if and only if α is odd.

Proof. Let $N = p_\alpha$ and k_i, $1 \leq i \leq N-1$ be the number (possibly zero) of adjacent segments between the i^{th} and the $(i+1)^{th}$ non-adjacent segment. Remembering that α_1 and α_k are non-adjacent, we then have

$$k = 1 + k_1 + 1 + \cdots + 1 + k_{N-1} + 1 = N + \sum_{i=1}^{N-1} k_i$$

so that

$$\frac{k}{2} = \frac{N + \sum_{i=1}^{N-1} k_i}{2} = \frac{2N - 1 + \sum_{i=1}^{N-1}(k_i - 1)}{2} = N - \frac{1}{2} + \sum_{i=1}^{N-1} \frac{k_i - 1}{2}.$$

Hence

$$\begin{aligned} \left\lceil \frac{k}{2} \right\rceil &\leq N + \sum_{i=1}^{N-1} \frac{k_i - 1}{2} \\ &\leq N + \sum_{i=1}^{N-1} \left\lfloor \frac{k_i}{2} \right\rfloor = p_\alpha + q_\alpha. \end{aligned}$$

The first inequality is actually strict when k is even and an equality when k is odd. The second inequality is an equality if and only if for all i, $\frac{k_i - 1}{2} = \left\lfloor \frac{k_i}{2} \right\rfloor$, that is k_i is odd and so α is odd. Since for odd saddle connections k is necessarily odd, equality overall is achieved exactly on odd saddle connections. □

4.3 Properties of (consecutive) adjacent segments

In this section, we give several properties of adjacent segments which we will use for the estimation of the intersections between two saddle connections. We start with a few definitions.

Definition 4.3.1 (Type of a segment)**.** Let α_i be a segment going from the interior of a side e to the interior of a side e'. We will say that α_i is of type $e \to e'$. If it goes from a vertex to the interior of a side e' (resp. from the interior of a side e to a vertex), we will say that α_i is of type $* \to e'$ (resp. $e \to *$).

4.3.1 Sector of adjacency

In this paragraph, we consider a convex polygon P whose sides are labeled in cyclic (clockwise) order $e_1, \cdots, e_N$, and a direction $\theta \in [0, 2\pi[$ which represent the direction of a saddle connection.

Lemma 4.3.2. *[and Definition] There exist two sides e_{u_-} and e_{u_+} such that for any adjacent segment α_i contained in P and having direction θ, the type of α_i is either:*

- $e_{u_+} \to e_{u_+ + 1}$,
- *or* $e_{u_-} \to e_{u_- - 1}$.

In the first case, we say that α_i has positive sign and in the second case we say that the segment is of type has negative sign.

Roughly speaking, we are saying that if we fix a direction, then an adjacent segment in that direction has only two possibilities for the edges that it can start from and end into. Moreover, the cyclic ordering of the sides of the polygon determine which pair of adjacent sides the segment touches.

Proof. Fixing two sides e_u and e_{u+1}, an (oriented) adjacent segment from e_u to e_{u+1} must have a direction within an angular sector determined by the directions of e_u and e_{u+1}. We will call this the *admissible sector for e_u and e_{u+1}*. For a convex polygon, the admissible sectors for each pair of adjacent sides form a partition of $[0, 2\pi[$. In particular, (if the direction of θ is not the direction of a side) there is only one pair of sides e_{u_+} and $e_{u_+ + 1}$ such that the direction θ lie in the admissible sector for e_{u_+} and $e_{u_+ + 1}$ (in this order).

Similarly, there is only one pair of sides e_{u_-} and $e_{u_- - 1}$ such that the direction θ lie in the admissible sector for e_{u_-} and $e_{u_- - 1}$ (in this order). □

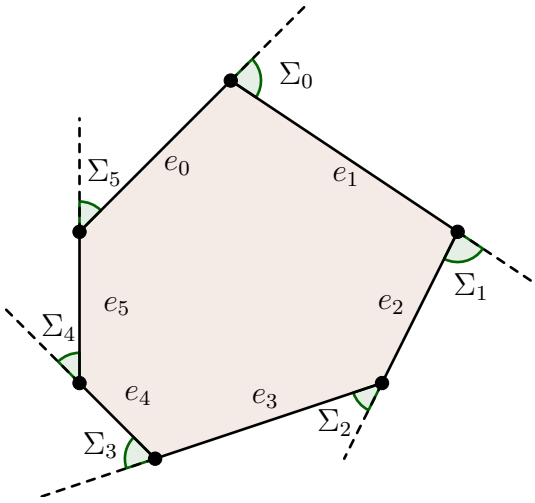

Figure 4.6: An adjacent segment from e_i to e_{i+1} has direction in the sector Σ_i defined by the directions of the sides e_i and e_{i+1}.

4.3.2 Sequences of consecutive adjacent segments

We now describe several properties of sequences of adjacent segments that will be used in the next section to estimate the intersections between two saddle connections using their polygonal decomposition.

Remark 4.3.3. In a sequence of consecutive adjacent segments, the sign of adjacent segments alternate. This is because two consecutive adjacent segments are as in Figure 4.7, so they must have opposite signs.

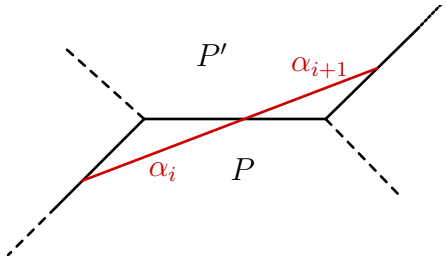

Figure 4.7: Two consecutive adjacent segment have opposite signs.

We can then use this remark to show:

Lemma 4.3.4. *We consider a maximal sequence of adjacent segments, and we assume that there are two adjacent segments inside the same polygon having the same sign. Then there is an even number of adjacent segments in the sequence.*

Proof. Let α_i and $\alpha_{i'}$ be two segments of the sequence inside the same polygon and having the same sign. Up to a change of orientation of α, we can assume

that they both have positive sign, and that we chose the indices i and i' so that we are in the configuration in Figure 4.8 (i.e. that α_i is closer than $\alpha_{i'}$ to the corner of P). We distinguish the cases $i < i'$ and $i' < i$.

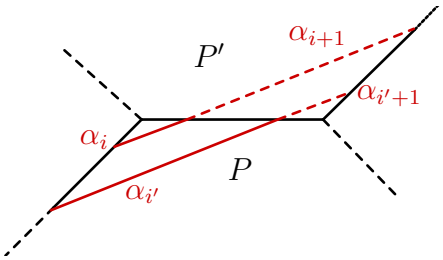

Figure 4.8: The segments α_i and $\alpha_{i'}$ are positive adjacent segments of the same type.

- Assume $i < i'$. All the segments between α_i and $\alpha_{i'}$ are adjacent segments. First, we will show that the last adjacent segment of a sequence has negative sign. Since α_{i+1} is an adjacent segment parallel to $\alpha_{i'+1}$, we directly deduce from Figure 4.8 that $\alpha_{i'+1}$ must be an adjacent segment (and has negative sign). Now, if $\alpha_{i'+2}$ is non-adjacent, then $\alpha_{i'+1}$ is the last adjacent segment and we saw it has negative sign. Otherwise, if $\alpha_{i'+2}$ is also adjacent, then α_{i+2} and $\alpha_{i'+2}$ have the same type and are in the same configuration as α_i and $\alpha_{i'}$, and hence $\alpha_{i'+3}$ is also adjacent. Repeating this argument, we obtain that the last adjacent segment of the sequence must be of negative sign.

  Now, we will prove that the first segment of the sequence has positive sign. Either α_i is the first adjacent segment and we have assumed it has positive sign, or α_{i-1} is an adjacent segment and then it must have negative sign and share its type with $\alpha_{i'-1}$. Next, $\alpha_{i'-2}$ is also an adjacent segment, and we deduce from Figure 4.9 that the segment α_{i-2}, parallel to $\alpha_{i'-2}$, must also be an adjacent segment (which then has positive sign). Then, α_{i-2} and $\alpha_{i'-2}$ are in the same configuration as α_i and $\alpha_{i'}$ and hence we can repeat the argument until we reach a non-adjacent segment. From this we conclude that the first segment of the sequence must be of positive sign.

  As a conclusion, the sequence starts with a positive adjacent segment and ends with a negative adjacent segment. Since the signs are alternating, there must be an even number of segments.

- Similarly, if $i' < i$, the above arguments give that the first segment of the sequence of consecutive adjacent segment must have negative sign while the last segment of the sequence has positive sign. Hence, there is also an even number of segments.

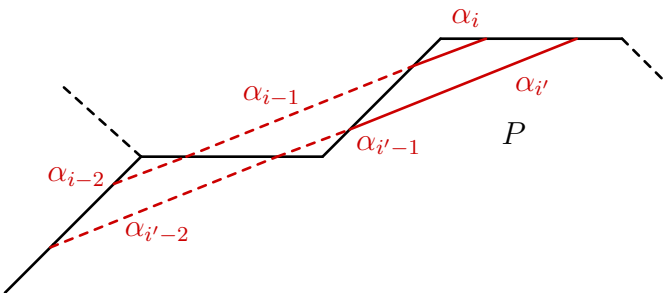

Figure 4.9: If α_{i-1} is adjacent, then the segments α_{i-2} and $\alpha_{i'-2}$ are positive adjacent segments of the same type.

□

To study the intersections, we distinguish three types of sequences of consecutive adjacent segments:

- **(Isolated adjacent segments)** An adjacent segment which is preceded and followed by non-adjacent segments will be called an *isolated* adjacent segment.

- **(Sequence of consecutive adjacent segments contained inside a short cylinder)** A sequence of consecutive adjacent segments containing at least two segments, and such that for each segment α_i of the sequence, α_{i+2} is either non-adjacent or have the same type as α_i.
  Formally, we are in this case if there exist two sides of the polygons e and e' such that the first segment of the sequence has type $e \to e'$, then the second segment has type $e' \to e$, and so on. A sequence of adjacent segments inside a short cylinder is represented in the left of Figure 4.10. Following the terminology of [BLM22], we say that the starting side e of the sequence is the sandwiching side of the sequence of adjacent segments while the side e' is the sandwiched side. By Lemma 4.3.4, a sequence of consecutive adjacent segments contained inside a short cylinder must contain an even number of segments. Further, if we decompose the segment by pairs, each pair $\alpha_i \cup \alpha_{i+1}$ goes from e to e, and the direction of α must lie in the sector defined by the direction of e' and the direction of the diagonal of the cylinder.

- **(Sequence of consecutive adjacent segments not contained inside a short cylinder)** The other sequences of consecutive adjacent segments are those which are not contained in a short cylinder. For those sequences, we have from Lemma 4.3.2 and Remark 4.3.3 that:

  Corollary 4.3.5. *Given three consecutive segments in a sequence of consecutive adjacent segments which is not contained in a short cylinder, no two segment lie inside the same polygon.*

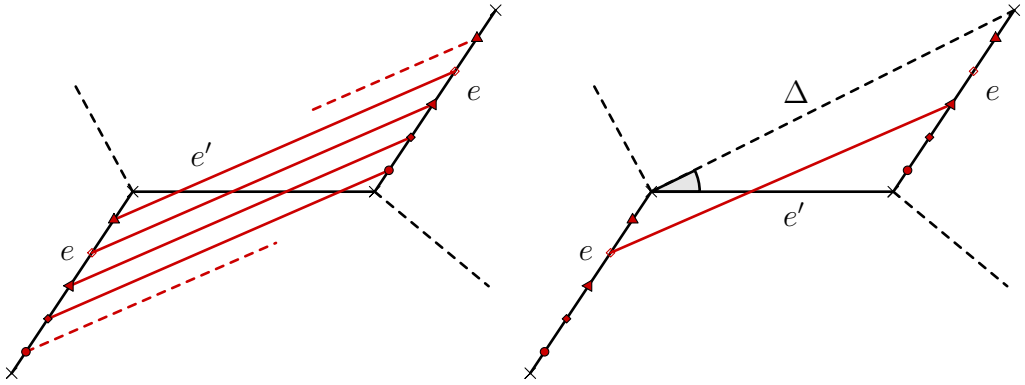

Figure 4.10: A sequence of adjacent segments contained inside a short cylinder. On the right, we show a single pair of adjacent segments in the sequence. Its direction is contained in the sector defined by the direction of e' and the direction of the diagonal Δ.

Proof. The second segment cannot lie in the same polygon than either the first or the third segment because by hypothesis $(H2)$ consecutive adjacent segments do not lie in the same polygon. By Lemma 4.3.2 and Remark 4.3.3, the first and the third segment cannot lie in the same polygon unless they have the same type, but this is not the case by assumption of not being in a small cylinder. □

4.4 Study of the intersections

We now study the intersections of two saddle connections $\alpha = \alpha_1 \cup \cdots \cup \alpha_k$ and $\beta = \beta_1 \cup \cdots \cup \beta_l$ depending on their polygonal decomposition. Namely, we show:

Proposition 4.4.1. *Let α and β be two saddle connections. We have:*

$$|\alpha \cap \beta| \leq (p_\alpha + q_\alpha)(p_\beta + q_\beta)$$

Further, if equality holds then between each non-adjacent segment there is an odd number of adjacent segments (that is, both α and β are odd saddle connections).

The proof of the proposition relies on the notion of *configuration* ★, which is defined in the next subsections and essentially states that an intersection involving an adjacent segment allows to remove one to the count of potential intersections.

Remark 4.4.2. The inequality of Proposition 4.4.1 is optimal, as given in the example of Figure 4.11.

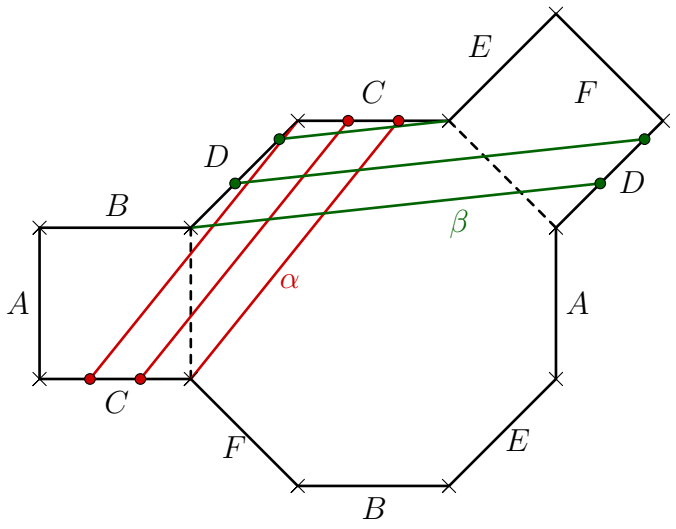

Figure 4.11: Example of odd saddle connections such that $|\alpha \cap \beta| = (p_\alpha + q_\alpha)(p_\beta + q_\beta)$.

4.4.1 Configurations ★

Roughly speaking, a configuration ★ gives two pieces α_i and β_j which intersect and have one endpoint on a shared side. Recall that we have $\alpha = \alpha_1 \cup \cdots \cup \alpha_k$ and $\beta = \beta_1 \cup \cdots \cup \beta_l$ the polygonal decompositions of the saddle connection α and β.

Definition 4.4.3. A *configuration* ★ is given by the ordered data of two pairs of indexes $((i,j),(i',j')) \in (\{1,\cdots,k\} \times \{1,\cdots,l\})^2$ such that :

(i) The segments α_i and β_j intersect

(ii) There is a side e of the polygon containing both α_i and β_j such that on the interior of e there is one endpoint of α_i and one endpoint of β_j.

(iii) $\alpha_{i'}$ and $\beta_{j'}$ are respectively the segments consecutive to α_i and β_j continued after this endpoint.

If $((i,j),(i',j'))$ are in a configuration ★, we will use the notation $(i,j) \xrightarrow{\star} (i',j')$. Moreover, we will say that (i,j) *induces a configuration* ★ if there exists (i',j') such that $((i,j),(i',j'))$ are in a configuration ★.

Note that i' and j' cannot just be any element of $\{1,\cdots,k\}$ and $\{1,\cdots,l\}$, but given i and j, we have $i' \in \{i-1, i+1\}$ and $j \in \{j-1, j+1\}$.

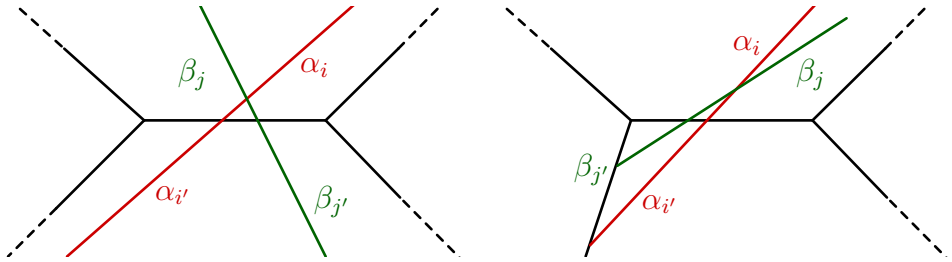

Figure 4.12: Examples of configuration $(i,j) \xrightarrow{\bigstar} (i',j')$.

The picture to have in mind is given by Figure 4.12. Let us now state several properties related to configurations $\bigstar$ which will turn out to be useful to count intersections.

Lemma 4.4.4. *1. If $(i,j) \xrightarrow{\bigstar} (i',j')$, then the segments $\alpha_{i'}$ and $\beta_{j'}$ lie in the same polygon but do not intersect.*

2. If given (i',j'), we have $(i,j) \xrightarrow{\bigstar} (i',j')$ and $(i'',j'') \xrightarrow{\bigstar} (i',j')$, then $i = i''$ and $j = j''$. In other words, the data of (i',j') in a configuration $\bigstar$ determines uniquely i and j.

3. Assume α_i is an adjacent segment and $j \neq 1, l$ be such that $\alpha_i \cap \beta_j \neq \varnothing$. Then (i,j) induces a configuration $\bigstar$.

4. Assume α_i is an adjacent segment, $\alpha_i \cap \beta_1 \neq \varnothing$ and $\alpha_i \cap \beta_l \neq \varnothing$, then either $(i,1)$ or (i,l) induce a configuration $\bigstar$.

Proof. 1. Looking at the two polygons glued along the side which contains an endpoint of α_i and β_j, the two lines defined by α and β can only intersect once, so if α_i and β_j intersect, then $\alpha_{i'}$ and $\beta_{j'}$ will not (see Figure 4.12).

2. If we have $(i,j) \xrightarrow{\bigstar} (i',j')$ and $(i'',j'') \xrightarrow{\bigstar} (i',j')$, with $i \neq i''$ and $j \neq j''$, then there exist two sides e and e' such that the interior of e contains one endpoint of $\alpha_{i'}$ and one endpoint of $\beta_{j'}$, while e' contains the other endpoints of $\alpha_{i'}$ and $\beta_{j'}$. Moreover, α_i and β_j are segments across e, while $\alpha_{i''}$ and $\beta_{j''}$ are segments across e'. Now, the straight lines defined by α and β can either be parallel or intersect once, so we cannot have both α_i and β_j and also $\alpha_{i''}$ and $\beta_{j''}$ to intersect, as required by the first part of the definition.

3. and 4. If α_i is an adjacent segment, then any segment β_j intersecting it must have one endpoint on one of the side containing and endpoint of α_i. The only case where it does not induce a configuration $\bigstar$ is when the endpoint lies on the vertex of the polygon which is between the two adjacent sides containing an endpoint of α_i; this case cannot happen if $j \neq 1, l$ and cannot happen simultaneously for $j = 1$ and $j = l$.

□

4.4.2 Counting the intersections

We are now ready to prove Proposition 4.4.1. For this purpose, we distinguish the intersections involving non-adjacent segments and adjacent segments. Namely, we define:

$I_1 := \{(i,j), \alpha_i \cap \beta_j \neq \varnothing, \alpha_i \text{ non-adjacent}\}$
$I_2 := \{(i,j), \alpha_i \cap \beta_j \neq \varnothing, \alpha_i \text{ adjacent}\}$

Further, since intersecting segments must lie in the same polygon, we have:

$I_1 \subset \tilde{I}_1 := \{(i,j), \alpha_i \text{ and } \beta_j \text{ lie in the same polygon }, \alpha_i \text{ non-adjacent}\}$

Next, we partition I_2 by distinguishing pairs of indexes of I_2 which induce configurations $\bigstar$ and pairs of I_2 which do not. We also distinguish pairs of indexes in I_2 inducing a configuration $\bigstar$ involving another adjacent segment or a non-adjacent segment, namely:

$I_2^{(0)} := \{(i,j) \in I_2 \text{ which do not induce a configuration } \bigstar\}$
$I_2^{(1)} := \{(i,j) \in I_2, \text{ with } (i,j) \xrightarrow{\bigstar} (i',j') \text{ and } \alpha_{i'} \text{ is non-adjacent}\}$
$I_2^{(2)} := \{(i,j) \in I_2 \backslash I_2^{(1)}, \text{ such that } (i,j) \xrightarrow{\bigstar} (i',j') \text{ and } \alpha_{i'} \text{ is adjacent}\}$

It should be noted that a pair of indexes may induce two configurations $\bigstar$ if they intersect and the endpoints of the segments on the interior of the same two sides. This is the reason why we do not take elements of $I_2^{(1)}$ in the definition of $I_2^{(2)}$, as it avoids counting an intersection twice. In this way, the three sets form a partition of I_2.

The main advantage of this partition is that by construction we have

$$\#I_2 = \#I_2^{(0)} + \#I_2^{(1)} + \#I_2^{(2)}.$$

Moreover, given a pair $(i,j) \in I_2^{(1)}$, the configuration $\bigstar$ determines (at least) one pair $(i',j') \in \tilde{I}_1 \backslash I_1$ since by part 1. of Lemma 4.4.4 $\alpha_{i'}$ and $\beta_{j'}$ do not intersect. The pairs (i',j') do not overlap by part 2. of Lemma 4.4.4 and hence

$$\#I_2^{(1)} \leq \#\left(\tilde{I}_1 \setminus I_1\right), \qquad \text{hence} \qquad \#I_1 \leq \#\tilde{I}_1 - \#I_2^{(1)}.$$

Then,

$$|\alpha \cap \beta| = \#I_1 + \#I_2 \leq \#\tilde{I}_1 - \#I_2^{(1)} + \#I_2^{(0)} + \#I_2^{(1)} + \#I_2^{(2)}$$

so that:

$$|\alpha \cap \beta| \leq \#\tilde{I}_1 + \#I_2^{(0)} + \#I_2^{(2)} \tag{4.4}$$

There is an easy estimate for $\#\tilde{I}_1$, as by hypothesis (H2) two consecutive segments cannot lie in the same polygon, thus for any non-adjacent segment α_i, there is at most $\left\lceil \frac{l}{2} \right\rceil$ segments of β in the polygon containing α_i, so that

$$\#\tilde{I}_1 \leq p_\alpha \left\lceil \frac{l}{2} \right\rceil. \tag{4.5}$$

Next, we study $I_2^{(0)}$ and $I_2^{(2)}$. For this purpose, we distinguish isolated adjacent segments (i.e. adjacent segments which are preceded and followed by non-adjacent segments) and sequences of (at least two) consecutive adjacent segments. The reason for this distinction is that isolated adjacent segments do not contribute to $I_2^{(2)}$, since α_i ans $\alpha_{i'}$ in a $\bigstar$ configuration are consecutive. Then, an intersection involving an isolated adjacent segment α_i must be either in $I_2^{(1)}$ or in $I_2^{(0)}$.

To compute $\#I_2^{(0)}$, we will split it further into two according to whether the adjacent segment is *isolated* or a sequence of *consecutive* ones and define

$$I_2^{(0,i)} := \{(i,j) \in I_2^{(0)}, \alpha_i \text{ is an isolated adjacent segment}\},$$
$$I_2^{(0,c)} := I_2^{(0)} \backslash I_2^{(0,i)} = \{(i,j) \in I_2^{(0)}, \alpha_i \text{ is not an isolated adjacent segment}\}.$$

Lemma 4.4.5. *We have:*

$$\#I_2^{(0,i)} \leq \#\{i, \alpha_i \textit{ is an isolated adjacent segment}\}.$$

Proof. The quantity $\#I_2^{(0,i)}$ counts the number of pairs (i,j) such that $\alpha_i \cap \beta_j \neq \varnothing$, α_i is adjacent and isolated and (i,j) do not induce a configuration $\bigstar$. Now, by part 3. of Lemma 4.4.4 we necessarily have that $j = 1$ or $j = l$, so for each i, the set contains at most two pairs. Now, from part 4. of Lemma 4.4.4, we cannot have both pairs $(i,1)$ and (i,l) because one of them must induce a configuration $\bigstar$. In other words, we are counting the number of i's such that α_i is adjacent and isolated and α_i intersects one of β_1 and β_l, which is certainly smaller than the number of i such that α_i is adjacent and isolated.

□

We are left to study the intersections of β with sequences of at least two consecutive adjacent segments, i.e. we want to estimate $\#I_2^{(0,c)}$. This is the purpose of the next section.

4.4.3 Intersections in sequences of consecutive adjacent segments

In this section we consider a maximal sequence of q consecutive adjacent segments $\alpha_{i_0+1} \cup \cdots \cup \alpha_{i_0+q}$ with $q \geq 1$, that is α_{i_0} and α_{i_0+q+1} are non-adjacent segments while all the in-between segments are adjacent. We show:

Lemma 4.4.6. *There are at most* $\left\lfloor \frac{q}{2} \right\rfloor \left\lfloor \frac{l}{2} + 1 \right\rfloor$ *intersections between* $\alpha_{i_0+1} \cup \cdots \cup \alpha_{i_0+q}$ *and* β *which are not in* $I_2^{(1)}$.

Note that this counts the number of intersections for the sequence of adjacent segments both in $I_2^{(2)}$ and in $I_2^{(0)}$. Hence this gives:

Corollary 4.4.7.

$$\#I_2^{(2)} + \#I_2^{(0,c)} \leq q_\alpha \left\lfloor \frac{l}{2} + 1 \right\rfloor.$$

Proof of Lemma 4.4.6. We distinguish 4 cases:

(i) The sequence of adjacent segments is contained inside a short cylinder.

(ii) q is even but the sequence of adjacent segment is not contained in a short cylinder.

(iii) $q = 3$,

(iv) $q \geq 5$ is odd.

Note that when q is odd, then the sequence cannot be contained in a small cylinder by Lemma 4.3.4.

For each of the cases, the idea is as follows: we first partition the sequence of maximal segments in pairs (with one triple if q is odd), and then show that for each of the $\left\lfloor \frac{q}{2} \right\rfloor$ pairs $\alpha_i \cup \alpha_{i+1}$ (or triple $\alpha_i \cup \alpha_{i+1} \cup \alpha_{i+2}$), we can pair consecutive pieces of β in such a way that each pair of pieces of β intersects $\alpha_i \cup \alpha_{i+1}$ (or $\alpha_i \cup \alpha_{i+1} \cup \alpha_{i+2}$) only once. We do this by associating to every piece β_j intersecting $\alpha_i \cup \alpha_{i+1}$ (or $\alpha_i \cup \alpha_{i+1} \cup \alpha_{i+2}$) a consecutive piece $\beta_{j'}$ which does not. Up to potentially add an extra intersection with β_1 and β_l, we get at most $\left\lfloor \frac{l}{2} + 1 \right\rfloor$ intersections.

More precisely, for each pair $\alpha_i \cup \alpha_{i+1}$ (resp. triple $\alpha_i \cup \alpha_{i+1} \cup \alpha_{i+2}$):

- β_1 (resp. β_l) intersect the pair (resp. triple) at most once (this is because of hypothesis (H2) – and Corollary 4.3.5 for the triple –), and
- given j such that β_j intersects one of the segments of the pair (resp. triple), and such that the intersection belongs to $I_2^{(2)}$, we can find $j' \in \{j-1, j+1\}$ such that $\#\left(\{i, i+1\} \times \{j, j'\} \cap \left(I_2^{(0} \cup I_2^{(2)}\right)\right) \leq 1$ (resp. $\#\left(\{i, i+1, i+2\} \times \{j, j'\} \cap \left(I_2^{(0} \cup I_2^{(2)}\right)\right) \leq 1$). Further, we can construct the (unordered) pairs $\{j, j'\}$ such that they do not overlap.

Here, β_1 and β_l may or may not be paired. In total,

- If neither β_1 nor β_l are paired, there are at most $\left\lfloor \frac{l-2}{2} \right\rfloor$ pairs, so that adding the intersections with β_1 and β_l, this implies that among all intersections between $\alpha_i \cup \alpha_{i+1}$ and β, at most $\left\lfloor \frac{l-2}{2} \right\rfloor + 2 = \left\lfloor \frac{l}{2} + 1 \right\rfloor$ intersections in $I_2^{(0)} \cup I_2^{(2)}$.

- If β_1 (resp. β_l) is paired but β_l (resp. β_1) is not, then we can construct at most $\left\lfloor \frac{l-1}{2} \right\rfloor$ pairs. Since β_1 (resp. β_l) is already paired, we only need to add the possible intersection with β_l (resp. β_1), and thus we get at most $\left\lfloor \frac{l-1}{2} \right\rfloor + 1 = \left\lfloor \frac{l+1}{2} \right\rfloor$ intersections for this pair.

- Finally, if both β_1 and β_l are paired, this gives $\left\lfloor \frac{l}{2} \right\rfloor$ intersections.

As a conclusion, we get at most $\left\lfloor \frac{l}{2} + 1 \right\rfloor$ intersections.

Although the intersections with pairs in $I_2^{(2)}$ induce a configuration $\bigstar$, this is not sufficient to construct the pairs $\{j, j'\}$, because some pairs might overlap. Here, we will investigate all possible configurations in each case to construct the pairs and to make sure that the pairs do not overlap.

Case (i). Assume the sequence of adjacent segments is contained inside a short cylinder. Then q is even by Lemma 4.3.4, and we can group the adjacent segments by pairs. Say each pair form a sandwiched segment of type $e \to e' \to e$. As explained in §4.3.2, we have a picture like Figure 4.10. In the following, we will denote by α_i and α_{i+1} the two adjacent segments of the pair, respectively of type $e \to e'$ and of type $e' \to e$.

Now, notice that a segment β_j intersecting $\alpha_i \cup \alpha_{i+1}$ must have an endpoint either on the side e or on e' (or on both). The corresponding endpoint is not on a vertex except maybe for $j = 1$ or $j = l$. We then define the index $j' = j \pm 1$ which will be paired to j as follows.

1. If β_j has one of its endpoints on e', we take j' such that β_j and $\beta_{j'}$ have this endpoint in common.

2. Else, β_j has one of its endpoints on e but no endpoint on e', and we take j' such that β_j and $\beta_{j'}$ have this endpoint in common.

With this construction, we have:

Lemma 4.4.8. *(a) If $j \in \{1, \cdots, l\}$ is such that β_j intersect $\alpha_i \cup \alpha_{i+1}$, then the segment $\beta_{j'}$ constructed as above does not intersect $\alpha_i \cup \alpha_{i+1}$.*

(b) Given j_1 and j_2 two distinct indices such that β_{j_1} and β_{j_2} intersect $\alpha_i \cup \alpha_{i+1}$ and such that the intersections belong to $I_2^{(2)}$, the pairs $\{j_1, j_1'\}$ and $\{j_2, j_2'\}$ constructed as above satisfy:

$$\{j_1, j_1'\} \cap \{j_2, j_2'\} = \varnothing.$$

Proof. (a) Let us assume up to a symmetry that β_j intersects the segment α_i. That means in particular that $\beta_{j'}$ does not lie in the same polygon as α_i, so these segments cannot intersect. Further,

1. if β_j has one of its endpoints on e', then it means that we have $(i,j) \xrightarrow{\bigstar} (i+1,j')$ and hence $\beta_{j'}$ do not intersect $\alpha_i \cup \alpha_{i+1}$ by part 1. of Lemma 4.4.4.
2. Else, β_j has one of its endpoints on e but no endpoint on e', and that means we have a configuration like Figure 4.13. In particular, since the direction of α is contained in the sector defined by the direction of e' and the direction of the diagonal Δ, we directly deduce that $\beta_{j'}$ cannot intersect α_{i+1}.

(b) As in the proof of (a), we will assume that β_{j_1} intersects the segment α_i. Since j_1 and j_2 are assumed to be distinct and both intersect the pair, we have by (a) that $j_2 \neq j_1'$ and $j_1 \neq j_2'$. It remains to show that $j_1' \neq j_2'$.

1&1. If β_{j_1} and β_{j_2} both have one endpoint on e' (case 1.), then this endpoint must be shared respectively with $\beta_{j_1'}$ and $\beta_{j_2'}$. In particular we cannot have $j_1' = j_2'$ as it would then imply $j_1 = j_2$.

1&2. Now, if β_{j_1} has an endpoint on e' (case 1.) but not β_{j_2} (which is then in case 2.), the condition $j_1' = j_2'$ would imply that $\beta_{j_1}, \beta_{j_1'} = \beta_{j_2'}$ and β_{j_2} are consecutive segments of β, and that $\beta_{j_1'} = \beta_{j_2'}$ has an endpoint on e' (shared with β_{j_1}) and an endpoint on e (shared with β_{j_2}). Further, since we assumed by symmetry that β_{j_1} intersects α_i, β_{j_1} lies in the polygon containing α_i, we have that $\beta_{j_1'}$ lies in the polygon containing α_{i+1}, and β_{j_2} lies in the polygon containing α_i. This means that β_{j_2} intersects α_i, and, combined with the fact that it has an endpoint on e and that its direction is comprised between the direction of α_i and the direction of e, it is easily seen to imply that β_{j_2} have an endpoint on e', which is not the case by assumption. This gives a contradiction.

By symmetry, this is the same if β_{j_2} has an endpoint on e' but β_{j_1} has not.

2&2. Else, both β_{j_1} and β_{j_2} have no endpoint on e' but one endpoint on e. That means that this endpoint must be shared with $\beta_{j_1'}$ (resp. $\beta_{j_2'}$) so that we cannot have $j_1' = j_2'$ unless $j_1 = j_2$.

Hence, in all cases we have $\{j_1, j_1'\} \cap \{j_2, j_2'\} = \varnothing$.

□

From Lemma 4.4.8 we obtain that for each pair $\alpha_i \cup \alpha_{i+1}$, we can group segments of β by pairs which are not overlapping and such that such that each

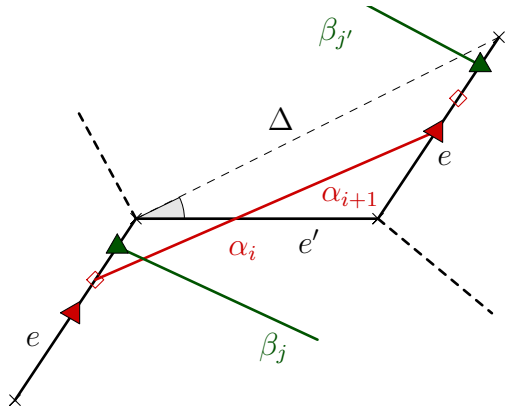

Figure 4.13: Example of pair of adjacent segments $\alpha_i \cup \alpha_{i+1}$ in case (i), with β_j having an endpoint on e but not on e'. We recall that the direction of α is contained in the sector defined by the direction of e' and the direction of the diagonal Δ. In particular, the segment $\beta_{j'}$ cannot intersect α_{i+1}.

pair intersects $\alpha_i \cup \alpha_{i+1}$ at most once. As already explained, β_1 and β_l could remain unpaired and we conclude that β can intersect $\alpha_i \cup \alpha_{i+1}$ at most $\left\lfloor \frac{l}{2} + 1 \right\rfloor$ times. Since the sequence of consecutive adjacent segments is made of $\frac{q}{2}$ pairs, we get that β intersects the sequence of adjacent segment at most $\frac{q}{2}\left\lfloor \frac{l}{2} + 1 \right\rfloor$, as required.

Case (ii). Now, **assume q is even but the sequence of consecutive adjacent segments is not contained in a small cylinder**, that is two adjacent segment of the sequence α_i and α_{i+2} are never contained in the same polygon (see Corollary 4.3.5). Since q is even we can group adjacent segments by pairs. Let $\alpha_i \cup \alpha_{i+1}$ be such a pair, as in Figure 4.14. We denote by e the side containing α_i^-, by e' the side containing $\alpha_i^+ = \alpha_{i+1}^-$ and by e'' the side containing α_{i+1}^+. The sides e, e' and e'' are different or the sequence of consecutive adjacent segments would be contained in a short cylinder.

Similarly to the first case, each segment β_j intersecting the sequence of adjacent segments must have an endpoint on at least one of the sides e, e' or e''. Assuming $j \neq 1, l$, the corresponding endpoint is not a vertex, and hence we define an index $j' = j \pm 1$ which will be paired to j as follows:

1. If β_j has an endpoint on e', then we choose j' such that β_j and $\beta_{j'}$ share their common endpoint on e'.

2. If β_j lies in the same polygon as α_i and has no endpoint on e' but an endpoint on e, then we choose j' such that β_j and $\beta_{j'}$ share their common endpoint on e.

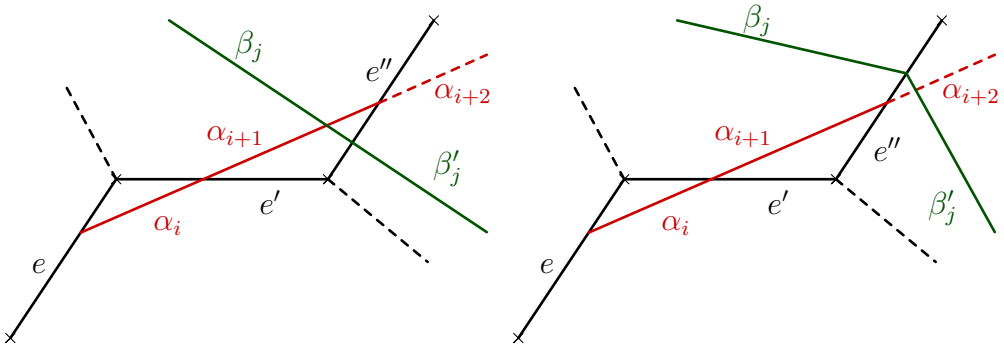

Figure 4.14: A pair of adjacent segments $\alpha_i \cup \alpha_{i+1}$ in case (ii). If a segment β_j intersect α_{i+1} and has one endpoint end e'' but no endpoint on e', we perform a small deformation of β so that the intersection of β_j with α_{i+1} moves to an intersection of $\beta_{j'}$ with α_{i+2}. This deformation does not change the type of the segments.

3. Else, β_j lies in the same polygon as α_{i+1} and has no endpoint on e' but one endpoint on e''. In this case, β_j intersects α_{i+1} and we have a configuration ★ given by $(i+1, j) \xrightarrow{\bigstar} (i+2, j')$. Then,

   - either α_{i+2} is non-adjacent and so $(i+1, j) \in I_2^{(1)}$, so that we do not have to count this intersection.
   - Or α_{i+2} is adjacent, and in this case we can perform a continuous deformation of β which will move the intersection of β_j and α_{i+1} to an intersection of α_{i+2} with $\beta_{j'}$, see Figure 4.14. This does not change the total number of intersections. In other words, instead of counting the intersection as an intersection between β_j and α_{i+1}, we count it as an intersection between $\beta_{j'}$ and α_{i+2} instead. Notice that this intersection would then become an intersection in case 1 for the pair $\alpha_{i+2} \cup \alpha_{i+3}$.

     The reason why we use this argument to move the intersection to the next pair is that otherwise there could be a segment β_j intersecting α_{i+1} and having an endpoint on e'', and then β_{j+1} could then have an endpoint on e and β_{j+2} intersect α_i. Following the rules, $j+1$ would appear in a pair with both j and $j+2$. Another way to understand this deformation argument is to notice that in the case where $j+1$ is paired with both j and $j+2$, none of the segments β_j, β_{j+1} and β_{j+2} intersect $\alpha_{i+2} \cup \alpha_{i+3}$, and so we "lose" an intersection of β with the pair $\alpha_{i+2} \cup \alpha_{i+3}$.

Lemma 4.4.9. *(a) If $j \in \{1, \cdots, l\}$ is such that β_j is either in case 1 or 2, then the segment $\beta_{j'}$ constructed as above does not intersect $\alpha_i \cup \alpha_{i+1}$.*

(b) Given j_1 and j_2 two distinct indices such that β_{j_1} and β_{j_2} are either in case 1 or 2, the pairs $\{j_1, j_1'\}$ and $\{j_2, j_2'\}$ constructed as above satisfy:

$$\{j_1, j_1'\} \cap \{j_2, j_2'\} = \varnothing.$$

Proof. (a) We distinguish two cases depending whether β_j has an endpoint on e' or not.

1. If β_j has an endpoint on e', then we have either $(i, j) \xrightarrow{\star} (i+1, j')$ or $(i+1, j) \xrightarrow{\star} (i, j')$ depending on whether α_i or α_{i+1} intersects β_j and the result holds by 1. of Lemma 4.4.4.
2. If β_j has no endpoint on e' but an endpoint on e, then in particular β_j intersects α_i, and $(i, j) \xrightarrow{\star} (i-1, j')$. Then, either α_{i-1} is non-adjacent and in this case $(i, j) \in I_2^{(1)}$ and we do not have to count this intersection, or α_{i-1} is adjacent but by Corollary 4.3.5 the segments α_{i-1} and α_{i+1} must lie in two different polygons. In particular, $\beta_{j'}$ and α_{i+1} also lie in different polygons and hence do not intersect.

(b) Similarly to the proof of (a), we distinguish two cases depending whether β_{j_1} has an endpoint on e' or not. Further, as in the proof of Lemma 4.4.8, we know that $j_1 \neq j_2'$ and $j_1' \neq j_2$ so that we only have to prove that $j_1 \neq j_2$. We will proceed by contradiction:

1&1. If β_{j_1} and β_{j_2} both have an endpoint on e', then by definition this endpoint must be shared respectively with $\beta_{j_1'}$ and $\beta_{j_2'}$, so that $j_1' = j_2'$ implies that $j_1 = j_2$.

1&2. If β_{j_1} has an endpoint on e' but not β_{j_2} (which is then in case (ii).2, that is it intersects α_i and has an endpoint on e, shared with $\beta_{j_2'}$), the condition $j_1' = j_2'$ implies that $\beta_{j_1'} = \beta_{j_2'}$ has one endpoint on e' and one endpoint on e, but does not belong to the polygon containing α_i since β_{j_2} already belongs to this polygon. In particular, both β_{j_1} and β_{j_2} belong to the polygon containing α_i while $\beta_{j_1'} = \beta_{j_2'}$ belongs to the polygon containing α_{i+1} (so that the side e is also identified to a side of the polygon containing α_{i+1}). Further, since $\beta_{j_1'}$ has its endpoints on e' and e, the direction of β is between the direction of e' and the direction of e, and hence the fact that β_{j_2} has an endpoint on e combined with the fact that it intersect α_i implies that it must have an endpoint on e', see Figure 4.15. This gives a contradiction.

By symmetry, this is the same if β_{j_2} has an endpoint on e'.

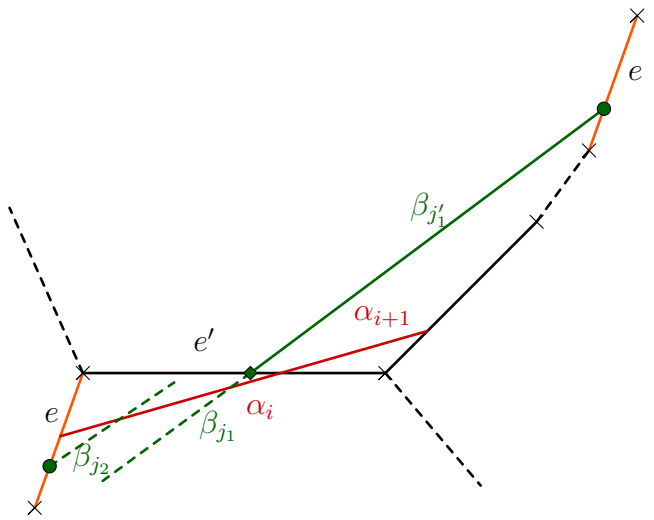

Figure 4.15: Illustration of the proof of Lemma 4.4.9 (b).2.

2&2. Else, β_{j_1} (resp. β_{j_2}) have no endpoint on e' but one endpoint on e. That means this endpoint must be shared with $\beta_{j'_1}$ (resp. $\beta_{j'_2}$), and hence $j'_1 = j'_2$ implies $j_1 = j_2$.

Hence, in both cases we have $\{j_1, j'_1\} \cap \{j_2, j'_2\} = \varnothing$.

□

Similarly to case (i), Lemma 4.4.9 together with the explanation in case (ii), part 3., imply that we can group segments of β by pairs (except β_1 and β_l which may remain alone) such that for each pair of β and each pair $\alpha_i \cup \alpha_{i+1}$, there is at most one intersection which does not belong to $I_2^{(1)}$. In total, this gives at most $\frac{q}{2}\left\lfloor \frac{l}{2} + 1 \right\rfloor$ intersections, as required.

Case (iii). Let us now deal with the case $q = 3$. As stated in Corollary 4.3.5, this means the sequence of adjacent segments is of the form $\alpha_i \cup \alpha_{i+1} \cup \alpha_{i+2}$ and the segments lie in three different polygons. Let e, e', e'' and e''' be respectively the sides of the polygons containing α_i^-, α_{i+1}^-, α_{i+2}^- and α_{i+2}^+. Since $q = 3$ is odd, the four sides are distinct by Lemma 4.3.4.

A segment β_j intersecting $\alpha_i \cup \alpha_{i+1} \cup \alpha_{i+2}$, must have at least one of its endpoints on e, e', e'' or e''', which is not a vertex if $j \neq 1, l$. Given $j \neq 1, l$, we then define an index j' which will be paired to j as follows:

1. If β_j has an endpoint on e', then we choose j' such that β_j and $\beta_{j'}$ share their common endpoint on e'.

2. If β_j has an endpoint on e'' (but no endpoint on e'), then we choose j' such that β_j and $\beta_{j'}$ share their common endpoint on e''.

3. Else, β_j has no endpoint on e' or e'' but an endpoint on e (resp. e'''). Since by assumption α_{i-1} (resp. α_{i+3}) is a non-adjacent segment, that means $(i,j) \in I_2^{(1)}$ (resp. $(i+2,j) \in I_2^{(1)}$) and we do not count the intersection.

With this construction, we have:

Lemma 4.4.10. *(a) If $j \in \{1, \cdots, l\}$ is such that β_j intersects $\alpha_i \cup \alpha_{i+1} \cup \alpha_{i+2}$ and such that the intersection belongs to $I_2^{(2)}$, then the segment $\beta_{j'}$ constructed as above does not intersect $\alpha_i \cup \alpha_{i+1} \cup \alpha_{i+2}$.*

(b) Given j_1 and j_2 two distinct indices such that β_{j_1} (resp. β_{j_2}) intersects $\alpha_i \cup \alpha_{i+1} \cup \alpha_{i+2}$ and such that the intersection belongs to $I_2^{(2)}$, the pairs $\{j_1, j_1'\}$ and $\{j_2, j_2'\}$ constructed as above satisfy:

$$\{j_1, j_1'\} \cap \{j_2, j_2'\} = \varnothing.$$

Proof. Since we assume that the intersections belong to $I_2^{(2)}$, we are either in the setting of case 1. or case 2.

(a) If β_j has an endpoint on the side e'. Then β_j intersects either α_i or α_{i+1}, so that we have either $(i,j) \xrightarrow{\bigstar} (i+1,j')$ or $(i+1,j) \xrightarrow{\bigstar} (i,j')$. In particular, $\beta_{j'}$ lies in the same polygon than α_{i+1} (resp. α_i) but these segments do not intersect. The other segments cannot intersect $\beta_{j'}$ since they do not lie in the same polygon.

By symmetry, the same argument holds if β_j has an endpoint on the side e''.

(b) We first deduce from (a) that $j_1 \neq j_2'$ and $j_1' \neq j_2$, hence we only have to show that $j_1' \neq j_2'$. Now, since $q = 3$ for every β_j intersecting $\alpha_i \cup \alpha_{i+1} \cup \alpha_{i+2}$ and such that the intersection belongs to $I_2^{(2)}$, the chosen index j' to be paired with j is such that either $(i,j) \xrightarrow{\bigstar} (i+1,j')$, $(i+1,j) \xrightarrow{\bigstar} (i,j')$, $(i+1,j) \xrightarrow{\bigstar} (i+2,j')$ or $(i+2,j) \xrightarrow{\bigstar} (i+1,j')$ and since α_i, α_{i+1} and α_{i+2} do not belong to the same polygon, the data of j' determines uniquely the corresponding index i' in the configuration $\bigstar$, and hence the configuration $\bigstar$ by 2. of Lemma 4.4.4. This exactly means that if $j_1' = j_2'$, then $j_1 = j_2$, and hence the pairs do not overlap.

□

As a conclusion, we get that among the intersections of β with $\alpha_i \cup \alpha_{i+1} \cup \alpha_{i+2}$, at most $\left\lfloor \frac{l}{2} + 1 \right\rfloor$ contribute to $I_2^{(2)} \cup I_2^{(0)}$, as required.

Case (iv). The remaining case is when q **is odd,** $q \geq 3$. In this case, we make one triple with the first three adjacent segment, and then we group the remaining adjacent segment by pairs. By the arguments of cases (ii) and (iii) and using to the deformation argument as in case (ii), we can directly conclude:

Lemma 4.4.11. *For each pair of adjacent segment, and any segment β_j intersecting this pair which is not as in configuration 3. of case (ii), we can choose $j' = j + 1$ such that:*

- *$\beta j'$ does not intersect the pair*
- *The pairs $\{j, j'\}$ constructed this way do not overlap.*

Proof. The construction of j' and the proof is exactly the same as in Lemma 4.4.9. □

Lemma 4.4.12. *For the triple $\alpha_{i_0+1} \cup \alpha_{i_0+2} \cup \alpha_{i_0+3}$, and for any segment β_j intersecting this triple which is not in the configuration 3. of case (iii), we can choose $j' = j + 1$ such that:*

- *$\beta j'$ does not intersect the pair*
- *The pairs $\{j, j'\}$ constructed this way do not overlap.*

The proof is exactly the same as the proof of Lemma 4.4.10. However, there is in fact a small difference for the reason why we do not have to consider intersections in case 3. With the notations of case (iii), we still have that if β_j intersects α_{i_0+1} and has not endpoint on e' but an endpoint of e, then the intersection belongs to $I_2^{(1)}$ so that we do not have to count this intersection. However, if β_j intersects the triple and has an endpoint on e''', the intersection is not in $I_2^{(1)}$ anymore if $q > 3$. In this case, we can again perform a small deformation of β in order to move the intersection on the next pair $\alpha_{i_0+3} \cup \alpha_{i_0+4}$.

As a conclusion, we get as required that among all intersections of β with the sequence of adjacent segment, at most $\left\lfloor \frac{q}{2} \right\rfloor \left\lfloor \frac{l}{2} + 1 \right\rfloor$ account for $I_2^{(2)} \cup I_2^{(0)}$. □

4.4.4 End of the proof of Proposition 4.4.1

The count of the intersections made in the last section allows us to conclude the proof of Proposition 4.4.1. We will start with the case where β is not an odd saddle connection, as when β is an odd saddle connection we need an additional argument.

Lemma 4.4.13. *Assume β is not an odd saddle connection. Then*

$$|\alpha \cap \beta| < (p_\alpha + q_\alpha)(p_\beta + q_\beta).$$

Proof. By Equation (4.4), we have

$$\begin{aligned}|\alpha \cap \beta| &\leq \#\tilde{I}_1 + \#I_2^{(0)} + \#I_2^{(2)} \\ &\leq \#\tilde{I}_1 + \#I_2^{(0,i)} + \#I_2^{(0,c)} + \#I_2^{(2)}\end{aligned}$$

Using Equation (4.5), Lemma 4.4.5 and Corollary 4.4.7, we have

$$\begin{aligned}|\alpha \cap \beta| &\leq p_\alpha \left\lceil \frac{l}{2} \right\rceil + \#\{i, \alpha_i \text{ is an isolated adjacent segment}\} + q_\alpha \left\lfloor \frac{l}{2} + 1 \right\rfloor \\ &\leq p_\alpha \left\lceil \frac{l}{2} \right\rceil + p_\alpha - 1 + q_\alpha \left\lfloor \frac{l}{2} + 1 \right\rfloor\end{aligned}$$

where we used that $\#\{i, \alpha_i \text{ is an isolated adjacent segment}\} \leq p_\alpha - 1$, which holds because the isolated adjacent segments are separated by the p_α non-adjacent ones. Using Lemma 4.2.9, we deduce that if β is not an odd saddle connection, then $\left\lceil \frac{l}{2} \right\rceil \leq p_\beta + q_\beta - 1$ and $\left\lfloor \frac{l}{2} + 1 \right\rfloor \leq p_\beta + q_\beta$ and hence

$$\begin{aligned}|\alpha \cap \beta| &\leq p_\alpha(p_\beta + q_\beta - 1) + p_\alpha - 1 + q_\alpha(p_\beta + q_\beta) \\ &\leq (p_\alpha + q_\alpha)(p_\beta + q_\beta) - 1 \\ &< (p_\alpha + q_\alpha)(p_\beta + q_\beta)\end{aligned}$$

as required. □

By symmetry, the same result holds if α is not an odd saddle connection. Thus, we are left to prove:

Lemma 4.4.14. *Assume that both α and β are odd saddle connections, then:*

$$|\alpha \cap \beta| \leq (p_\alpha + q_\alpha)(p_\beta + q_\beta).$$

Proof. In this case, we need to make an additional remark in order to show the required result:

> Assume the (isolated adjacent) segment α_i intersects β_1 (resp. β_l), then the (non-adjacent) segments α_{i-1} and α_{i+1} do not lie in the same polygon as β_1 (resp. β_l). In particular, there are at most $\left\lceil \frac{l-1}{2} \right\rceil$ segments of β in the same polygon as α_{i-1}, because α_{i-1} can intersect at most half of the $l-1$ segments $\beta_2 \cdots \beta_l$. Similarly, there are at most $\left\lceil \frac{l-1}{2} \right\rceil$ segments of β in the same polygon as α_{i+1}.

If β is an odd saddle connection, then l is an odd integer and $\left\lceil \frac{l-1}{2} \right\rceil = \left\lceil \frac{l}{2} \right\rceil - 1$. In particular, for each intersection in $I_2^{(0,i)}$ (corresponding to the intersection of an isolated adjacent segment α_i with either β_1 or β_l) we can remove one in the count of $\#\tilde{I}_1$ (and more precisely in the count of intersections of α_{i-1} with β). Further, for the index $i_{max} = \max\{i, \alpha_i \text{ is an isolated adjacent segment intersecting either } \beta_1 \text{ or } \beta_l\}$, we can remove one more intersection in the count of $\#\tilde{I}_1$ (and more precisely in the count of intersections of $\alpha_{i_{max}+1}$ with β). Hence, we have shown:

Lemma 4.4.15. *Assume β is odd and $\#I_2^{(0,i)} \neq 0$, then:*

$$\#\tilde{I}_1 \leq p_\alpha \left\lceil \frac{l}{2} \right\rceil - \#I_2^{(0,i)} - 1$$

As a corollary, we get that:

$$\begin{aligned} |\alpha \cap \beta| &\leq \#\tilde{I}_1 + \#I_2^{(0,i)} + \#I_2^{(0,c)} + \#I_2^{(2)} \\ &\leq p_\alpha \left\lceil \frac{l}{2} \right\rceil + q_\alpha \left\lceil \frac{l}{2} \right\rceil \\ &\leq (p_\alpha + q_\alpha)(p_\beta + q_\beta) \end{aligned}$$

with equality only if $\#I_2^{(0,i)} = 0$. □

Remark 4.4.16. Notice that having an equality above thus requires that $\#\tilde{I}_1 = p_\alpha \left\lceil \frac{l}{2} \right\rceil$, and that any element of $\tilde{I}_1$ appears either as an intersection or as pair (i', j') of a configuration ★.

This concludes the proof of Proposition 4.4.1.

4.5 Proof of Theorem 4.1.5

Having studied both the length of the segments and the intersections of saddle connections according to their polygonal decomposition, we can now prove Theorem 4.1.5, which will follow from Equation (4.3), Lemma 4.2.8 and Proposition 4.4.1. We will deal with the cases where one of the saddle connections is either a side or a diagonal separately. In fact, an additional argument is required in the case where one of the saddle connections is a diagonal.

4.5.1 Non diagonals

Proposition 4.5.1. *Assume that neither α nor β is a side or a diagonal of the polygons. Then:*

$$\frac{|\alpha \cap \beta| + 1}{l(\alpha) l(\beta)} < \frac{1}{l_0^2}.$$

Proof. 1. If either α or β is not an odd saddle connection, we have by Proposition 4.4.1,

$$|\alpha \cap \beta| < (p_\alpha + q_\alpha)(p_\beta + q_\beta)$$

and by Equation (4.3),

$$l(\alpha) l(\beta) \geq (p_\alpha + q_\alpha)(p_\beta + q_\beta) l_0^2 \tag{4.6}$$

Hence we have:

$$\frac{|\alpha \cap \beta| + 1}{l(\alpha) l(\beta)} \leq \frac{1}{l_0^2}. \tag{4.7}$$

Let us show that the above inequality is strict. This is because:

- If there is at least one adjacent segment, then the inequality of Equation (4.6) is strict, and hence it is also the case for Equation (4.7)
- Else, there are no adjacent segments, and $k = p_\alpha$ and $l = p_\beta$. We easily deduce from hypothesis (H2) that as soon as $k, l \geq 2$, we have

$$|\alpha \cap \beta| \leq \left\lceil \frac{kl}{2} \right\rceil \leq kl - 2 \leq p_\alpha p_\beta - 2,$$

and this allows to conclude that the inequality of equation (4.7) is strict.

2. Else, both α and β are odd, but neither sides or diagonals of the polygons. From Lemma 4.2.8, we know that:

$$l(\alpha) \geq (p_\alpha + q_\alpha + \sqrt{2} - 1)l_0$$

and similarly

$$l(\beta) \geq (p_\beta + q_\beta + \sqrt{2} - 1)l_0$$

Thus

$$l(\alpha)l(\beta) \geq [(p_\alpha + q_\alpha)(p_\beta + q_\beta) + (\sqrt{2} - 1)(p_\alpha + q_\alpha + p_\beta + q_\beta) + (\sqrt{2} - 1)^2]l_0^2$$

But $p_\alpha \geq 2$ as well as p_β, so that

$$\begin{aligned} l(\alpha)l(\beta) &\geq [(p_\alpha + q_\alpha)(p_\beta + q_\beta) + 4(\sqrt{2} - 1) + (\sqrt{2} - 1)^2]l_0^2 \\ &> [(p_\alpha + q_\alpha)(p_\beta + q_\beta) + 1]l_0^2 \end{aligned}$$

This gives the required inequality.

□

4.5.2 The case of sides

We now turn to the case where one of the saddle connections is a side of a polygon. We can assume up to permutation that it is α. We show:

Lemma 4.5.2. *Assume α is a side of a polygon. Then*

$$\frac{|\alpha \cap \beta| + 1}{l(\alpha)l(\beta)} \leq \frac{1}{l_0^2}.$$

Further, equality holds if and only if $l(\alpha) = l_0$ and:

1. *either $|\alpha \cap \beta| = 0$ and β has length l_0. In particular it is either is a side or a diagonal.*

2. *or* $|\alpha \cap \beta| = 1$ *and* β *is the union of two non adjacent segments, of total length* $2l_0$*, and intersecting* α *once on its interior.*

Proof. Each non-singular intersection between α and β corresponds to the union of two consecutive segments $\beta_j \cup \beta_{j+1}$ which share their common endpoint on the side α, and since by (H2) pairs of segments cannot overlap, we directly obtain:

$$|\alpha \cap \beta| \leq \left\lfloor \frac{l}{2} \right\rfloor \leq (p_\beta + q_\beta) - 1, \tag{4.8}$$

Further, $l(\beta) \geq (p_\beta + q_\beta) l_0$ by Lemma 4.2.1. Hence, we conclude that

$$\frac{|\alpha \cap \beta| + 1}{l(\alpha) l(\beta)} \leq \frac{1}{l_0^2}. \tag{4.9}$$

Notice that a necessary condition to have an equality above is that $l(\alpha) = l_0$. Further,

1. If β is either a side or a diagonal, then $|\alpha \cap \beta| = 0$ and we have equality in (4.9) if and only if $l(\beta) = l_0$.

2. Else, β is neither a side nor a diagonal and:

   - either there is an adjacent segment in the polygonal decomposition of β and, since the length of two consecutive adjacent segments is greater than l_0 by Lemma 4.2.1, and since we do not take into account the presence of isolated adjacent segments in the estimation of Equation (4.3), we obtain $l(\beta) > (p_\beta + q_\beta) l_0$ and hence we cannot have equality in (4.9)
   - or there are no adjacent segments in the polygonal decomposition of β and $l = p_\beta$. In particular, as soon as $l \geq 3$, we have $\left\lfloor \frac{l}{2} \right\rfloor \leq p_\beta - 2$ and hence
   $$l(\beta) \geq p_\beta l_0 > \left(\left\lfloor \frac{l}{2} \right\rfloor + 1 \right) l_0$$
   so that by Equation (4.8) we conclude that we cannot have equality in (4.9).

   In particular, we cannot have equality in (4.9) unless β is the union of two non-adjacent segments and $|\alpha \cap \beta| = 1$. In that case the length of β must be $2l_0$.

□

4.5.3 The case of diagonals

It remains to deal with the case where either α or β is the diagonal of a polygon. Up to permutation we will assume it is α. Namely, we show

Lemma 4.5.3. . *Assume α is a diagonal of a polygon (and β is not a side of a polygon). Then*

$$\frac{|\alpha \cap \beta| + 1}{l(\alpha)l(\beta)} \leq \frac{1}{l_0^2}.$$

Further, equality holds if and only if:

1. *either $l(\alpha) = l_0$, $|\alpha \cap \beta| = 1$ and β is the union of two non adjacent segments, of total length $2l_0$, and intersecting α once on its interior.*

2. *or α and β are two diagonals, of length $\sqrt{2}l_0$, and intersecting once on their interior.*

We will proceed to the proof as follows. First, we investigate the case where β is not an odd saddle connection. Then we continue with the case where β is also a diagonal, and finally we deal with the case where β is an odd saddle connection.

A diagonal and a non-odd saddle connection. Given a saddle connection β, it is easily shown that

$$|\alpha \cap \beta| \leq \lfloor \frac{l}{2} \rfloor$$

with equality only if β is either a diagonal or an odd saddle connection. In particular, if β is neither a diagonal nor an odd saddle connection, we directly deduce from Equation (4.3) that:

$$\frac{|\alpha \cap \beta| + 1}{l(\alpha)l(\beta)} \leq \frac{1}{l_0^2},$$

and, as before, the inequality is strict unless $l(\alpha) = l_0$ and β is the union of two non-adjacent segments such that $|\alpha \cap \beta| = 1$ and $l(\beta) = 2l_0$ (recall that we assumed β not to be a side or a diagonal).

Intersections of diagonals. We now investigate the case where both α and β are diagonals. Namely, we show:

Lemma 4.5.4. *Let α and β be two distinct diagonals of a convex polygon P with obtuse or right angles. Let l_0 be the length of the shortest side of the polygon. Then, if α and β intersect on their interior, we have $l(\alpha)l(\beta) \geq 2l_0^2$. Further, equality holds if and only if both diagonals have length $\sqrt{2}l_0$.*

Proof. First, if $\min(l(\alpha), l(\beta)) \geq \sqrt{2}l_0$, then we obviously have $l(\alpha)l(\beta) \geq 2l_0^2$. In the rest of the proof, we will assume, up to permuting α and β, that $l(\alpha) \leq \sqrt{2}l_0$. Let P be the polygon containing α and θ_{min} be the minimal angle between α and the sides of P having a common endpoint with α. Since the polygon has obtuse or right angles, we know from Lemma 4.2.2 that the distance from any vertex of P to a point in a side which does not have this vertex as an endpoint is at least l_0. In particular, we must have $\sin\theta_{min} \geq \frac{l_0}{l(\alpha)}$, otherwise by convexity there would be an endpoint of α and a point of P in a segment which does not contain this endpoint at a distance less than l_0, as in Figure 4.16.

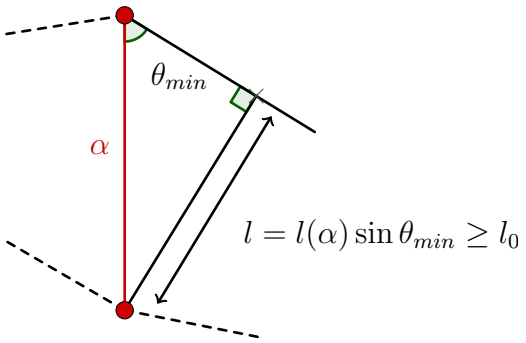

Figure 4.16: The distance from the bottom vertex of α to a non-adjacent side of the polygon is at least l_0.

In particular, no vertex of P lie inside the hexagon having as sides the four segments making an angle θ_{min} with α at one of its vertex and having length l_0 (this hexagon degenerates to a square when $l(\alpha) = \sqrt{2}l_0$). Adding this to the fact that no side of P lies at a distance less than l_0 from the two endpoints of α (except the sides adjacent to the endpoints of α), we get that no vertex of P which is not a vertex of α lies inside the gray zone of Figure 4.17. In particular, the length of β has to be at least $2l_0\sin\theta_{min}$, and we get

$$l(\alpha)l(\beta) \geq l(\alpha) \times 2l_0\sin\theta_{min} \geq 2l_0^2.$$

In fact, one can easily show that $l(\beta) > 2\sin\theta_{min}l_0$ unless $l(\alpha) = l(\beta) = \sqrt{2}l_0$.

- If $\min(l(\alpha), l(\beta)) > \sqrt{2}l_0$, then we directly have that $l(\alpha)l(\beta) > 2l_0^2$.
- Else, we can assume that $l(\alpha) \leq \sqrt{2}l_0$. Of course, if $\sin\theta_{min} > \frac{l_0}{l(\alpha)}$ then we have $l(\alpha)l(\beta) > 2l_0^2$. Otherwise, $\sin\theta_{min} = \frac{l_0}{l(\alpha)}$, and one can check that the two angles between α and the sides of P at a vertex of α cannot be simultaneously equal to θ_{min} (unless $l(\alpha) = \sqrt{2}$), and hence we have $l(\beta) > 2\frac{l_0}{l(\alpha)}$.

□

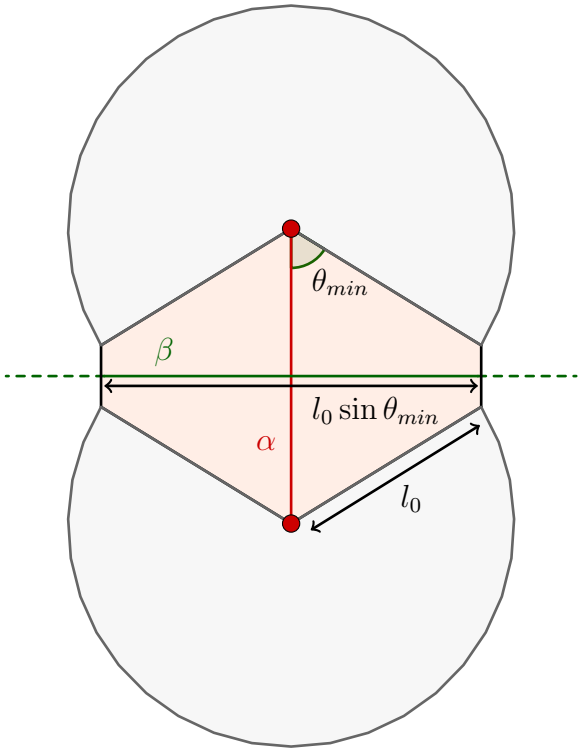

Figure 4.17: No point on a side of the polygon which is not adjacent to one of the two endpoints of α lies inside the hexagon or inside the disks of radius l_0 centered at the endpoints of α. In particular, the length of β is at least $2 \sin \theta_{min} l_0$.

As a direct corollary of Lemma 4.5.4, we get:

Corollary 4.5.5. *If α and β are both diagonals, then:*

$$\frac{|\alpha \cap \beta| + 1}{l(\alpha)l(\beta)} \leq \frac{1}{l_0^2}.$$

Further, the inequality is strict unless $l(\alpha) = l(\beta) = \sqrt{2}l_0$ and $|\alpha \cap \beta| = 1$.

Proof. Either α and β do not intersect on their interior and the result comes from the fact that $l(\alpha)l(\beta) \geq l_0^2$, or they do intersect once in their interior and the result comes from Lemma 4.5.4. □

A diagonal and an odd saddle connection. In fact, the above argument can be easily generalised to the case where, α is a diagonal but β is an odd saddle connection which is not a diagonal. In this case, recall that:

$$|\alpha \cap \beta| \leq \left\lfloor \frac{l}{2} \right\rfloor \leq (p_\beta + q_\beta),$$

and

$$l(\beta) > (p_\alpha + q_\alpha).$$

(Notice that from Lemma 4.2.8 the inequality is strict.). Hence:

1. if $|\alpha \cap \beta| < p_\beta + q_\beta$, we directly deduce that

$$\frac{|\alpha \cap \beta| + 1}{l(\alpha)l(\beta)} < \frac{1}{l_0^2}.$$

2. Else, $|\alpha \cap \beta| = p_\beta + q_\beta$ and in particular β_1 must intersect α. Then similarly to the proof of Lemma 4.5.4, we construct the region of Figure 4.17, and the endpoints β_1^- and β_2^+ cannot lie inside this region, giving:

$$l(\beta_1 \cup \beta_2)l(\alpha) > 2l_0^2.$$

Since β is odd, we can group the other adjacent segments after β_2 by pairs to obtain

$$l(\alpha)l(\beta) > (p_\beta + q_\beta + 1)l_0^2.$$

Using Proposition 4.4.1, we conclude that

$$\frac{|\alpha \cap \beta| + 1}{l(\alpha)l(\beta)} < \frac{1}{l_0^2},$$

as required.

In fact, it is also possible to make this argument if both α and β are odd saddle connections (this means we do not need to use Lemma 4.2.8 and Lemma 4.2.4), but this argument does not seem to generalize to the case where the angles are no longer assumed to be obtuse.

This completes the proof of Lemma 4.5.3.

Conclusion. Combining Proposition 4.5.1, Lemma 4.5.2 and Lemma 4.5.3, we finally obtain Theorem 4.1.5, and thus Theorem 4.1.1.

4.5.4 Additional remarks

Before moving to the specific case of Bouw-Möller surfaces, let us make a few remarks on the proof of Theorem 4.1.1, and in particular discuss the hypotheses of this result.

General flat surfaces. The first thing that has to be noted is that although we deal here with translation surfaces, we specifically use properties of polygons (namely the fact that they are convex with obtuse angles) and gluings (which is only combinatorial). In particular, Theorem 4.1.1 should still hold is the surface is no longer assumed to be a translation surface, namely it should generalize to any flat surface constructed from a collection of polygons by gluing pairs of sides (without assuming that the sides which are paired are parallel and of the same length).

Notice that in this general setting there are two main issues:

- Since the resulting flat surface does not necessarily have trivial holonomy, closed geodesics do not have a well defined direction. However, the polygonal decomposition still makes sense and Equation (4.3) is still valid as well as Lemma 4.2.8 and Lemma 4.2.9. Further, we can still define the positive and negative endpoints of a segment as well as the sign of an adjacent segment. In particular, Lemma 4.3.4 still holds.

  The main issue is that Lemma 4.3.2 is not true anymore as well as Corollary 4.3.5. In fact, it is believed that one can modify the proof of Lemma 4.4.6 using deformation processes as we did in the proof of case (ii) (Lemma 4.4.9) as well as a case by case analysis (in the bad cases) to take into account these changes.

  Notice that Lemma Lemma 4.4.6 is the key lemma here and the rest of section 3. does not change (as well as section 4).

- Further, in this general setting it may not be true that closed geodesics are always homologous to union of vertex-to-vertex trajectories having the same length, and as such we also have to show that if either α or β is a closed geodesic which does not go through a singularity, we still have

$$\frac{|\alpha \cap \beta|}{l(\alpha)l(\beta)} \leq \frac{1}{l_0^2}.$$

  This case is in fact simpler as then we do not have to count additional intersections at the singularities. The only change is that for saddle connections, the first and the last segments in the polygonal decomposition

were both non-adjacent segments, whereas in general this may not be true (for example, there may be no non-adjacent segments at all). Nevertheless, one can check that only small changes are required to deal with these cases. Namely:

- The inequality of Lemma 4.2.9 still holds, but the equality case also includes closed geodesics having either no non-adjacent segments in their polygonal decomposition [1], or closed geodesics for which, cyclically speaking, between two non-adjacent segment there is an odd number of adjacent segments.
- Now the inequality of Proposition 4.4.1 is still valid, but as before the equality cases must include closed geodesics having either no non-adjacent segments in their polygonal decomposition or closed geodesics for which, cyclically speaking, between two non-adjacent segment there is an odd number of adjacent segments. The modifications in the proof are that:
  * $I_2^{(0)} = \varnothing$ if β is not a vertex-to-vertex trajectory.
  * In Equation (4.5), we should replace $\lceil \frac{l}{2} \rceil$ by $\lfloor \frac{l}{2} \rfloor$ if β is not a vertex-to-vertex trajectory.
  * In Lemma 4.4.6, we should replace $\lfloor \frac{l}{2} + 1 \rfloor$ by $\lfloor \frac{l}{2} \rfloor$ if β is not a vertex-to-vertex trajectory.

  In particular, if β is not a vertex-to-vertex trajectory, we have:

$$\begin{aligned} |\alpha \cap \beta| &\leq \#\tilde{I}_1 + \#I_2^{(2)} \\ &\leq p_\alpha \lfloor \frac{l}{2} \rfloor + q_\alpha \lfloor \frac{l}{2} \rfloor \\ &\leq (p_\alpha + q_\alpha)(p_\beta + q_\beta) \end{aligned}$$

  Since the estimates on the length of the segments given in Equation (4.3) is left unchanged, this implies that if β is not a vertex-to-vertex trajectory, we have:

$$\frac{|\alpha \cap \beta|}{l(\alpha) l(\beta)} \leq \frac{1}{l_0^2}.$$

  This argument is still valid if α is a diagonal of a polygon. If α is a side of a polygon, we have $|\alpha \cap \beta| \leq \lfloor \frac{l}{2} \rfloor \leq (p_\beta + q_\beta)$ and hence

$$\frac{|\alpha \cap \beta|}{l(\alpha) l(\beta)} \leq \frac{1}{l_0^2},$$

  and in fact, the inequality is strict.

[1] Recall from Lemma 4.3.4 that in this case there would be an even number of adjacent segments

Surfaces made of polygons with acute angles. In light of Theorem 4.1.1, one may wonder what happens if the angles are no longer assumed to be obtuse or right (that is we remove hypothesis (H1)). The main issue in this case is that two consecutive adjacent segment may have very small length, as in the example of Figure 4.18. However, it is possible to avoid this issue by making the following assumption:

(H1') The sum of two consecutive angles is at least π.

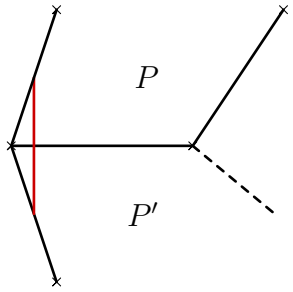

Figure 4.18: If we do not assume the angles of the polygons to be obtuse or right, pairs of adjacent segments can have arbitrarily small length.

Now, given a translation surface X constructed from a collection of convex polygons and satisfying hypothesis (H1') and (H2), we can denote by θ_0 the smallest internal angle of the polygons defining X [2]. Although Theorem 4.1.1 deals with the case $\theta_0 \geq \frac{\pi}{2}$, we can make similar estimates on the lengths of saddle connections in this more general setting if we replace l_0 by $l_0 \sin\theta_0$, namely:

- The length of a saddle connection α is at least $(p_\alpha + q_\alpha) l_0 \sin\theta_0$.
- The length of an odd saddle connection α which is neither a side or a diagonal of a polygon is at least $\left(p_\alpha + q_\alpha + 2\dfrac{\sin(\frac{\theta_0}{2})}{\sin\theta_0} - 1 \right) l_0 \sin\theta_0$.
- The product of the length of two intersecting diagonals is at least $2l_0^2(\sin\theta_0)^2$.
- If α is a diagonal and β is an odd saddle connection such that β_1 intersects α, we have $l(\alpha)l(\beta_1 \cup \beta_2) \geq 2l_0^2(\sin\theta_0)^2$ and in particular $l(\alpha)l(\beta) \geq (p_\alpha + q_\alpha + 1)l_0^2(\sin\theta_0)^2$.

We do not prove these properties as the proof is exactly the same as in Lemmas 4.2.1, 4.2.2, 4.2.4 and 4.5.4. Further, the count of the intersections is only combinatorial and does not depend on the angles of the sides of the polygons.

[2] This kind of hypothesis is for example satisfied for some twisted origamis.

In particular, assuming $4\left(\frac{2\cos\frac{\theta_0}{2}}{\sin\theta_0}-1\right)\geq 1$ (which is needed in our proof, see the second bullet of the proof of Proposition 4.5.1), we conclude that for any two closed curves α and β on X, we have:

$$\frac{\mathrm{Int}(\alpha,\beta)}{l(\alpha)l(\beta)}\leq\frac{1}{(\sin(\theta_0)l_0)^2}.$$

Notice that the inequality $4\left(\frac{2\sin\frac{\theta_0}{2}}{\sin\theta_0}-1\right)\geq 1$ is true for $\theta_0\geq 2\arccos(\frac{4}{5})\simeq 0.409\pi$. We believe that this inequality is in fact not needed an that the same result holds for any $\theta_0>0$.

Chapitre 5

The case of Bouw-Möller surfaces

Résumé en Français. Dans ce chapitre, on s'intéresse aux surfaces de Bouw-Möller, qui sont des surfaces construites à partir de polygones semi-réguliers. I. Bouw et M. Möller [BM10] ont démontré que ce sont exactement les surfaces de translation dont le groupe de Veech est un groupe triangulaire, et P. Hooper [Hoo12] a donné un modèle polygonal de ces surfaces. Après avoir introduit les surfaces de Bouw-Möller ainsi que quelques unes de leurs propriétés, on démontre le Théorème B qui donne une borne pour KVol sur chacune des surfaces de Bouw-Möller, et une égalité spécifiquement dans le cas où la surface possède une unique singularité.

Nous généralisons ensuite la méthode d'extension au disque de Teichmüller présentée aux chapitres 2 et 3 en démontrant le Théorème 1.3.10. Pour pouvoir appliquer la méthode, il faut savoir démontrer que les connexions de selles horizontales des surfaces de Bouw-Möller ne s'intersectent pas : dans ce cadre nous utilisons la notion de diagramme de séparatrices introduite par M. Kontsevich et A. Zorich [KZ03] et démontrons le Théorème 1.3.12. Cela nous permettra d'utiliser le critère sur le caractère borné ou non sur les disques de Teichmüller de surfaces de Veech obtenu au Chapitre 3 (voir Théorème D) et ainsi démontrer le Théorème E. Enfin, nous démontrerons le Théorème C qui donne une formule close pour KVol sur chaque disque de Teichmüller associé à une surface de Bouw-Möller ayant une seule singularité. Comme le chapitre précédent, il s'agit d'un travail réalisé en commun avec I. Pasquinelli.

In this chapter, we are interested in Bouw-Möller surfaces, which are surfaces built from semi-regular polygons. I. Bouw and M. Möller [BM10] proved that these are exactly the translation surfaces whose Veech group is a triangular group, and P. Hooper [Hoo13] gave a polygonal model of these surfaces. After introducing the Bouw-Möller surfaces as well as some of their properties, we prove Theorem B which gives an upper bound for KVol on each Bouw-Möller surface, and equality specifically in the case where the surface has a unique singularity.

We then generalize the method used in Chapters 2 and 3 to extend the computation of KVol on Teichmüller disks of Veech surfaces by proving Theorem 1.3.10. In order to apply the method, it must be shown that closed curves made of horizontal saddle connections do not intersect: for this purpose we rely on the notion of separatrix diagram introducted by M. Kontsevich and A. Zorich [KZ02], and we show Theorem 1.3.12. This will allow to use the boundedness criterion given in Theorem D and obtained in Chapter 3, from which we will deduce Theorem E. We end this chapter by proving Theorem C, which gives a close formula for KVol on the Teichmüller disks associated with Bouw-Möller surfaces having a single singularity. As in the preceding chapter, the work presented here is joint with I. Pasquinelli.

5.1 Introduction

The first goal of this chapter is to calculate the value of KVol for Bouw-Möller surfaces. More precisely, we show:

Theorem 5.1.1. *Let $m, n \geq 2$ with $nm \geq 6$ and let $S_{m,n}$ be the corresponding Bouw-Möller surface. Then, for any pair (α, β) of closed curves on $S_{m,n}$, we have*

$$\frac{\mathrm{Int}(\alpha, \beta)}{l(\alpha)l(\beta)} \leq \frac{1}{l_0^2}$$

where $l_0 = \sin(\pi/m)$ is the length of the smallest side of the polygons forming $S_{m,n}$. Moreover, equality holds if and only if

- *m and n are coprime and α and β are intersecting systoles (of length l_0),*
- *or $n = 4$ and $m \equiv 3 \mod 4$ and α and β are diagonals of $P(0)$ (resp. $P(m-1)$), intersecting twice and having length $\sqrt{2}l_0$.*

From this result we deduce:

Corollary 5.1.2. *Let $m, n \geq 2$, $mn \geq 6$. Then :*

$$KVol(S_{m,n}) \leq \frac{Vol(S_{m,n})}{\sin(\pi/m)^2}$$

with equality if and only if m and n are coprime.

In fact, Theorem 5.1.1 is a direct consequence of Theorem 4.1.1 (obtained in the preceding chapter) for Bouw-Möller surfaces $S_{m,n}$ with $n \geq 4$. In this paper we will deal specifically with the case $n = 3$ and extend the proof of Theorem 4.1.1 to this case. Namely, we assume both closed curves are geodesics and subdivide them into smaller segments whose length, as well as the intersection of two pairs of segments, can be controlled. In the case where the resulting Bouw-Möller has a single singularity (i.e. for $S_{m,n}$ with m and n coprime), we show that the obtained inequality is in fact an equality by showing that there are intersecting systoles, thus obtaining Corollary 5.1.2. On the contrary, if the surface has several singularities, the inequality of Theorem 5.1.1 is in fact strict.

In light of the above result, it is interesting to wonder how KVol varies in the Teichmüller disk $\mathcal{T}_{m,n}$ of $S_{m,n}$. This question has been investigated in the case of the double regular n-gon for odd n in [BLM22] (Chapter 2) and in the case of the regular n-gon for even n in [Bou23] (Chapter 3), and the second goal of this paper is to calculate how KVol varies in the Teichmüller disc of Bouw-Möller surfaces. More precisely, we give an explicit expression for KVol on $\mathcal{T}_{m,n}$ in the case where $S_{m,n}$ has a unique singularity:

Theorem 5.1.3. *Let $m, n \geq 2$ coprime. Then for any $X \in \mathcal{T}_{m,n}$, we have:*

$$KVol(X) = K_0 \cdot \frac{1}{\cosh d_{\mathbb{H}^2}(X, \gamma_{\infty,\pm\cot(\pi/n)})}$$

where $d_{\mathbb{H}^2}$ denotes the hyperbolic distance and $\gamma_{\infty,\pm\cot(\pi/n)}$ is the union of the two hyperbolic geodesics of respective endpoints $(\infty, \cot(\pi/n))$, and $(\infty, -\cot(\pi/n))$ [1], and $K_0 > 0$ is an explicit constant.

The case where m and n are not coprime is much more complicated, as there are several distinct singularities. In this case we do not obtain an explicit formula for KVol on the Teichmüller disk of $S_{m,n}$, but we can still show that KVol is bounded on the Teichmüller disk. This is done using Theorem 1.5 of [Bou23]. The following result is also stated as Corollary 5.4.4:

Theorem 5.1.4. *KVol is bounded on the Teichmüller disk of $S_{m,n}$.*

Further, we describe a general approach for showing boundedness on Teichmüller disk of Veech surfaces by investigating horizontal separatrix diagrams in every periodic direction. Namely, we show in Section 5.4 that;

Theorem 5.1.5. *Closed curves made with horizontal saddle connections are pairwise non-intersecting if and only if the associated horizontal separatrix diagram is planar.*

[1] The geodesics of endpoints $(\infty, \cot(\pi/n))$ and $(\infty, -\cot(\pi/n))$ are the same if $n = 2$.

The notion of separatrix diagram has been introduced by M. Kontsevich and A. Zorich in [KZ02]. It is a ribbon graph which represents the cyclic ordering of the horizontal saddle connections while turning around the singularities. As explained in [EMM13], a ribbon graph is planar if and only if it can be embedded into a sphere.

Organisation of the chapter. We first define Bouw-Möller surfaces in Section 5.2 and give some properties which will be used in the next sections. Then, we show Theorem 5.1.1 and Corollary 5.1.2 in Section 5.3. In Section 5.4, we introduce horizontal separatrix diagrams and show Theorem 5.1.5 as well as boundedness of KVol on Teichmüller disks (Theorem 5.1.4). Then, in sections 5.5.1 and 5.2.2 we show Theorem 5.1.3. The proof uses Theorem 5.5.8 (see Theorem I in the first chapter), which will be proven in Section 5.7.

5.2 Bouw-Möller surfaces

In this section we will define Bouw-Möller surfaces, which are examples of translation surfaces and the main setting of our discussion. For more details on translation surfaces, see [Mas06] and for more details on Bouw-Möller surfaces see [?].

5.2.1 Generalities on Bouw-Möller surfaces

Given $m, n \geq 2$ with $mn \geq 6$, the Bouw-Möller surface $S_{m,n}$ is a translation surface made with m semi-regular polygons, each having a symmetry of order n. In this section we will explain how to describe the surface $S_{m,n}$ using polygons, following [Hoo13], and we will mention some useful facts that will be needed later on.

Definition of Bouw-Möller surfaces. Given $m, n \geq 2$ with $mn \geq 6$, the Bouw-Möller surface $S_{m,n}$ is a translation surface obtained by identifying the sides of a collection of m semi-regular polygons $P(0), \dots, P(m-1)$. More precisely, for $n \geq 2$ and $a, b \in \mathbb{R}^+$, let $P_n(a, b)$ be the semi regular polygon having all angles equal to $\frac{(n-1)\pi}{n}$ and sides of length alternating between a and b, as in Figure 5.1. The edges $(v_j)_{j=0,\dots,2n-1}$ of $P_n(a, b)$ are given by the vectors:

$$v_j = \begin{cases} a(\cos(\frac{j\pi}{n}), \sin(\frac{j\pi}{n})) \text{ if } j \text{ is even} \\ b(\cos(\frac{j\pi}{n}), \sin(\frac{j\pi}{n})) \text{ if } j \text{ is odd} \end{cases}$$

In the case where $a = 0$ (resp. $b = 0$), $P_n(a, b)$ is a regular n-gon of side length b (resp. a).

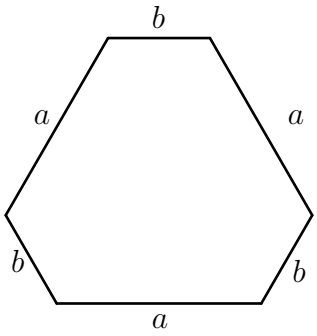

Figure 5.1: The polygon $P_6(a, b)$

Now, if n is odd, then define

$$P(i) = P_n(\sin(\frac{(i+1)\pi}{m}), \sin(\frac{i\pi}{m})).$$

If n is even, define

$$P(i) = \begin{cases} P_n(\sin(\frac{(i+1)\pi}{m}), \sin(\frac{i\pi}{m})) & \text{if } i \text{ is even,} \\ P_n(\sin(\frac{i\pi}{m}), \sin(\frac{(i+1)\pi}{m})) & \text{if } i \text{ is odd,} \end{cases}$$

Finally, the Bouw-Möller surface $S_{m,n}$ is obtained by identifying the even sides of $P(i)$, $i = 1, \dots m-2$, with the parallel (odd) sides of $P(i-1)$ while odd sides of $P(i)$ are identified with parallel (even) sides of $P(i+1)$. Note that $P(0)$ and $P(m-1)$ are regular n-gons and hence for them, this means that the sides are glued to the parallel sides of $P(1)$ and $P(m-2)$ respectively. The examples of $S_{3,4}$ and $S_{4,3}$ are represented in Figure 5.2.

Remark 5.2.1. Note that given two adjacent sides of the polygon $P(i)$, $0 < i < m-1$, one is paired to a side in $P(i-1)$ while the other is paired to a side in $P(i+1)$.

Remark 5.2.2. With this construction, the side v_0 of $P(0)$ is always horizontal. This convention will be used later.

Properties of Bouw-Möller surfaces. Given $m, n \geq 2$, with $mn \geq 6$, the surface $S_{m,n}$ is a translation surface of genus $(mn - m - n - \gamma)/2 + 1$ and $\gamma = \gcd(m, n)$ singularities. More precisely, one has

Proposition 5.2.3 (Proposition 24 of [Hoo13])**.** *Let $\gamma = \gcd(m, n)$. There are γ equivalence classes of vertices in the decomposition into polygons. In particular, $S_{m,n}$ will have γ cone singularities. Each of these singularities has cone angle $2\pi(mn - m - n)/\gamma$.*

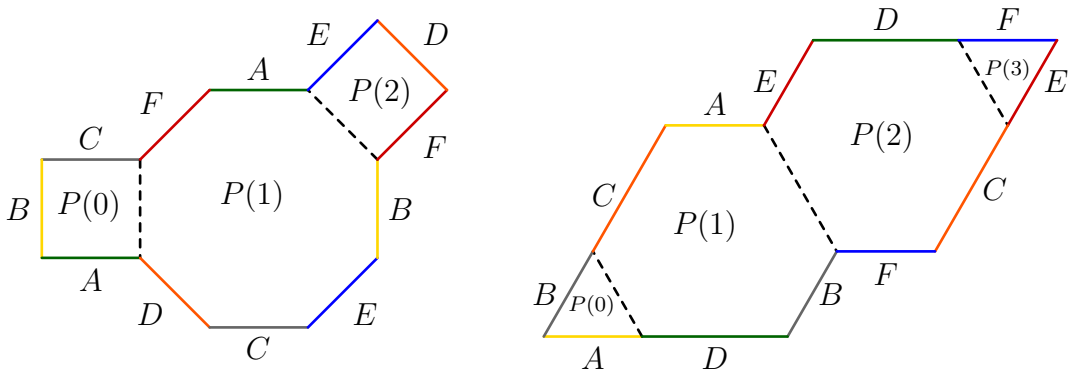

Figure 5.2: The surfaces $S_{3,4}$ and $S_{4,3}$.

In particular $S_{m,n}$ has only one singularity if and only if m and n are coprime. Notice that in this case saddle connections are closed curves, and hence we have

Proposition 5.2.4. *If m and n are coprime, then the systoles of $S_{m,n}$ are exactly the sides of $P(0)$ and $P(m-1)$.*

Proof. Any closed curve on $S_{m,n}$ has length at least the length of the shortest side of the polygons defining $S_{m,n}$. Since the sides have length $\sin\frac{k\pi}{m}$, the shortest sides are for the case $k=1$ or $k=m-1$, which corresponds to the length of the sides of $P(0)$ and $P(m-1)$. □

5.2.2 Veech group and Fundamental domain

In this section, we recall results about the Veech group of $S_{m,n}$ and give a model for the Teichmüller curve associated to $S_{m,n}$.

Definition 5.2.5 (Parametrization of the Teichmüller curve $\mathcal{T}_{m,n}$)**.** Given $M = \begin{pmatrix} a & b \\ c & d \end{pmatrix} \in SL_2(\mathbb{R})$, we send the surface $M \cdot S_{m,n} \in \mathcal{T}_{m,n}$ to an element of $\mathbb{H}^2$ using the identification:

$$M \cdot S_{m,n} \in \mathcal{T}_{m,n} \mapsto \frac{di+b}{ci+a} \in \mathbb{H}^2,$$

We can describe precisely the shape of the fundamental domain of $S_{m,n}$ when n and m are coprime using the following results:

Theorem 5.2.6 ([BM10], [Hoo13])**.** *Let m, n coprime. The Veech group of $S_{m,n}$ is the triangle group $\Delta^+(m,n,\infty)$. Further, $S_{m,n}$ and $S_{n,m}$ are affinely equivalent.*

Then, the Teichmüller disk of $S_{m,n}$ can be identified with two copies of a hyperbolic triangle of angles $(0, \frac{\pi}{n}, \frac{\pi}{m})$.

Theorem 5.2.7 ([Hoo13], [DPU19]). *The horizontal cylinders of $S_{m,n}$ have all the same moduli, namely:*

$$s := 2\cot(\frac{\pi}{n}) + \frac{2\cos(\pi/m)}{\sin(\pi/n)} = \frac{2(\cos(\pi/n)+\cos(\pi/m))}{\sin(\pi/n)}.$$

In particular, the element $\begin{pmatrix} 1 & s \\ 0 & 1 \end{pmatrix}$ belongs to the Veech group of $S_{m,n}$ and the fundamental domain looks like Figure 5.3, where $S_{m,n}$ corresponds to the point of coordinates $(0, i)$ and is stabilised by the action of the rotation of angle $\frac{2\pi}{n}$ while the other corners (which are identified) correspond to the surface $S_{n,m}$, which lies in the same Teichmüller disk (up to normalizing the area) and is stabilised by the action of the rotation of angle $\frac{2\pi}{m}$.

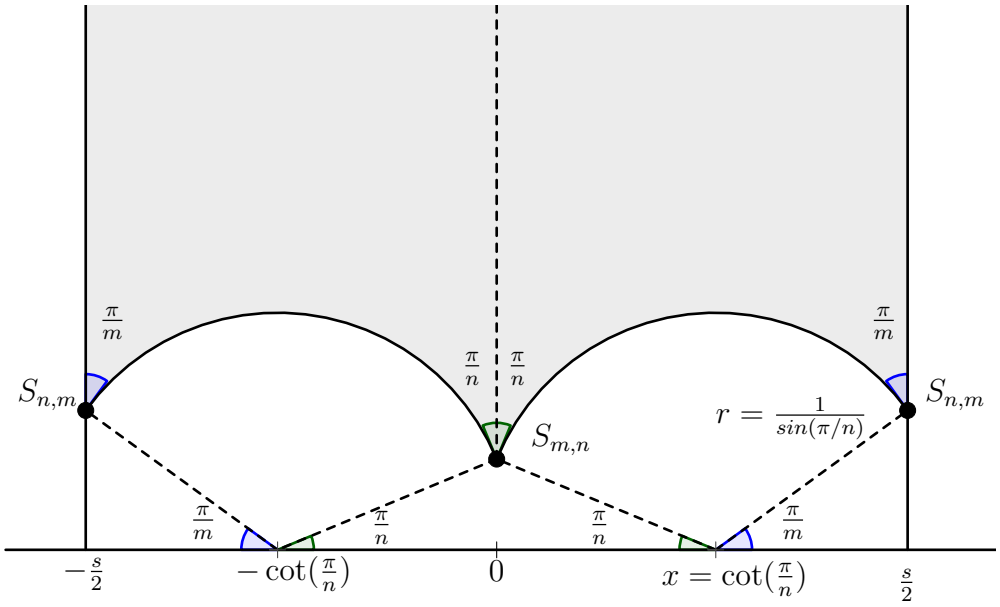

Figure 5.3: The fundamental domain $\mathcal{T}_{m,n}$ of the Teichmüller disk of $S_{m,n}$.

Next, we compute the parameters x and r (which are respectively the abscissa of the center and the radius of the circle which defines the fundamental domain, see Figure 5.3) and the coordinates of $S_{n,m}$ using the data of Figure 5.3 on the angles, giving $x = \cot(\frac{\pi}{n})$, $r = \frac{1}{\sin(\pi/n)}$ and that $S_{n,m}$ has coordinates $\pm\frac{s}{2} + \frac{\sin(\pi/m)}{\sin(\pi/n)}$.

Finally, notice that since $S_{m,n}$ and $S_{n,m}$ belong to the same Teichmüller disk (up to normalising the area), this gives two distinct parametrisations of $\mathcal{T}_{m,n}$. In the following, we will use the parametrisation given by $S_{m,n}$ with $n < m$.

5.3 KVol on Bouw-Möller surfaces

In this section, we study KVol specifically on Bouw-Möller surfaces, and we prove Theorem 5.1.1. By construction, the Bouw-Möller surface $S_{m,n}$ satisfies the hypotheses (H1) and (H2) of Theorem 4.1.1 as soon as $n = 4$, and as such the conclusion of Theorem 4.1.1 holds. Further:

- On Bouw-Möller surfaces for $n = 2$, the hypothesis (H1) holds but not (H2). In fact it is still possible to show that Theorem 5.1.1 holds using cylinder decompositions, as done in Chapter 2 for the staircase model of the double m-gon, m odd. The case where m is even is similar.
- On Bouw-Möller surfaces for $n = 3$, the hypothesis (H2) holds but not (H1) because there are two triangles among the polygons defining $S_{m,3}$. However, notice that it satisfies the hypothesis (H1'), and in fact it will be possible to adapt the proof of Theorem 5.1.1 to this case. Namely:
  - Although Lemma 4.2.1 does not hold anymore, we show below that:

    Lemma 5.3.1. *Let $m \geq 3$ and let α be a saddle connection on $S_{m,3}$, then*

    $$l(\alpha) \geq (p_\alpha + q_\alpha) l_0.$$

    Further, if α is odd but it is not a side or a diagonal of a polygon, then

    $$l(\alpha) \geq (p_\alpha + q_\alpha + \sqrt{2} - 1) l_0.$$

  - The count of the intersections does not change, and Proposition 4.4.1 still holds (this is because $S_{m,3}$ satisfies (H1')).
  - The case of sides and diagonals do not change (as there are no diagonals on a triangle).

Hence, we have:

Corollary 5.3.2. *Let γ and δ be two closed curves on $S_{m,n}$, then:*

$$\frac{\mathrm{Int}(\gamma, \delta)}{l(\gamma) l(\delta)} \leq \frac{1}{l_0^2}.$$

Further, equality holds if and only m and n are coprime and γ and δ are sides of length l_0 intersecting at the singularity, or diagonals of length $\sqrt{2} l_0$ intersecting once at the singularity, and once outside the singularity with the same sign.

Before proving Lemma 5.3.1, let us explain specifically the equality case for Bouw-Möller surfaces. First, we can deduce from Equation (4.1) that equality may hold only if γ and δ are both closed saddle connections. If m and n are not coprime, there are several distinct singularities, and in fact there are no closed

saddle connections of length l_0. Further, there are closed diagonals of length $\sqrt{2}l_0$ only if $n = 4$ and $m \equiv 2 \mod 4$, but in this case the two diagonals of $P(0)$ intersect only once (outside the singularities), giving a ratio of $\frac{1}{2l_0^2}$ instead of $\frac{1}{l_0^2}$.

Next, if m and n are coprime then saddle connections are automatically closed and from Theorem 4.1.6 we deduce that equality holds only if α and β are sides of length l_0 intersecting at the singularity (diagonals of the polygons defining Bouw-Möller surfaces have length greater than l_0), or if α and β are diagonals of length $\sqrt{2}l_0$ and intersecting twice. We will see (Proposition 5.3.6) that this latter case can only arise if $n = 4$ and $m \equiv 3 \mod 4$.

5.3.1 Proof of Lemma 5.3.1

The Bouw-Möller surface $S_{m,3}$ is made of two equilateral triangles of side l_0 (namely $P(0)$ and $P(m-1)$) and $m-2$ hexagons which are convex with obtuse angles. In particular, non-adjacent segments which do not lie inside $P(0)$ or $P(m-1)$ have length least l_0. Furthermore, only the initial and terminal segments α_1 and α_k can be non-adjacent on one of the triangles $P(0)$ and $P(m-1)$. Similarly, the length of two adjacent segments can be smaller than l_0, but this can only happen if one of the adjacent segments is contained in $P(0)$ or in $P(m-1)$. One way to compensate is then to take into account the next non-adjacent segment. More precisely, we have:

Lemma 5.3.3. *Assume α is not a side nor a diagonal of the polygons defining $S_{m,n}$. Then*

1. *If α_1 (resp. α_k) lies in either $P(0)$ or $P(m-1)$, then α_2 (resp. α_{k-1}) is a non-adjacent segment and $l(\alpha_1 \cup \alpha_2) > 2l_0$ (resp. $l(\alpha_{k-1} \cup \alpha_k) > 2l_0$).*

2. *Assume α_i and α_{i+1} are two adjacent segments, being respectively contained in $P(0)$ and $P(1)$. Then the segment α_{i+2} is non-adjacent and the total length of $\alpha_i \cup \alpha_{i+1} \cup \alpha_{i+2}$ is at least $2l_0$.*

Proof. 1. By symmetry, we can consider the case of α_1 and assume it lies inside $P(0)$. Then we have a configuration like the left of Figure 5.4 and the length of $\alpha_1 \cup \alpha_2$ is at least $\min(H_0, L)$ (and in fact, if the minimum is L, the inequality must be strict). Recall that, by definition, the length of the sides of $P(0)$ and $P(1)$ is at least l_0 and the internal angles of $P(1)$ are $\frac{2\pi}{3}$. In particular, $H_0 = (\sqrt{3}+\sqrt{3}\cos(\pi/m))l_0) > 2l_0$ and $L = (1+2\cos(\pi/m))l_0 \geq 2l_0$, with equality when $m = 3$. Hence we deduce that the length of $\alpha_1 \cup \alpha_2$ must be greater than $2l_0$.

2. The segments α_i, α_{i+1} and α_{i+2} can be represented as in the right of Figure 5.4. The segment α_{i+2} is non-adjacent because for α_i and α_{i+1} to be adjacent, the angle between the direction of α and the vertical must be

less than $\frac{\pi}{6}$. In particular, the total length of $\alpha_i \cup \alpha_{i+1} \cup \alpha_{i+2}$ is at least $\min(H_0, L) \geq 2l_0$. Further, as in 1. the bound $2l_0$ cannot be achieved.

□

Now, the first part of Lemma 5.3.1 is a direct corollary of Lemma 5.3.3.

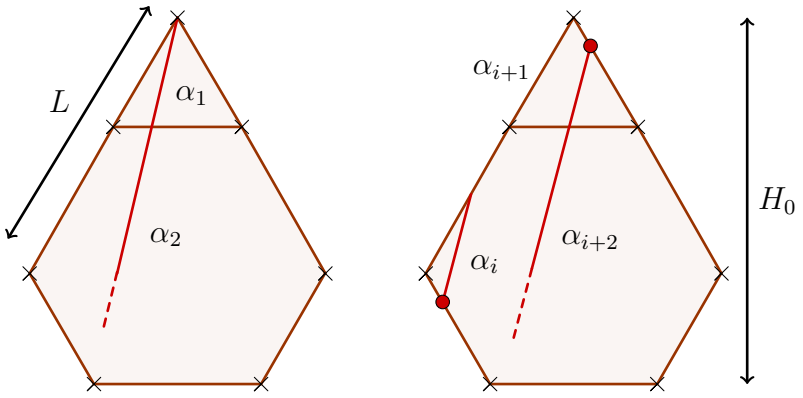

Figure 5.4: On the left, the case where α_1 belongs to the triangle $P(0)$. On the right, the case where α_i and α_{i+1} are two consecutive adjacent segments and one of them lies in $P(0)$ (here, α_{i+1}). Further, we have $L = (1 + 2\cos\frac{\pi}{m})l_0$ and $H_0 = (2\frac{\sqrt{3}}{2} + 2\cos\frac{\pi}{m})l_0$.

Concerning the length of odd saddle connections, we have:

Lemma 5.3.4. *(i) The total length of three consecutive adjacent segments is at least $\sqrt{2}l_0$.*

(ii) Given three consecutive segments in the polygonal decomposition of α such that the first and the third segments are non-adjacent while the second segment is adjacent, the total length of the three segments is at least $2\sqrt{2}l_0$.

Proof. Let us first notice that if none of the adjacent segment are contained in $P(0)$ or $P(m-1)$, then the result is a direct corollary of Lemma 4.2.4. Hence, we can assume by symmetry that at least one of the adjacent segments is contained in $P(0)$.

(i) Given three consecutive adjacent segments such that one is contained in $P(0)$, the geometry of Bouw-Möller surfaces imply that the other two segments must be contained respectively in $P(1)$ and $P(2)$. Then, we are in the setting of Figure 5.5 and hence the total length of the three adjacent segments is at least $H_1 = \frac{\sqrt{3}}{2}(1 + 2\cos(\pi/m))l_0 \geq \sqrt{3}l_0$, which is greater than $\sqrt{2}l_0$.

(ii) As in (i), we can assume by symmetry that the adjacent segment is contained in $P(0)$. The preceding and following non-adjacent segment are then both contained in $P(1)$. We can see from Figure 5.6 that the total length of the three segments must be at least

$$\min((1+4\cos\frac{\pi}{m})l_0, (2+4\cos\frac{\pi}{m})\frac{\sqrt{3}}{2}l_0),$$

which is greater than $2\sqrt{2}l_0$, as required. (In fact, it is even greater than $3l_0$).

□

Putting together Lemma 5.3.3 and Lemma 5.3.4 allows to conclude that the length of an odd saddle connection α which is not a side or a diagonal of a polygon is at least $(p_\alpha + q_\alpha + \sqrt{2} - 1)l_0$. This concludes the proof of Lemma 5.3.1.

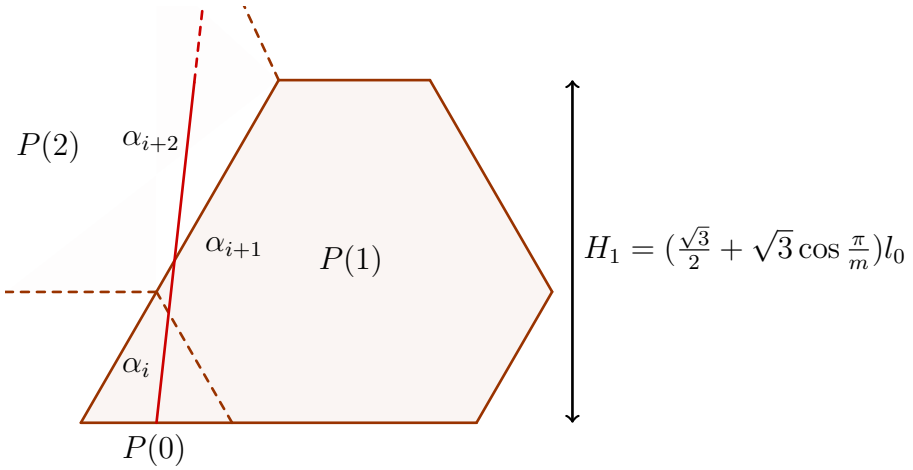

Figure 5.5: The total length of three consecutive adjacent segments, one being in $P(0)$, is at least H_1. Note that in this configuration α_{i-1} cannot be an adjacent segment.

5.3.2 Intersection of systoles and diagonals

We now show that if m and n are coprime, there are indeed intersecting systoles. Specifically if $n = 4$ and $m \equiv 3 \mod 4$, we also show that the diagonals of the square $P(0)$ (resp. $P(m-1)$), which projects to closed curves on the surface, intersect twice: once at the singularity, and once outside the singularity with the same sign. Combined with Theorem 5.1.1, this will show Corollary 5.1.2. We first recall how to compute the intersection of two closed curves at a singular point.

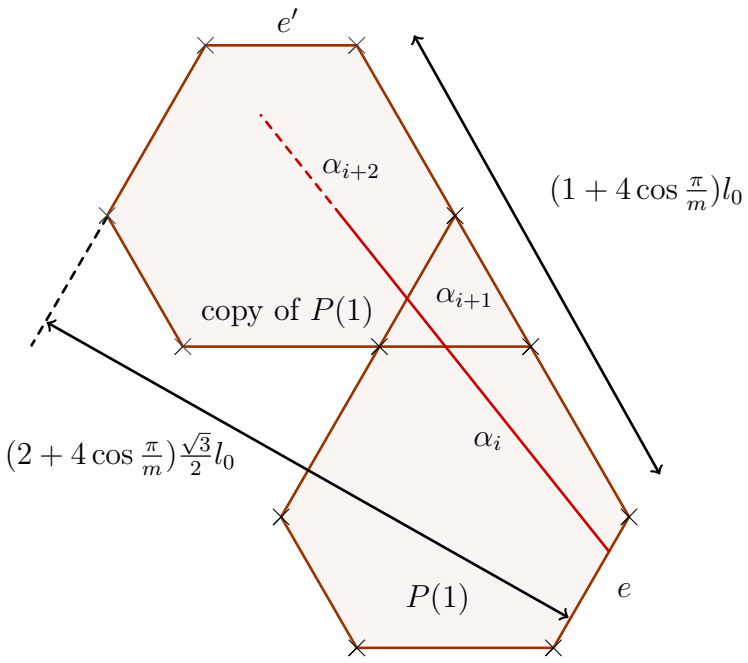

Figure 5.6: Example of three consecutive segments, the first and the third (α_i and α_{i+2}) being non-adjacent, while the second (α_{i+1}) is adjacent and contained in $P(0)$. (Since either α_i has an endpoint on e or α_{i+1} as an endpoint on e', we assumed by symmetry that α_i has an endpoint on e.) The total length of the three segments is at least $\min((1 + 4\cos\frac{\pi}{m})l_0, (2 + 4\cos\frac{\pi}{m})\frac{\sqrt{3}}{2}l_0) > (1 + \sqrt{2})l_0$.

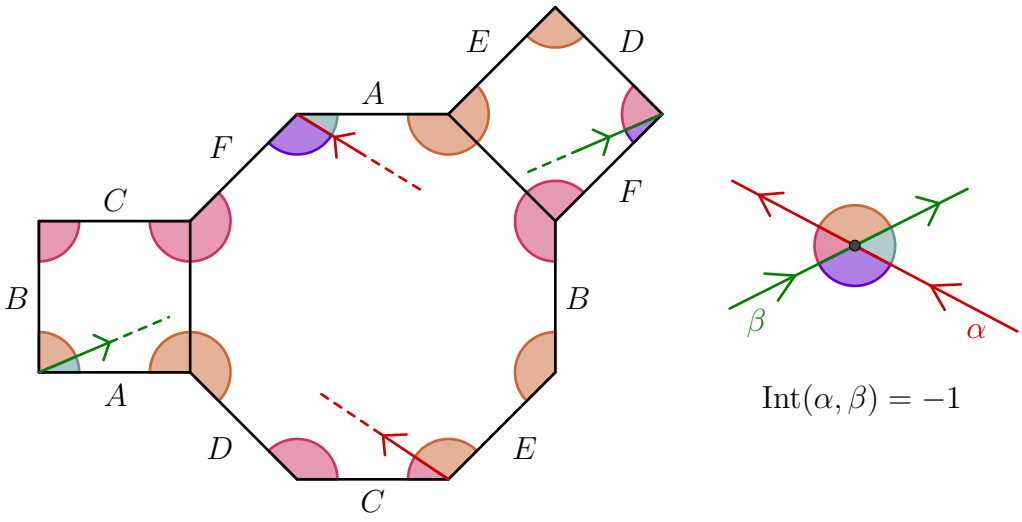

Figure 5.7: In the example of this picture, the curves α and β intersect once at the singularity. Furthermore, the sign is given by $\mathrm{Int}(\alpha, \beta) = -1$.

Intersection at singular points. Given two (simple) closed oriented curves α and β on a translation surface, the algebraic intersection is given by the sum of each intersection point with its sign. Recall that for a transverse intersection point P, we have $\mathrm{Int}_P(\alpha, \beta) = +1$ if the tangent vectors at P of α and β form an ordered basis with the normal to the sheet of paper, and $\mathrm{Int}_P(\alpha, \beta) = -1$ otherwise.

For closed saddle connections, one looks at the incoming and outgoing pieces of α and β in a neighbourhood of the singularity, as in Figure 5.7. Then, the intersection will be determined by the circular order of these, in the sense that two saddle connections will intersect if and only if the two entries of one saddle connection alternate with the two entries of the other saddle connection. Intuitively, this means that one cannot pull the two curves apart at the singularity to obtain two curves that do not intersect.

Intersection of systoles. In the case of Bouw-Möller surfaces, this method allows to prove useful results about how some saddle connections intersect.

Proposition 5.3.5. *Assume m and n are coprime. Then there is a pair of intersecting systoles in $S_{m,n}$. More precisely, the horizontal systole α corresponding to the side v_0 of $P(0)$ intersects at least one systole having a direction making an angle $\frac{\pi}{n}$ with the horizontal.*

Proof. As mentioned, the systoles of $S_{m,n}$ are exactly the sides of $P(0)$ and $P(m-1)$ (Proposition 5.2.4). Since they cannot intersect outside the singularity, we only

need to show that we can find two systoles that intersect at the singularity whose directions make an angle of $\frac{\pi}{n}$. In order to compute the algebraic intersection of systoles at the singularity, we need to understand in which order we encounter the sides of $P(0)$ and $P(m-1)$ while turning around the singularity.

The strategy of the proof is the following. Denote as α the side v_0 of the polygon $P(0)$, which is horizontal by Remark 5.2.2 and it is a systole. Since there is only one singularity, when looking at all the sides of polygons in a neighbourhood of the singularity, we will see two occurrences of each side corresponding to the two extremities of the side. Now choose the extreme of α on the left and start turning around the singularity counter-clockwise. If we look at the two occurrences of α, they will be separated by a certain number of other sides and we will define a certain β to be the side that we encounter when we are in some sense half way from meeting α again. In the following we will prove that α and β are two systoles which intersect and which form an angle of $\frac{\pi}{n}$.

Recall that the polygons $P(i)$ for $i \neq 0, m-1$ are semi-regular $2n$-gons, so their internal angles are all equal to $\frac{(n-1)\pi}{n}$, while $P(0)$ and $P(m-1)$ are both regular n-gons so their internal angles are all $\frac{(n-2)\pi}{n}$. From Remark 5.2.1, one deduces that going around the singularity and starting from a sector of $P(0)$ we will encounter one sector in each polygon $P(i)$ for $i = 1$ to $m-2$, then one sector in $P(m-1)$ and then again one sector in each $P(i)$ for $i = m-2$ to 1 until getting back to $P(0)$.

Now start turning counter-clockwise around the singularity from the left endpoint of the horizontal systole α. We want to understand what happens in the neighbourhood of the singularity before we get back to α. The next side we encounter is the consecutive side in $P(0)$ (which is also a side in $P(1)$) having the left endpoint of α as an endpoint, which we encounter after having turned by an angle $\frac{(n-2)\pi}{n}$. Then, by Remark 5.2.1, we cross an angular sector in $P(1)$, then one in $P(2)$, and so on until $P(m-2)$. In the sector contained in $P(m-2)$, if we start from a common side of $P(m-2)$ and $P(m-3)$, then the next side we encounter going around the singularity is a common side of $P(m-2)$ and $P(m-1)$. This side is also a systole and we encounter it after having turned by a total angle $\frac{(n-2)\pi}{n} + (m-2)\frac{(n-1)\pi}{n}$, where the first term comes from the sector in $P(0)$ and the second term comes from the $m-2$ sectors in $P(1)$ to $P(m-2)$. Next, following the same reasoning, we encounter a second side of $P(m-1)$ after having turned by an angle $(m-2)\frac{(n-1)\pi}{n} + 2\frac{(n-2)\pi}{n}$ in total (so, an extra $\frac{(n-2)\pi}{n}$ from the first systole we encounter in $P(m-1)$). We can then continue turning around the singularity and meeting sectors in $P(m-2)$ to $P(1)$ until we are back in $P(0)$ after an angle of $\frac{2(n-2)\pi}{n} + 2(m-2)\frac{(n-1)\pi}{n}$.

Repeating this argument, we can see that every time we turn around the singularity by $2l\frac{(n-2)\pi}{n} + 2l(m-2)\frac{(n-1)\pi}{n}$, with l integer, we are back on a systole which is a side of $P(0)$ and if we add one more sector, so after an angle $(2l +$

$1)\frac{(n-2)\pi}{n} + 2l(m-2)\frac{(n-1)\pi}{n}$ we encounter another systole which is a side of $P(0)$. Moreover, when we are halfway and we turn by $l\frac{(n-2)\pi}{n} + l(m-2)\frac{(n-1)\pi}{n}$, we encounter a systole (which is either a side of $P(0)$ or a side of $P(m-1)$ depending on the parity of l). Now, the next occurrence of α in the neighbourhood of the singularity must be at the end of a sector in $P(0)$, when turning counterclockwise around the singularity. This means that we will be encountering α again after an angle of $(2l_0+1)\frac{(n-2)\pi}{n} + 2l_0(m-2)\frac{(n-1)\pi}{n}$ for a certain integer l_0. We now define β to be the systole that we will be encountering after an angle of $l_0\frac{(n-2)\pi}{n} + l_0(m-2)\frac{(n-1)\pi}{n}$. To find the correct value of l_0, we need the new systole we found to be parallel to α and this is enough because if the systole was another systole parallel to α but not α, then it would be at the beginning of a sector in $P(0)$ because of the structure of Bouw-Möller surfaces. In other words, l_0 is the smallest integer such that

$$2l_0(m-2)\frac{(n-1)\pi}{n} + (2l_0+1)\frac{(n-2)\pi}{n} \equiv \pi \mod 2\pi.$$

This implies that

$$2l_0(m-2)\frac{(n-1)\pi}{n} + 2l_0\frac{(n-2)\pi}{n} \equiv \pi - \frac{(n-2)\pi}{n} \mod 2\pi.$$

and hence

$$l_0(m-2)\frac{(n-1)\pi}{n} + l_0\frac{(n-2)\pi}{n} \equiv \frac{\pi}{n} \mod \pi.$$

Now, the left hand side is exactly the angle after which we encounter β and hence it makes an angle $\frac{\pi}{n}$ with the horizontal.

Furthermore, the above argument applied to β tells by symmetry that the two occurences of β in the neighbourhood of the singularity are separated by an angle $2l_0(m-2)\frac{(n-1)\pi}{n} + (2l_0+1)\frac{(n-2)\pi}{n}$. This implies that turning around the singularity, we first see α, then β (after an angle $l_0(m-2)\frac{(n-1)\pi}{n} + l_0\frac{(n-2)\pi}{n}$), then α (after an angle $2l_0(m-2)\frac{(n-1)\pi}{n} + (2l_0+1)\frac{(n-2)\pi}{n}$) and finally again β (after an angle $3l_0(m-2)\frac{(n-1)\pi}{n} + (3l_0+1)\frac{(n-2)\pi}{n}$). We conclude that $\mathrm{Int}(\alpha,\beta) = \pm 1$ (depending on the choice of the orientation of both α and β). □

Intersection of diagonals. Similarly, we can compute the algebraic intersection of the closed saddle connections given by the diagonals of the square $P(0)$ in the surfaces $S_{m,4}$ for m odd.

Proposition 5.3.6. *Let $m \geq 3$ odd. On the surface $S_{m,4}$, the diagonals of the square $P(0)$ have algebraic intersection 2 if $m \equiv 3 \mod 4$ and 0 otherwise.*

Proof. As in Figure 5.8, we denote the two diagonals as α (positive slope) and β (negative slope) and four sectors Σ_i for $i = 1, 2, 3, 4$ as being a neighbourhood

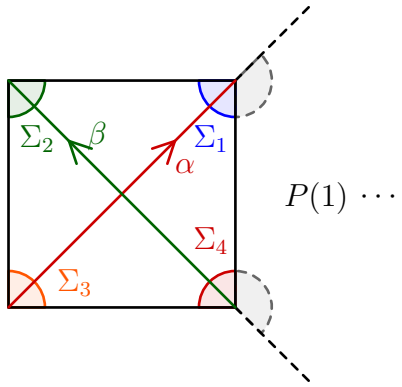

Figure 5.8: If $n = 4$ and m odd, the cyclic ordering of $\Sigma_1, \Sigma_2, \Sigma_3$ and Σ_4 determines the intersection at the singularity between the diagonals α and β of $P(0)$.

of the singularity intersecting the square $P(0)$ in the corners, moving counterclockwise starting from the top-right corner. In order to compute the algebraic intersection number at the singularity, we need to understand in which order one would encounter the sectors Σ_i around the singularity. This would determine the order of occurrences of α and β and hence their intersection at the singularity. One would then just need to add the (positive) intersection in the centre of the square.

The polygons $P(i)$ for $i \neq 0, m-1$ are semi-regular octagons, so the internal angles are all equal to $\frac{3\pi}{4}$, while $P(m-1)$ is a square, so its internal angles are $\frac{\pi}{2}$. In order to detect in which order we would see the Σ_is around the singularity, we need to determine what is the angle of a sector sitting in between two of them. This, plus the gluing rules of translation surfaces, will tell us uniquely which sector follows a given Σ_i. Recalling Remark 5.2.1, one can easily see that going around the singularity and starting from $P(0)$, we will encounter one vertex in each polygon $P(i)$ for $i = 1$ to $m-2$, then one vertex in $P(m-1)$ and then again one vertex in each $P(i)$ for $i = m-2$ to 1 until getting back to $P(0)$. This means that between each pair Σ_1, Σ_j, there is a cone angle of $2(m-2) \cdot \frac{3\pi}{4} + \frac{\pi}{2}$.

In particular, writing $m = 4k + r$, we turn around the singularity by an angle $2(4k + r - 2) \cdot \frac{3\pi}{4} + \frac{\pi}{2} = (3k - 2) \cdot 2\pi + (3r + 3)\frac{\pi}{2}$. Recalling that $r \neq 0, 2$ because m is odd, this gives an integer number of turns for $r = 3$, and a half turn for $r = 1$. Hence the order of the sectors is:

$$\begin{aligned} &\Sigma_1, \Sigma_2, \Sigma_3, \Sigma_4 && \textit{for} && r = 3, \\ &\Sigma_1, \Sigma_4, \Sigma_3, \Sigma_2 && \textit{for} && r = 1. \end{aligned}$$

This would then give a positive intersection at the singularity in the first case and a negative intersection at the singularity in the second case. □

5.4 Intersection of horizontal saddle connections

In this section, we move back to the general case of translation surfaces. Namely, we consider a translation surface X which is completely periodic in the horizontal direction. As such, we have a horizontal cylinder decomposition. Following Kontsevich-Zorich [KZ02, Section 4.1], we define the *separatrix diagram* associated to the horizontal saddle connections of X. This diagram is in fact a graph with a cyclic orientation of the edges incident to each vertex (a *ribbon graph*). Further, the separatrix diagram allows to understand the intersection of horizontal closed curves on X, that is closed curves which are union of horizontal saddle connections. More precisely:

Proposition 5.4.1. *Horizontal closed curves are pairwise non-intersecting if and only if the separatrix diagram is planar.*

Remark 5.4.2. Let us insist on the fact that the separatrix diagram comes with a cylic orientation of the edges at each vertex. As such, a separatrix diagram is planar if there exist a planar representation of the separatrix diagram respecting the cyclic orientation at each vertex. In general, given a ribbon graph one can define its genus as the minimal genus of surfaces onto which it can be embedded (respecting the cyclic orientation at each vertex). Equivalently, a ribbon graph of genus g can be seen as a cell complex in a surface of genus g, see [EMM13]. In particular, a ribbon graph is planar if and only if it has genus zero.

Next, we define a *dual separatrix diagram*, which is planar if and only if the separatrix diagram is. We give an alternative definition of the dual separatrix diagram using the horizontal cylinder decomposition, which is easily understood in the case of Bouw-Möller surfaces and allows to show:

Proposition 5.4.3. *Horizontal closed curves on Bouw-Möller surfaces are pairwise non-intersecting.*

Using Theorem 1.5 of [Bou23], we deduce that:

Corollary 5.4.4. *KVol is bounded on the Teichmüller disk of Bouw-Möller surfaces.*

An introduction to graphs on surfaces and ribbon graphs is presented in [EMM13].

5.4.1 The horizontal separatrix diagram

Following [KZ02], we define the horizontal separatrix diagram associated to a translation surface which is completely periodic in the horizontal direction as the graph whose edges are the horizontal saddle connections and the vertices are the singularities. The edge corresponding to the saddle connection A connects the

vertices corresponding to the singularities represented by the endpoints of A. The orientation on the edges at a vertex comes from the circular orientation at the corresponding singularity.

In particular, a horizontal closed curve correspond to a closed path on the horizontal separatrix diagram. Further, the algebraic intersection of such closed curves on X is exactly the intersection of the paths on the horizontal separatrix diagram. In particular, if the horizontal separatrix diagram is planar then closed paths on the horizontal separatrix diagram are pairwise non-intersecting since the plane is simply connected.

Conversely, if the horizontal separatrix diagram is not planar, we can construct two closed paths on the separatrix diagram having non-zero intersection. Indeed, the fact that the graph is not planar implies that we have a configuration like Figure 5.9. We then choose the curves α and β, corresponding to horizontal closed curves on the surface X and intersecting once. We have proven Proposition 5.4.1.

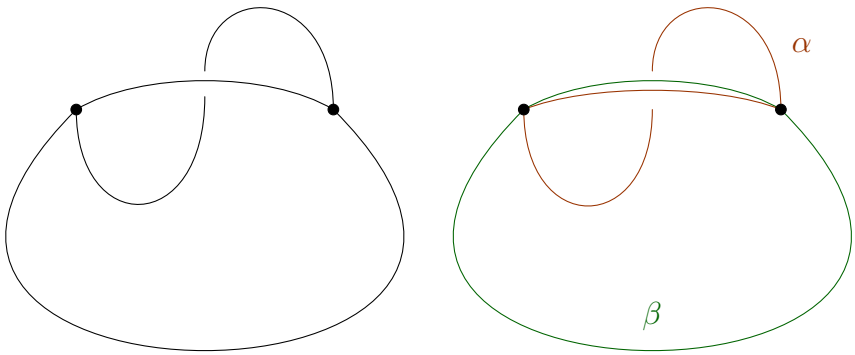

Figure 5.9: A configuration in a non-planar ribbon graph (the two vertices could also be collapsed as one). From this configuration, one constructs curves α and β intersecting once.

5.4.2 The dual separatrix diagram

The dual graph. As we have seen, ribbon graphs are equivalent to cell complexes on a surface. In particular, there is a well defined notion of faces and it is possible to define the dual of a ribbon graph: replace each face by a vertex, and each edge would then become an edge connecting the two faces it separates (it could be the same face, and in this case we just get a loop around the vertex) and the orientation of the vertex at each edge is just the circular orientation of the edges of the corresponding face. Finally, the vertices of the ribbon graph give the faces of the dual ribbon graph. The dual ribbon graph is then just the dual cell complex and it can be embedded on the same surface. In particular, the dual graph of a planar ribbon graph is planar, and conversely. Hence, we have:

Proposition 5.4.5. *Horizontal closed curves are pairwise non-intersecting if and only if the dual separatrix diagram is planar.*

In the next paragraph we give an alternative definition of the dual separatrix diagrams which comes directly from the cylinder decomposition.

An alternative definition. Let X be a translation surface which is completely periodic in the horizontal direction. As such, it is decomposed into cylinders: let $\mathcal{C}_1, \ldots, \mathcal{C}_n$ be the horizontal cylinders. We define the dual separatrix diagram $\mathfrak{G}(X)$ having $2n$ vertices as follows:

- **Vertices.** For every horizontal cylinder $\mathcal{C}$, we define two vertices of the graph, denoted $\mathcal{C}^+$ and $\mathcal{C}^-$.
- **Edges.** For a horizontal saddle connection A connecting the top of a cylinder $\mathcal{C}_i$ to the bottom of a cylinder $\mathcal{C}_{i'}$, we define an edge between the vertices of label $\mathcal{C}_i^+$ and $\mathcal{C}_{i'}^-$.
- **Cyclic orientation on the vertices.** Given a vertex $\mathcal{C}^+$, corresponding to the top of the cylinder $\mathcal{C}$, define the cyclic orientation on the edges from $\mathcal{C}^+$ as the left to right order on the horizontal saddle connections on the top of $\mathcal{C}^+$.
  Given a vertex $\mathcal{C}^-$, corresponding to the bottom of the cylinder $\mathcal{C}$, define the cyclic orientation on the edges from $\mathcal{C}^-$ as the right to left order on the horizontal saddle connections on the bottom of $\mathcal{C}^-$. See Figure 5.10.

An example of such graph is depicted in Figure 5.11. We explain in the next paragraph why it is the dual graph of the horizontal separatrix diagram.

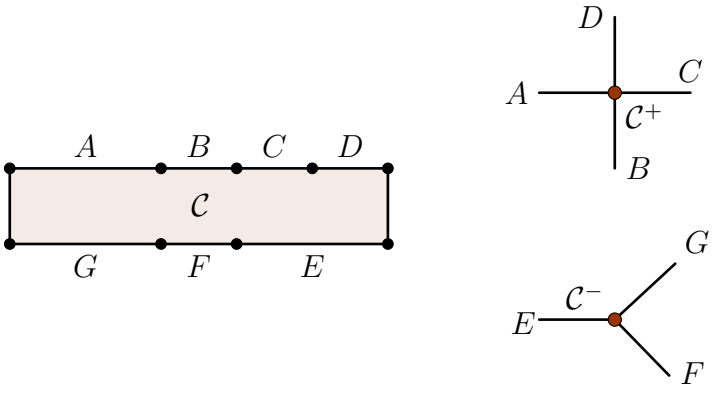

Figure 5.10: The two vertices $\mathcal{C}^+$ and $\mathcal{C}^-$ from a cylinder $\mathcal{C}$ and the emanating edges in cyclic order.

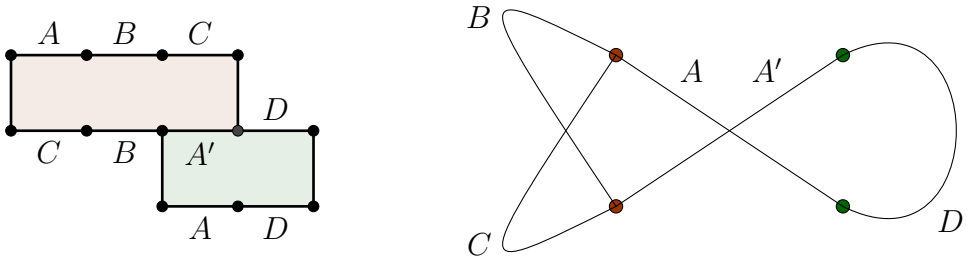

Figure 5.11: Example of decomposition into cylinders and its associated graph.

5.4.3 Turning aroung the singularity

Let us make clear how to tell the cyclic sequence of horizontal saddle connections crossed while turning around the singularity, as it will explain how to recover the separatrix diagram from the dual separatrix diagram.

Assume we turn around the singularity in the trigonometric order. Then:

- After crossing the side top A, we cross the side top B, following the top order from left to right.

- After crossing the bottom side A, we cross the bottom side C, following the bottom order from right to left.

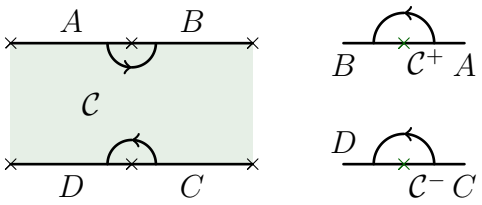

Figure 5.12: Turning around the singularity on the surface X and on the graph $\mathfrak{G}(X)$.

In particular, turning around the singularity reduces to follow the edges of the graph, and at each vertex follow the trigonometric order. The sequence of encountered edges determines the separatrix diagram at the singularity, as in Figure 5.13. Each edge is crossed twice, once in each direction. Furthermore, it gives that the number of cycles determine the number of singularities. In particular, when X has a single singularity, the associated graph is automatically connected.

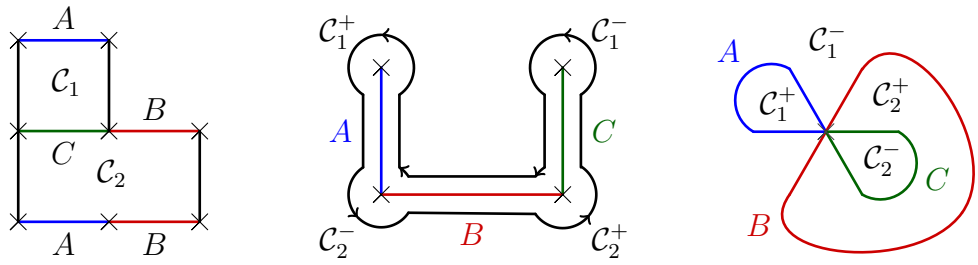

Figure 5.13: From the dual separatrix diagram to the separatrix diagram.

5.4.4 Saddle connections on Bouw-Möller surfaces

In this paragraph we use the criterion of Proposition 5.4.5 to show that horizontal closed curves are pairwise non-intersecting on Bouw-Möller surfaces.

Let $m, n \geq 2$, $mn \geq 3$. We consider the Bouw-Möller surface $S_{m,n}$, which has $gcd(m, n)$ singularities. $S_{m,n}$ is a Veech surface and as such it is completely periodic in every saddle connection direction. Furthermore, the cylinder decomposition in every periodic direction look the same and we have:

Lemma 5.4.6. *$S_{m,n}$ is decomposed into $\frac{(m-1)\times(n-1)}{2}$ cylinders, and every cylinder has either one or two top saddle connections and one or two bottom saddle connections.*

Proof of Lemma 5.4.6. This is just because all cylinders are by construction contained in two polygons, and there is at most one horizontal top or bottom saddle connection of a cylinder in each polygon. □

From this lemma we draw that each vertex of the dual separatrix diagram $\mathfrak{G}(S_{m,n})$ of $S_{m,n}$ has either one or two incident edges. Thus, every connected component of $\mathfrak{G}(S_{m,n})$ is either a tree or a cycle, and $\mathfrak{G}(S_{m,n})$ is planar. Hence, Proposition 5.4.3 follows from Proposition 5.4.5.

5.4.5 Additional comments

It is easily shown that for translation surfaces having a single singularity, having a planar separatrix diagram is equivalent to having exactly g cylinders. This is for example the case for periodic directions in any algebraically primitive Veech surface which has a single singularity (see [HL06]). In particular Proposition 5.4.5 and [Bou23, Theorem 1.5] imply that KVol is always bounded on the Teichmüller disk of an algebraically primitive Veech surface. As stated in [BLM22, Theorem 1.4], the converse is true in $\mathcal{H}(2)$: KVol is bounded on the Teichmüller disk of a Veech surface if and only if the Veech surface is non-arithmetic.

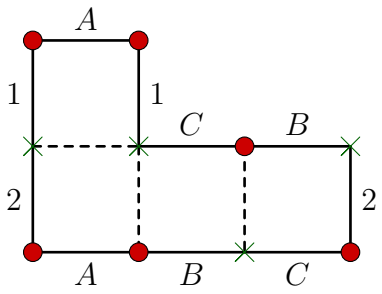

Figure 5.14: Example of squared tiled surface having bounded KVol on its Teichmüller disk.

In fact, this result is not true in $\mathcal{H}(1,1)$: the squared-tiled surface of Figure 5.14 decomposes into two cylinders in each periodic direction and we can check easily that the associated separatrix diagrams are planar. In particular, KVol is bounded on the Teichmüller disk of the squared-tiled surface of Figure 5.14.

5.5 Extension to the Teichmüller disk

In the rest of the paper we study KVol as a function on the Teichmüller disk of $S_{m,n}$, with m, n coprime. More precisely, we extend the techniques of [BLM22] developed in the case of the double regular n-gon. This section is devoted to introduce the preliminary material from [BLM22]. We will then study the cylinder decompositions of $S_{m,n}$ in Section 5.6 in order to derive estimates which allows to compute KVol on the Teichmüller disk.

5.5.1 Preliminaries : Direction decomposition

In this paragraph, we follow Sections 4 and 5 of [BLM22] and give another convenient expression for KVol on the Teichmüller disk of $S_{m,n}$. Recall that we have a parametrization of the Teichmüller disk given by Definition 5.2.5. We start with a few definitions.

Definition 5.5.1 (Direction of a saddle connection on $X \in \mathcal{T}_{m,n}$). (i) Given a saddle connection α on $S_{m,n}$, of holonomy vector $\vec{\alpha} = \begin{pmatrix} \alpha_x \\ \alpha_y \end{pmatrix}$, we define the direction of α as $d_\alpha := -\dfrac{\alpha_x}{\alpha_y} \in \mathbb{R} \cup \{\infty\}$, that is minus the co-slope of the holonomy vector $\vec{\alpha}$. If α is horizontal, the co-slope is defined as ∞.
Using the classical identification $\mathbb{R} \cup \{\infty\} \equiv \partial\mathbb{H}^2$, it means that to each

saddle connection on $S_{m,n}$ we associate a direction in $\partial\mathbb{H}^2$.

(ii) Further, for any $M \in GL_2^+(\mathbb{R})$, the direction of the saddle connection $\alpha \subset M \cdot S_{m,n}$ is defined as the direction of the preimage $M^{-1} \cdot \alpha$, which is a saddle connection on the surface $S_{m,n}$.

This definition allows to make a consitent choice for the direction of a saddle connection in $S_{m,n}$ and all its images when transforming the surface $S_{m,n}$ by a matrix M. Using Definitions 5.2.5 and 5.5.1, the locus of surfaces $X \in \mathcal{T}_{m,n}$ where saddle connections of respective direction d and d' make an angle θ on X has a nice expression:

Proposition 5.5.2. *[BLM22, §4] The locus of surfaces $X \in \mathcal{T}_{m,n}$ where the directions d and d' make an (unoriented) angle $\theta \in]0, \frac{\pi}{2}]$ is the banana neighborood*

$$\gamma_{d,d',r} = \{z \in \mathbb{H}^2 : \mathrm{dist}_{\mathbb{H}^2}(z, \gamma_{d,d'}) = r\}$$

where $\cosh r = \dfrac{1}{\sin\theta}$, *and $\gamma_{d,d'}$ is the hyperbolic geodesic having endpoints $d, d' \in \partial\mathbb{H}^2$ (see Figure 5.15).*

In particular, the locus of surfaces in $\mathcal{T}_{m,n}$ where the directions d and d' are orthogonal is the hyperbolic geodesic $\gamma_{d,d'}$.

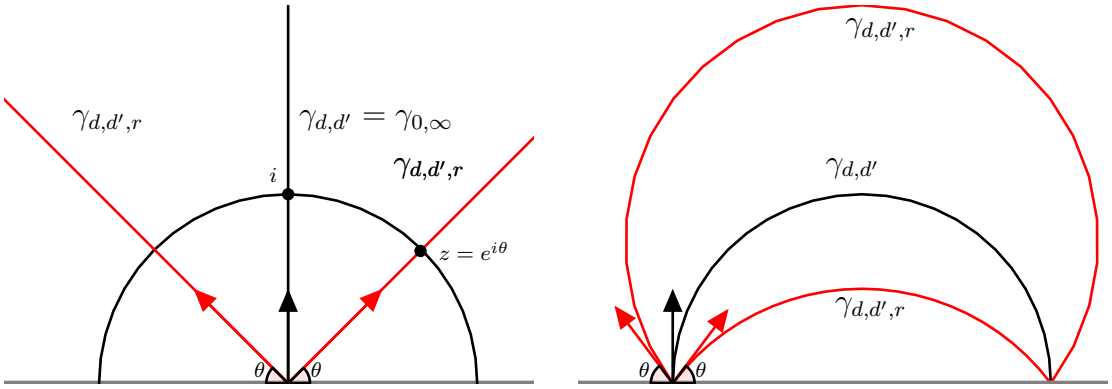

Figure 5.15: The set $\gamma_{d,d',r}$ for $\cosh r = \frac{1}{\sin\theta}$.

In the rest of the paper, we use the following

Notation 5.5.3. Given $X = M \cdot \mathcal{S} \in \mathcal{T}_{m,n}$, and d, d' distinct directions, we define $\theta(X, d, d') \in]0, \frac{\pi}{2}]$ as the (unoriented) angle between the directions d and d' in the surface X. With this notation, we have by Proposition 5.5.2:

$$\sin\theta(X, d, d') = \frac{1}{\cosh(d_{\mathbb{H}^2}(X, \gamma_{d,d'}))}. \tag{5.1}$$

5.5.2 Another look at KVol

The above geometric interpretation allows to rewrite KVol as a supremum over pairs of directions instead of saddle connections by grouping together all pairs of saddle connections (α, β) having directions (d, d'). More precisely, we have:

Proposition 5.5.4. *[BLM22, Proposition 5.1] Let $\mathcal{P}$ be the set of periodic directions in $S_{m,n}$. Then for any surface $X \in \mathcal{T}_{m,n}$ we have:*

$$KVol(X) = \mathrm{Vol}(X) \cdot \sup_{\substack{d, d' \in \mathcal{P} \\ d \neq d'}} K(d, d') \cdot \sin\theta(X, d, d'), \tag{5.2}$$

where $K(d, d') = \sup_{\substack{\alpha \subset \mathcal{S} \text{ saddle connection in direction } d \\ \beta \subset \mathcal{S} \text{ saddle connection in direction } d'}} \frac{\mathrm{Int}(\alpha,\beta)}{\alpha \wedge \beta}$.

Although stated in the Teichmüller disk of the double regular n-gon in [BLM22], the proof is obvious and extends to the case of all Teichmüller disks of Veech surfaces having a single singularity and no pairs of intersecting saddle connections in the same direction, which is the case in $S_{m,n}$ as seen in Section 5.4.

Remark 5.5.5.

- The Veech group Γ of $S_{m,n}$ acts on $S_{m,n}$ while preserving the intersection form, and acts linearly on $\mathbb{R}^2$, hence preserving the wedge product. In particular, $K(d, d') = K(g \cdot d, g \cdot d')$ for any element $g \in \Gamma$.
- Further, notice that by invariance under the action of $SL_2(\mathbb{R})$, the quantity $K(d, d')$ can be computed on any surface of the Teichmüller disk, giving the same result. In the following we will compute $K(d, d')$ on the base surface $S_{m,n}$, $n < m$.

From Proposition 5.5.4 and Equation (5.1), the statement of Theorem 5.1.3 can be formulated again as:

Theorem 5.5.6. *For any $X \in \mathcal{T}_{m,n}$, we have*

$$KVol(X) = Vol(X) \cdot K(\infty, \pm\cot\frac{\pi}{n}) \cdot \max(\sin\theta(X, \infty, +\cot\frac{\pi}{n}), \sin\theta(X, \infty, -\cot\frac{\pi}{n})).$$

Further, as seen in Section 5.3 and Proposition 5.3.5, the supremum in the definition of $\mathrm{KVol}(S_{m,n})$ is achieved (for $m, n \geq 3$ coprime) by the horizontal systole of $P(0)$ and another systole of $P(m-1)$ of direction $\pm\cot(\frac{\pi}{n})$, and hence we deduce from Proposition 5.5.4 that:

Corollary 5.5.7.

$$KVol(S_{m,n}) = Vol(S_{m,n}) \cdot K(\infty, \pm\cot\frac{\pi}{n}) \cdot \sin\theta(S_{m,n}, \infty, \pm\cot\frac{\pi}{n})$$

Notice that in this case $\theta(S_{m,n}, \infty, \cot\frac{\pi}{n}) = \theta(S_{m,n}, \infty, -\cot\frac{\pi}{n}) = \frac{\pi}{n}$.

5.5.3 Strategy for the proof of Theorem 5.5.6

In order to show Theorem 5.5.6, we use the following result, proven in Section 5.7, which states in a general setting what has been proven in [BLM22, Section 7] in the case of the double regular n-gon.

Theorem 5.5.8. *Let $a, b, c \in \mathbb{R}$ with $|b| \leq |c|$. Let $\mathcal{D}$ be the hyperbolic domain delimited by the geodesics $\gamma_{a,\infty}$, $\gamma_{a+b,\infty}$ and $\gamma_{a-c,a+c}$, and X_0 be the intersection point of $\gamma_{a+b,\infty}$ and $\gamma_{a-c,a+c}$, which exist by the assumption $|b| \leq |c|$. Assume that the angle between the geodesics $\gamma_{a+b,\infty}$ and $\gamma_{a+c,a-c}$ is of the form $\frac{\pi}{n}$, for $n \geq 2$ so that the group generated by the reflections along the geodesics $\gamma_{a+b,\infty}$ and $\gamma_{a-c,a+c}$ is a dihedral group. Let $\mathcal{P} \subset \partial\mathbb{H}^2$ containing at least ∞, a, and $a + 2b$, and $K(\cdot,\cdot) : \mathcal{P} \times \mathcal{P}\backslash\Delta \to \mathbb{R}$ be a map which is symmetric with respect to its two coordinates (Δ is the diagonal $\{(x, x), x \in \mathcal{P}\}$.) and invariant under the diagonal action of the dihedra group generated by the reflections along the geodesics $\gamma_{a+b,\infty}$ and $\gamma_{a-c,a+c}$.*

Assume that

(H1) For any distinct $d, d' \in \mathcal{P}$,

$$K(d, d') \sin(X_0, d, d') \leq K(\infty, a) \sin\theta(X_0, \infty, a)$$

(H2) For any distinct $d, d' \in \mathcal{P}$,

$$K(d, d') \leq K(\infty, a)$$

(H3) For any distinct $d, d' \in \mathcal{P}$ such that $\gamma_{d,d'}$ intersects $\mathcal{D}$ and $(d, d') \neq (\infty, a)$,

$$K(d, d') \leq \sin(\frac{\pi}{4}) K(\infty, a)$$

(H4) For any distinct $d, d' \in \mathcal{P}$ such that $\gamma_{d,d'}$ intersects $\mathcal{D}$ and $(d, d') \neq (\infty, a)$,

$$K(d, d') \leq \frac{\sin\theta(X_0, \infty, a)}{\sin\theta(X_0, a, a + 2b)} K(\infty, a)$$

Then, for any $X \in \mathcal{D}$ and any distinct $d, d' \in \mathcal{P}$

$$K(d, d') \sin(X, d, d') \leq K(\infty, a) \sin\theta(X, \infty, a).$$

In particular, it suffices to show that the function $K(\cdot,\cdot)$ defined over the set $\mathcal{P}$ of periodic directions satisfy the hypotheses of Theorem 5.5.8 in each of the domains $\mathcal{D}_1$, $\mathcal{D}_2$, $\mathcal{D}_3$ and $\mathcal{D}_4$ of Figure 5.16. Notice that $(H1)$ comes directly from Corollary 5.5.7. We show $(H2)$, $(H3)$ and $(H4)$ in the next section.

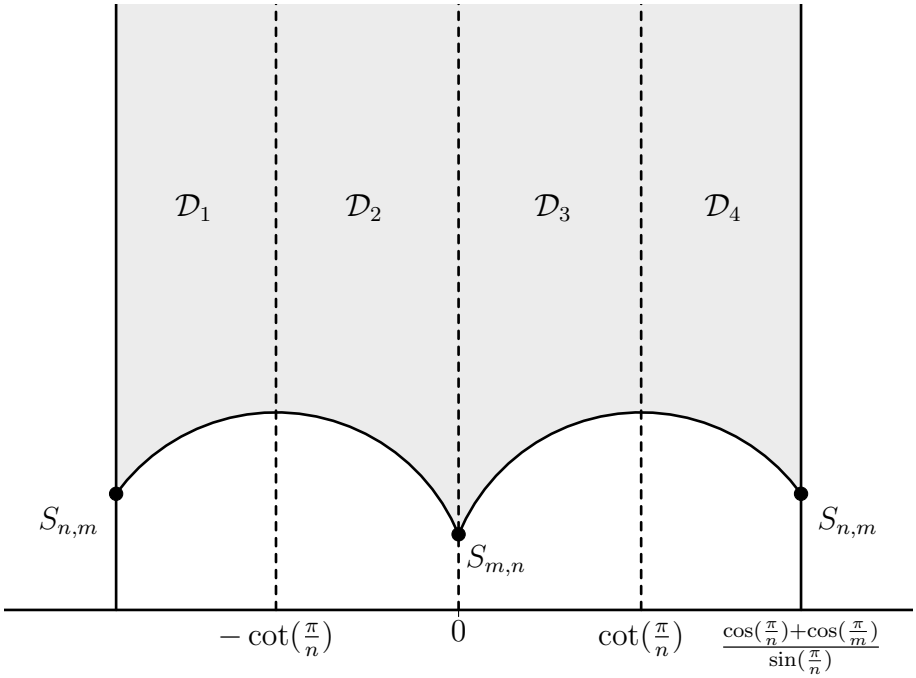

Figure 5.16: The fundamental domain $\mathcal{T}_{m,n}$ of the Teichmüller disk of $S_{m,n}$ and the four domains $\mathcal{D}_1$, $\mathcal{D}_2$, $\mathcal{D}_3$ and $\mathcal{D}_4$.

Remark 5.5.9. It is clear that the same result holds under the following modified hypotheses:

$(H2)$ For any distinct $d, d' \in \mathcal{P}$,

$$K(d, d') \leq K(\infty, a)$$

$(H3)$ For any distinct $d, d' \in \mathcal{P}$ such that $\gamma_{d,d'}$ intersects $\mathcal{D}$ and $(d, d') \neq (\infty, a)$,

$$K(d, d') \leq \sin(\frac{\pi}{4}) K(\infty, a)$$

$(H\star)$ $\theta(X_0, \infty, a) \geq \frac{\pi}{4}$.

This is because $(H\star)$ and $(H3)$ automatically imply $(H1)$ and $(H4)$. In general, $(H\star)$ do not hold but we can see from §5.2.2 that it is the case on $\mathcal{D}_2$ and $\mathcal{D}_3$ if $n \leq 4$ and on $\mathcal{D}_1$ and $\mathcal{D}_4$ if $m \leq 4$.

5.6 Study of $K(d, d')$

In this section we give estimates on $K(d, d')$ which ensures that hypotheses $(H2)$, $(H3)$ and $(H4)$ are satisfied on each of the domains $\mathcal{D}_1$ to $\mathcal{D}_4$. More precisely:

Proposition 5.6.1. *Let m, n coprime, with $3 \leq n < m$. Then,*

(i) $K(\infty, \pm\cot(\pi/n)) = \dfrac{1}{\sin(\pi/n) l_0^2}$

(ii) $K(\infty, \pm\cot(2\pi/n)) \leq \dfrac{1}{2\cos(\pi/n)\sin(\pi/n) l_0^2}$

(iii) $K(\infty, \pm\dfrac{1 + 2\cos(\pi/n)\cos(\pi/m)}{2\sin(\pi/n)\cos(\pi/m)}) \leq \dfrac{1}{2\cos(\pi/m)\sin(\pi/n) l_0^2}$

Moreover, for every pair of distinct periodic directions (d, d') which is not the image of one of the preceeding pairs of directions by the diagonal action of the Veech group,

$$K(d, d') \leq \frac{1}{2\cos(\pi/m)\sin(\pi/n) l_0^2}.$$

Remark 5.6.2.

- Notice that for $n = 3$ we have $\cot(2\pi/3) = -\cot(\pi/3)$ and $2\cos(\pi/3) = 1$. In fact, Cases (i) and (ii) are merged.
- For $n = 4$, notice that $\cot(2\pi/n) = 0$. Interestingly, $K(\infty, \cot(2\pi/n))$ is realised by horizontal and vertical sides of $P(0)$ if $m \equiv 1 \mod 4$, while such sides do not intersect if $m \equiv 3 \mod 4$. In the latter case, it is the diagonals of $P(m-1)$, which are intersecting twice by Proposition 5.3.6, that achieve the best ratio for $K(\infty, \cot(2\pi/n))$.
- In cases (ii) and (iii), instead of having an equality we only give an upper bound. This is because the equality does not hold in general. More precisely, equality holds in case (ii) if and only if a horizontal side of $P(0)$ intersects a side of $P(0)$ (or $P(m-1)$) in direction $d' = \pm\cot(2\pi/n)$. Similarly, equality holds in case (iii) if and only if a horizontal side of $P(0)$ intersects a small diagonal of $P(1)$ (or $P(m-2)$) in direction $d' = \dfrac{1 + 2\cos(\pi/n)\cos(\pi/m)}{2\sin(\pi/n)\cos(\pi/m)}$. However, the upper bounds are sufficient to show that the hypotheses of Theorem 5.5.8 are satisfied.

Before proving the proposition, we start with a few preliminaries about the horizontal cylinder decomposition of $S_{m,n}$.

5.6.1 Length and height of horizontal cylinders

Lemma 5.6.3 (Length of horizontal saddle connections)**.** *Let m, n coprime, with $3 \leq n < m$. The three shortest length of horizontal saddle connections of $S_{m,n}$ are*

$$l_0 = \sin\frac{\pi}{m}, \qquad l_1 := 2\cos(\pi/n) l_0 \qquad \text{and} \qquad l_2 := 2\cos(\pi/m) l_0.$$

Further,

- *l_0 is the length of the systole of $S_{m,n}$ which is realised by sides of $P(0)$ and $P(m-1)$. There are two horizontal saddle connections of length l_0, and both lie in $P(0) \cap P(1)$ if n is even while if n is odd there is one such saddle connection in $P(0) \cap P(1)$ and one in $P(m-1) \cap P(m-2)$.*

- *l_1 is the length of the smallest diagonal of $P(0)$ and $P(m-1)$. If $n = 3$, there are no such diagonals but then $l_0 = l_1$. If $n = 4$ (then m is odd) and there is only one horizontal saddle connection of length l_1, the diagonal of $P(m-1)$. Else, there are two horizontal saddle connections of length l_1: both lie in $P(m-1)$ if n is odd while if n is even then one lie inside $P(0)$ and the other in $P(m-1)$.*

- *l_2 is the length of the long sides of $P(1)$ and $P(m-2)$. There are two such horizontal sides: both are sides of $P(m-2)$ if n is even while if n is odd then there is one such side in $P(m-2)$ and another in $P(1)$.*

Proof. First, the saddle horizontal saddle connections contained in $P(0)$ or $P(m-1)$ correspond by construction to sides or diagonals of a regular n-gon of side length $\sin(\frac{\pi}{m})$, and hence have length $\sin(\frac{\pi}{m})$, $2\cos(\frac{\pi}{n})\sin(\frac{\pi}{m})$ (if $n \geq 3$), $1 + 2\cos(\frac{2\pi}{n})\sin(\frac{\pi}{m})$ (if $n \geq 7$), and so on. Notice that $1 + 2\cos(\frac{2\pi}{n})\sin(\frac{\pi}{m})$ is already greater than l_2.
Next, apart from the small sides which correspond to sides of $P(0)$ or $P(m-1)$ and have already been counted, the smallest horizontal saddle connections contained in $P(1)$ or $P(m-1)$ are the long sides having length $l_2 = \sin(\frac{2\pi}{m}) = 2\cos(\frac{\pi}{m})\sin(\frac{\pi}{m})$.
Finally, all other horizontal saddle connections (which are not contained in $P(0)$, $P(1)$, $P(m-2)$ or $P(m-1)$) are longer. □

Similarly, we can compute the height of the smallest horizontal cylinders:

Lemma 5.6.4 (Height of horizontal cylinders)**.** *Let m, n coprime, with $3 \leq n < m$. The three smallest height of horizontal cylinders of $S_{m,n}$ are*

$$h_0 := \sin(\pi/n)l_0, \qquad h_1 := 2\cos(\pi/n)h_0 \qquad \text{and} \qquad h_2 := 2\cos(\pi/m)h_0.$$

Further,

- *There are two horizontal cylinders of height h_0. If m is odd and n is even then both are contained in $P(m-1) \cup P(m-2)$ and otherwise there is one such cylinder inside $P(m-1) \cup (m-2)$ and another contained in $P(0) \cup P(1)$.*

- *If $n \geq 5$, there are two horizontal cylinders of height h_1: if m is odd and n is even then both are contained in $P(0) \cup P(1)$ and otherwise there is one such cylinder inside $P(m-1) \cup P(m-2)$ and another contained in $P(0) \cup P(1)$. Else, if $n = 3$ then $h_0 = h_1$ and this case is the same as the preeceding, and if for $n = 4$ there is a single such horizontal cylinder, contained in $P(0) \cup P(1)$.*

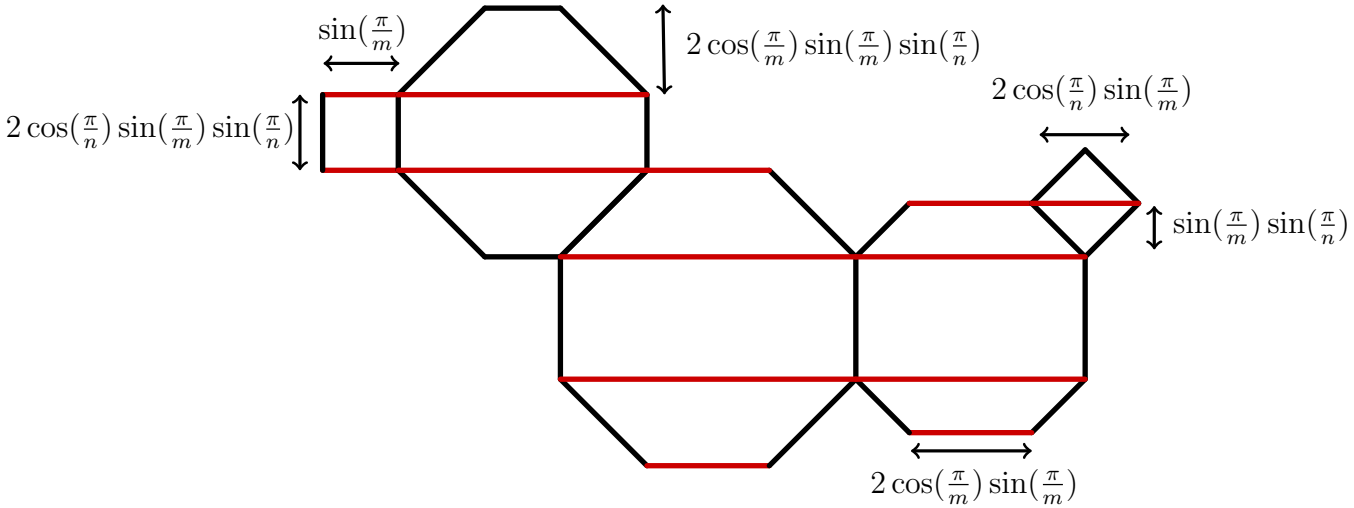

Figure 5.17: Lengths of horizontal saddle connections and height of the cylinders for $n = 4$ and $m = 5$.

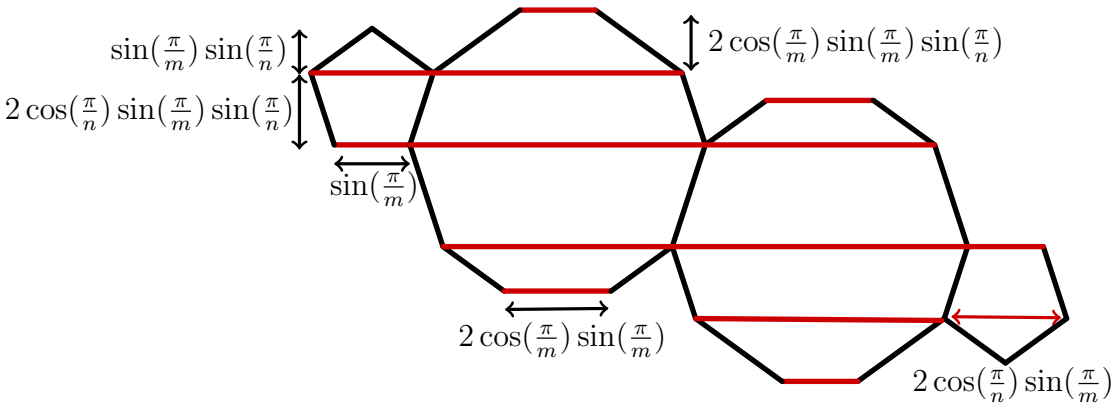

Figure 5.18: Lengths of horizontal saddle connections and height of the cylinders for $n = 5$ and $m = 4$.

- *h_2 is the height of the smallest horizontal cylinder which does not not intersect $P(0) \cup P(m-1)$. There are two such cylinders: if n is even then both cylinders are contained in $P(1) \cup P(2)$ and otherwise there is one such cylinder inside $P(1) \cup P(2)$ and the other inside $P(m-2) \cup P(m-3)$.*

Proof. First, the horizontal cylinders intersecting $P(0)$ or $P(m-1)$ have height among $\sin(\frac{k\pi}{n})\sin(\frac{\pi}{m})$ for $1 \leq k \leq n-1$. For $k \geq 3$, this is already higher than h_2.
Next, the horizontal cylinders intersecting $P(1)$ (resp. $P(m-2)$) but not $P(0)$ (resp. $P(m-1)$) have height among $\sin(\frac{k\pi}{n})\sin(\frac{2\pi}{m})$. The smallest such cylinder ($k=1$) have height h_2, and all other cylinders are bigger.
Finally, all other horizontal cylinders, which are not intersecting $P(0)$, $P(1)$, $P(m-2)$ or $P(m-1)$, have height greater than $\sin(\frac{k\pi}{n})\sin(\frac{3\pi}{m})$ and hence greater than h_2. □

We are now able to prove Proposition 5.6.1.

5.6.2 Proof of Proposition 5.6.1

Recall from Remark 5.5.5 that we can assume $d = \infty$ and compute $K(d, d')$ on $S_{m,n}$ directly. Let $d' \neq \infty$ and let α and β be two saddle connections on $S_{m,n}$ in respective directions $d = \infty$ and d'.

Case 1. If there are no non singular intersection. In this case $\mathrm{Int}(\alpha, \beta) \leq 1$ with at most a single singular intersection. In particular:

$$\frac{\mathrm{Int}(\alpha, \beta)}{\alpha \wedge \beta} \leq \frac{1}{l_v(\beta) l(\alpha)}$$

where $l_v(\beta)$ denotes the vertical length of β. This length is minimal if β crosses once a horizontal cylinder with small height. From Lemma 5.6.4, we deduce:

- If β is contained in a cylinder of height h_0, then

$$\frac{\mathrm{Int}(\alpha, \beta)}{\alpha \wedge \beta} \leq \frac{1}{l_0 h_0} = \frac{1}{\sin(\pi/n) l_0 l(\alpha)}$$

with equality if $\mathrm{Int}(\alpha, \beta) = 1$. The only such saddle connections β are, up to an horizontal twist, saddle connections in directions $d' = \pm\cot(\pi/n)$. As seen in Proposition 5.3.5, choosing α a horizontal side of $P(0)$ (hence of minimal possible length, l_0) and β a convenient side of either $P(m-1)$ or $P(0)$ in direction $d' = \cot(\pi/n)$ (resp. $d' = -\cot(\pi/n)$), and hence of length l_0, we obtain $\mathrm{Int}(\alpha, \beta) = 1$ so that

$$\frac{\mathrm{Int}(\alpha, \beta)}{\alpha \wedge \beta} = \frac{1}{l_0 h_0} = \frac{1}{\sin(\pi/n) l_0^2}.$$

- If β is contained in a cylinder of height h_1, and $n \neq 3$, then

$$\frac{\mathrm{Int}(\alpha,\beta)}{\alpha \wedge \beta} \leq \frac{1}{l_0 h_1} = \frac{1}{2\cos(\pi/n)\sin(\pi/n) l_0 l(\alpha)}$$

  with equality if $\mathrm{Int}(\alpha,\beta) = 1$. Outside the case $d' = \pm\cot(\pi/n)$, the only such β are saddle connections in direction $d' = \pm\cot(2\pi/n)$, corresponding to directions of sides of $P(0)$ (and $P(m-1)$ if n is odd).

- If β is contained in a cylinder of height h_2, then

$$\frac{\mathrm{Int}(\alpha,\beta)}{\alpha \wedge \beta} \leq \frac{1}{l_0 h_2} = \frac{1}{2\cos(\pi/m)\sin(\pi/n) l_0^2}$$

  with equality if $\mathrm{Int}(\alpha,\beta) = 1$. Outside the case $d' = \pm\cot(\pi/n)$, the only such β are saddle connections in direction $d' = \pm\dfrac{1+2\cos(\pi/n)\cos(\pi/m)}{2\sin(\pi/n)\cos(\pi/m)}$.

In all other cases, the vertical length of β is greater[2] so that we have:

$$\frac{\mathrm{Int}(\alpha,\beta)}{\alpha \wedge \beta} \leq \frac{1}{l_0 h_2} = \frac{1}{2\cos(\pi/m)\sin(\pi/n) l_0^2}.$$

Case 2 If there is at least one non-singular intersection, we distinguish two cases.

Case 2.1 If α has length l_0, we can assume by symmetry that α is a horizontal side of $P(0)$. Then,

(i) for every non singular intersection with α, β has to cross both cylinders adjacent to alpha, see Figure 5.19, hence a non-singular intersection with α accounts for a vertical length at least $h_1 + h_2 = (2\cos(\pi/m) + 2\cos(\pi/n))\sin(\pi/n) l_0$,

(ii) further, there are no simple curve contained in C_1 and C_1' which intersect α once outside the singularity, because such a saddle connection would have direction both smaller and greater than $\cot(\pi/n)$ (assuming the direction lie on the first quadrant, or $-\cot(\pi/n)$ if the direction lie on the second quadrant) . In particular, if there is exactly one non singular intersection, then β has to cross vertically another cylinder C', and hence the vertical length of β must be at least $h_1 + h_2 + h_0 = (2\cos(\pi/m) + 2\cos(\pi/n) + 1)\sin(\pi/n) l_0$.

From the first remark we deduce that if there are $p \geq 2$ non singular intersections, then $\mathrm{Int}(\alpha,\beta) \leq p+1$ and

[2]Notice that crossing at least two horizontal cylinders gives a vertical lenght at least $2\sin(\pi/n) l_0$, which is greater than $2\cos(\pi/m)\sin(\pi/n) l_0^2$.

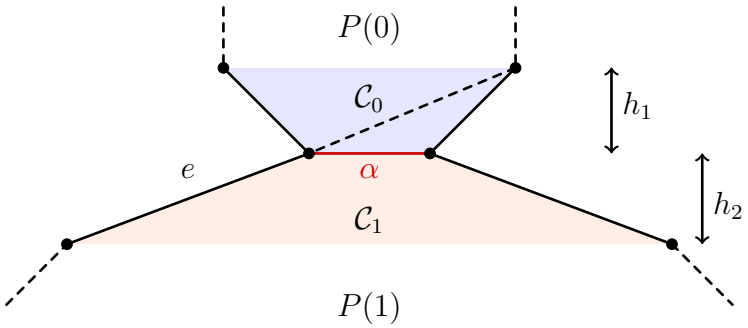

Figure 5.19: The two cylinders adjacent to α have height h_1 and h_2. Further, the direction of the side e of $P(1)$ is the same as the direction of the dashed diagonal of $P(0)$.

$$\begin{aligned}\frac{\mathrm{Int}(\alpha,\beta)}{\alpha\wedge\beta} &\leq \frac{p+1}{p(2\cos(\pi/m)+2\cos(\pi/n))\sin(\pi/n)l_0^2}\\ &\leq \frac{3}{2(2\cos(\pi/m)+2\cos(\pi/n))\sin(\pi/n)l_0^2},\end{aligned}$$

which is easily shown to be less than $\dfrac{1}{2\cos(\pi/m)\sin(\pi/n)l_0^2}$ for $3 \leq n < m$.

From the second remark we deduce that if there is a single non singular intersection, then $\mathrm{Int}(\alpha,\beta) \leq 2$ and

$$\frac{\mathrm{Int}(\alpha,\beta)}{\alpha\wedge\beta} \leq \frac{2}{(2\cos(\pi/m)+2\cos(\pi/n)+1)\sin(\pi/n)l_0^2}.$$

which is again less than $\dfrac{1}{2\cos(\pi/m)\sin(\pi/n)l_0^2}$.

Case 2.2 if α is not a systole, we have by Lemma 5.6.3

- If $n = 3$, $l(\alpha) \geq l_2 = 2\cos(\pi/m)l_0$.
- If $n \neq 3$, $l(\alpha) \geq l_1 = 2\cos(\pi/n)l_0$

Further, similarly to Case 2.1, β has to cross vertically a horizontal cylinder C before any non singular intersection with α, and another horizontal cylinder C' after any non-singular intersection with α (the two cylinders are not the same as no cylinder is glued to itself on $S_{m,n}$). In particular, if there are p non-singular intersections, then

$$l_v(\beta) \geq p \times (h(C) + h(C')).$$

Now, $h(C) + h(C') \geq 2h_0$, and equality can occur only if the two cylinders of height h_0 are adjacent, which is possible if and only if either $n = 4$ or by symmetry $m = 4$ (and hence $n = 3$ since we assumed $n < m$). Further,

(a) If $n = 3$, given that $l(\alpha) \geq l_2$ the inequality $h(C) + h(C') \geq 2h_0$ is sufficient to obtain

$$\frac{\mathrm{Int}(\alpha, \beta)}{\alpha \wedge \beta} \leq \frac{p+1}{2ph_0l_2} \leq \frac{2}{2h_0l_2} = \frac{1}{2\cos(\pi/m)\sin(\pi/n)l_0^2}$$

as required.

(b) If $n = 4$, then m is odd and the two cylinders of height h_0 are the two cylinders intersecting $P(m-1)$, so that we have equality above only when α and β are the two diagonals of $P(m-1)$ (up to a horizontal twist). As we have seen in Proposition 5.3.6, these diagonals intersect twice if and only if $m \equiv 3 \mod 4$, giving

$$\frac{\mathrm{Int}(\alpha, \beta)}{\alpha \wedge \beta} = \frac{2}{2h_0l(\alpha)} = \frac{1}{2\cos(\pi/n)\sin(\pi/n)l_0^2}.$$

The second possible case is $h(C) + h(C') = h_0 + h_1$, giving:

$$\begin{aligned}\frac{\mathrm{Int}(\alpha, \beta)}{\alpha \wedge \beta} &\leq \frac{p+1}{p(h_0+h_1)l_1} \\ &\leq \frac{2}{(h_0+h_1)l_1} = \frac{2}{(2\cos(\pi/n)+1)\times 2\cos(\pi/n)\sin(\pi/n)l_0^2}\end{aligned}$$

For $n \geq 5$, this last quantity is easily shown to be less than $\dfrac{1}{2\cos(\pi/m)\sin(\pi/n)l_0^2}$. However, this is not the case for $n = 4$, and one has to further notice that if $4 = n < m$ and if we are not in the setting of (b), then the two cylinders of height h_0 (which are contained in $P(m-1) \cup P(m-2)$) are not adjacent to the (single) cylinder of height h_0 which is contained in $P(0) \cup P(1)$, so that $h(C) + h(C') \geq h_0 + h_2$ and we get:

$$\begin{aligned}\frac{\mathrm{Int}(\alpha, \beta)}{\alpha \wedge \beta} &\leq \frac{p+1}{p(h_0+h_2)l_1} \\ &\leq \frac{2}{(h_0+h_2)l_1} = \frac{2}{(2\cos(\pi/m)+1)\times 2\cos(\pi/n)\sin(\pi/n)l_0^2} \\ &< \frac{1}{2\cos(\pi/m)\sin(\pi/n)l_0^2}\end{aligned}$$

as required.

End of the proof. According to the above study, we have

$$\frac{\mathrm{Int}(\alpha,\beta)}{\alpha\wedge\beta}\leq\frac{1}{2\cos(\pi/m)\sin(\pi/n)l_0^2}$$

unless:

- α is a systole and β is, up to a horizontal twist, a side of $P(m-1)$ (or $P(0)$), having direction $\pm\cot(\pi/n)$ and intersecting α once, and then

  $$\frac{\mathrm{Int}(\alpha,\beta)}{\alpha\wedge\beta}\leq\frac{1}{\sin(\pi/n)l_0^2}.$$

  Further, by Proposition 5.3.5, one can always find such intersecting sides, giving

  $$K(\infty,\pm\cot(\pi/n))=\frac{1}{\sin(\pi/n)l_0^2}$$

- α is a systole and, up to a horizontal twist, β has direction $\pm\cot(\frac{2\pi}{n})$, and then:

  $$\frac{\mathrm{Int}(\alpha,\beta)}{\alpha\wedge\beta}\leq\frac{1}{2\cos(\pi/n)\sin(\pi/n)l_0^2}.$$

5.6.3 Verifying (H2), (H3) and (H4)

Using Proposition 5.6.1, we directly deduce that $(H2)$ and $(H3)$ are satisfied on each of the domains $\mathcal{D}_i$. To show that $(H4)$ holds as well (for $m,n\leq 4$, see Remark 5.5.9), we first draw the images of the geodesics $\gamma_{\infty,\pm\cot(\pi/n)}$, $\gamma_{\infty,\pm\cot(2\pi/n)}$ and $\gamma_{\infty,\pm\frac{1+2\cos(\pi/n)\cos(\pi/m)}{2\sin(\pi/n)\cos(\pi/m)}}$ by the action the Veech group which intersect the fundamental domain $\mathcal{T}_{m,n}$. Those geodesics are represented in Figure 5.20.

Next,

1. On $\mathcal{D}_1$, the setting is $a=-\cot(\pi/n)$, $b=-\frac{\cos(\pi/m)}{\sin(\pi/n)}$, $c=\sin(\pi/n)$ and $X_0=S_{n,m}$ so that

   - $\theta(X_0,\infty,a)=\theta(X_0,\infty,-\cot(\pi/n))=\frac{\pi}{n}$
   - $\theta(X_0,a,a+2b)=\theta(X_0,-\cot(\pi/n),-\cot(\pi/n)-2\sin(\pi/n))=\frac{2\pi}{n}$

   And hence

   $$\frac{\sin\theta(X_0,\infty,a)}{\sin\theta(X_0,a,a+2b)}=\frac{sin(\pi/n)}{\sin(2\pi/n)}=\frac{1}{2\cos(\pi/n)}.$$

   But since by Proposition 5.6.1, for any (d,d') which is not the image of the pair $(\infty,\pm\cot(\pi/n))$,

   $$K(d,d')\leq\frac{1}{2\cos(\pi/n)}K(\infty,\pm\cot(\pi/n))$$

   we directly have that $(H4)$ is satisfied.

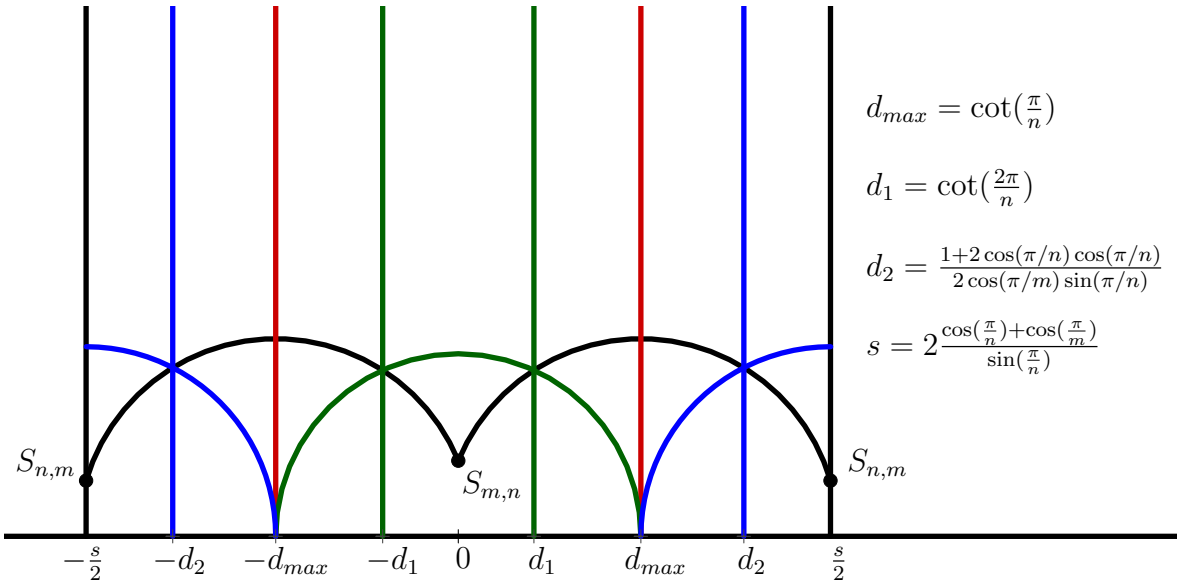

Figure 5.20: The geodesics $\gamma_{\infty,\pm\cot(\pi/n)}$, $\gamma_{\infty,\pm\cot(2\pi/n)}$ and $\gamma_{\infty,\pm\frac{1+2\cos(\pi/n)\cos(\pi/m)}{2\sin(\pi/n)\cos(\pi/m)}}$ and their images by the Veech group intersecting the fundamental domain.

2. On $\mathcal{D}_2$, the setting is $a = -\cot(\pi/n)$, $b = \frac{\cos(\pi/m)}{\sin(\pi/n)}$, $c = \sin(\pi/n)$ and $X_0 = S_{m,n}$ so that

   - $\theta(X_0, \infty, a) = \theta(X_0, \infty, -\cot(\pi/n)) = \frac{\pi}{m}$
   - $\theta(X_0, a, a+2b) = \theta(X_0, -\cot(\pi/n), -\cot(\pi/n) - 2\sin(\pi/n)) = \frac{2\pi}{m}$

   And hence

   $$\frac{\sin\theta(X_0,\infty,a)}{\sin\theta(X_0,a,a+2b)} = \frac{sin(\pi/m)}{\sin(2\pi/m)} = \frac{1}{2\cos(\pi/m)}.$$

   But since by Proposition 5.6.1, for any (d, d') which is not the image of the pairs $(\infty, \pm\cot(\pi/n))$, and $(\infty, \pm\cot(2\pi/n))$

   $$K(d,d') \leq \frac{1}{2\cos(\pi/m)} K(\infty, \pm\cot(\pi/n)),$$

   we directly have that $(H4)$ is satisfied.

By symmetry, we also deduce that $(H4)$ holds in the domains $\mathcal{D}_3$ and $\mathcal{D}_4$.

Conclusion. The hypotheses (H1), (H2), (H3) and (H4) are satisfied on any of the domains $\mathcal{D}_1$ to $\mathcal{D}_4$. Using Theorem 5.5.8, we conclude that

$$K(d,d')\sin\theta(X,d,d') \leq K(\infty, \pm\cot\frac{\pi}{n})\sin\theta(X,\infty,\pm\cot\pi n)$$

is satisfied on the whole fundamental domain associated to the surface $S_{m,n}$. As a conclusion, we obtain Theorem 5.1.3.

5.7 Proof of Theorem 5.5.8

Although the ideas of the proof of Theorem 5.5.8 are already explained in [BLM22, Section 7], we provide a proof in this section. Let $X \in \mathcal{D}$ and (d, d') and admissible pair of directions. Recall that we want to show

$$K(d, d') \sin \theta(X, d, d') \leq K(\infty, a) \sin \theta(X, \infty, a) \qquad (\clubsuit)$$

By convenience we will assume that $b > 0$, which is possible by symmetry. We start with the following Proposition, which is a direct generalisation of Proposition 7.8 of [BLM22] and hence which we will not prove (see also Proposition 5.7 of [Bou23]).

Proposition 5.7.1. *Let $a \in \mathbb{R}$, and $0 < b < c$. Let $\mathcal{D} \subset \mathbb{H}^2$ be the domain delimited by the geodesics $\gamma_{a,\infty}$, $\gamma_{a+b,\infty}$ and $\gamma_{a-c,a+c}$ and X_0 be the intersection point of $\gamma_{a+b,\infty}$ and $\gamma_{a-c,a+c}$. Then for any (d, d') with $a \leq d \leq a + b \leq d'$, and such that $\gamma_{d,d'}$ intersect the domain $\mathcal{D}$, the function*

$$F_{(d,d')} : X \in \mathcal{D} \mapsto \frac{\sin \theta(X, \infty, a)}{\sin \theta(X, d, d')}$$

is minimal at X_0 on the domain $\mathcal{D}$.

Case 1: $\gamma_{d,d'} \cap \mathcal{D} \neq \varnothing$. In this case, let us first remark that if $X \in \mathcal{R} := \{X \in \mathcal{D}, \theta(X, a, \infty) \geq \frac{\pi}{4}\}$, then we can directly deduce $(\clubsuit)$ from $(H3)$. In the following we will then assume that $X \notin \mathcal{R}$, see Figure 5.21.

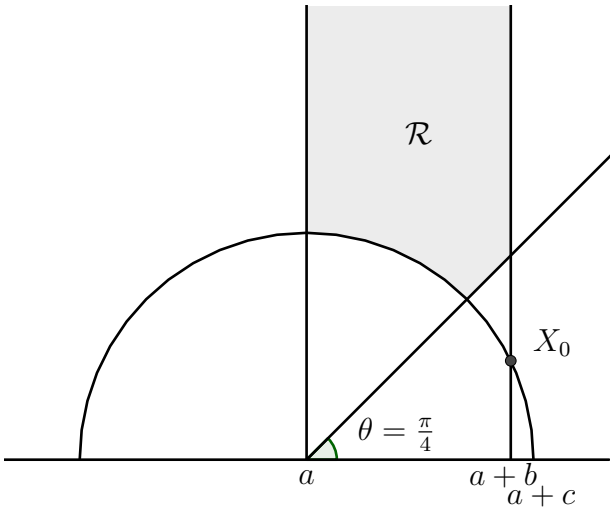

Figure 5.21: The domain $\mathcal{R}$.

Then, notice that we are in one of the three following cases:

(i) $a \leq d < a + b < d'$

(ii) $d < a < a + b < d'$

(iii) $d < a < d' \leq a + b$

Case 1.i: If $a \leq d < a + b < d'$, we deduce from $(H1)$ and Proposition 5.7.1 that

$$\begin{aligned}
K(d,d')\sin\theta(X,d,d') &\leq K(d,d')\frac{\sin\theta(X,d,d')}{\sin\theta(X,\infty,a)} \times \sin\theta(X,\infty,a) \\
&\leq K(d,d')\frac{\sin\theta(X_0,d,d')}{\sin\theta(X_0,\infty,a)} \times \sin\theta(X,\infty,a) \quad \text{by Proposition 5.7.1} \\
&\leq K(d,d')\sin\theta(X_0,d,d') \times \frac{\sin\theta(X,\infty,a)}{\sin\theta(X_0,\infty,a)} \\
&\leq K(d,d')\sin\theta(X_0,a,\infty) \times \frac{\sin\theta(X,\infty,a)}{\sin\theta(X_0,\infty,a)} \quad \text{by } (H1) \\
&\leq K(d,d')\sin\theta(X,a,\infty).
\end{aligned}$$

Case 1.ii: If $d < a < a + 2b < d'$, then for all $X \notin \mathcal{R}$, we have

$$\sin\theta(X,d,d') \leq \sin(\theta,X,a,a+2b)$$

so that by $(H4)$, we have

$$\begin{aligned}
K(d,d')\sin\theta(X,d,d') &\leq K(d,d')\sin\theta(X,a,a+2b) \\
&\leq K(\infty,a)\frac{\sin\theta(X_0,\infty,a)}{\sin\theta(X_0,a,a+2b)} \times \sin\theta(X,a,a+2b) \quad \text{by } (H4) \\
&\leq K(\infty,a)\sin\theta(X_0,\infty,a) \times \frac{\sin\theta(X,a,a+2b)}{\sin\theta(X_0,a,a+2b)} \\
&\leq K(\infty,a)\sin\theta(X,\infty,a) \quad \text{by Proposition 5.7.1}
\end{aligned}$$

Case 1.iii: If $d < a < d' \leq a + b$, let g_c be the reflection along the geodesic $\gamma_{a+c,a-c}$ and $(e,e') = (g_c \cdot d, g_c \cdot d')$. The hypotheses on d and d' entails $e' \geq a + b$ so that (e,e') correspond to a pair of direction in Case 1.i or Case 1.ii, and in particular for any $X \in \mathcal{D}$

$$K(e,e')\sin\theta(X,e,e') \leq K(\infty,a)\sin\theta(X,\infty,a) \tag{5.3}$$

Further,

- For any X inside the domain delimited by the geodesics $\gamma_{a+c,a-c}$, $\gamma_{\infty,a+b}$ and $\gamma_{e,e'}$, we have
$$\sin\theta(X,d,d') \leq \sin\theta(X,e,e').$$
By (5.3), we directly deduce (♣).

- If X lies outside this domain, we can find $X^* \in \gamma_{e,e'} \cap \mathcal{D}$ such that:

$$\theta(X^*, \infty, a) \leq \theta(X, \infty, a)$$

(see Figure 5.22). Using (5.3), we deduce:

$$\begin{aligned} \underbrace{K(d,d')}_{=K(e,e')} \sin\theta(X,d,d') &\leq K(e,e') \underbrace{\sin\theta(X^*,e,e')}_{=1} \\ &\leq K(\infty,a)\sin\theta(X^*,\infty,a) \\ &\leq K(\infty,a)\sin\theta(X,\infty,a) \end{aligned}$$

as required.

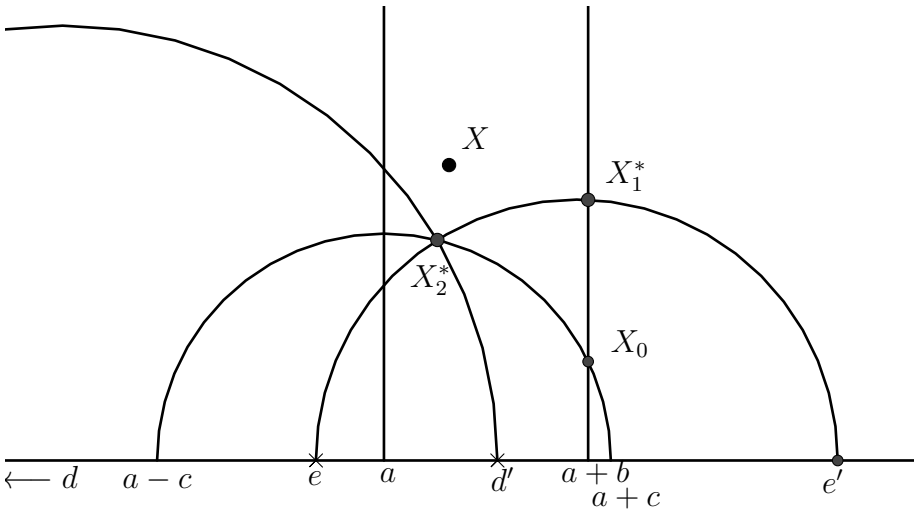

Figure 5.22: If $X \in \mathcal{D}$ lies outside the domain delimited by the geodesics $\gamma_{a+c,a-c}$, $\gamma_{\infty,a+b}$ and $\gamma_{e,e'}$, then $\min(\theta(X_1^\star, a, \infty), \theta(X_2^\star, a, \infty)) \leq \theta(X, a, \infty)$.

Case 2: $\gamma_{d,d'} \cap \mathcal{D} = \varnothing$**.** Let us distinguish two cases.

Case 2.1: If $\gamma_{d,d'}$ does not intersect one of images of the domain $\mathcal{D}$ adjacent to X_0, then for all $X \in \mathcal{D}$,

$$\sin\theta(X,d,d') \leq \sin\theta(X,a,\infty)$$

so that ($\clubsuit$) holds by $(H1)$.

Case 2.2: Else, for every $X \in \mathcal{D}$, we can always find an element g of the dihedral group generated by the reflections along $\gamma_{\infty,a+b}$ and $\gamma_{a+c,a-c}$ [3] such that:

[3] which may depend on X.

- $\gamma_{g\cdot d, g\cdot d'} \cap \mathcal{D} \neq \varnothing$
- $\sin\theta(X, d, d') \leq \sin\theta(X, g\cdot d, g\cdot d')$.

Hence, we deduce from Case 1 that

$$\begin{aligned} K(d,d')\sin\theta(X,d,d') &\leq K(g\cdot d, g\cdot d')\sin\theta(X, g\cdot d, g\cdot d') \\ &\leq K(\infty, a)\sin\theta(X,\infty,a) \end{aligned}$$

as required.

Bibliography

[BLM22] Julien Boulanger, Erwan Lanneau, and Daniel Massart. Algebraic intersection in regular polygons. 2022.

[BM10] Irene Bouw and Martin Möller. Teichmuller curves, triangle groups, and Lyapunov exponents. *Annals of Mathematics*, 172(1):85–139, 2010.

[Bou23] Julien Boulanger. Algebraic intersection, lengths and veech surfaces. *arXiv:2309.17165*, 2023.

[DPU19] Diana Davis, Irene Pasquinelli, and Corinna Ulcigrai. Cutting sequences on Bouw-Möller surfaces : an s-adic characterization. *Annales scientifiques de l'ENS*, 2019.

[EMM13] Joanna A. Ellis-Monaghan and Iain Moffatt. Graphs on surfaces - dualities, polynomials, and knots. In *Springer Briefs in Mathematics*, 2013.

[HL06] Pascal Hubert and Erwan Lanneau. Veech groups without parabolic elements. *Duke Mathematical journal*, 133, 2006.

[Hoo13] W. Patrick Hooper. Grid graphs and lattice surfaces. *International mathematics research notices*, 12:2657–2698, 2013.

[KZ02] Maxim Kontsevich and Anton Zorich. Connected components of the moduli space of abelian differentials with prescribed singularities. *Inventiones Mathematicae*, 153, 01 2002.

[Mas06] Howard Masur. Ergodic theory of translation surfaces. In *Handbook of dynamical systems. Vol. 1B*, pages 527–547. Elsevier B. V., Amsterdam, 2006.

[MM14] Daniel Massart and Bjoern Muetzel. On the intersection form of surfaces. *Manuscr. Math.*, 143(1-2):19–49, 2014.

Chapitre 6

Lower bound for KVol on the minimal stratum of translation surfaces

Résumé en français. Dans ce chapitre, correspondant à l'article [Bou23b] (soumis pour publication), on s'intéresse à la question de la borne inférieure de KVol sur l'ensemble des surfaces de translation de genre g à une seule singularité. On démontre le Théorème F, avec une discussion concernant chacune des composantes connexes de $\mathcal{H}(2g-2)$.

Lower bound for KVol on the minimal stratum of translation surfaces

Julien Boulanger

Abstract

In this paper we are interested in algebraic intersection of closed curves of a given length on translation surfaces. We study the quantity KVol, defined in [6] and studied in [6, 7, 2, 3], and we construct families of translation surfaces in each connected component of the minimal stratum $\mathcal{H}(2g-2)$ of the moduli space of translation surfaces of genus $g \geq 2$ such that KVol is arbitrarily close to the genus of the surface, which is conjectured to be the infimum of KVol on $\mathcal{H}(2g-2)$.

1 Introduction

Given a closed oriented surface X, the algebraic intersection $\mathrm{Int}(\cdot,\cdot)$ defines a symplectic bilinear form on the first homology group $H_1(X,\mathbb{R})$. When X is endowed with a Riemannian metric, we can define the quantity

$$\mathrm{KVol}(X) := \mathrm{Vol}(X) \sup_{\alpha,\beta} \frac{\mathrm{Int}(\alpha,\beta)}{l_g(\alpha) l_g(\beta)}$$

where the supremum ranges over all piecewise smooth closed curves α and β in X. Here, $\mathrm{Vol}(X)$ denotes the Riemannian volume, and $l_g(\alpha)$ (resp. $l_g(\beta)$) denotes the length of α (resp. β) with respect to the metric.

The study of KVol originates in the work of Massart [10] and Massart-Muetzel [12]. In fact, KVol is also well defined if the Riemannian metric has isolated singularities, and it has been studied recently specifically in the case of translation surfaces (see [6], [7], [2], [3]) for which one could hope to get explicit computations of KVol.

Although it is easy to make KVol go to infinity by pinching a non-separating curve, it cannot be made arbitrarily small: Massart and Muetzel [12] showed that for any closed oriented surface X with a Riemannian metric, we have $\mathrm{KVol}(X) \geq 1$ with equality if and only if X is a torus and the metric is flat. In light of this result, it is interesting to wonder what are the Riemannian (resp. hyperbolic,

flat) surfaces of fixed genus g having small KVol. This question turns out to be difficult to answer. In [12], KVol is studied as a function over the moduli space of hyperbolic surfaces of fixed genus: they provide asymptotic bounds when the systolic length goes to zero. In [7] Cheboui, Kessi and Massart extend the study of KVol to the moduli space of translation surfaces of genus 2 having a single singularity. Namely, they investigate the following quantity:

$$\mathcal{K}(\mathcal{H}(2)) := \inf_{X \in \mathcal{H}(2)} \mathrm{KVol}(X)$$

In particular, they conjecture that $\mathcal{K}(\mathcal{H}(2)) = 2$ and show that $\mathcal{K}(\mathcal{H}(2)) \leq 2$ by exhibiting a family of (square-tiled) translation surfaces $L(n+1, n+1)$ having KVol converging to 2 as n goes to infinity.

In this note, we tackle the same question in any genus $g \geq 2$. More precisely, we conjecture that:

$$\mathcal{K}(\mathcal{H}(2g-2)) := \inf_{X \in \mathcal{H}(2g-2)} \mathrm{KVol}(X) = g$$

and we construct surfaces in $\mathcal{H}(2g-2)$ having their KVol arbitrarily close to g, showing:

Theorem 1. *For all $g \geq 2$,*

$$\mathcal{K}(\mathcal{H}(2g-2)) \leq g.$$

It has to be remarked that translation surfaces with a single singularity are very specific surfaces and that the infimum of KVol over all Riemannian surfaces of genus g does not grow linearly with the genus as it is expected in the case of $\mathcal{H}(2g-2)$. In particular, as suggested by Sabourau to the author, a construction of [5] gives a surface X_g for each genus $g \geq 1$ such that

$$\mathrm{KVol}(X) \leq C \frac{g}{\log(g+1)^2}$$

for a given constant $C > 0$. This bound can be obtained using Theorem 1.5 of [12], which compares KVol and the systolic volume, and the fact that the (homological) systolic volume of the surfaces constructed in [5] grows as $C' \dfrac{g}{\log(g+1)^2}$.

However, in the case of translation surfaces having a single singularity, it is not possible to construct similar surfaces, as Boissy and Geninska [1] (and independantly Judge and Parlier [8]) showed that in this setting the systolic volume has a linear bound in the genus. This is the reason why we expect the infimum of KVol over $\mathcal{H}(2g-2)$ to grow linearly with g.

Remark 1.0.1. Concerning the lower bound on KVol, Theorem 1.1 of [4] gives directly that for any constant $A > 0$, there exist $c_A > 0$ such that for any Riemannian surface X of genus g and such that $\mathrm{SysVol}(X) < A$, we have:

$$c_A \frac{g}{\log(g+1)^2} \leq \mathrm{KVol}(X).$$

It would be interesting to know whether the same inequality holds with a universal constant $c > 0$ which does not depend on A. It should be noted that such a result has recently been shown for hyperbolic surfaces in the case where the algebraic intersection is replaced by the geometric intersection, see [13]. The proof in this later case relies on the existence of a short figure eigth geodesic.

Connected components of $\mathcal{H}(2g-2)$. With Theorem 1 in mind, it is interesting to wonder whether the bound g can be achieved in any connected component of $\mathcal{H}(2g-2)$. Kontsevich and Zorich [9] classified the connected components of any stratum of translation surfaces, and showed in particular that for any $g \geq 4$, $\mathcal{H}(2g-2)$ has three connected components: the hyperelliptic component $\mathcal{H}^{hyp}(2g-2)$, and two other connected components $\mathcal{H}^{even}(2g-2)$ and $\mathcal{H}^{odd}(2g-2)$ distinguished by the spin invariant. In genus 2, the only connected component is hyperelliptic while in genus 3 there are two connected components : odd spin and hyperelliptic. It turns out that the family of surfaces we construct in Section 2 belongs to odd spin for any $g \geq 2$. In Section 3 we give a family of hyperelliptic surfaces H_g^n and even spin M_g^n surfaces such that both $\mathrm{KVol}(H_g^n)$ and $\mathrm{KVol}(M_g^n)$ converge to g as n goes to infinity. In particular, we show:

Theorem 2.

- $\mathcal{K}(\mathcal{H}^{hyp}(2g-2)) \leq g$ *for any* $g \geq 2$.
- $\mathcal{K}(\mathcal{H}^{odd}(2g-2)) \leq g$ *for any* $g \geq 3$.
- $\mathcal{K}(\mathcal{H}^{even}(2g-2)) \leq g$ *for any* $g \geq 4$.

We assume familiarity with the geometry of translation surfaces, and encourage the reader to check out the surveys [15], [14] and [11].

Acknoledgments. I would like to thank E. Lanneau, D. Massart and S. Sabourau for useful and enlightening discussions related to the work presented here.

2 Proof of Theorem 1

In this section, we prove Theorem 1 by exhitibing a family of surfaces L_g^n for $g, n \geq 2$, (having odd spin parity and) such that L_g^n has genus g for each $n \geq 2$ and

$$\lim_{n\to\infty} \mathrm{KVol}(L_g^n) = g.$$

2.1 Construction of the surface L_g^n.

Given $g \geq 2$ and $n \geq 2$, define L_g^n as the $(g(n+1)-1)$-square translation surface of genus g with a single conical point which forms a staircase with steps of lengths and height n, as in Figure 1.

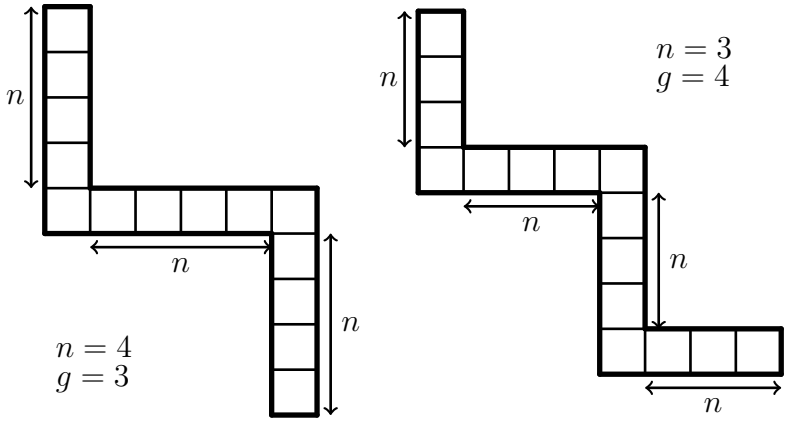

Figure 1: The surface L_3^4 on the left, and L_4^3 on the right. The identifications are such that each horizontal (resp. vertical) rectangle is a cylinder.

A basis of the homology. Let $e_1, \cdots, e_g$ (resp. $f_1, \cdots f_g$) be the horizontal (resp. vertical) saddle connections (see Figure 2), seen as homology classes. Notice that for odd i, e_i can be represented by a closed geodesic which do not pass through the singularity. We will refer to such homology classes as *non singular* homology classes. This is also the case of f_j for even j. On the contrary, for even i (resp. odd j), the class e_i (resp. f_j) will be called *singular* as it can only be represented by closed geodesics passing through the singularity.

The intersection matrix of the e_i and f_j is given by the following table:

$\text{Int}(e_i, f_j)$	e_1	e_2	e_3	e_4	e_5	$\cdots$	e_g
f_1	1	-1	0	0	0	$\cdots$	0
f_2	0	1	0	0	0		0
f_3	0	-1	1	-1	0		0
f_4	0	0	0	1	0		0
f_5	0	0	0	-1	1	$\cdots$	0
$\cdots$						$\cdots$	$\cdots$
f_g	0	0	0	0	0	$\cdots$	1

To see this, notice that for odd i, the fact that e_i can be represented by a non-singular closed curve gives $\text{Int}(e_i, f_j) = \delta_{i,j}$. The same holds for f_j for

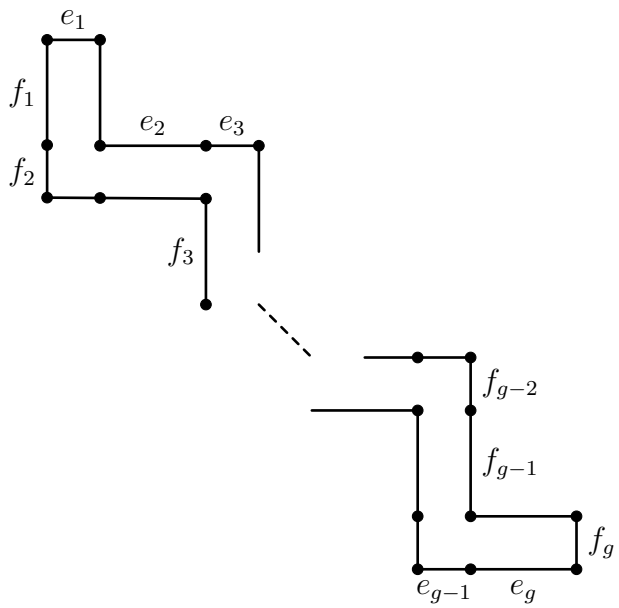

Figure 2: The horizontal and vertical saddle connections $e_1, \cdots, e_g$, resp. $f_1, \cdots, f_g$.

even j. Next, given i even, the holomogy class $e_{i-1} + e_i + e_{i+1}$ corresponds to a non-singular curve in L_g^n which intersects f_j if and only if $j = i$. In particular,

$$\mathrm{Int}(e_{i-1}, f_j) + \mathrm{Int}(e_i, f_j) + \mathrm{Int}(e_{i+1}, f_j) = \delta_{i,j}$$

But the fact that both $i-1$ and $i+1$ are odd gives $\mathrm{Int}(e_{i-1}, f_j) = \delta_{i-1,j}$ and $\mathrm{Int}(e_{i+1}, f_j) = \delta_{i+1,j}$, so that

$$\mathrm{Int}(e_i, f_j) = \delta_{i,j} - \delta_{i-1,j} - \delta_{i+1,j}$$

Further, as $\mathrm{Int}(e_{i-1}+e_i+e_{i+1}, e_i) = 0$ for even i (resp. $\mathrm{Int}(f_{j-1}+f_j+f_{j+1}, f_j) = 0$ for odd j), the same arguments gives that the e_i's (resp. the f_j's) do not intersect each other.

As a concluding remark, notice that closed geodesics representing e_1 and f_1 are intersecting once and have respective length 1 and n, and in particular:

$$\mathrm{KVol}(L_g^n) \geq \mathrm{Vol}(L_g^n) \cdot \frac{\mathrm{Int}(e_1, f_1)}{l(e_1)l(f_1)} = (g(n+1) - 1) \cdot \frac{1}{n}.$$

Computation of the spin. As explained in [9, Section 3], it is easy to compute the spin parity of an abelian differential ω given a symplectic basis of the first homology group $(a_i, b_i)_{1 \leq i \leq g}$ represented by smooth curves, and we have:

$$\varphi(\omega) = \sum_{i=1}^{g} \Omega(a_i)\Omega(b_i) \mod 2.$$

where $\Omega(a_i) = ind_{a_i} + 1$ and $2\pi \cdot ind_{a_i}$ is the total change of angle between the tangent vector to the curves and the horizontal foliation. Further, for any $a, b \in H^1(X, \omega)$, we have:

$$\Omega(a+b) = \Omega(a) + \Omega(b) + \mathrm{Int}(a,b). \tag{1}$$

In the case of L_g^n, we use the basis $(a_i, b_i)_{1 \leq i \leq g}$ defined by:

$$a_i = \begin{cases} e_i & \text{if } i \text{ is even} \\ e_{i-1} + e_i + e_{i+1} & \text{if } i \text{ is odd} \end{cases} \qquad \text{and} \qquad b_i = f_i.$$

The index of each a_i is 0 as well as the index of each b_i for even i because they correspond to non-singular homology classes. Further, using (1) we show that $\Omega(b_1) = 0$, as well as $\Omega(b_g) = 0$ if g is odd, while $\Omega(b_i) = 1$ for odd i, $1 < i < g$. In particular, we deduce that the spin structure of L_g^n has odd parity.

Further, it should be remarked that although L_2^n is hyperelliptic for any $n \geq 2$, L_g^n is not hyperelliptic if $g \geq 3$. This is because an hyperelliptic involution would have to fix each cylinder, and hence must act as an involution of $R_1 \cup C_1$ (with the notations of Figure 3) so that it must act as an involution on C_1, but it must also act as an involution of $C_1 \cup R_2 \cup C_2$, which is then impossible.

A useful model for the surfaces L_g^n. Let us finish this section by giving another model for L_g^n, which, although less intuitive at first sight, turns out to be helpful for the study of the intersections of saddle connections on L_g^n. This model is obtained from a cut and paste procedure which is described in Figure 3 in the example of L_4^3. The main idea is to glue together all the squares at the corners of L_g^n to form a *core staircase* to which are attached the *long rectangles*. A general picture is given in Figure 4.

2.2 An upper bound on $KVol(L_g^n)$

In this section we provide estimates for KVol on the surface L_g^n. Recall from [12, Section 3] that the supremum in the definition of KVol can be taken over pairs of simple closed geodesics. In the case of translation surfaces, closed geodesics are homologous to unions of saddle connections. Since saddle connections are closed curves on L_g^n (which has a single singularity), we have:

$$\mathrm{KVol}(L_g^n) = \sup_{\alpha,\beta \text{ saddle connections}} \frac{\mathrm{Int}(\alpha,\beta)}{l(\alpha)l(\beta)}$$

In this setting, we show:

Theorem 2.2.1. *For any pair of saddle connections α, β on L_g^n, we have*

$$\frac{Int(\alpha,\beta)}{l(\alpha)l(\beta)} \leq \frac{1}{n}(\frac{n+1}{n})^2 + \frac{6}{n^2} \tag{2}$$

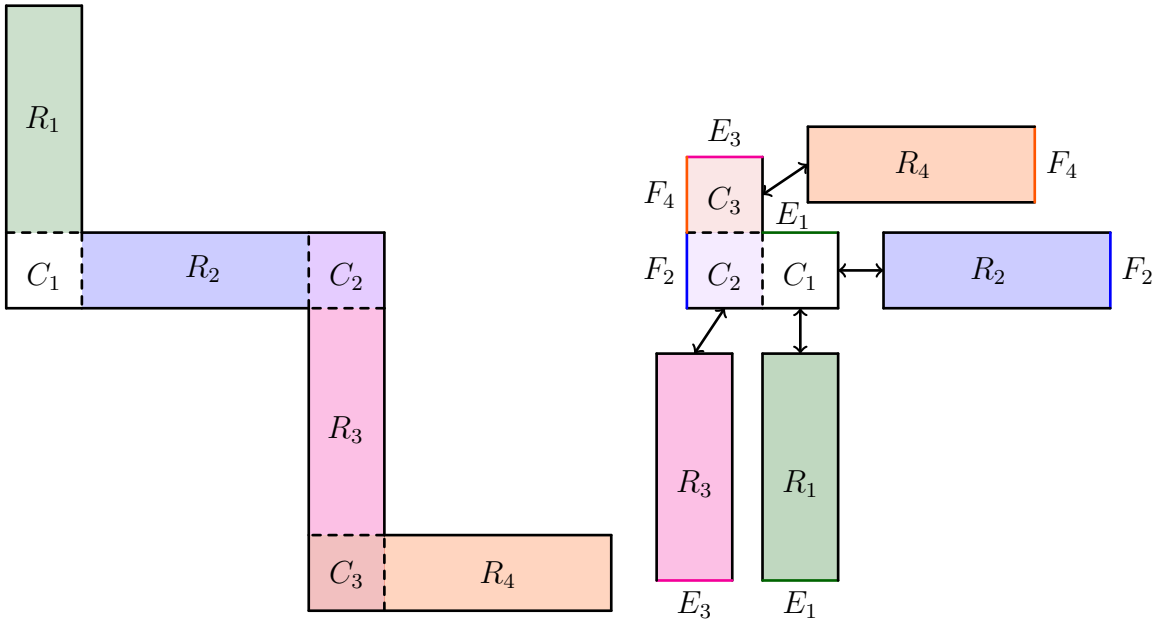

Figure 3: L_4^3 and its alternative model.

From this result, we deduce directly that

$$\mathrm{KVol}(L_g^n) \leq (g(n+1)-1)(\frac{(n+1)^2}{n^3} + \frac{6}{n^2}).$$

Further, as remarked in Section 2,

$$\frac{g(n+1)-1}{n} \leq KVol(L_g^n),$$

so that, in particular, $\mathrm{KVol}(L_g^n) \longrightarrow g$ as n goes to infinity, proving Theorem 1.

Proof of Theorem 2.2.1. Let α and β be two saddle connections on L_g^n. We decompose the homolgy class of α (resp. β) in the basis $(e_1, \cdots, e_g, f_1, \cdots, f_g)$ of the homology. The first case we deal with is as follows:

Lemma 2.2.2. *For any saddle connection α in $L_{g,n}$ being in homology an integer combination of the e_i, i odd, and the f_j, j even, and any saddle connection β, we have*

$$l(\beta) \geq n|Int(\alpha, \beta)|$$

In particular

$$\frac{Int(\alpha, \beta)}{l(\alpha)l(\beta)} \leq \frac{1}{n}.$$

Proof of Lemma 2.2.2. As seen in the table of the intersections, the non-singular e_i or f_j do not intersect each other, and in particular do not intersect α. It

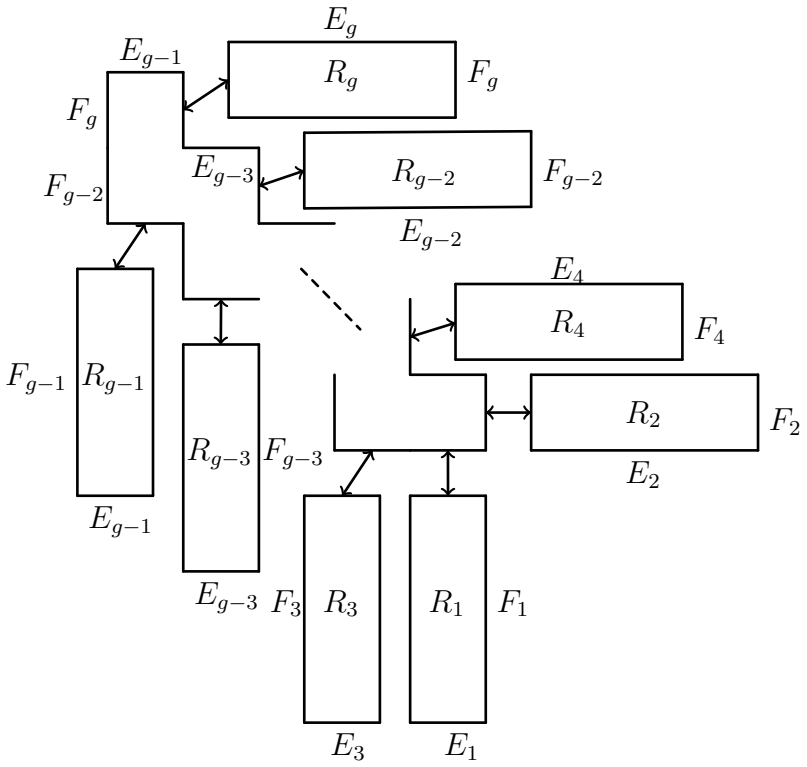

Figure 4: The alternative model for L_g^n is made of a core staircase to which are attached the long rectangles R_i. The curve E_i (resp. F_j) represents the homology class e_i (resp. f_j).

follows that if we decompose β in the basis of the homology $(e_1, f_1, \cdots, e_g, f_g)$, the intersection $\text{Int}(\alpha, \beta)$ will be at most the number of singular e_i and f_j in the decomposition. But each singular e_i or f_j in the decomposition of β corresponds to a trip through a long rectangle R_i and accounts for a length at least n, so that:

$$l(\beta) \geq n|\text{Int}(\alpha, \beta)|.$$

Given that $l(\alpha) \geq 1$, we get

$$\frac{\text{Int}(\alpha, \beta)}{l(\alpha)l(\beta)} \leq \frac{1}{n}.$$

□

In particular, we deduce from Lemma 2.2.2 that Equation (2) holds if either α or β is an integer combination of the non-singular e_i and f_j only. In the rest of the proof, we will assume that neither α nor β correspond to such saddle connections. In the alternative model for L_g^n, this says exactly that α and β have to cross a long rectangle R_i.

In particular, we can decompose the saddle connections α and β by cutting them each time they enters or leaves a rectangle R_i (lengthwise). This gives a decomposition into smaller (non-closed) segments $\alpha = \alpha_1 \cup \cdots \cup \alpha_k$ (resp. $\beta = \beta_1 \cup \cdots \cup \beta_l$) alternating between:

(i) long segments (of length at least n) inside a long rectangle R_i,

(ii) short segments which stay inside the core staircase of Figure 4.

By convention, we will include the endoints in the short segments, apart from the singularities (the possible singular intersection will be counted separately). Since long segments and short segments are alternating, there are at least $\max(\lfloor k/2 \rfloor, 1)$ long segments and there are at most $\lceil k/2 \rceil$ short segments for α. Notice that:

- Long segments and short segments do not lie in the same part of the surface, hence they cannot intersect.
- Any two short segments α_i and β_j intersect at most once, as no side of the core staircase is identified to another side of the core staircase.
- Concerning the intersection of long segments, we have:

Lemma 2.2.3. *Given two long segments α_i and β_j in the same rectangle R, we have*

$$\frac{\#\alpha_i \cap \beta_j}{l(\alpha_i) l(\beta_j)} \leq \frac{1}{n} (\frac{n+1}{n})^2 + \frac{1}{n^2}$$

where $\#\alpha_i \cap \beta_j$ denotes the cardinal of the set of intersection points.

Proof. The proof of this Lemma is similar to the proof of Proposition 2.5 in [7]. We first identify the sides of each long rectangle R to form a torus T. Then, for each long segment α_i (resp. β_j) contained in the long rectangle R, we construct a closed curve $\tilde{\alpha}_i$ (resp. $\tilde{\beta}_j$) on the corresponding torus T. This construction can be done by adding to α_i (resp. β_j) a small portion of curve of length at most one, and removes at most one intersection, so that

(a) $\mathrm{Int}(\tilde{\alpha}_i, \tilde{\beta}_j) \geq \#\alpha_i \cap \beta_j - 1$.

(b) $l(\tilde{\alpha}_i) \leq l(\alpha_i) + 1$ and $l(\tilde{\beta}_j) \leq l(\beta_j) + 1$.

Moreover, $l(\alpha_i) \geq n$ and $l(\beta_j) \geq n$ so that:

(c) $l(\alpha_i) + 1 \leq l(\alpha_i)(1 + 1/n)$ (and the same holds for β_j),

(d) $1 \leq \dfrac{l(\alpha_i) l(\beta_j)}{n^2}$.

Now, since $\mathrm{KVol}(T) = 1$ on the flat torus T, and given that the rectangle R has area n (and so does the torus T), we get:

$$\frac{\mathrm{Int}(\tilde{\alpha}_i, \tilde{\beta}_j)}{l(\tilde{\alpha}_i) l(\tilde{\beta}_j)} \leq \frac{1}{n}.$$

In particular

$$\begin{aligned}
\#\alpha_i \cap \beta_j &\leq \mathrm{Int}(\tilde{\alpha}_i, \tilde{\beta}_j) + 1 && \text{by (a)} \\
&\leq \frac{1}{n}(l(\tilde{\alpha}_i) l(\tilde{\beta}_j)) + 1 \\
&\leq \frac{1}{n}(l(\alpha_i) + 1)(l(\beta_j) + 1) + 1 && \text{by (b)} \\
&\leq \frac{1}{n} l(\alpha_i)(1 + \frac{1}{n}) l(\beta_j)(1 + \frac{1}{n}) + \frac{l(\alpha_i) l(\beta_j)}{n^2} && \text{by (c) and (d).}
\end{aligned}$$

This gives Theorem 2.2.1. □

End of the proof. Counting all intersections, we have:

$$\mathrm{Int}(\alpha, \beta) \leq (\sum_{i,j} \#\alpha_i \cap \beta_j) + 1$$

where the added intersection accounts for the possible singular intersection. Using the preceeding estimates, we have:

$$\begin{aligned}
\mathrm{Int}(\alpha, \beta) &\leq \left(\sum_{\alpha_i, \beta_j \text{ long segments}} \#\alpha_i \cap \beta_j \right) + \left(\sum_{\alpha_i, \beta_j \text{ short segments}} \#\alpha_i \cap \beta_j \right) + 1 \\
&\leq \left(\sum_{\alpha_i, \beta_j \text{ long segments}} (\frac{1}{n}(\frac{n+1}{n})^2 + \frac{1}{n^2}) l(\alpha_i) l(\beta_j) \right) + \left(\sum_{\alpha_i, \beta_j \text{ short segments}} 1 \right) + 1 \\
&\leq (\frac{1}{n}(\frac{n+1}{n})^2 + \frac{1}{n^2}) \left(\sum_{\alpha_i, \beta_j \text{ long segments}} l(\alpha_i) l(\beta_j) \right) + \lceil \frac{k}{2} \rceil \lceil \frac{l}{2} \rceil + 1 \\
&\leq (\frac{1}{n}(\frac{n+1}{n})^2 + \frac{1}{n^2}) l(\alpha) l(\beta) + \lceil \frac{k}{2} \rceil \lceil \frac{l}{2} \rceil + 1
\end{aligned}$$

Now, since there are at least $\max(\lfloor k/2 \rfloor, 1)$ long segments of α, each long segment having length at least n, we get $l(\alpha) \geq \max(\lfloor k/2 \rfloor, 1) n$, so that $\frac{k-1}{2} \leq \frac{l(\alpha)}{n}$, and

$$\lceil \frac{k}{2} \rceil \leq \frac{k+1}{2} \leq \frac{l(\alpha)}{n} + 1 \leq \frac{2 l(\alpha)}{n}$$

where the last inequality comes from $l(\alpha) \geq n$. Similarly, we have

$$\lceil \frac{l}{2} \rceil \leq \frac{l+1}{2} \leq \frac{2 l(\beta)}{n}$$

so that

$$\begin{aligned}\mathrm{Int}(\alpha,\beta) &\leq (\frac{1}{n}(\frac{n+1}{n})^2+\frac{1}{n^2})l(\alpha)l(\beta)+\frac{4}{n^2}l(\alpha)l(\beta)+1\\ &\leq (\frac{1}{n}(\frac{n+1}{n})^2+\frac{5}{n^2})l(\alpha)l(\beta)+\frac{l(\alpha)l(\beta)}{n^2}\end{aligned}$$

again using that $l(\alpha)\geq n$ and $l(\beta)\geq n$. □

3 Even spin and hyperelliptic families

We conclude this paper by giving a hyperelliptic family of surfaces H_g^n for $g\geq 3$ and an even spin family of surfaces M_g^n (for $g\geq 4$) such that for fixed g, $\mathrm{KVol}(H_g^n)$ and $\mathrm{KVol}(M_g^n)$ converge to g as n goes to infinity.

The proof is in fact similar to the case of L_g^n, as each surface can be decomposed into core polygons (giving rise to short segments) and long rectangles (giving rise to long segments). These two families of surfaces have the property that each edge of a core polygon is glued to an edge of a long rectangle, which allows to generalize Lemma 2.2.3. Further, the curves staying in the core polygons do not intersect each other and the conclusion of Lemma 2.2.2 can be generalized to these families of surfaces. This allows to give bounds for $\mathrm{KVol}(H_g^n)$ and $\mathrm{KVol}(M_g^n)$ which are easily shown to converge to g as g is fixed and n goes to infinity.

3.1 The family H_g^n

A convenient way to construct a family of hyperelliptic surfaces is to copy the staircase model of the double regular $(2g+1)$-gon. However, we need each *long rectangle* to have area n. One way to do this is to set the lengths of the horizontal and vertical curves e_i and f_j drawn in the left of Figure 5 as

$$l(e_i)=n^{\frac{g-i-1}{g-1}} \text{ and } l(f_j)=n^{\frac{j-1}{g-1}}.$$

Next, we distinguish the core polygons C_i and the big rectangles R_i and proceed with the proof as in the case of L_g^n. Notice that the e_i's (resp. the f_j's) are pairwise non-intersecting and that the intersection of the e_i and the f_j is given by the following table:

$\mathrm{Int}(e_i,f_j)$	e_1	e_2	e_3	e_4	e_5	$\cdots$
f_1	1	0	0	0	0	$\cdots$
f_2	-1	1	0	0	0	$\cdots$
f_3	1	-1	1	0	0	$\cdots$
f_4	-1	1	-1	1	0	$\cdots$
f_5	1	-1	1	-1	1	$\cdots$
$\cdots$	$\cdots$	$\cdots$	$\cdots$	$\cdots$	$\cdots$	$\cdots$

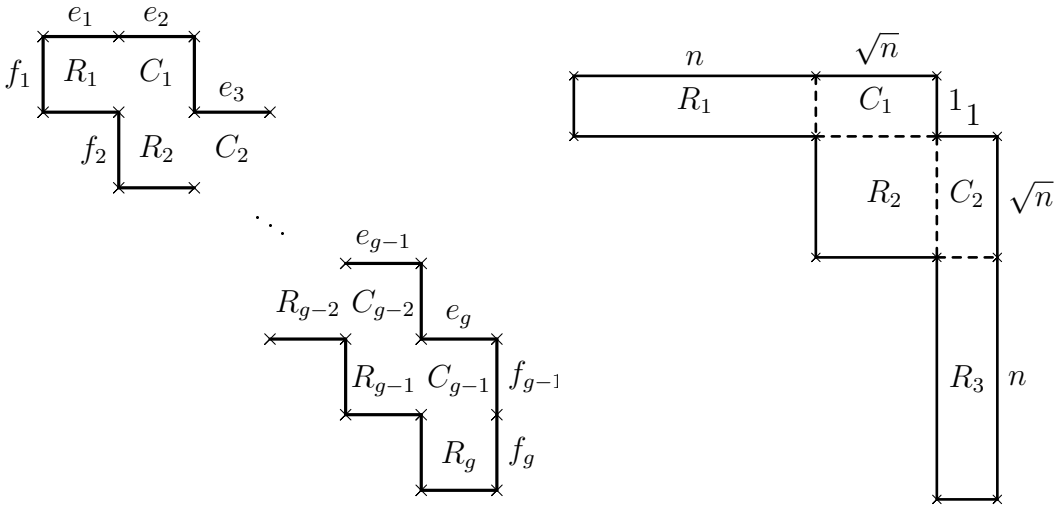

Figure 5: On the left, a combinatorial model for H_g^n. On the right, the example of H_3^n.

This allows to get an adapted version of Lemma 2.2.2:

Lemma 3.1.1. *The closed saddle connections γ contained in the core polygons correspond to the homology classes e_i, f_{i-1} and $e_i + f_{i-1}$ for $2 \leq i \leq g$.*
For any such saddle connection γ and any other saddle connection g, we have:

$$\frac{Int(\gamma, g)}{l(\gamma)l(g)} \leq \frac{1}{n}.$$

Further, similarly to Lemma 2.2.3, we have:

Lemma 3.1.2. *For any two saddle connections α and β which are not contained in the core polygons C_i, we have*

$$\frac{Int(\alpha, \beta)}{l(\alpha)l(\beta)} \leq \frac{1}{n}(1 + n^{-\frac{1}{g}})^2 + \frac{6}{n^2}.$$

Using that the area of H_g^n is $gn + (g-1)n^{\frac{g-1}{g}}$, we get that

$$g + (g-1)n^{\frac{-1}{g}} \leq KVol(H_g^n) \leq (g + (g-1)n^{\frac{-1}{g}})((1 + n^{-\frac{1}{g}})^2 + \frac{6}{n}),$$

where the lover bound comes from the fact that e_1 and f_1 are intersecting once, and $l(e_1)l(f_1) = n$. Hence, for fixed g, $\mathrm{KVol}(H_g^n)$ goes to g as n goes to infinity.

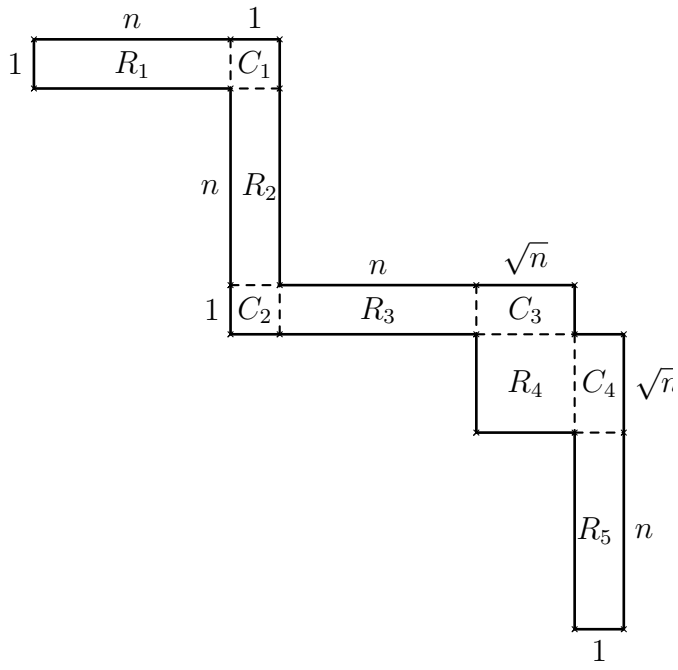

Figure 6: The surface M_5^n.

3.2 The family M_g^n

Similarly to L_g^n and H_g^n, it is possible to construct an even spin family of translation surfaces M_g^n, such that for any fixed $g \geq 4$, $\mathrm{KVol}(M_g^n)$ goes to g as n goes to infinity. For example, construct each M_g^n from H_3^n by adding steps as in L_g^n, see Figure 6. As we have seen in the case of L_g^n, the operation of adding steps do not change the parity of the spin structure. In particular, the parity of the spin structure of M_g^n is the same as H_3^n, that is even. Further, similarly to L_g^n, the surface M_g^n is not hyperelliptic as an hyperelliptic involution would have to fix each cylinder, and hence act as an involution of C_2, R_3 and C_3 but also $C_2 \cup R_3 \cup C_3$, which is impossible. In the case of M_g^n, an argument similar to the previous cases show:

$$\frac{gn + 2\sqrt{n} + (g-3)}{n} \leq \mathrm{KVol}(M_g^n) \leq \frac{gn + 2\sqrt{n} + (g-3)}{n}((1 + \frac{1}{\sqrt{n}})^2 + \frac{6}{n}).$$

References

[1] Boissy, C. and Geninska, S. "Systoles in translation surfaces." *Bull. de la SMF* 149, no. 2 (2021): 417-438.

[2] Boulanger, J. and Lanneau, E. and Massart, D. "Algebraic intersection in regular polygons." *arXiv 2110.14235* (2022).

[3] Boulanger, J. "Algebraic intersection, lengths and Veech surfaces." *arXiv* (2023).

[4] , Balacheff, F. and Parlier, H. and Sabourau, S. "Short loop decompositions of surfaces and the geometry of jacobians." *Geometric And Functionnal Analysis* 22 (2012): 37-73.

[5] Buser, P. and Sarnak, P, "On the period matrix of a Riemann surface of large genus (with an Appendix by J.H. Conway and N.J.A. Sloane)." *Invent. Math.* 117 (1994): 27–56.

[6] Cheboui, S. and Kessi, A. and Massart, D. "Algebraic intersection for translation surfaces in a family of Teichmüller disks." *Bull. Soc. Math. France* 149, no. 4 (2021): 613–640.

[7] Cheboui, S. and Kessi, A. and Massart, D. "Algebraic intersection for translation surfaces in the stratum $\mathcal{H}(2)$." *C. R. Math. Acad. Sci. Paris*, 359 (2021): 65–70.

[8] Judge, C. and Parlier, H. "The maximum number of systoles for genus two Riemann surfaces with abelian differentials." *Comment. Math. Helv.* 94, no. 2 (2019): 399-437.

[9] , Kontsevich, M. and Zorich, A. "Connected components of the moduli spaces of Abelian differentials with prescribed singularities." *Invent. Math.* 153 (2003): 631–678.

[10] Massart, D. "Normes stables des surfaces." *Comptes Rendus de l'Académie des Sciences - Series I - Mathematics* 324, no. 2 (1997): 221-224.

[11] Massart, D. "A short introduction to translation surfaces, Veech surfaces, and Teichmüller dynamics." *Surveys in geometry I*, Springer, (2022): 343–388.

[12] Massart, D. and Muetzel, B. "On the intersection form of surfaces." *Manuscr. Math.* 143, no. 1-2 (2014): 19–49.

[13] Torkaman, T. "Intersection number, length and systole on compact hyperbolic surfaces." *arXiv:2306.09249* (2023).

[14] Wright, A. "From rational billards to dynamics on moduli spaces." *Bull. Amer. Math. Soc.* 53, no. 1 (2016): 41-56.

[15] Zorich, A. "Flat surfaces." *Frontiers in number theory, physics, and geometry. I*, Springer, Berlin, 2006: 437–583.

Chapitre 7

Connection points on the double heptagon

Résumé en français. Ce chapitre correspond à l'article [Bou], publié au *Bulletin de la SMF*. On s'intéresse au flot directionnel sur les surfaces de translation obtenues à partir de deux $(2n+1)$-gones dont on a recollé les côtés parallèles. On donne une condition suffisante pour qu'une direction soit hyperbolique, c'est-à-dire fixée par une direction hyperbolique du groupe de Veech, en termes d'un algorithme de fractions continues naturel sur les directions de la surface. En particulier, cela nous permet d'exhiber des points sur le double heptagone à coordonnées dans le corps de trace qui ne sont pas des points de connexion. Parmi ces points on peut notamment trouver les points centraux des heptagones, ce qui donne une réponse négative à une question de P. Hubert et T. Schmidt.

Central points of the double heptagon translation surface are not connection points.

Les points centraux du double heptagone ne sont pas des points de connexion.

Julien Boulanger *

November 3, 2021

Abstract

We consider flow directions on the translation surfaces formed from double $(2n+1)$-gons, and give a sufficient condition in terms of a natural gcd algorithm for a direction to be hyperbolic in the sense that it is the fixed direction for some hyperbolic element of the Veech group of the surface. In particular, we give explicit points in the holonomy field of the double heptagon translation surface which are not so-called connection points. Among these are the central points of the heptagons, giving a negative answer to a question by P. Hubert and T. Schmidt [HS].

Résumé

On s'intéresse au flot directionnel sur les surfaces de translation obtenues à partir de deux $(2n+1)$-gones dont on a recollé les côtés parallèles, et on donne une condition suffisante pour qu'une direction soit hyperbolique, c'est à dire fixée par une direction hyperbolique du groupe de Veech, en termes d'un algorithme de pgcd naturel sur les directions de la surface. En particulier, cela nous permet d'exhiber des points sur le double heptagone à coordonnées dans le corps d'holonomie qui ne sont pas des points de connexion. Parmi ces points on peut notamment trouver les points centraux des heptagones, ce qui donne une réponse négative à une question de P. Hubert et T. Schmidt [HS].

*julien.boulanger@univ-grenoble-alpes.fr
Institut fourier, UMR 5582, Laboratoire de Mathématiques.
Université Grenoble alpes, CS 40700, 38058 Grenoble cedex 9, France.

1 Introduction and statement of the results.

A translation surface is a genus g topological surface with an atlas of charts on the surface minus a finite set of points such that all transition functions are translations. These surfaces can also be described as the surfaces obtained by gluing pairs of opposite parallel sides of a collection of euclidean polygon by translations. Such surfaces arise naturally in the study of billiard table dynamics : the Katok-Zemlyakov unfolding procedure, which consists in reflecting the billiard every time the trajectory hits an edge instead of reflecting the trajectory, replaces the billiard flow on a polygon by a directional flow on isometric translation surfaces. The study of translation surfaces has been flourishing, with major recent advances such as the results in [EMM15], [EFW18] or [EMMW20] but there still remains various open questions, for instance in the area of Veech groups. One of these questions is to characterize so-called connection points, for which little is known for translation surfaces whose trace field is of degree 3 or more over $\mathbb{Q}$. In this paper we look at two particular points of the double heptagon surface, whose trace field is cubic over $\mathbb{Q}$, and show that they are not connection points. For surveys about translation surfaces see [Zor06], [Wri14], and for Veech groups see [HS06].

Before looking at connection points, one needs to understand better parabolic (resp. hyperbolic) directions, that is directions fixed by a parabolic (resp. hyperbolic) element of the Veech group. For Veech surfaces, periodic directions, saddle connection directions and directions fixed by parabolic elements of the Veech group coincide. For these terms, see the background and [HS06]. For translation surfaces whose trace field is quadratic or $\mathbb{Q}$, C. McMullen showed in [McM03] that (after a natural normalization) the periodic directions are exactly those with slopes in the trace field. When the trace field is of higher degree, it is no longer true and the periodic directions in general form a proper subset of the directions whose slope belong to the trace field. D. Davis and S. Lelièvre [DL19] characterized the parabolic directions for the double pentagon surface using a gcd algorithm. Their results can be directly extended to the $(2n+1)$-gon which has a holonomy field of degree n over $\mathbb{Q}$.

In this paper we use the algorithm to characterize hyperbolic directions whose slope belong to the trace field for each double $(2n+1)$-gon surface, which are made of two copies of a $(2n+1)$-gon with parallel opposite sides glued together. We find explicit examples of such directions for the double heptagon. This allows us to prove that central points of the double heptagon are not connection points, see Theorem 1.3. This answers negatively a question of P. Hubert and T. Schmidt. Recall that the central points of the double heptagon are the centers of the heptagons. A nonsingular point of a translation surface is called a connection point if every separatrix passing through this point can be extended to a

saddle connection. In fact, the author do not know any example of non periodic connection point [1] for a translation surface whose trace field is of degree 3 over $\mathbb{Q}$ or higher.

Theorem 1.1. *Let $n \geq 2$, for the double $(2n+1)$-gon surface, directions which ends in a periodic sequence (of period ≥ 2) for the gcd algorithm are hyperbolic directions.*

Proposition 1.2 (Double heptagon case)**.** *For the double heptagon surface, there are hyperbolic directions in the trace field.*

This proposition is already known from [AS09] and [HMTY08], where they use a different method. Our method provides an answer to the question of central points as connection points, which was not known.

Theorem 1.3. *Central points of the double heptagon are not connection points.*

Moreover, one can look at double $(2n+1)$-gons with more sides. For example, the same result holds for the double nonagon :

Theorem 1.4. *Central points of the double nonagon are not connection points.*

Moreover, different tests we conducted suggests the following conjecture, which is not new since we found the same ideas in [HMTY08].

Conjecture 1.5. *For the double heptagon and the double nonagon, all the directions in the trace field are either parabolic or hyperbolic.*

What is interesting is that these results don't seem to genralize to the double hendecagon for example. In fact, for the double hendecagon we couldn't find any direction in the trace field which ends in a periodic sequence. These questions will be discussed in Section 5.

Acknowledgments. I'm grateful to Erwan Lanneau for all the explanations and the discussions and for the many remarks about preliminary versions of this paper. I would like to thank Samuel Lelièvre for the discussions and his help about Sage, Curt McMullen for interesting questions and remarks, and the anonymous reviewer as well for careful reading and helpful suggestions.

1. A point is *periodic* if its orbit under the action of the affine group is finite, otherwise it is non-periodic, see [HS04].

2 Background.

A *translation surface* (X, ω) is a real compact genus g surface X with an atlas ω such that all transition functions are translations except on a finite set of singularities Σ, along with a distinguished direction. Alternatively, it can be seen as a surface obtained from a finite collection of polygons embedded in $\mathbb{C}$ by gluing pairs of parallel opposite sides by translation. We get a surface X with a flat metric and a finite number of singularities. We define $X' = X - \Sigma$, which inherits the translation structure of X and defines a Riemannian structure on X'. Therefore, we have notions of geodesics, length, angle, and geodesic flow (called directional flow). This allows us make the following definitions, which will be useful in Section 4.

Definitions 2.1. (i) A *separatrix* is a geodesic line emanating from a singularity.
(ii) A *saddle connection* is a separatrix connecting singularities without any singularities on its interior.
(iii) A nonsingular point of the translation surface is called a *connection point* if every separatrix passing through this point can be extended to a saddle connection.

The action of $GL_2^+(\mathbb{R})$ on polygons induces an action on the moduli space of translation surfaces (see for example [Zor06]). Two surfaces are affinely equivalent if they lie in the same orbit. The stabilizer of a given translation surface X is called the *Veech group* of X, and is denoted by $SL(X)$. In particular, affinely equivalent surfaces have conjugated Veech group. As well as introducing the notion (altough not the name) W.A. Veech showed in [Vee89] that they are discrete subgroups of $SL_2(\mathbb{R})$. Hence, we can classify elements of the Veech group into three types : elliptic ($|\mathrm{tr}(M)| < 2$), parabolic ($|\mathrm{tr}(M)| = 2$) and hyperbolic ($|\mathrm{tr}(M)| > 2$). Any element of the Veech group induces a diffeomorphism of the surface. Such diffeomorphisms are called *affine diffeomorphisms*.

Trace field The *trace field* of a group $\Gamma \subset SL_2(\mathbb{R})$ is the subfield of $\mathbb{R}$ generated over $\mathbb{Q}$ by $\{\mathrm{tr}(M), M \in \Gamma\}$. One defines the trace field of a translation surface to be the trace field of its Veech group.

Let X be a genus g translation surface. We have the following theorems :

Theorem 2.2 (see [KS00])**.** *The trace field of X has degree at most g over $\mathbb{Q}$. Assume the Veech group of X contains a hyperbolic element M. Then the trace field is exactly $\mathbb{Q}[tr(M)]$.*

It is a classical result (see for instance [Thu88]) that after a normalization, there exists an atlas such that every parabolic direction has its slope in the trace field and every connection point has coordinates in the trace field. Specifically in the quadratic case, we have the following result :

Theorem 2.3 ([McM03], Theorem 5.1, see also [Bos88]). *If the trace field is quadratic over $\mathbb{Q}$ then every direction whose slope lies in the trace field is parabolic.*

3 Hyperbolic directions for the double $(2n+1)$-gon.

I. Bouw and M. Möller in [BM10] gave a large class of Veech surfaces. W. P. Hooper gave a geometric interpretation of these surfaces in [Hoo12] and proved in particular that the double $(2n+1)$-gon is affinely equivalent to a staircase polygonal model. See also [Dav14], [DPU19] and [Mon05]. See Figure 1 for the double heptagon's staircase model. We will use this model to construct the gcd algorithm at the heart of this paper which is a direct generalization of that described in [DL19] in the setting of the double pentagon. For more results on the double pentagon, see also [DFT11].

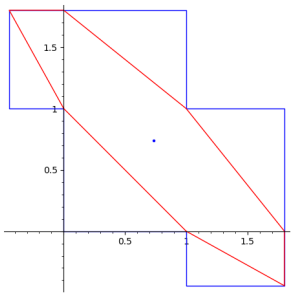

Figure 1 – The staircase model for the double heptagon (in red we show one of the two heptagons).

The staircase model can be constructed as follows : Let each $R_i, i = 1, ..., 2n-1$ be the rectangle of side $\sin(\frac{i\pi}{2n+1})$ and $\sin(\frac{(i+1)\pi}{2n+1})$. Glue R_i and R_{i+1} such that edges of the same size are glued together, each side being glued to the opposite side of the other rectangle as shown in Figure 2. Parallel edges of R_1 (resp. R_{2n-1}) that are not glued to an edge of another rectangle are glued together.

It is then an easy calculation to establish the following lemma, which in fact is a particular case of Lemma 6.6 from [Dav14] (see also [Vee89]).

Lemma 3.1. *Let $n \geq 2$ be an integer. Then in the staircase model for the double $(2n+1)$-gon translation surface, there is a horizontal (resp. vertical) decomposition into cylinders such that all cylinders have modulus equal to $a_n = 2\cos(\frac{\pi}{2n+1})$.*

In fact, for computationnal reasons it will be more convenient to rescale the staircase by a factor $\frac{1}{sin(\frac{n\pi}{2n+1})}$ so that each side can be expressed in the trace field and the longer side has lengh 1.

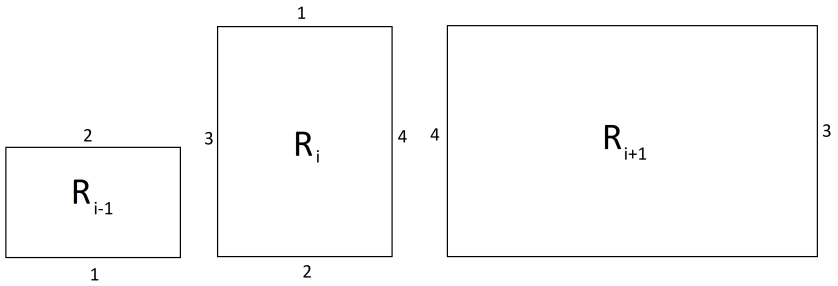

Figure 2 – How to glue the rectangles R_i. Each edge of R_i is glued to the one with the same number in R_{i-1} or R_{i+1}.

Let us now look at the short diagonals of the staircase. We get $2n-1$ short diagonal vectors denoted by $D_i, i \in [\![1, 2n-1]\!]$. We set D_0 to be the shortest horizontal vector and D_{2n} the shortest vertical vector. We rescale such that D_0 and D_{2n} are length 1 vectors. We drew the diagonals in a graph as shown in Figure 3 for the double heptagon ($n = 3$). All the D_i's have euclidean norm bigger than 1 (except D_0 and D_{2n} with norm equal to 1).

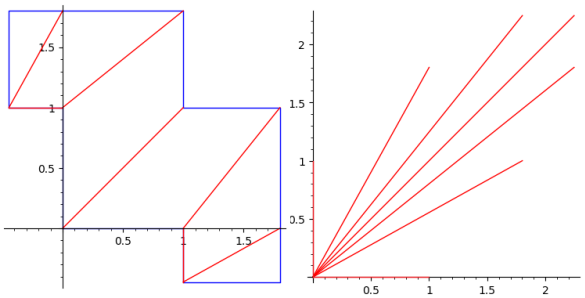

Figure 3 – The diagonals of the double heptagon staircase divides the positive cone into 6 subcones. The diagonals are rescaled so that D_0 and D_{2n} are length 1 vectors. We have $D_0 = (1, 0)$, $D_1 = (a_3, 1)$, $D_2 = (a_3^2-1, a_3)$, $D_3 = (a_3^2-1, a_3^2-1)$, and the other diagonals are symetrical about the first bisector.

Let M_i, $i \in [\![0, 2n-1]\!]$ be the matrix that maps $D_0 = (1, 0)$ to D_i and $D_{2n} = (0, 1)$ to D_{i+1}. Let Σ denote the first quadrant, and Σ_i its image under M_i (we include D_i in M_i). The matrix M_i is in the Veech group of the staircase and is associated to an affine homeomorphism of the staircase surface which we still denote by M_i. This homeomorphism sends parabolic (resp. hyperbolic) directions [2] to parabolic (resp. hyperbolic) directions which are in the i^{th} cone. Iterating this process, we obtain a way to construct new parabolic (resp. hyperbolic) directions once we have found one. Conversely, we have a gcd algorithm given by the following definition.

2. Here and thoughout, we mean by direction an element of the projective line $\mathbb{P}(\mathbb{R}^2)$.

Definition 3.2 (gcd algorithm[3] for the staircase model)**.** Given a direction in the first quadrant as entry, apply the following procedure :
1) If the direction lies in the i^{th} cone, apply M_i^{-1}.
2) If the direction is neither horizontal nor vertical, go back to step 1.

The following theorem is due to D.Davis and S.Lelièvre. It is stated in [DL19] in the case of the double pentagon but the same arguments can be directly extended to the double $(2n+1)$-gon.

Theorem 3.3 ([DL19])**.** *A direction on the double $(2n+1)-$gon is parabolic if and only if the gcd algorithm terminates at the horizontal direction.*

This theorem gives the first possibility for this algorithm to end. The other possibility would be an eventually periodic ending, i.e if we apply the algorithm a certain number of times the direction we get is a direction we already got in a previous step. Here we characterize these directions in the trace field and we prove Theorem 1.1, which can be stated more formally in the following way :

Theorem 3.4. *The gcd algorithm is eventually periodic for a direction θ (which is neither horizontal nor vertical) in the trace field if and only if θ is the image by a matrix $M_{i_k}...M_{i_1}$ of an eigendirection for a hyperbolic matrix of the form $M_{j_1}...M_{j_l}$. In particular, every eventually periodic direction for the gcd algorithm is an eigendirection for a hyperbolic matrix of the Veech group.*

Proof. If θ is eventually periodic for the gcd algorithm, let k denote the length of the preperiod of θ. Then, we have matrices $M_{i_1}, ..., M_{i_k}$ such that $\theta' = (M_{i_k}...M_{i_1})^{-1}(\theta)$ is periodic for the algorithm. That is, there exist $M_{j_1}, ..., M_{j_l}$ such that $M_{j_1}...M_{j_l}(\theta') = \theta'$. Then $M = M_{j_1}...M_{j_l}$ is indeed a hyperbolic matrix since all M_js dilates lengths in the first quadrant, which means that the eigenvalue of $M_{j_1}...M_{j_l}$ for the direction θ' has to be strictly bigger than 1. Moreover, M belongs to the Veech group, being a product of elements of the Veech group.

Conversely, let us suppose there is $i_1, ..., i_k, j_1, ..., j_l$ such that $M_{j_1}...M_{j_l}(\theta') = \theta'$, where $M = M_{j_1}...M_{j_l}$ is hyperbolic and $\theta = M_{i_k}...M_{i_1}(\theta')$. First, it is clear that θ' belongs to the first quadrant by the Perron-Frobenius theorem since all the matrices M_i have positive entries, and that the only sequences $j_1, ...j_l$ such that $M = M_{j_1}...M_{j_l}$ have possible zero entries are if $j_1 = ... = j_l = 0$ or $j_1 = ... = j_l = 2n$, which gives a matrix M that is parabolic and not hyperbolic. Thus, θ belongs to the first quadrant as well because the M_i's are contractions of the first quadrant. Moreover, at every step q, $M_{i_q}...M_{i_1}(\theta')$ belongs to the first quadrant. By construction of the gcd algorithm, it follows that applying the gcd algorithm to the direction θ leads to θ' after k steps. By the same argument, since $M_{j_1}...M_{j_l}(\theta') = \theta'$ and θ' belongs to the first quadrant, we conclude that the sequence $j_l, ..., j_1$ is exactly the sequences of indices we would have got if

3. The name comes from the geometric version of Euclide algorithm for the torus.

we would have applied the algorithm to θ', and that θ' is a periodic direction for the gcd algorithm. Hence, θ is an eventually periodic direction for the gcd algorithm. □

Remark 3.5. A point worth noting is that the sequence of sectors along the algorithm allows us to construct the matrix M which stabilizes the original direction. This will allow us, for the double heptagon, to find a separatrix whose direction is eventually periodic for the gcd algorithm and hence is not parabolic, which means that the separatrix does not extend to a saddle connection.

Remark 3.6. This theorem implies that eventually periodic directions for the gcd algorithm are hyperbolic directions, but the converse is not necessarily true. However, we guess that for the double heptagon surface this gives all hyperbolic directions and, moreover, all directions in the trace field are either hyperbolic or parabolic.

Exemple 3.7. For the gcd algorithm on the double heptagon :
- The direction of slope $a_3^2 + 1$ is 2-periodic and fixed by the hyperbolic matrix $M_5 M_0$.
- The direction of slope $-\frac{33}{29}a_3^2 + \frac{3}{29}a_3 + \frac{103}{29}$ is 28-periodic and fixed by the hyperbolic matrix $M_5^{12} M_4^2 M_0^{12} M_2 M_0$.

4 Connection points.

In this section, we finally show that central points of the double heptagon are not connection points. We first give some motivation to their study.

Connection points have been studied in [HS04] by P. Hubert and T. Schmidt who gave a construction of translation surfaces with infinitely generated Veech groups as branched covers over non-periodic connection points. C. McMullen proved in [McM06] the existence of these points in the case of a quadratic trace field, and implicitely showed that the connection points are exactly the points with coordinates in the trace field. But in higher degree there is no such result, neither concerning connection points nor about infinitely generated Veech groups. One of the easiest non-quadratic surfaces is the double-heptagon whose trace field is of degree 3 over $\mathbb{Q}$. P.Arnoux and T.Schmidt implicitely showed (see [AS09]) that for the double heptagon surface there are points with coordinates in the trace field that are not connection points. Still, it was not known whether or not central points of the double heptagon were connection points. We provide here a negative answer to this question.

By definition, for proving that a point is not a connection point, it suffices to find a separatrix passing throught it which cannot be extended to a saddle

connection, for instance because the separatrix lies in a hyperbolic direction. We managed to find such a separatrix for a central point, which is drawn in Figure 4. Of course, both central points plays a symetric role, so it suffices to consider either one of the central points.

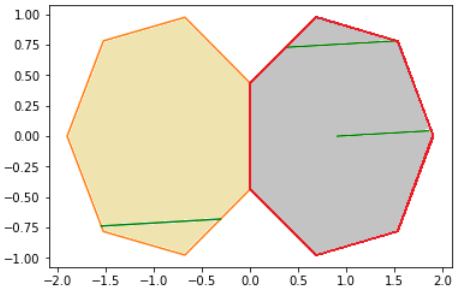

Figure 4 – The green separatrix, passing through one of the central points with slope $\sin(\frac{\pi}{7})(-\frac{8}{3}\cos(\frac{\pi}{7})^2 + 4\cos(\frac{\pi}{7}) - \frac{4}{3})$, does not extend to a saddle connection.

We are now able to prove Proposition 1.2. More precisely :

Proposition 4.1. *The green separatrix in Figure 4 has a hyperbolic direction.*

Proof. Let us work with the staircase model. Recall that it is affinely equivalent to the double heptagon model. The transition matrix is given by

$$T = \begin{pmatrix} \cos(\frac{\pi}{7}) + 1 & \cos(\frac{\pi}{7}) + 1 \\ -\sin(\frac{\pi}{7}) & \sin(\frac{\pi}{7}) \end{pmatrix}.$$

In this setting, we get Figure 5 and the slope of the new green direction is $\frac{3}{13}a^2 + \frac{6}{13}a - \frac{1}{13}$, where $a = a_3 = 2cos(\frac{\pi}{7})$.

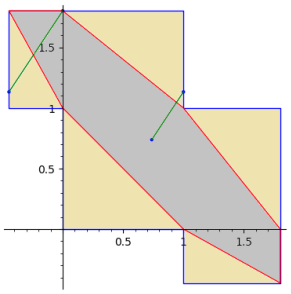

Figure 5 – The same green separatrix in the staircase model does not extend to a saddle connection.

We apply the gcd algorithm to the green direction and notice that it ends in a periodic sequence of directions, which means the green direction is fixed by a

hyperbolic matrix of the Veech group , namely

$$M = M_4^2 M_5 M_1 (M_4^{-1})^2 = \begin{pmatrix} -34a^2 - 26a + 19 & 22a^2 + 21a - 14 \\ -50a^2 - 41a + 28 & 35a^2 + 26a - 17 \end{pmatrix}.$$

It follows that M is hyperbolic (of trace $2 + a^2$) and belongs to the Veech group. Explicitely,

$$M = \begin{pmatrix} a & 1 \\ a^2 - 1 & a \end{pmatrix} \begin{pmatrix} a & 1 \\ a^2 - 1 & a \end{pmatrix} \begin{pmatrix} 1 & 0 \\ a & 1 \end{pmatrix} \begin{pmatrix} 1 & a \\ 0 & 1 \end{pmatrix} \begin{pmatrix} a & -1 \\ -a^2 + 1 & a \end{pmatrix} \begin{pmatrix} a & -1 \\ -a^2 + 1 & a \end{pmatrix}.$$

Finally, going back to the Veech group of the double heptagon model, we get that TMT^{-1} fixes the green direction of Figure 4, which is then a hyperbolic direction.

□

It follows from this proof that the central points are not connection points, since the green separatrix of Figure 4, having a hyperbolic direction, cannot be extended to a saddle connection. This proves Theorem 1.3.

Remark 4.2. The green separatrix used for the proof is not the only separatrix passing through one of the central points whose direction is hyperbolic. For example, one could have taken the separatrix of Figure 6 which is hyperbolic and fixed (in the staircase model) by the matrix $SM_5^3 M_0 M_5^{-2} S^{-1}$. Here S is the half turn $\begin{pmatrix} 0 & -1 \\ 1 & 0 \end{pmatrix}$ in the Veech group.

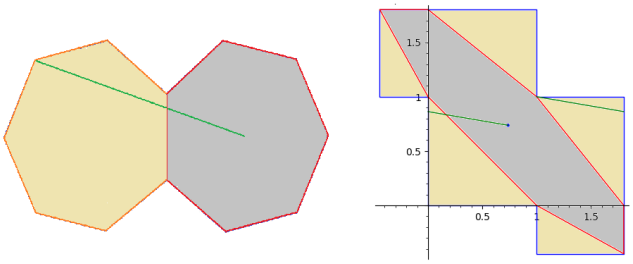

Figure 6 – Another example of a separatrix whose direction is hyperbolic and in the trace field.

5 Further directions.

In the previous sections we looked at an algorithm defined for all $(2n+1)$-gons and used it for the case of the double heptagon to show that the central points are not connection points. One can ask what happens if we look at double $(2n+1)$-gons with more sides. It appears that the same result holds for the double nonagon. More precisely :

Proposition 5.1. *The green direction of Figure 7 is hyperbolic. Hence the central points of the double nonagon are not connection points.*

Proof. The proof is similar to the case of the double heptagon. We work with the staircase model and use the gcd algorithm to find a separatrix passing through one of the central points whose direction is hyperbolic. It appears that the green direction of Figure 7, starting at a singularity with slope $a_4^2+2a_4+1$ and reaching one of the central point is hyperbolic and fixed by the matrix :

$$M = M_0^4 M_5 M_7^2 = \begin{pmatrix} 23a_4^2 + 12a_4 - 1 & 9a_4 + 4 \\ 5a_4 + 3 & a_4^2 - 1 \end{pmatrix}$$

Where $a_4 = 2\cos(\frac{\pi}{9})$ and the M_i's correspond to the matrix of the algorithm for the double nonagon staircase. Namely :

$$M_0 = \begin{pmatrix} 1 & a_4 \\ 0 & 1 \end{pmatrix} \ , \ M_5 = \begin{pmatrix} a_4^2 - 1 & a_4 \\ a_4 + 1 & a_4^2 - 1 \end{pmatrix} \ , \ M_7 = \begin{pmatrix} 1 & 0 \\ a_4 & 1 \end{pmatrix}$$

□

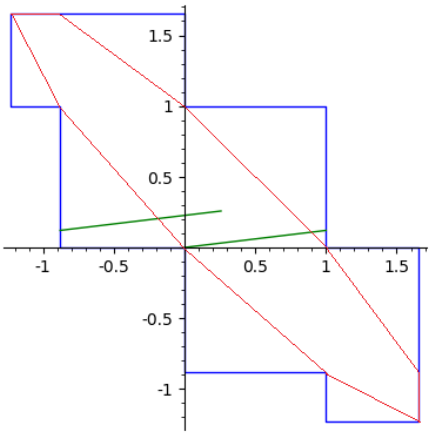

Figure 7 – The green separatrix in the staircase model for the double nonagon does not extend to a saddle connection.

Conversely, we conducted tests for the double hendecagon but found no directions with periodic ending. This is closely related to Remark 9 of [HMTY08] made in the setting of λ-continued fractions for Hecke groups, saying the authors didn't find any hyperbolic direction in the trace field for $11 \leq 2n+1 \leq 29$. The interpretation in our setting relies on Veech having shown in [Vee89] that the Veech group of the double $(2n+1)$-gon is conjugated to the Hecke group H_{2n+1} [4] [5]. In particular, we do not know whether central points of the double

4. for $k \geq 3$, $H_k = < \begin{pmatrix} 0 & -1 \\ 1 & 0 \end{pmatrix} ; \begin{pmatrix} 1 & \lambda_k \\ 0 & 1 \end{pmatrix} >$, where $\lambda_k = 2\cos(\frac{\pi}{k})$

5. While the Veech group of the $2n$-gon is conjugated to a subgroup of order 2 of the Hecke group H_{2n}.

hendecagon are connection points or not. See also [AS09] and [CS13] for related results.

Moreover, the study of directions in the double heptagon and the double nonagon had shown that there are either parabolic or hyperbolic directions in the trace field. But could there be something else ? It is *a priori* possible that the algorithm doesn't terminate for a given direction. In fact, our tests suggests this doesn't happen in those cases, which leads to a precised version of conjecture 1.5 :

Conjecture 5.2. *For the double heptagon and the double nonagon, every direction in the trace field terminates for the gcd algorithm. In particular, every direction in the trace field would be either parabolic or hyperbolic.*

In fact, this conjecture is also related to a conjecture in [HMTY08] about the possible orbits on $\widehat{\mathbb{Q}}(\cos(\frac{\pi}{2n+1}))$ under the projective action of the Hecke triangle group H_{2n+1}. Once again, the behaviour appears to be very different for the double hendecagon : there seems to be directions in the trace field which never terminates for the gcd algorithm.

Another interesting corollary of this result is related to billiards trajectories and has been suggested to the author by C. McMullen. Recall that the double heptagon surface arises from the unfolding of the triangular billiard with angles $(\frac{\pi}{2}, \frac{\pi}{7}, \frac{5\pi}{14})$. The green separatrix in the proof of Proposition 4.1 is the lift of a vertex-to-vertex trajectory, drawn in Figure 8. In particular, there exists vertex-to-vertex trajectories whose direction are not parabolic (which means there also exists a billiard trajectory in this direction which equidistributes).

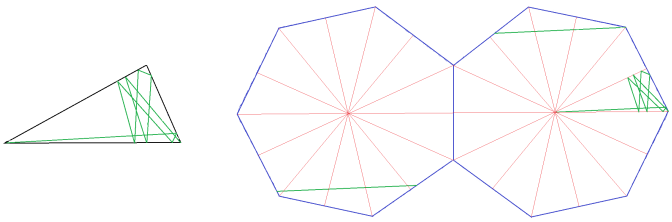

Figure 8 – The green vertex-to-vertex trajectory on the triangular billiard unfolds to a directionnal trajectory whose direction is hyperbolic according to Section 4.

References

[AS09] Pierre Arnoux and Thomas Schmidt. Veech surfaces with non periodic directions in the trace field. *J. Mod. Dyn. 3*, pages 611–629, 2009.

[BM10] Irene Bouw and Martin Möller. Teichmuller curves, triangle groups, and Lyapunov exponents. *Annals of Mathematics, 172, no. 1*, pages 85–139, 2010.

[Bos88] Michael D. Boshernitzan. Rank two interval exchange transformations. *Ergod. Th. and Dynam. Sys., 8*, 379–394, 1988.

[CS13] Kariane Calta and Thomas Schmidt. Infinitely many lattice surfaces with special pseudo-Anosov maps. *J. Mod. Dyn, 7*, pages 239–254, 2013.

[Dav14] Diana Davis. Cutting sequences on translation surfaces. *New York Journal of Mathematics, Vol. 20*, pages 399–429, 2014.

[DFT11] Diana Davis, Dmitry Fuchs, and Serge Tabachnikov. Periodic trajectories in the regular pentagon. *Moscow Mathematical Journal, Vol. 3*, 2011.

[DL19] Diana Davis and Samuel Lelièvre. Periodic paths on the pentagon, double pentagon and golden L. *Preprint*, 2019.

[DPU19] Diana Davis, Irene Pasquinelli, and Corinna Ulcigrai. Cutting sequences on Bouw-Möller surfaces : an s-adic characterization. *Annales scientifiques de l'ENS*, 2019.

[EFW18] Alex Eskin, Simion Filip, and Alex Wright. The algebraic hull of the Kontsevich-Zorich cocycle. *Ann. of Math.*, 2018.

[EMM15] Alex Eskin, Maryam Mirzakhani, and Amir Mohammadi. Isolation, equidistribution, and orbit closures for the $Sl(2,\mathbb{R})$ action on moduli space. *Annals of Mathematics, 182*, pages 1–49, 2015.

[EMMW20] Alex Eskin, Curtis McMullen, Ronen Mukamel, and Alex Wright. Billiards, quadrilaterals and moduli spaces. *J. Amer. Math. Soc.*, 2020.

[HMTY08] Elise Hanson, Adam Merberg, Christopher Towse, and Elena Yudovina. Generalized continued fractions and orbits under the action of Hecke triangle groups. *Acta Arithmetica, 134.4*, 2008.

[Hoo12] W.Patrick Hooper. Grid graphs and lattice surfaces. *International Mathematics Research Notices, Vol. 2013, No. 12*, pages 2657–2698, 2012.

[HS04] Pascal Hubert and Thomas Schmidt. Infinitely generated Veech groups. *Duke mathematical journal, 123*, pages 49–69, 2004.

[HS06] Pascal Hubert and Thomas Schmidt. An introduction to Veech surfaces. Volume 1 of *Handbook of Dynamical Systems*, pages 501–526. 2006.

[HS] Private communication.

[KS00] Richard Kenyon and John Smillie. Billiards on rational-angled triangles. *Commentarii Mathematici Helvetici, 75*, pages 65–108, 2000.

[McM03] Curt McMullen. Teichmüller geodesics of infinite complexity. *Acta Math., 191*, pages 191–223, 2003.

[McM06] Curt McMullen. Teichmüller curves in genus two : torsion divisors and the ratio of sines. *Inventionnes Mathematicae, 165*, pages 651–672, 2006.

[Mon05] Thierry Monteil. On the finite blocking properties. *Annales de l'institut Fourier, 55*, 1195–1217, 2005.

[Thu88] William Thurston. On the geometry and dynamics of diffeomorphism of surfaces. *Bull. Amer. Math. Soc. (N.S.) 19(2)*, pages 417–431, 1988.

[Vee89] W.A. Veech. Teichmüller curves in moduli spaces, Eisenstein series and application to triangular billiards. *Invent. math. 97*, pages 553–583, 1989.

[Wri14] Alex Wright. Translation surfaces and their orbit closures: an introduction for a broad audience. *Bull. Amer. Math. Soc. 2016*, 2014.

[Zor06] Anton Zorich. Flat surfaces. *Frontiers in Number Theory, Physics, and Geometry Vol.1*, pages 439–456, 2006.

Chapitre 8

There are no primitive Teichmüller curves on Prym(2,2)

Résumé en français. Dans ce chapitre, on présente un travail en commun avec Sam Freedman, accepté pour publication aux *Comptes rendus de l'académie des sciences*, où l'on démontre qu'il n'existe pas de surfaces de Veech géométriquement primitives dans le lieu $Prym(2,2)$ des surfaces de $\mathcal{H}(2,2)$ munies d'une involution prym. Ce résultat fait suite à un travail d'E. Lanneau et M. Möller [LM19] qui démontrent qu'en dehors de 92 candidats potentiels, il n'y a pas de surfaces de Veech géométriquement primitives dans $Prym(2,2)$. Nous implémentons chacun de ces 92 candidats sous Sage et démontrons que ces surfaces ne sont pas de Veech en utilisant le package *Flatsurf*, qui permet de donner une borne inférieure sur la dimension de l'adhérence de la $SL_2(\mathbb{R})$-orbite d'une surface donnée et ainsi de certifier qu'une surface n'est pas de Veech.

Le code associé à l'article est disponible à l'adresse `https://github.com/sfreedman67/92-candidates`.

There are no primitive Teichmüller curves in Prym(2, 2)

Julien Boulanger and Sam Freedman

November 18, 2022

Abstract

We complete the work of Lanneau–Möller [4] to show that there are no primitive Teichmüller curves in $\mathrm{Prym}(2,2)$.

1 Introduction

Teichmüller curves are closed $\mathrm{GL}(2,\mathbb{R})$-orbits in the moduli space of translation surfaces $\Omega\mathcal{M}_g$ that descend to isometrically-immersed algebraic curves in the moduli space of genus g Riemann surfaces $\mathcal{M}_g$. Lanneau–Möller [4] searched for *geometrically primitive* Teichmüller curves, i.e., those not arising from a covering construction, in a certain locus $\mathrm{Prym}(2,2)$ of genus 3 translation surfaces with two cone-points called *Prym eigenforms*. In the spirit of McMullen's proof that the decagon is the unique primitive Teichmüller curve in $\Omega\mathcal{M}_2(1,1)$ (see [6, Theorem 6.3]), they reduced their search to considering whether any of 92 candidate Prym eigenforms generate a Teichmüller curve. In this note, we analyze those 92 candidates and show:

Theorem 1.1. *The Prym locus* $\mathrm{Prym}(2,2) \subset \Omega\mathcal{M}_3$ *contains no primitive Teichmüller curves.*

Our main tool is the newly-available SageMath package *Flatsurf* which partially computes the $\mathrm{GL}(2,\mathbb{R})$-orbit closure of an input translation surface. (See Appendix B of Delecroix–Rüth–Wright [2] for an introduction to *Flatsurf*.) Using *Flatsurf*, we construct the 92 candidates Prym eigenforms and find a periodic direction that violates the Veech dichotomy. See §§2.2 for details.

We thank Erwan Lanneau for his assistance with this project.

Background

Classifying the translation surfaces that generate Teichmüller curves, called *Veech surfaces*, is a central problem in Teichmüller dynamics. See Hubert–Schmidt [3]

for an introduction to Veech surfaces, Möller [8] for a list of known examples of Teichmüller curves, Lanneau–Möller [4] for a history of classification results, and McMullen [7] for a general survey.

While McMullen [5] classified all primitive Teichmüller curves in genus two, we do not have a complete classification of primitive Teichmüller curves in all other genera. In genus three, Bainbridge–Habegger–Möller [1] found a numerical bound on the number of *algebraically primitive* Teichmüller curves, yet the bound is too large for a complete classification. (An *algebraically primitive* Teichmüller curve is one for which the trace field of the generating Veech surface has maximal degree, i.e., degree the genus of the Veech surface. We remark that algebraically primitive Teichmüller curves are automatically geometrically primitive, yet the converse does not hold.) In fact, all but finitely many geometrically primitive Teichmüller curves in genus 3 lie in the Prym loci (see McMullen [7, Theorem 5.5]).

At another level, Lanneau–Möller [4] began searching for Teichmüller curves among translation surfaces having a certain *Prym involution* that generalizes the hyperelliptic involution in genus 2. (See Lanneau–Möller [4] for the definition.) They showed that there are no *geometrically primitive* Teichmüller curves in $\mathrm{Prym}(2,1,1)$ and initiated the proof for $\mathrm{Prym}(2,2)$ that we finish in this note. The remaining case of whether there are primitive Teichmüller curves in the locus $\mathrm{Prym}(1,1,1,1)$ is still open and seems interesting. Outside the Prym loci, Winsor [9] showed that the Veech 14-gon generates the unique algebraically primitive Teichmüller curve in the hyperelliptic component of the stratum $\Omega\mathcal{M}_3(2,2)$.

2 Proof of Theorem 1.1.

2.1 Candidate surfaces

In this section we review, following Lanneau–Möller [4], how to construct the 92 candidate surfaces that could generate a Teichmüller curve.

Every surface in $\mathrm{Prym}(2,2)$ decomposes into horizontal cylinders (after possibly rotating the surface). The combinatorics of the horizontal separatrices matches one of the eight polygonal models in Figure 1. (See also Figure 3 in Lanneau–Möller [4].) In each underlying polygonal model, the Prym involution fixes one cylinder, called C_2, and permutes the other two, called C_1 and C_3. The surface is then determined by choices of the widths, heights and twists of the cylinders C_1 and C_2, as well as of the length of a relative period called the *slit parameter* s. See Proposition 8.1 in Lanneau–Möller [4] for an example of one of the eight possible separatrix diagrams.

In this respect, Lanneau–Möller [4] determine a finite list of possible values for the width and the height of C_2, the surface being normalized with $w(C_1) = h(C_1) = 1$. More precisely, they first show (see their Theorem 4.5 and §6.2) that

Trace field	Reduced intersection matrix	$w(C_2)$	$h(C_2)$
$\mathbb{Q}[\sqrt{2}]$	$\begin{pmatrix} 72 & 48 \\ 24 & 18 \end{pmatrix}$	$\frac{\sqrt{2}}{2}$	$2\sqrt{2}$
$\mathbb{Q}[\sqrt{3}]$	$\begin{pmatrix} 72 & 24 \\ 12 & 6 \end{pmatrix}$	$\frac{-1+\sqrt{3}}{2}$	$-2+2\sqrt{3}$
$\mathbb{Q}[\sqrt{3}]$	$\begin{pmatrix} 72 & 24 \\ 48 & 18 \end{pmatrix}$	$\frac{1+\sqrt{3}}{2}$	$2+2\sqrt{3}$
$\mathbb{Q}[\sqrt{3}]$	$\begin{pmatrix} 36 & 12 \\ 30 & 12 \end{pmatrix}$	$\sqrt{3}$	$\frac{2\sqrt{3}}{3}$
$\mathbb{Q}[\sqrt{33}]$	$\begin{pmatrix} 6 & 24 \\ 12 & 54 \end{pmatrix}$	$\frac{3+\sqrt{33}}{2}$	$\frac{3+\sqrt{33}}{6}$

Table 1: The list of trace fields and reduced matrices that could give rise to Teichmüller curves[2], and the corresponding width and height of the cylinder C_2.

the only possible trace fields are $\mathbb{Q}[\sqrt{D}]$ for $D \in \{2, 3, 33\}$. They then encode the data of the widths and the heights of the horizontal and vertical cylinders in a *reduced intersection matrix*. In Proposition 5.5 and §§6.3–6.5, they compute a finite list of such matrices that could give rise to Teichmüller curves; we recall this list in Table 1 along with the associated width and height of C_2.

Having established the width and height parameters of the cylinders, it remains to control the length of the slit parameter and the twists of the cylinders. In §8.2 of Lanneau–Möller [4] and the corresponding code, they explicitly enumerate the finite list of possible values for such parameters that would lead to one of each admissible reduced intersection matrix. This amounts to a finite list of candidate surfaces (see Table 2 of Lanneau–Möller [4]). In the code joint to this note, we list all those candidate surfaces and construct them using *Flatsurf*.

2.2 Cylinder decompositions

Given a translation surface M, Flatsurf can efficiently generates many saddle connections on M. For each such saddle connection, it can compute the decomposition of the straight-line flow on M in that direction into cylinders and minimal components. Observe that if Flatsurf finds a direction for which M decomposes completely into cylinders, yet those cylinders have incommensurable moduli, then this direction witness that M does not satisfy the Veech dichotomy (See Hubert—Schmidt [3, Theorem 1]). Our code analyzes each of the 92 candidates and in each case finds a direction that is not completely parabolic. We conclude that none of the candidates is Veech, proving Theorem 1.1.

[2]The last two reduced matrices of Lanneau–Möller[4] do not generate Teichmüller curves according to Table 2 of [4], so we do not consider them.

References

[1] Matt Bainbridge, Philipp Habegger, and Martin Möller. Teichmüller curves in genus three and just likely intersections in $\mathrm{G}_m^n \times \mathrm{G}_a^n$. *Publications mathématiques de l'IHÉS*, 124, 10 2014. doi:10.1007/s10240-016-0084-6.

[2] Vincent Delecroix, Julian Rüth, and Alex Wright. A new orbit closure in genus 8, 2021. doi:10.48550/ARXIV.2110.05407.

[3] Pascal Hubert and Thomas Schmidt. An introduction to Veech surfaces. *Handbook of Dynamical Systems, vol. 1B*, 01 2006.

[4] Erwan Lanneau and Martin Moeller. Non-existence and finiteness results for Teichmüller curves in prym loci. *Experimental Mathematics*, 31:621 – 636, 2019. doi:https://doi.org/10.1080/10586458.2019.1671920.

[5] Curtis McMullen. Dynamics of $\mathrm{SL}_2(\mathbb{R})$ over moduli space in genus two. *Annals of Mathematics*, 165(2):397–456, March 2007. doi:10.4007/annals.2007.165.397.

[6] Curtis T. McMullen. Teichmüller curves in genus two: Torsion divisors and ratios of sines. *Inventiones mathematicae*, 165(3):651–672, April 2006. doi:10.1007/s00222-006-0511-2.

[7] Curtis T. McMullen. Billiards and Teichmülller curves. 2021. URL: https://people.math.harvard.edu/~ctm/papers/home/text/papers/tsurv/tsurv.pdf.

[8] Martin Möller. Geometry of Teichmüller curves. In *Proceedings of the International Congress of Mathematicians—Rio de Janeiro 2018. Vol. III. Invited lectures*, pages 2017–2034. World Sci. Publ., Hackensack, NJ, 2018. doi:10.1142/9789813272880_0128.

[9] Karl Winsor. Uniqueness of the Veech 14-gon. 2022. doi:10.48550/ARXIV.2210.09702.

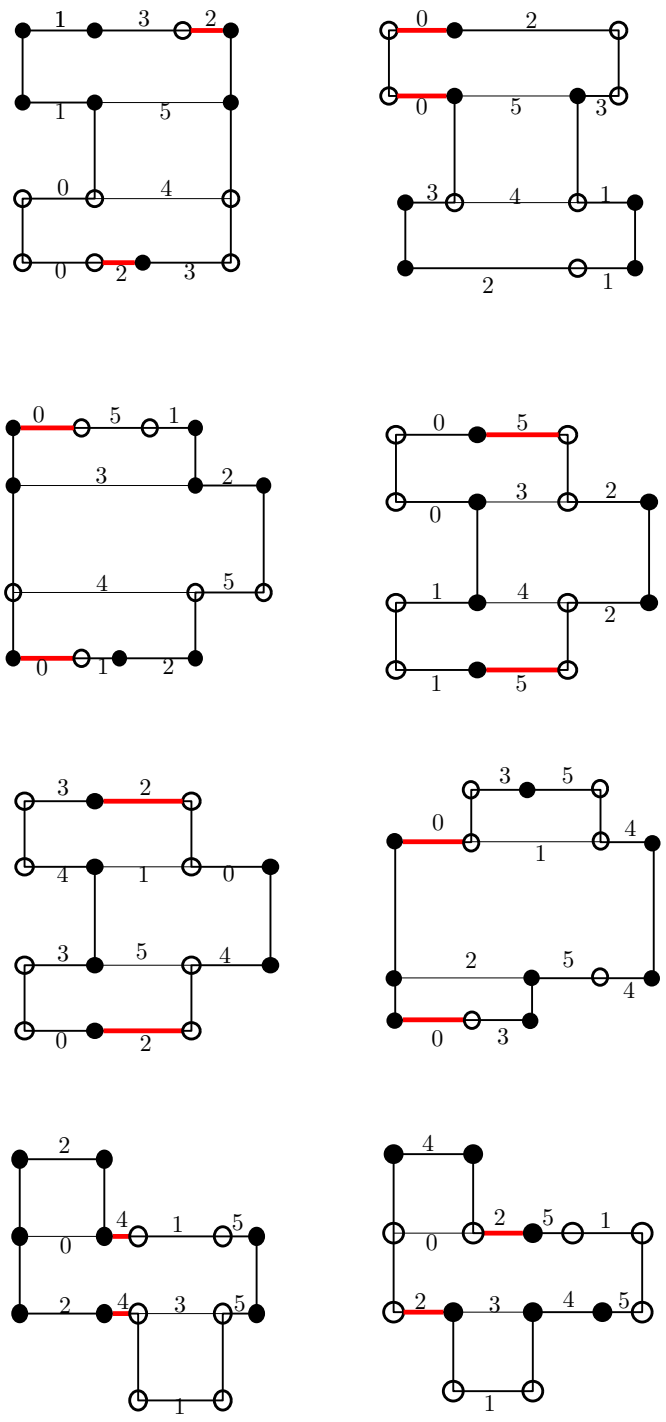

Figure 1: The 8 polygonal models. The slit parameter encodes the length of the bold red relative period.

Bibliographie

[AS09] Pierre Arnoux and Thomas Schmidt. Veech surfaces with non periodic directions in the trace field. *J. Mod. Dyn. 3*, pages 611–629, 2009.

[Bal] Florent Balacheff. *Mémoire d'habilitation à diriger des recherches.*

[BF22] Julien Boulanger and Sam Freedman. There are no primitive Teichmüller curves in Prym$(2,2)$. *accepted for publication at the Comptes rendus de l'académie des sciences*, 2022.

[BG21] Corentin Boissy and Slavyana Geninska. Systoles in translation surfaces. *Bull. de la SMF*, 149(2) :417–438, 2021.

[BK04] V. Bangert and M. Katz. An optimal Loewner-type systolic inequality and harmonic one forms of constant norms. *Comm. Anal. Geom.*, 12(3) :703–732, 2004.

[BKP18] Florent Balacheff, Steve Karam, and Hugo Parlier. The minimal length product over homology bases of manifolds. *Mathematische Annalen*, 380 :825–854, 2018.

[BLM22] Julien Boulanger, Erwan Lanneau, and Daniel Massart. Algebraic intersection in regular polygons. 2022.

[BM10] Irene Bouw and Martin Möller. Teichmuller curves, triangle groups, and Lyapunov exponents. *Annals of Mathematics*, 172(1) :85–139, 2010.

[Bor73] W. Borho. Kettenbrüche im Galoisfeld. *Abh. Math. Sem. Univ. Hamburg*, 39 :76–82, 1973.

[Bos88] Michael D. Boshernitzan. Rank two interval exchange transformations. *Ergod. Th. and Dynam. Sys.*, 8 :379–394, 1988.

[Bou] Julien Boulanger. Central points of the double heptagon are not connection points. *Bulletin de la SMF*, 150.

[Bou23a] Julien Boulanger. Algebraic intersection, lengths, and veech groups. *arXiv :2309.17165*, 2023.

[Bou23b] Julien Boulanger. Lower bound for KVol on the minimal stratum of translation surfaces. *arXiv :2310.00130*, 2023.

[BPS12] Florent Balacheff, Hugo Parlier, and Stéphane Sabourau. Short loop decompositions of surfaces and the geometry of Jacobians. *Geometric And Functionnal Analysis*, 22 :37–73, 2012.

[BR73] W. Borho and G. Rosenberg. Eine Bemerkung zur Hecke-Gruppe g(λ). *Abh. Math. Sem. Univ. Hamburg*, 39 :83–87, 1973.

[BS94] P. Buser and P Sarnak. On the period matrix of a Riemann surface of large genus (with an Appendix by J.H. Conway and N.J.A. Sloane). *Invent. Math.*, 117 :27–56, 1994.

[Cha21] Yann Chaubet. Closed geodesics with prescribed intersection numbers. 2021.

[CHMWS22] Tobias Columbus, Frank Herrlich, Bjoern Muetzel, and Gabriela Weitze-Schmithüsen. Systolic geometry of translation surfaces. *Experimental Mathematics*, 0(0) :1–22, 2022.

[CKM21a] Smail Cheboui, Arezki Kessi, and Daniel Massart. Algebraic intersection for translation surfaces in a family of Teichmüller disks. *Bull. Soc. Math. France*, 149(4) :613–640, 2021.

[CKM21b] Smail Cheboui, Arezki Kessi, and Daniel Massart. Algebraic intersection for translation surfaces in the stratum $\mathcal{H}(2)$. *C. R. Math. Acad. Sci. Paris*, 359 :65–70, 2021.

[CS12] Kariane Calta and Thomas Schmidt. Continued fractions for a class of triangle groups. *J. Austral. Math. Soc. 93*, pages 21–42, 2012.

[CS13] Kariane Calta and Thomas Schmidt. Infinitely many lattice surfaces with special pseudo-Anosov maps. *J. Mod. Dyn, 7*, pages 239–254, 2013.

[DL18] Diana Davis and Samuel Lelièvre. Periodic paths on the pentagon, double pentagon and golden L. *arXiv : Dynamical Systems*, 2018.

[DPU19] Diana Davis, Irene Pasquinelli, and Corinna Ulcigrai. Cutting sequences on Bouw-Möller surfaces : an s-adic characterization. *Annales scientifiques de l'ENS*, 2019.

[DRW21] Vincent Delecroix, Julian Rüth, and Alex Wright. A new orbit closure in genus 8, 2021.

[EFW18] Alex Eskin, Simion Filip, and Alex Wright. The algebraic hull of the Kontsevich-Zorich cocycle. *Ann. of Math.*, 2018.

[EMM13] Joanna A. Ellis-Monaghan and Iain Moffatt. Graphs on surfaces - dualities, polynomials, and knots. In *Springer Briefs in Mathematics*, 2013.

[EMM15] Alex Eskin, Maryam Mirzakhani, and Amir Mohammadi. Isolation, equidistribution, and orbit closures for the $SL(2, \mathbb{RR})$ action on moduli space. *Annals of Mathematics 182*, pages 1–49, 2015.

[EMMW20] Alex Eskin, Curtis McMullen, Ronen Mukamel, and Alex Wright. Billiards, quadrilaterals and moduli spaces. *J. Amer. Math. Soc.*, 2020.

[FP15] Federica Fanoni and Hugo Parlier. Systoles and kissing numbers of finite area hyperbolic surfaces. *Algebr. Geom. Topol.*, 15(6) :3409–3433, 2015.

[GH94] P. Griffiths and J Harris. *Principles of algebraic geometry*. 1994.

[GL08] Sebastien Gouëzel and Erwan Lanneau. Un théorème de Kerckhoff, Masur et Smillie : Unique ergodicité sur les surfaces plates. *Séminaires et Congrès, Société Mathématique de France*, 19, 2008.

[Gro83] Mikhael Gromov. Filling Riemannian manifolds. *Journal of Differential Geometry*, 18 :1–147, 1983.

[HMTY08] Elise Hanson, Adam Merberg, Christopher Towse, and Elena Yudovina. Generalized continued fractions and orbits under the action of Hecke triangle groups. *Acta Arithmetica, 134.4*, 2008.

[Hoo12] W.Patrick Hooper. Grid graphs and lattice surfaces. *International Mathematics Research Notices, Vol. 2013, No. 12*, page 2657–2698, 2012.

[HS04] Pascal Hubert and Thomas Schmidt. Infinitely generated Veech groups. *Duke mathematical journal, 123*, pages 49–69, 2004.

[HS06] Pascal Hubert and Thomas Schmidt. An introduction to Veech surfaces. volume 1 of *Handbook of Dynamical Systems*, pages 501–526. 2006.

[JP19] Chris Judge and Hugo Parlier. The maximum number of systoles for genus two Riemann surfaces with abelian differentials. *Comment. Math. Helv.*, 94(2) :399–437, 2019.

[Kap00] Michael Kapovich. Hyperbolic manifolds and discrete groups. 2000.

[KS00] Richard Kenyon and John Smillie. Billiards on rational-angled triangles. *Commentarii Mathematici Helvetici, 75*, pages 65–108, 2000.

[KS21] Mikhail G. Katz and Stéphane Sabourau. Systolically extremal nonpositively curved surfaces are flat with finitely many singularities. *J. Topol. Anal.*, 13(2) :319–347, 2021.

[KZ03] Maxim Kontsevich and Anton Zorich. Connected components of the moduli spaces of abelian differentials with prescribed singularities. *Invent. Math.*, 153 :631–678, 2003.

[Lal14] Steven P. Lalley. Statistical regularities of self-intersection counts for geodesics on negatively curved surfaces. *Duke Mathematical Journal*, 163(6) :1191 – 1261, 2014.

[Leu67] Armin Leutbecher. Über die Heckeschen Gruppen $\mathfrak{G}(\lambda)$. *Abh. Math. Sem. Univ. Hamburg*, 31 :199–205, 1967.

[LM19] Erwan Lanneau and Martin Moeller. Non-existence and finiteness results for Teichmüller curves in prym loci. *Experimental Mathematics*, 31 :621 – 636, 2019.

[LN13] Erwan Lanneau and Duc-Manh Nguyen. $\mathrm{GL}_2^+(\mathbb{R})$–orbits in Prym eigenform loci. *Geometry & Topology*, 20 :1359–1426, 2013.

[Mas97] Daniel Massart. Normes stables des surfaces. *Comptes Rendus de l'Académie des Sciences - Series I - Mathematics*, 324(2) :221–224, 1997.

[Mas00] Howard Masur. Ergodic theory of translations surfaces. 2000.

[Mas22] Daniel Massart. A short introduction to translation surfaces, Veech surfaces, and Teichmüller dynamics. In *Surveys in geometry I*, pages 343–388. Springer, Cham, 2022.

[McM05a] Curt McMullen. Teichmüller curves in genus two : the decagon and beyond. *Jounal für die reine und angewandte Mathematik*, 2005.

[McM05b] Curtis T. McMullen. Teichmüller curves in genus two : Discriminant and spin. *Math. Ann.*, 333(1) :87–130, 2005.

[McM06a] Curt McMullen. Teichmüller curves in genus two : torsion divisors and the ratio of sines. *Inventionnes Mathematicae, 165*, pages 651–672, 2006.

[McM06b] Curtis T. McMullen. Prym varieties and Teichmüller curves. *Duke Mathematical Journal*, 133 :569–590, 2006.

[McM21] Curtis T. McMullen. Billiards and Teichmüllller curves. 2021.

[Mir08] Maryam Mirzakhani. Growth of the number of simple closed geodesics on hyperbolic surfaces. *Annals of Mathematics*, 168 :97–125, 2008.

[MM14] Daniel Massart and Bjoern Muetzel. On the intersection form of surfaces. *Manuscr. Math.*, 143(1-2) :19–49, 2014.

[Möl04] Martin Möller. Periodic points on Veech surfaces and the Mordell-Weil group over a Teichmüller curve. *Inventiones mathematicae*, 165 :633–649, 2004.

[Möl18] Martin Möller. Geometry of Teichmüller curves. In *Proceedings of the International Congress of Mathematicians—Rio de Janeiro 2018. Vol. III. Invited lectures*, pages 2017–2034. World Sci. Publ., Hackensack, NJ, 2018.

[Mon05] Thierry Monteil. On the finite blocking property. *Ann. Inst. Fourier*, 55(4) :1195–1217, 2005.

[Ros54] David Rosen. A class of continued fractions associated with certain properly discontinuous groups. *Duke Mathematical Journal*, 21 :549–563, 1954.

[Sch93] P. Schmutz. Riemann surfaces with shortest geodesic of maximal length. *Geometric and functional analysis*, 3(6) :564–631, 1993.

[SS95] Thomas Schmidt and Mark Sheingorn. Lenght spectra of the Hecke triangle group. *Mathematische Zeitschrift*, 220 :369–398, 1995.

[Tor23] Tina Torkaman. Intersection number, length, and systole on compact hyperbolic surfaces. 2023.

[Vee89] W. A. Veech. Teichmüller curves in moduli space, Eisenstein series and an application to triangular billiards. *Invent. Math.*, 97(3) :553–583, 1989.

[Win22] Karl Winsor. Uniqueness of the Veech 14-gon. 2022.

[Wri16] Alex Wright. From rational billiards to dynamics on moduli spaces. *Bull. Amer. Math. Soc. (N.S.)*, 53(1) :41–56, 2016.

[ZK76] A. N. Zemlyakov and A. B. Katok. Topological transitivity of billiards in polygons. *Math. Notes*, 18 :760–764, 1976.

[Zor06] Anton Zorich. Flat surfaces. In *Frontiers in number theory, physics, and geometry. I*, pages 437–583. Springer, Berlin, 2006.